anal-OL

JUN

U.S. DEPARTMENT OF COMMERCE

BUREAU OF STANDARDS JOURNAL OF RESEARCH

Vol. 10 JUNE 1933 No. 6

CONTENTS

RP. No.	TITLE AND AUTHOR	Page
561.	The compressometer, an instrument for evaluating the thickness, compressibility, and compressional resilience of textiles and similar materials. Herbert F. Schiefer	705
562.	The thermal expansion of refractories to 1,800° C. R. A. Heindl	715
563.	Fire tests of columns protected with gypsum. Nolan D. Mitchell	737
564.	The infrared arc spectra of manganese and rhenium. William F. Meggers	757
565.	Recombination radiation in the cesium positive column. F. L. Mohler	771
566.	The viscosity of sulphuric-acid solutions used for battery electrolytes. G. W. Vinal and D. N. Craig	781
567.	Composition of grids for positive plates of storage batteries as a factor influencing the sulphation of negative plates. G. W. Vinal, D. N. Craig, and C. L. Snyder	795
568.	The freezing point of iridium. F. Henning and H. T. Wensel	809
569.	The precipitation and titration of magnesium oxyquinolate in the presence of calcium oxalate, and its application in the analysis of portland cement and similar silicates. John C. Redmond	823
570.	A new description and analysis of the arc spectrum of chlorine. C. C. Kiess	827
571.	The effect of gasoline volatility on the miscibility with ethyl alcohol. Oscar C. Bridgeman and Dale W. Querfeld	841
572.	Creep and structural stability of nickel-chromium-iron alloys at 1,600° F. W. A. Tucker and S. E. Sinclair	852
	Index	863

A monthly periodical of pure and applied science published by our National Government

BUREAU OF STANDARDS JOURNAL OF RESEARCH

PUBLISHED AT WASHINGTON, D.C.

¶With the January issue the JOURNAL began its tenth semiannual volume. The JOURNAL contains the Bureau's research papers and critical reviews in the fields of science and technology. These will be comparable in interest and importance with the Bureau papers formerly issued as Scientific and Technologic Papers.

¶Several hundred researches are always in progress at the Bureau of Standards and the outlet for the results is the "BUREAU OF STANDARDS JOURNAL OF RESEARCH."

¶If you are interested in following the latest developments in science and technology you need the BUREAU OF STANDARDS JOURNAL OF RESEARCH. If you are a subscriber, renew your subscription promptly; if not, your subscription will be appreciated. Copies are limited and it is not always possible to supply back numbers.

PRICES

New subscription (or renewal)[1] to Journal of Research for United States, Canada, Cuba, Mexico, Newfoundland, and the Republic of Panama (vol. 8, and thereafter)		$2.50*
Blue buckram bound	Volume 1, July to December 1928	$2.75*
	Volume 2, January to June 1929	$2.75*
	Volume 3, July to December 1929	$2.75*
	Volume 4, January to June 1930	$2.75*
	Volume 5, July to December 1930	$2.75*
	Volume 6, January to June 1931	$2.75*
	Volume 7, July to December 1931	$2.75*
	Volume 8, January to June 1932	$2.50*

[1] Yearly subscription, 12 issues. * For other countries, add 75 cents.

Research papers (printed separately with durable paper cover and priced according to cost)—see list of research papers on cover pages 2 and 3 of this issue.

Address orders only to
Superintendent of Documents, Government Printing Office
Washington, D.C.

The value of prompt and adequate news of the latest research results cannot be measured by ordinary standards. They are permanent gainful assets for the expert. He cannot afford to be without such basic sources

U.S. DEPARTMENT OF COMMERCE
DANIEL C. ROPER, Secretary
BUREAU OF STANDARDS
LYMAN J. BRIGGS, Acting Director

BUREAU OF STANDARDS JOURNAL OF RESEARCH

June 1933
Vol. 10, No. 6

UNITED STATES
GOVERNMENT PRINTING OFFICE
WASHINGTON : 1933

For sale by the Superintendent of Documents, Washington, D.C. - - Price 25 cents; $2.50 per year on subscription

For a partial list of previous research papers appearing in BUREAU OF STANDARDS JOURNAL OF RESEARCH see pages 2 and 3 of the cover

THE COMPRESSOMETER, AN INSTRUMENT FOR EVALUATING THE THICKNESS, COMPRESSIBILITY, AND COMPRESSIONAL RESILIENCE OF TEXTILES AND SIMILAR MATERIALS

By Herbert F. Schiefer

ABSTRACT

The instrument described in this paper provides a convenient means for measuring the thickness and the change in thickness of a textile or similar material when it is subjected to increasing or decreasing pressures. The foot of the instrument can be lowered or raised by means of a rack and pinion acting through a helical spring. The pressure applied to the specimen by the foot is indicated on a dial micrometer and the corresponding thickness of the specimen on a second dial micrometer. Readings are taken under increasing pressures and then under decreasing pressures.

Curves for the compression and recovery of several materials are shown. Definitions are proposed for the terms thickness, compressibility, and compressional resilience as applied to textiles. The results of tests on rug underlays, blankets, felts, on knit, woven, and pile fabrics, and on sheet rubber and paper are given.

CONTENTS

		Page
I.	Introduction	705
II.	The instrument	706
III.	Test procedure	708
IV.	Discussion and application	708

I. INTRODUCTION

The thickness of textiles and many other similar materials depends greatly upon the pressure applied to the surfaces of the specimen. It decreases as the pressure is increased. The thickness of these materials is purely a matter of definition. Many definitions of thickness and methods for measuring thickness are published. The resulting confusion is described by Emley.[1] He points out the need for general agreement on one method and proposes a specification for a standard thickness gage and a standard definition of thickness.

The purpose of this paper is to describe an instrument for measuring the thickness under a known pressure which can be increased or decreased gradually and continuously.[2] Using this instrument the thickness under a given pressure can be measured. The change in thickness under either increasing or decreasing pressure can also be

[1] W. E. Emley, Measurement of Thickness of Textiles and Similar Materials, Am. Soc. Testing Materials 1931. Preprint Report of Committee B-1 on Methods of Testing, pp. 23-27.

[2] In a paper entitled "An Instrument for Measurement of Thickness of Compressible Solids," J. Sci. Instruments, vol. 6, pp, 382-385, 1929, M. C. Marsh has described an instrument suitable for measuring the thickness at a known pressure. The pressure may be varied by increments in a range between 1 mg and 100 g per square centimeter.

measured. The compressibility and compressional resilience of the material are computed from these data. These properties affect the sensations that contribute to what is usually called the softness or hardness of cloth.

Curves for the compression and recovery of several materials are shown. Definitions are proposed for the terms thickness, compressibility, and compressional resilience as applied to textiles. The results of tests on rug underlays, blankets, felts, on knit, woven, and pile fabrics, and on sheet rubber and paper are given.

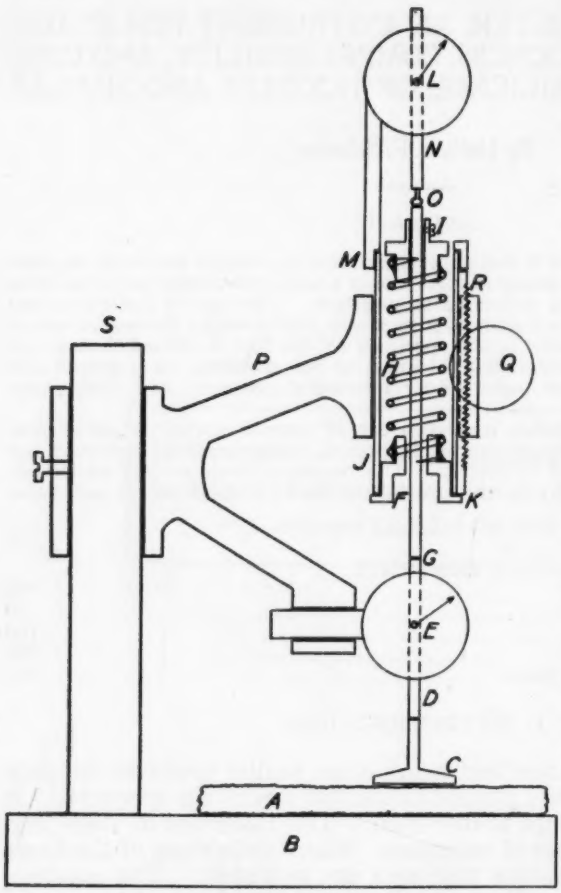

FIGURE 2.—*Schematic diagram of compressometer.*

II. THE INSTRUMENT

The instrument is shown in figure 1. A schematic diagram is shown in figure 2. The specimen, *A*, is placed upon the anvil, *B*. The foot, *C*, is circular in shape and 1 inch in diameter. It is fastened to the bottom of the spindle, *D*, of the lower dial micrometer, *E*. The lower surface of the foot is plane and parallel to the upper surface of the anvil. The rod, *F*, is fastened to the top of the spindle at *G* and to the top of a helical spring, *H*, at *I*. The bottom of the spring is fastened to the tube, *J*, at *K*. The upper dial micrometer, *L*, is fastened to the top of the tube at *M*. The spindle, *N*, of the upper dial micrometer rests on the top of the rod at *O*. The tube may be moved up or down relative to the frame, *P*, by turning the knob, *Q*, of the rack and pinion, *R*. By turning the knob the foot may be lowered upon the specimen. The pressure which is applied to the specimen by the foot may be ascertained from the upper dial reading and a calibration curve of the spring. The upper dial indicates the elongation of the spring. The distance between the face of the foot and the anvil; that is, the thickness of the specimen, is indicated on the lower dial. Each dial is graduated to read directly to 0.001 inch.

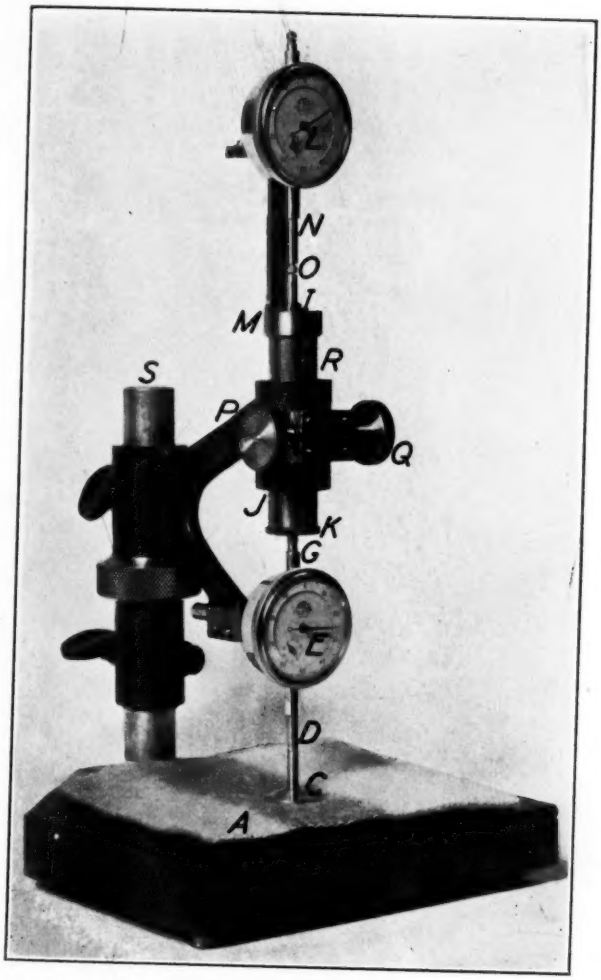

FIGURE 1.—*The compressometer.*

To calibrate the spring, the frame of the instrument is rotated through 180° about the vertical post, *S*. The foot is placed above the center of one pan of a balance. A load is placed on the other pan. The foot is lowered until the two pans are in balance and the elongation of the spring is read on the upper dial. The foot is lowered beyond the balanced position and then is raised until the two pans are again in balance. The elongation of the spring is read on the upper dial. The difference between the two upper dial readings is due to friction. Similar readings are taken for various loads. The spring elongations are plotted against the pressure; that is, the load divided by 0.7854 square inch which is the area of the foot.

The results are shown in figure 3 where curve *A* is obtained when the foot is lowered and curve *B* is obtained when the foot is raised.

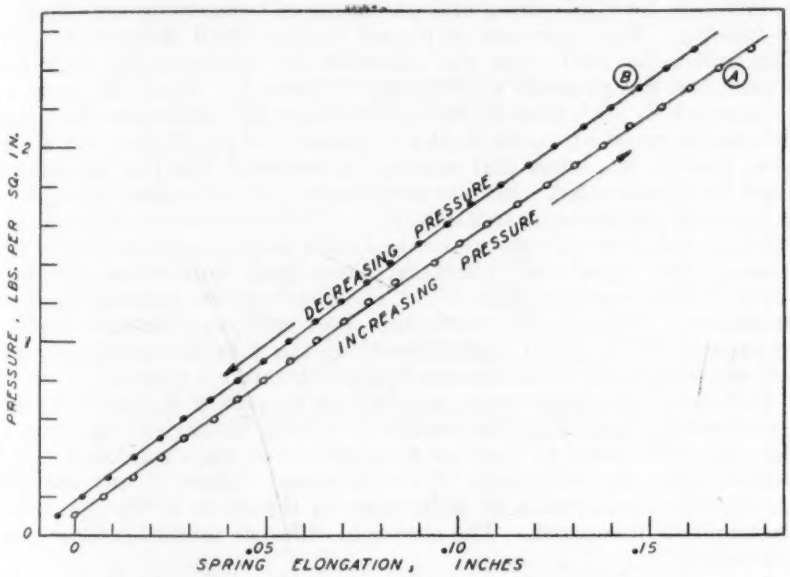

FIGURE 3.—*Calibration curves of helical spring.*

Curves *A* and *B* differ from each other because of friction in the moving parts of the dial micrometer. The friction gradually increases from the equivalent of about 0.1 lb./in.^{2} at low pressures to about 0.2 lb./in.^{2} at high pressures. It is probably high in the present instrument and could be reduced by changes in the design. For the present instrument where the friction in the moving parts is appreciable, curve *A* is used when the pressure on the specimen is increased, while curve *B* is used when the pressure is decreased.

The small helical spring of the lower dial micrometer was removed because it would alter the calibration curves when specimens of various thicknesses are measured.

The lower dial micrometer was calibrated for periodic and hysteresis errors. In the calibration a load of 1 pound was placed upon the spindle. The periodic error was less than 0.0005 inch. The hysteresis error was less than 0.0001 inch.

The periodic and hysteresis errors of the lower dial micrometer were also determined under the conditions in which the instrument is used. The periodic error was practically the same as that determined on the dial alone. The hysteresis error, however, increased from 0.0001 inch at a pressure of 0.1 lb./in.^{2} to 0.0003 inch at a pressure of 2 lb./in.^{2}.

The elastic deformation of the frame of the instrument when the pressure exerted by the foot is increased or decreased 1 lb./in.^{2} is about 0.0002 inch. The maximum departure from parallelism of the foot from the anvil is about 0.0003 inch.

These errors are negligible and were neglected in reporting the results.

III. TEST PROCEDURE

The data for the loading and unloading of a specimen are obtained as follows. The specimen is placed on the anvil without tension. The foot is lowered upon the specimen by means of the rack and pinion and the pressure is gradually increased. When the pressure reaches 0.1 lb./in.^{2}; that is, when the upper dial indicates the spring elongation given by curve A at the pressure of 0.1 lb./in.^{2}, the thickness; that is, the lower dial reading, is recorded, the ten thousandth place being estimated. Similar simultaneous observations are made at seven other pressures up to 2.0 lb./in.^{2}. The pressure is then gradually reduced and observations are made at the same pressures during unloading, the upper dial indicating the spring elongations given by curve B at the various pressures. The observations are made in rapid succession. With a little practice an observation can be made in about 10 seconds. The time required to obtain the data for the compression and recovery cycle of a specimen is approximately 3 minutes.

Curves of the compression and recovery cycle of several materials are shown in figure 4. The curves are drawn through the average of the values obtained at three or more places on each specimen. It is evident that the variations of the observed values of any material are mainly attributable to differences in thickness of the specimens at the places measured. The curves of different materials show great differences.

IV. DISCUSSION AND APPLICATION

In order to evaluate the thickness of fabrics and similar materials and to evaluate the properties of compressibility and compressional resilience, it is necessary to define each in terms of measurable properties. The definitions must of necessity specify the size and shape of the foot and the pressure exerted by the foot. The pressure of 1 pound per square inch proposed by Emley [3] is used in the tentative definition of standard thickness. The definition for compressional resilience of textiles requires the selection of a standard pressure range. The range from 0.1 to 2.0 lb./in.^{2} is suggested. The definitions which follow are for textile fabrics, but may be applicable to other materials.

It is assumed that unless otherwise specified tests made with the compressometer will be carried out on specimens that are in equilibrium with an atmosphere of 65 percent relative humidity at a temperature of 70° F., the standard conditions for textile testing.

[3] See footnote 1, p. 705.

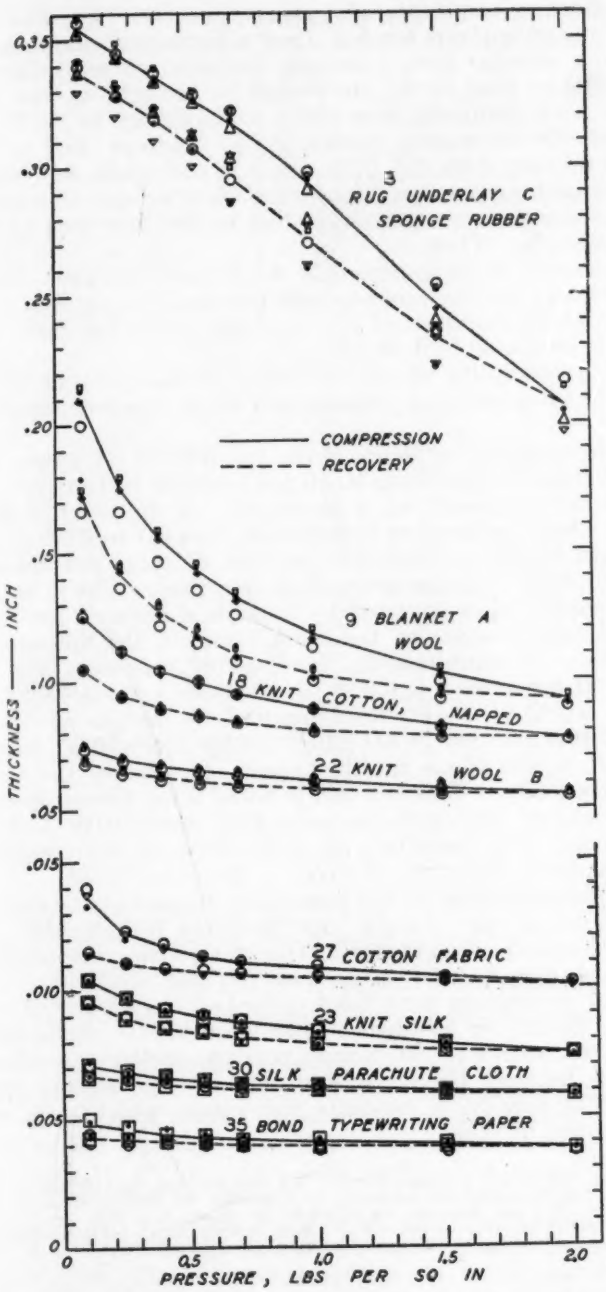

FIGURE 4.—*Typical curves of compression and recovery.*

The following conditions of test are specified. (1) The specimen shall be placed without tension upon a horizontal plane surface, the anvil; (2) a circular foot, 1 inch in diameter whose surface is plane and parallel to that of the anvil shall be brought to bear upon the specimen with gradually increasing pressures up to 2.0 lb./in.^{2} and then gradually decreasing pressures; (3) readings shall be taken at pressures 0.1, 0.2, 0.35, 0.5, 0.75, 1.0, 1.5, and 2.0 lb./in.^{2}; and (4) the time interval between two consecutive observations of points on the curve of compression or recovery shall be not less than 10 nor more than 15 seconds. Then:

The thickness of the specimen is the distance between the foot and the anvil when the pressure has been increased to a stated amount.

The standard thickness of the specimen is the thickness when the pressure is increased to 1 lb./in.^{2}.

The compressibility of the specimen is the ratio of the rate of decrease in thickness at a pressure of 1 lb./in.^{2} to the standard thickness.

The compressional resilience of the specimen is the amount of work recovered from the specimen when the pressure is decreased from 2.0 to 0.1 lb./in.^{2} expressed as a percentage of the work done on the specimen when the pressure is increased from 0.1 to 2.0 lb./in.^{2}.

The data for the numerical expression of these properties can be readily obtained with the instrument described. The area under the curve of compression bounded by horizontal lines at the initial and final thickness is equal to the work done on the specimen during compression. If simultaneous readings of thickness and pressure are taken at pressures 0.1, 0.2, 0.35, 0.5, 0.75, 1.0, 1.5, and 2.0 lb./in.^{2} then the work done can be computed by means of the formula $W=0.025\ (6A+5B+6C+8D+10E+15F+20G-70H)$, where A, B, C, D, E, F, G, and H are the thicknesses in inches at the above pressures, respectively. This formula is based upon the assumption that the segments of the curve between two consecutive pressures are straight lines. The same formula gives the work recovered when the thicknesses from the curve of recovery are substituted.

The numerical values of the properties defined above appear to be useful criteria of the "handle" or "feel" of fabrics when they are squeezed between the fingers. Together with the coefficient of friction and the flexural work and flexural resilience, for which methods of evaluation have been described elsewhere,[4] they offer a means for describing the tactile and kinaesthetic characteristics of farbrics quantitatively. However, pending further consideration of the relation between the physical stimuli and the sensory responses,[5] it will suffice simply to tabulate the values which were obtained. They are given in table 1.

---

[4] A. A. Mercier, Coefficient of Friction of Fabrics. B.S. Jour. Reserach, vol. 5 (RP196), pp. 243-246, 1930. H. F. Schiefer, The Flexometer, An Instrument for Evaluating the Flexural Properties of Cloth and Similar Materials. B.S. Jour. Research, vol. 10 (RP555), pp. 647-657, May 1933.

[5] Wm. D. Appel and the author are attempting to enumerate and define what may be called the kinaesthetic and tactile characteristics of cloth and the related physical properties.

TABLE 1.—*Results of tests* [1]

No.	Description of specimen	Total compression pressure range of 0.1 to 2.0 lb./in.[2]	Standard thickness	Compressibility	Compressional resilience	
						Average deviation
		Inch	*Inch*	*In.²/lb.*	*Percent*	*Percent*
1	Rug underlay A, cotton and paper	[3] 0.290	[3] 0.357	[3] 0.32	[4] 35	[4] 2
2	Rug underlay B, jute	.058	.268	.10	31	1
3	Rug underlay C, sponge rubber	.146	.292	.28	81	4
4	Rug underlay D, sponge rubber	.0075	.1635	.02	74	1
5	Sheet rubber A, pure gum	.003	.1915	.006	86	4
6	Sheet rubber B, packing	.0015	.153	.003	74	1
7	Felt A	.038	.1395	.09	35	1
8	Felt B	.0195	.075	.09	37	1
9	Blanket A, wool	.118	.117	.38	54	1
10	Blanket B, wool	.077	.116	.27	48	1
11	Blanket B after 1 washing	.097	.134	.27	42	1
12	Blanket B after 3 washings	.105	.145	.28	36	1
13	Blanket B after 5 washings	.103	.144	.27	36	1
14	Blanket C, cotton warp, wool filling	.081	.123	.25	45	1
15	Blanket C after 1 washing	.101	.145	.27	39	1
16	Blanket C after 3 washings	.101	.148	.26	36	2
17	Blanket C after 5 washings	.096	.144	.26	36	1
18	Knit cotton, napped	.0485	.089	.21	43	1
19	Knit cotton	.0115	.0415	.10	39	2
20	Knit cotton and wool	.0195	.0475	.14	45	1
21	Knit wool A	.0345	.0825	.16	53	1
22	Knit wool B	.020	.061	.13	55	1
23	Knit silk	.003	.0085	.14	56	1
24	Knit rayon	.002	.014	.06	56	4
25	Wool pile fabric	.025	.137	.06	42	2
26	Mohair pile fabric	.0105	.149	.02	48	2
27	Cotton fabric	.0035	.011	.08	41	2
28	Cotton balloon cloth	.0045	.0065	.15	28	5
29	Wool fabric	.003	.015	.07	66	4
30	Silk parachute cloth	.0015	.006	.06	67	5
31	Rayon fabric	.0015	.0095	.05	51	2
32	Weighted silk fabric	.002	.0125	.07	47	2
33	Weighted silk fabric, weighting removed chemically	.002	.011	.06	55	2
34	Filter paper	.002	.0085	.07	53	3
35	Bond typewriting paper	.001	.004	.06	56	9

[1] The results in the table are the average of 3 determinations except for specimens nos. 3, 4, and 9, which are the average of 7, 4, and 4 determinations, respectively.

[2] The total compression and standard thickness are reported to nearest 0.001 inch for those materials having a total compression greater than 0.05 inch and to nearest 0.0005 inch for those materials having a total compression equal to or less than 0.05 inch.

[3] The compressibility is reported to nearest 0.01 inch[2] per pound except specimens nos. 5 and 6, which are reported to nearest 0.001.

[4] The compressional resilience and average deviation are reported to the nearest percent.

The total compression in the pressure range of 0.1 to 2.0 lb./in.[2] and standard thickness are reported to nearest 0.001 inch for those specimens which have a total compression greater than 0.05 inch and to nearest 0.0005 inch for those specimens which have a total compression equal to or less than 0.05 inch. The compressibility is reported to nearest 0.01 inch[2] per pound except specimens nos. 5 and 6, which are reported to nearest 0.001. The compressional resilience is reported to the nearest percent. The average deviation of the compressional resilience is also given in the table. It is 1 percent for 18 specimens, 2 percent for 9 specimens, and greater than 2 percent for the remaining 8 specimens. The average deviation is large, 9 percent for bond typewriting paper, for specimens which have a small total compression. Rug underlay *C* of sponge rubber appears

to be an exception. For it the average deviation of 4 percent is probably attributable to the nonuniformity of the underlay. (See fig. 4.)

The following observations are of interest. The compressibility of the blanket is roughly six times that of the silk parachute cloth and the bond typewriting paper. The order of increasing compressional resilience is different from that of compressibility. For the specimens measured, it ranges from 28 to 86 percent. As was to be expected, the rubber specimens have the highest compressional resilience. The silk, wool, rayon, cotton, and jute specimens come next in order. The increase in thickness and total compression and the decrease in compressional resilience of the blankets after washing is marked. The difference between a weighted silk and the same silk after removal of the weighting is also marked.

The compressional resilience of the specimens of pure gum sheet rubber and of sheet rubber packing are lower than might be expected. Applying corrections for the instrumental errors to the results for these specimens decreases the compressional resilience a few percent. The explanation for the low compressional resilience of these rubber specimens therefore must be sought elsewhere. The conditions of the surfaces of the rubber specimens, whether clean, dirty, or lubricated affect the curves of compression and recovery. The total compression and the compressional resilience for the pressure range of 0.1 to 2.0 lb./in.^{2} were found to be lower for specimens with clean surfaces than for the same specimens with the surfaces lubricated with graphite. The total compression and the compressional resilience for the above pressure range were found to increase with the thickness of the specimen. The total compression for the second compression cycle was found to be smaller and the compressional resilience was found to be greater than for the first cycle when the second cycle was obtained without removing the specimen from the instrument. The results of tests are given in table 2 for two specimens of pure gum sheet rubber.

TABLE 2.—*Results showing effect of thickness and condition of surface of pure gum sheet rubber on total compression and compressional resilience*

Specimen No.	Condition of surface	Standard thickness	Total compression pressure range of 0.1 to 2.0 lb./in.^{2}	Compressional resilience
		Inch	*Inch*	*Percent*
1	Clean, first cycle	0.389	0.0018	64
1	Clean, second cycle	.389	.0013	79
1	Lubricated with graphite	.389	.0032	77
2	Clean, first cycle	1.08	.0195	90
2	Clean, second cycle	1.08	.0175	95
2	Lubricated with graphite	1.08	.0210	92

The shape and size of the foot and the dimensions of the rubber specimen relative to them probably affect the magnitude of the compressional resilience. The manner in which these affect the compressional resilience is beyond the scope of this paper.

The present instrument was designed primarily for the measurement of relatively thick textiles, such as blankets and napped underwear. The results shown in tables 1 and 2 and figure 4 indicate that

it can be used satisfactorily for measuring thin fabrics, paper, and rubber. However, measurements of such materials should be significant to the fourth decimal place and an instrument accurate to 0.0001 inch should therefore be used. Moreover, to measure to this degree of precision, the following precautions must be observed: (1) The instrument must be constructed with greater rigidity to reduce the elastic deformation of the frame to less than 0.0001 inch; (2) tolerances consistent with this degree of precision must be set for the parallelism and planeness of the surfaces of the anvil and foot; and (3) the periodic and hysteresis errors of the lower dial micrometer must be determined and corrections consistent with this degree of precision must be applied.

The results given indicate what may be expected from the use of the instrument. From the data available it would seem that the compressibility depends mainly upon the structure of the specimen whereas the compressional resilience depends upon the kind of material and the structure of the specimen.

NOTE.—Drawings of the instrument showing the details of construction may be obtained from the textile section of the Bureau of Standards.

WASHINGTON, March 16, 1933.

THE THERMAL EXPANSION OF REFRACTORIES TO 1,800° C.

By R. A. Heindl

ABSTRACT

The linear thermal expansions of the following 36 materials were measured: African chrome sand; Cuban, Grecian, Friable African, Rhodesian Imperial, Indian and Turkish chrome ores; Austrian, Californian, and electrically fused magnesites; a periclase brick; a spinel brick; two types of fire-clay bricks and two of fire clays; Kentucky, Tennessee, and English ball clays; Georgia kaolin and and English china clay; an 80 percent alumina brick; artificial corundum, diaspore, bauxite; five mullites, each of which was prepared from different raw materials; two zircon bricks and a furnaced zirconium silicate; silicon carbide, a silica brick, and an insulating brick. Data are also given on artificial graphite which had been preheated several times to 1,800° C. Measurements were made below 1,000° C. in both an oxidizing and a reducing atmosphere. Above, 1,000° C. the materials were tested in a reducing atmosphere only. When the refractoriness of the materials permitted they were tested up to 1,800° C. Petrographic analyses of the materials were made before and after the several heat treatments.

CONTENTS

	Page
I. Introduction	715
II. Materials and specimens	716
III. Apparatus	716
1. Description	716
2. Calibration	718
IV. Method of testing	719
V. Results	720
1. Linear thermal expansion	721
2. Petrographic analyses	731
VI. Summary	735

I. INTRODUCTION

The need for information relative to the expansion of refractory materials, up to and beyond the temperature range in which they are now used, is evidenced by an increasing number of reports [1] dealing with the subject. Norton [2] gave reasons regarding the value of such

[1] F. H. Norton, The Thermal Expansion of Refractories, J.Am.Cer. Soc., vol. 8, no. 12, pp. 799–815, 1925.
K. Becker, X-ray Method of Determining Coefficient of Expansion at High Temperatures, Z. Physik, vol. 40, pp. 37–41, 1926.
W. Miehr, J. Kratzert, and H. Immke, The Importance of Thermal Expansion in the Valuation of Refractory Material, Tonin. Ztg., vol. 51 (26), pp. 417–422, 1927.
Hans Hirsch and Max Pulfrich, Expansion Measurements at high Temperatures, Tonin. Ztg., vol. 52 (36), pp. 712–713, 1928.
K. Endell and W. Steger, The Measurement of the Thermal Expansion of Refractory Materials to 1,600° C., Archiv. Eisenhüttenives, vol. 1 (11), 1928; Feuerfest vol. 5 (1), pp. 3–4, 1929.
Willi M. Cohn, Expansion Measurements from 20° to 1,400° C., Keramos, vol. 9 (7), pp. 215–218, 1930.
H. Reich, A New Apparatus for Measuring the Thermal Expansion of Refractory Materials in the Temperature Range 0° to 1,700° C., Berichte Deut. Ker. Gesell., vol. 13 (4), pp. 157–166, 1932.

[2] F. H. Norton, The Thermal Expansion of Refractories, J.Am.Cer. Soc., vol. 8, no. 12, pp. 799–815, 1925.

information. It may also be pointed out that it is not at all unusual for refractories to be used at temperatures considerably higher than those at which they had been heated during the manufacturing process. In such cases physical and chemical changes not completed during the manufacturing stage continue to progress. In many cases the linear thermal expansion is affected by such additional heating which in turn may greatly affect the stresses set up in the refractory during use.

The present report deals not only with the expansion of the well-known types of refractory materials to temperatures sufficiently high to cause many of them to soften or deform but also with the effect on the expansion when the materials are heated to a higher temperature than that at which they had been heated preliminary to the first test.

II. MATERIALS AND SPECIMENS

Seven chrome ores, four magnesites, five mullites, two fire-clay bricks, two fire clays, three ball clays, two kaolins, three zircons, and one each of spinel, silicon carbide, artificial corundum, diaspore, bauxite, 80 percent alumina fire brick, silica brick, and insulating brick were included in this investigation. A large proportion of these materials were furnished by manufacturers [3] and the others were available in the bureau laboratories.

Test specimens approximately 5⅞ inches long and ⅞ inch square were cut from commercial bricks if available, but if bricks were not available specimens of similar dimensions were prepared from raw materials which had been ground to pass a 40-mesh sieve. The specimens were prepared by adding sufficient water or gum tragacanth to each ground material so it could be readily molded. After removing the damp specimens from the mold they were dried, heated, and cut to the required dimensions. The specimens cut from the bricks were tested without further treatment whereas most of those prepared from the raw material were tested after having been heated at 1,400° C. for 5 hours and cooled with the furnace in about 36 hours.

III. APPARATUS

1. DESCRIPTION

A furnace of the high frequency induction type shown in figure 1 was used for determining the expansion of the various materials up to 1,800° C. The heat is generated through the medium of a cylindrical graphite muffle 12 inches long, 6 inches in diameter, and having a wall ½ inch thick. The gradual oxidation of the graphite muffle was the cause of a reducing atmosphere within the furnace. The converter for controlling the power input to the furnace is shown on the right in the figure. An Ames micrometer dial graduated in ten thousandth inch was supported independently of the furnace by a framework, the legs of which were fused quartz tubes.

The set-up of the specimen is indicated by the sketch in figure 2. This set-up formed a continuous system which also could expand and contract independently of the furnace. Tungsten plates ⅞ inch

[3] E. J. Lavino & Co., Philadelphia, Pa.; Harbison-Walker Refractories Co., Pittsburgh, Pa.; Norton Co., Worcester, Mass.; A. P. Green Fire Brick Co., Mexico, Mo.; Champion Spark Plug Co., Detroit, Mich.; Titanium Alloy Manufacturing Co., Niagara Falls, N.Y.; Babcock & Wilcox Co., New York, N.Y.

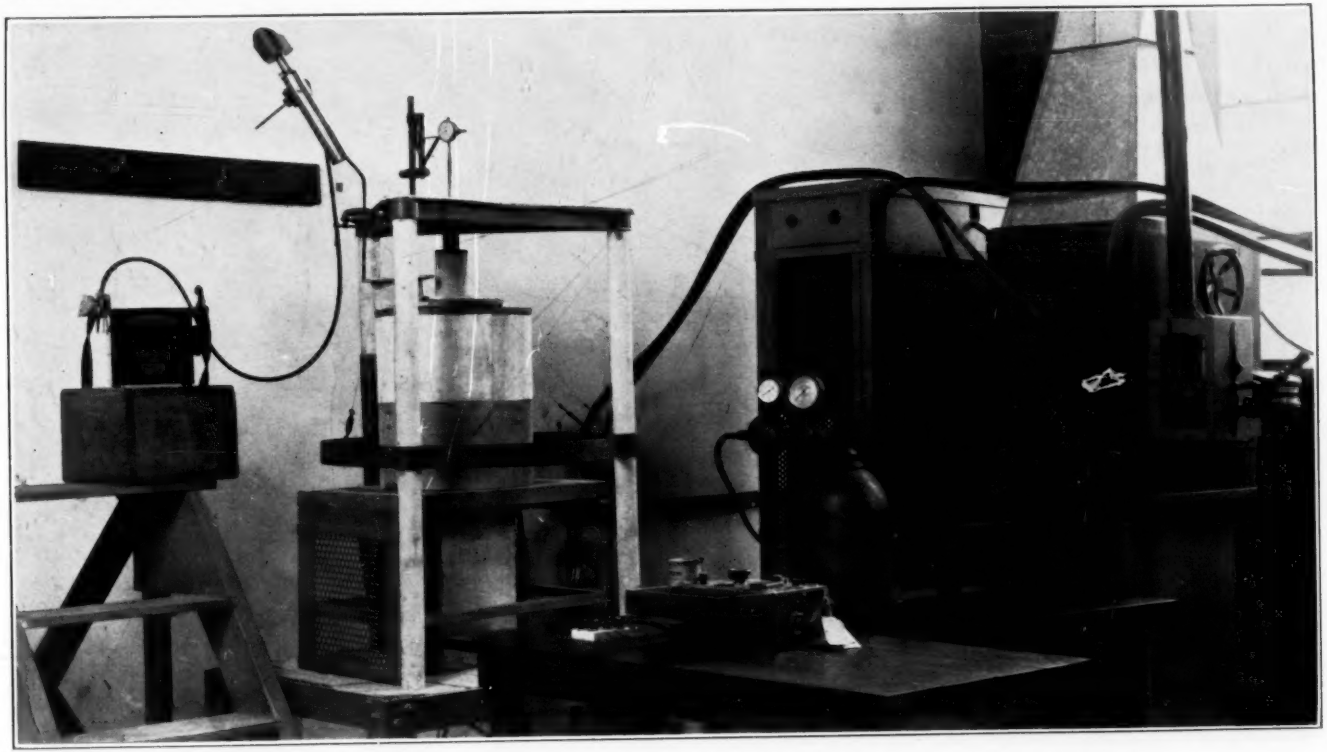

FIGURE 1.—*Apparatus used for obtaining linear thermal expansion measurements to 1,800° C.*

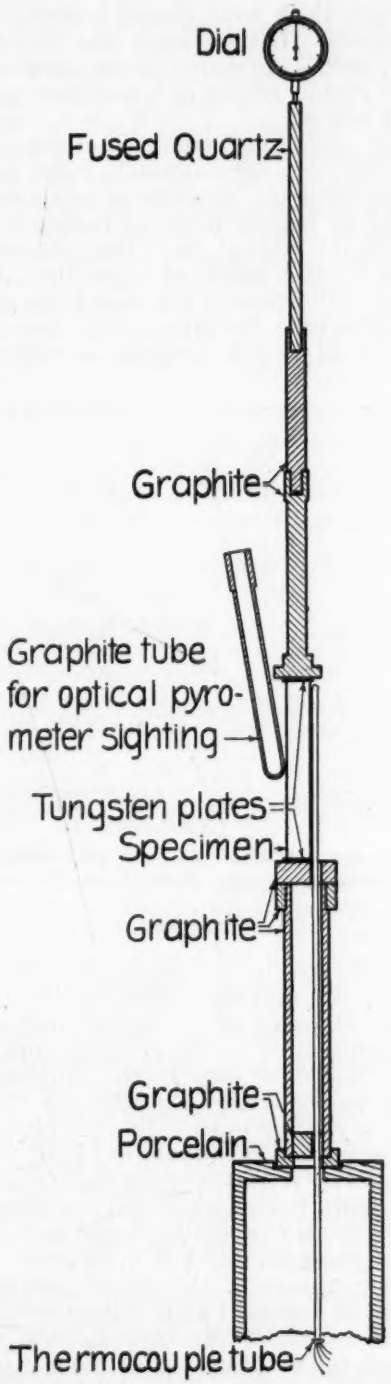

FIGURE 2.—*Showing the specimen, specimen support, and the system transmitting the expansion to the micrometer dial.*

The fused quartz rod does not extend into the furnace.

square and 0.015 inch thick were placed between the test specimen and the graphite pieces. The specimen was placed within a muffle, inside diameter 2¼ inches, prepared from zirconium silicate. The weight of the pieces resting on top of a specimen and making contact with the dial was 4 ounces.

Two platinum to platinum-rhodium thermocouples were placed alongside the specimen, one approximately three fourths inch below the top end and the other the same distance above the bottom end. These couples could be readily removed during a test through the lower end of the furnace without disturbing the set-up. The optical pyrometer shown in figure 1 was fixed in position, preceding the test, so that it sighted on the bottom of the closed end graphite tube indicated in figure 2. This tube was placed near the middle of the specimen and as close to it as possible without actually touching it.

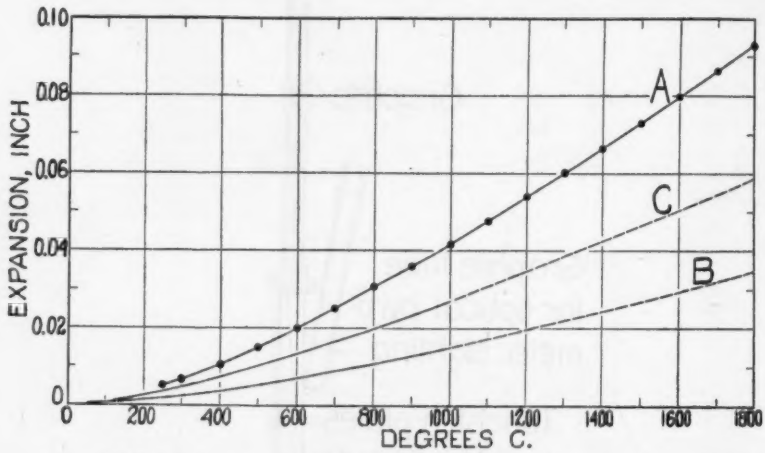

FIGURE 3.—*Calibration curve C for the apparatus when samples approximately 5⅞ inches long were tested and curves A and B involved in its derivation.*

2. CALIBRATION

The movements indicated by the micrometer dial during an expansion test represented the difference between the total expansion of the built-up column composed of the various parts shown in figure 2 and the vertical expansion of the outer framework and dial support shown in figure 1. The first step in the calibration was to make several tests with a bar of artificial graphite, 5.737 inches long and 1 inch in diameter, as the specimen. In each of these tests the temperatures were increased to a maximum of 1,800° C. at the same rate and the dial readings were recorded in the same manner as in the later tests. After preliminary heatings the dial readings for like temperatures in different tests were nearly the same and when plotted were found to lie along the smooth curve *A* in figure 3. This established the fact that the expansions of the entire measuring system were practically the same in repeated tests with the same specimen and set-up. During the course of the investigation several additional tests were made with the graphite bar as the specimen and in these, the readings, beginning at approximately 250° C. did not deviate more than 2.0 percent from curve *A*, figure 3.

Repeated readings over a temperature range of 20° to 1,000° C. were then made with a bar (5.852 inches long) of fused quartz, the thermal expansion of which was known. In these tests the rate of increase of temperature was the same as in other tests. Dial readings in the different tests of fused quartz checked, which confirmed the indications of the previous tests that the effects of expansions of supports for the specimen and the dial did not vary significantly. Deducting the expansion of the fused quartz bar from these dial readings gave the corrections which should be deducted from dial readings in later tests to obtain the expansion of specimens investigated. These corrections are shown by solid portion of curve *C*, figure 3. Appying these corrections to the readings obtained with the graphite bar (curve *A*) gave the values for the expansion of the bar itself below 1,000° C. which are shown by the solid portion of curve *B*, figure 3.[4]

Curve *A* showed no irregularities between 1,000° and 1,800° C.; consequently it is logical to assume that neither curve *B* nor *C* above 1,000° C. should show irregularities. Moreover, as the curvature of curve *A* in the temperature range 500 to 1,800° C. and also that of curve *B* in the range 500° to 1,000° C. were approximately constant, it seemed reasonable to assume that the curvature of curve B would remain approximately constant from 500° to 1,800° C. Accordingly curve *B* was extended from 1,000° to 1,800° C. based on that assumption. The calibration or correction curve *C* was then extrapolated to 1,800° C. by taking the difference between curves *A* and *B* at 100° C. intervals in the range 1,000° to 1,800° C.

A further precaution was taken in that the furnace was calibrated to 1,000° C. with the specimen of fused quartz preceding practically every test of a material.

IV. METHOD OF TESTING

Linear thermal expansion measurements were made of the same specimen, of each of the materials, in steps as follows: (1) Up to 1,000° C. at approximately 100° C. intervals, using either the entire specimen and the apparatus described in the Second Progress Report of the Sagger Investigation[5] or chips of the specimen and the interferometer.[6] (2) In the induction furnace to some temperature above 1,000° C., but in no case above 1,800° C. (3) The procedure described under (1) was repeated with the specimen taken from the induction furnace. (4) After the measurements described under (3) were completed, the specimen was again tested in the induction furnace at the higher temperatures. There were two reasons for this procedure, (*a*) the time for making the tests in the induction furnace could be considerably lessened because only a few observations below 1,000° C. would be necessary, and (*b*) an error in the set-up of the specimen in the induction furnace would be quickly detected because the data obtained below 1,000° C. with the induction furnace should generally

[4] The values obtained checked the expansion of the graphite bar determined over the range 20° to 500° C. by means of an apparatus described elsewhere. R. F. Geller and R. A. Heindl, II. Progress Report on Investigation of Sagger Clays—Some Observations as to the Significance of Their Thermal Expansions, J.Am.Cer.Soc., vol. 9, no. 9, pp. 555-575, 1926.

[5] See footnote 4.

[6] C. G. Peters and C. H. Cragoe, B.S.Sci. Paper No. 393, and G. E. Merritt, B.S.Sci. Paper No. 485. The specimens from which the chips were cut did not always receive the corrseponding heat treatment to 1,000° C.

agree with those previously obtained in the furnaces operating only to 1,000° C.

Temperatures in the induction furnace were measured with the thermocouples up to approximately 1,500 C., following which the couples were removed and the temperatures observed with an optical pyrometer. In testing with the induction furnace, temperature readings to and including 1,000° C. were taken at approximately 250° C. intervals, thereafter at approximately 100° C. intervals. It was always the practice to check the optical pyrometer against the thermocouples before their removal. Temperatures were maintained for approximately 15 minutes before the final micrometer dial readings were recorded for each temperature up to 1,500° C.; thereafter no effort was made to stop at any specific temperature. However, an attempt was made to regulate the power input so that readings were taken only while the furnace temperature was increasing at a comparatively slow rate or not at all.

The maximum temperature at which expansion or contraction movements were observed depended on the refractoriness of the material, but in no case did it exceed 1,800° C.

In most instances observations at temperatures above 1,000° C. were made of each specimen twice, namely, (1) after its preparation, and (2) after its initial test in the induction furnace. This procedure afforded the means of determining whether any changes had occurred in the expansions of the materials as a result of having been heated in the induction furnace at temperatures considerably higher than those at which they had been initially heated.

V. RESULTS

1. LINEAR THERMAL EXPANSION

Linear thermal expansion or contraction values for all the materials are shown in the curves given in figures 4 to 9, inclusive. Observations (filled in circles) with the induction furnace below 1,000° C. are not given in figures 5 to 9 because they very nearly coincided with the observations (clear circles) obtained in the furnaces operated only to 1,000° C.

Pertinent data are summarized in table 1. A detailed discussion of the data, therefore, is not necessary. The data obtained up to 1,000° C. have an accuracy of ±2½ percent [7] and it is estimated those above 1,000° C. have ar. accuracy of ±5 percent. The curves give the following information relative to expansion of the materials: (*a*) Type, whether uniform or nonuniform, (*b*) the effect, if any, of reheating, and (*c*) the temperature at which bloating or contraction begins. Table 1 gives the average coefficients of expansion for various temperature ranges.

[7] See footnote 4, p. 719, for reference to report giving calibration of apparatus.

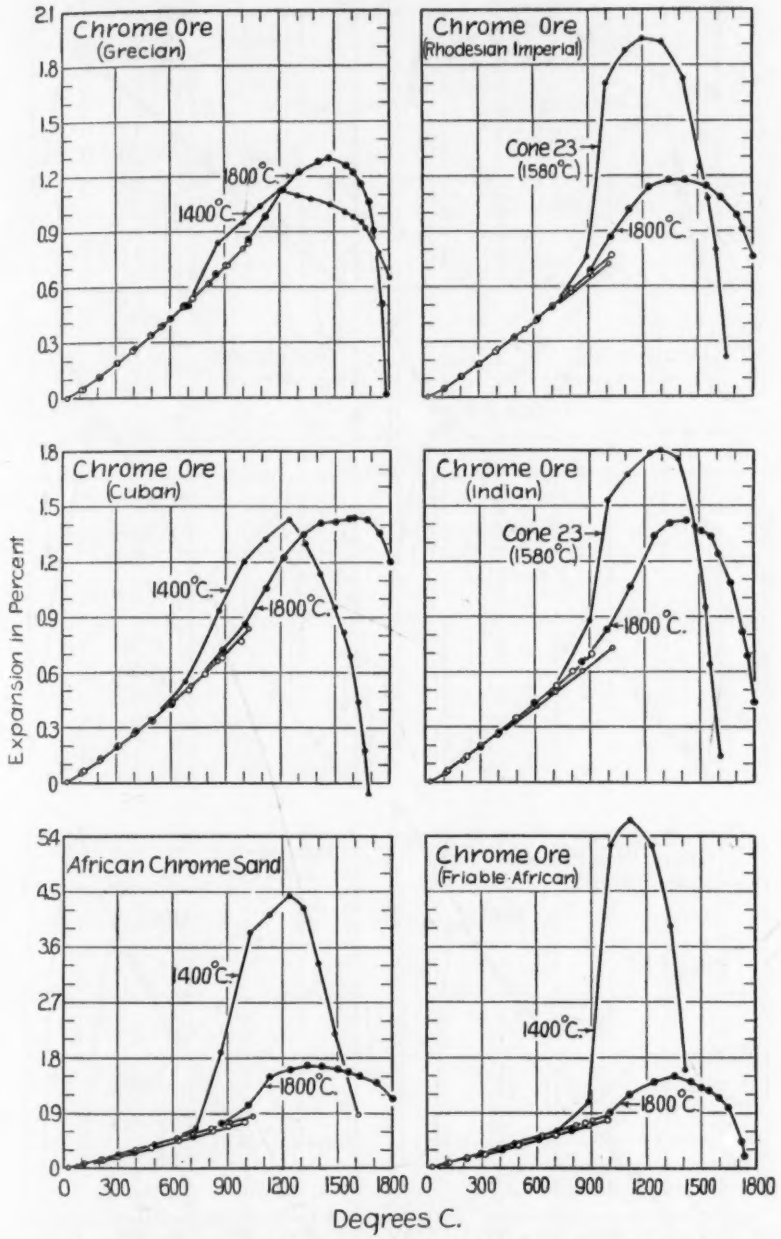

FIGURE 4.—*Thermal expansion curves for five chrome ores and a chrome sand.*

The temperatures adjacent to the curves indicate the maximum heat treatment the specimen had received previous to testing. The filled in circles on the curves represent the values obtained in a reducing atmosphere and the clear circles those obtained in an oxidizing atmosphere.

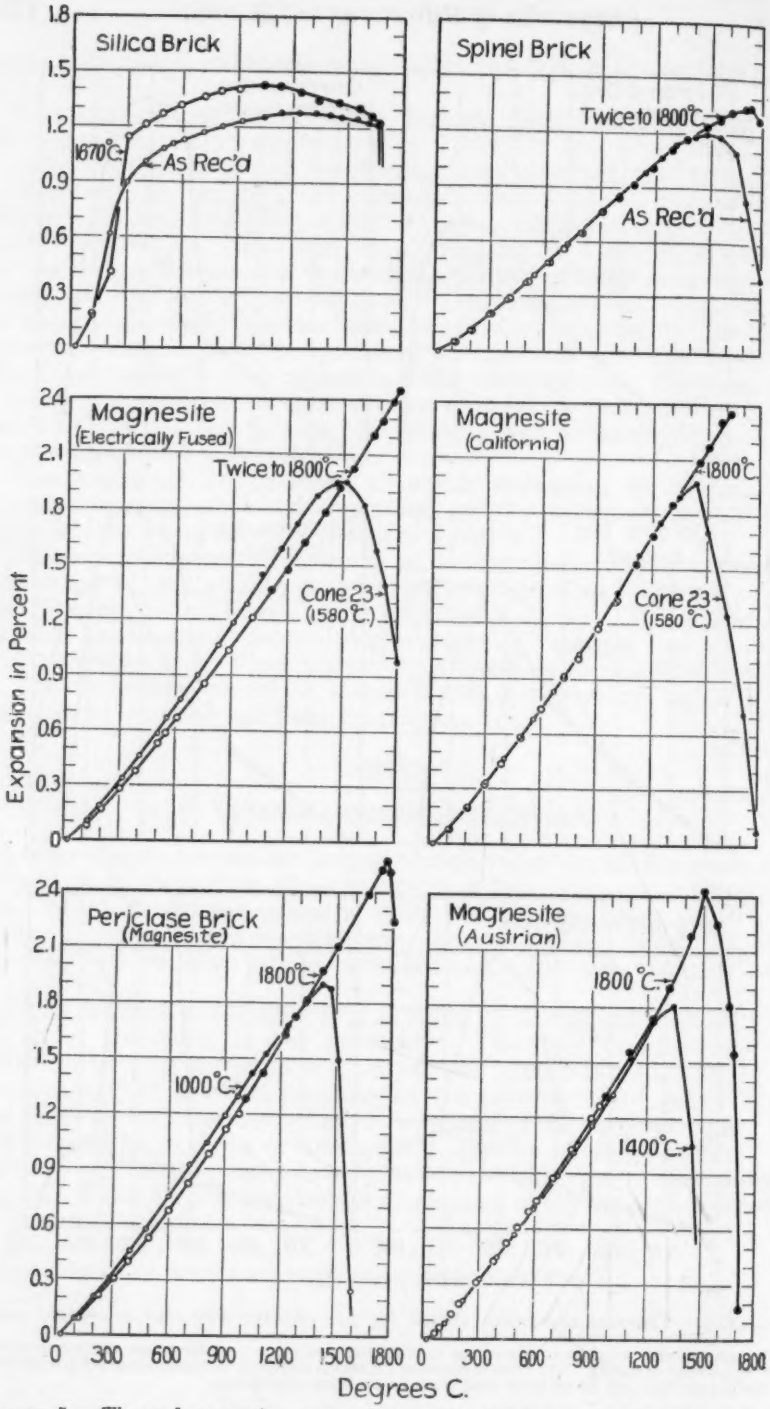

FIGURE 5.—*Thermal expansion curves for a silica brick, a spinel brick, and four magnesites.*

The temperatures adjacent to the curves indicate the maximum heat treatment the specimen had received previous to testing. (For additional details, see p. 721.)

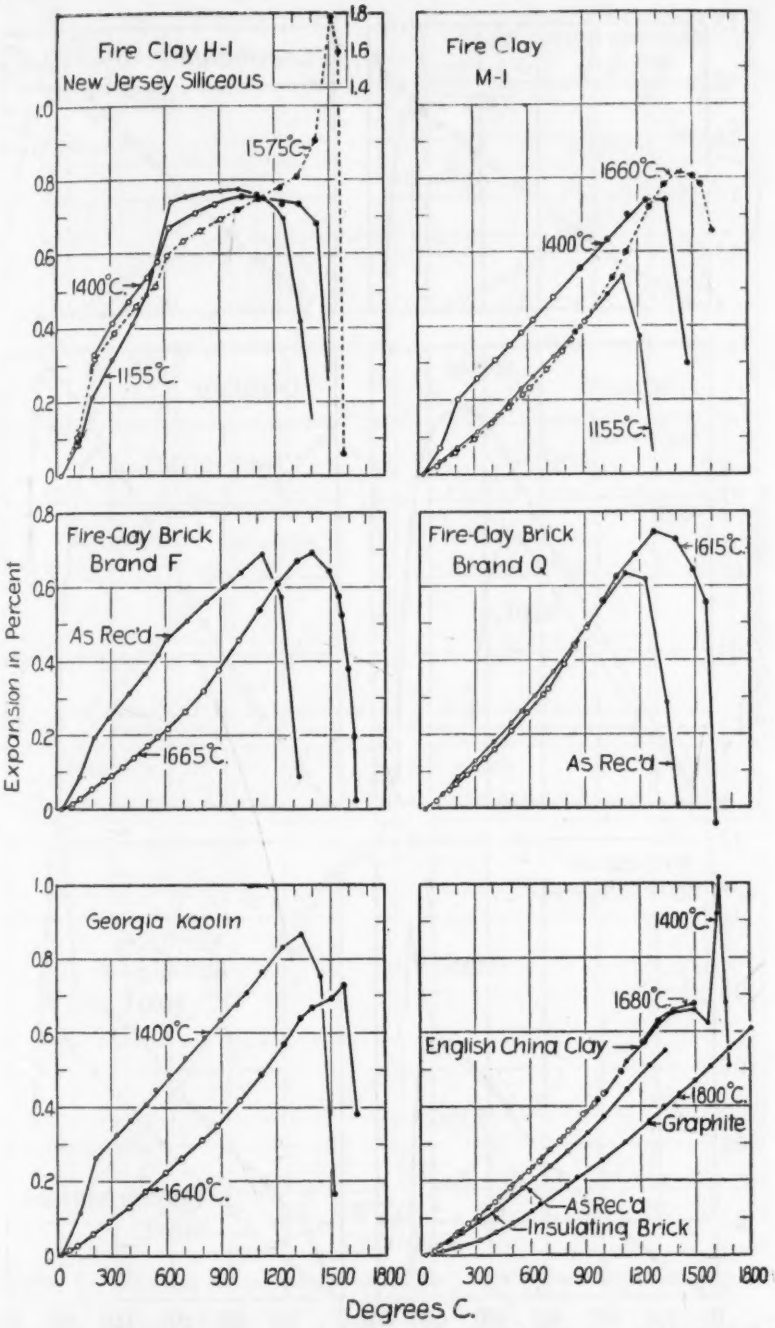

FIGURE 6.—*Thermal expansion curves for two types of fire clays and fire-clay bricks, a Georgia kaolin, an English china clay, insulating brick, and graphite.*

The temperatures adjacent to the curves indicate the heat treatment the specimen had received previous to testing. (For additonal details, see p. 721.)

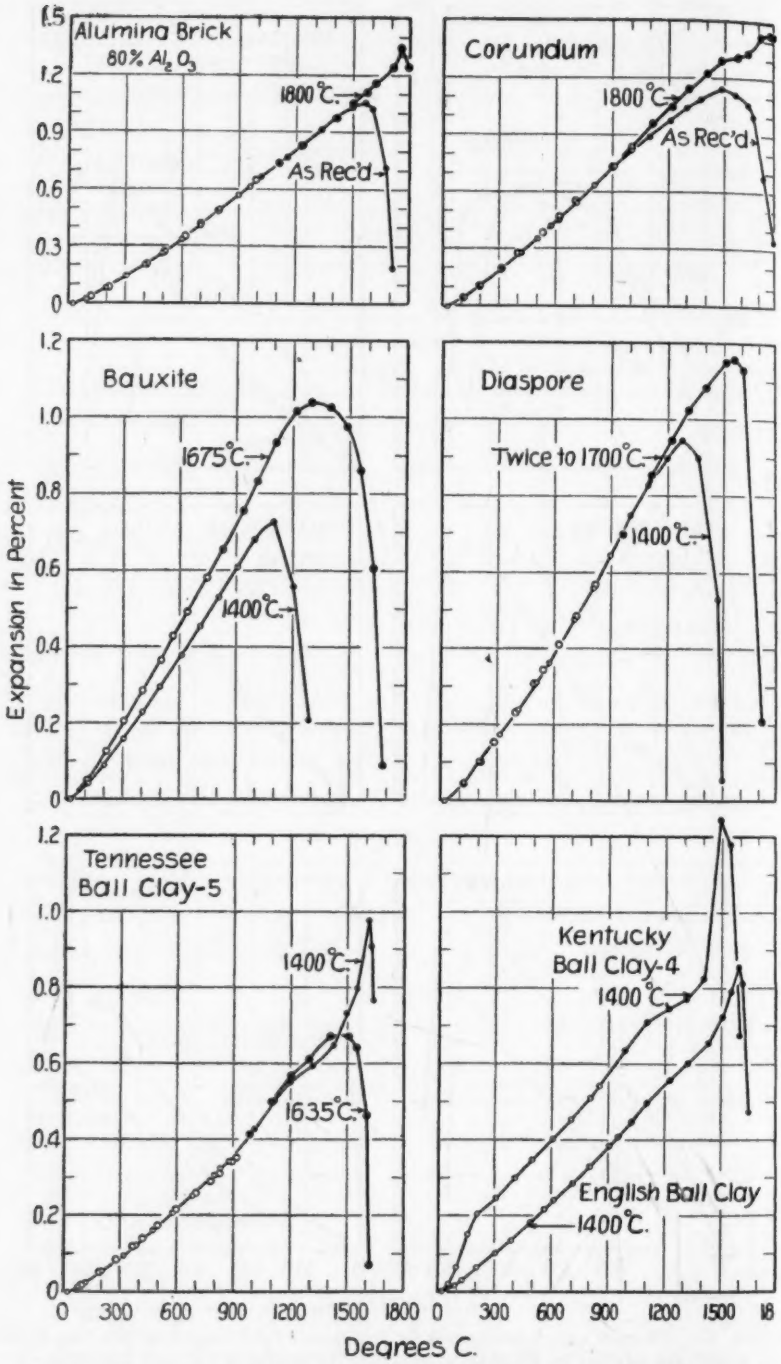

FIGURE 7.—*Thermal expansion curves for a high alumina fire brick, corundum, bauxite, diaspore, and Tennessee, Kentucky, and English ball clays.*

The temperatures adjacent to the curves indicate the heat treatment the specimen had received previous to the testing. (For additional details, see p. 721.)

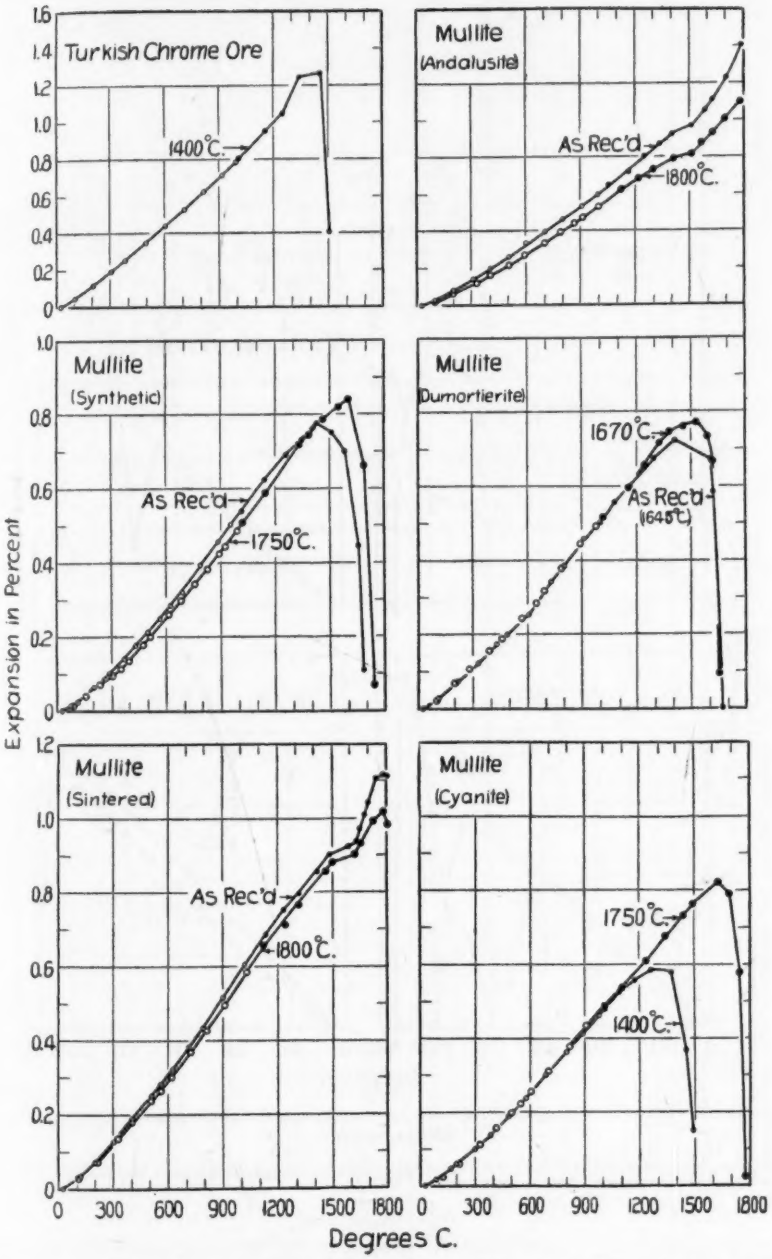

FIGURE 8.—*Thermal expansion curves for five mullites from different sources, and a chrome ore.*

The temperatures adjacent to the curves indicate the heat treatment the specimen had received previous testing. (For additional details, see p. 721.)

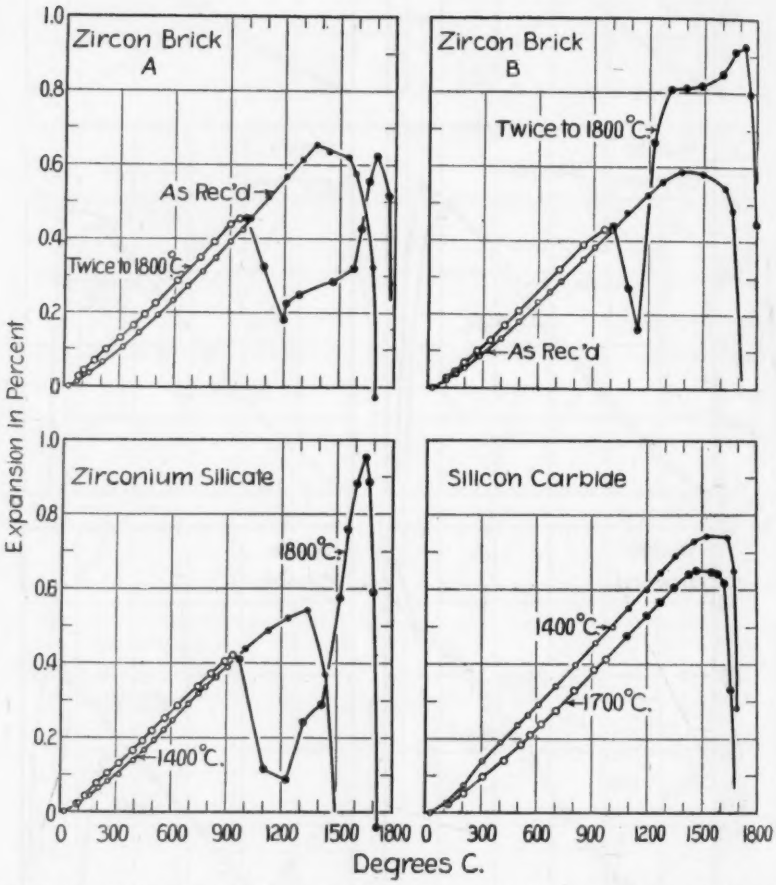

FIGURE 9.—*Thermal expansion curves for two zircon bricks, zirconium silicate, and silicon carbide.*

The temperatures adjacent to the curves indicate the heat treatment the specimen had received previous to testing. (For additional details, see p. 721.)

TABLE 1.—*Average coefficients of linear thermal expansion of refractories after different heat treatments*

Material	Chemical analyses [1]									Original heat treatment [2]	Maximum temperature reached in induction furnace		Linear thermal expansion in—						Total gain (+) or loss (−) after completion of tests, in—		Extent of deformation at end of tests
													Induction furnace				Resistance wire furnace [5]				
													First test		Second test		Average coefficient of expansion between 20° and 1,000° C.—				
	Ignition loss	SiO_2	FeO	Fe_2O_3	Al_2O_3	TiO_2	CaO	Cr_2O_3	MgO		First test	Second test	Temperature range [3]	Average coefficient of expansion [4]	Temperature range [3]	Average coefficient of expansion [4]	Before first test in induction furnace	After first test in induction furnace	Weight	Length	
	Per-cent	*Per-cent*	*Per-cent*	*Per-cent*	*Per-cent*	*Per-cent*	*Per-cent*	*Per-cent*	*Per-cent*	°C.	°C.	°C.	°C.	$\times 10^{-6}$	°C.	$\times 10^{-6}$	$\times 10^{-6}$	$\times 10^{-6}$	*Per-cent*	*Per-cent*	
African chrome sand	-----	4.5	-----	-----	-----	-----	----	51.3	-----	1,400	1,800	1,800	20–700 700–1,000 1,000–1,235	8.1 108.0 28.0	20–700 700–1,000 1,000–1,125 1,125–1,475	7.5 15.4 40.0 8.6	8.2	7.2	−5.3	−3.3	Slight.
Cuban chrome ore	1.3	2.4	15.1	-----	29.7	-----	----	34.2	16.5	1,400	1,800	1,800	20–700 700–1,000 1,000–1,250	7.6 20.5 8.9	20–700 700–1,000 1,000–1,215 1,215–1,600	7.4 10.9 17.0 5.7	8.3	7.9	−3.7	−2.3	Do.
Grecian chrome ore	1.1	3.8	13.3	-----	24.8	-----	----	40.8	15.3	1,400	1,800	1,800	20–700 700–865 865–1,200	7.4 21.0 8.3	20–700 700–1,030 1,030–1,300 1,300–1,470	7.6 10.2 13.3 4.8	8.2	8.2	−3.1	−4.3	Do.

[1] The analyses for the chrome ores, magnesites, 80 percent alumina brick, corundum, and bauxite were furnished by the companies which supplied the materials; the remainder of those given were made at the Bureau of Standards by J. F. Klekotka and F. W. Glaze.

[2] Materials marked "As received" were tested without preliminary heating in the laboratory furnaces, since they have been heated in commercial furnaces previous to their receipt.

[3] Shrinkage occurred above the highest temperatures given in this column except in the case of the California magnesite (second test).

[4] The negative sign preceding a value indicates contraction.

[5] Description of furnace and method given in J. Am. Ceramic Soc. vol. 9 (9), pp. 556-574, 1926.

TABLE 1.—*Average coefficients of linear thermal expansion of refractories after different heat treatments*—Continued

Material	Chemical analyses									Original heat treatment	Maximum temperature reached in induction furnace		Linear thermal expansion in—						Total gain (+) or loss (−) after completion of tests, in—		Extent of deformation at end of tests
													Induction furnace				Resistance wire furnace				
													First test		Second test		Average coefficient of expansion between 20° and 1,000° C.—				
	Ignition loss	SiO_2	FeO	Fe_2O_3	Al_2O_3	TiO_2	CaO	Cr_2O_3	MgO		First test	Second test	Temperature range	Average coefficient of expansion	Temperature range	Average coefficient of expansion	Before first test in induction furnace	After first test in induction furnace	Weight	Length	
	Per cent	*Per cent*	*Per cent*	*Per cent*	*Per cent*	*Per cent*	*Per cent*	*Per cent*	*Per cent*	°C.	°C.	°C.	°C.	×10⁻⁶	°C.	×10⁻⁶	×10⁻⁶	×10⁻⁶	*Per cent*	*Per cent*	
Friable African chrome ore.	2.0	5.6	15.4	-----	13.3	-----	-----	49.0	13.7	1,400	1,800	1,740	20–700 700–900 900–1,115	8.4 25.0 199.0	20–700 700–1,000 1,000–1,350	7.5 12.4 16.7	8.8	7.8	−10.3	−4.9	Slight.
Imperial chrome ore, Rhodesian.	2.1	5.2	13.4	-----	15.8	-----	-----	50.4	12.1	Cone 23 (1,580)	1,800	1,800	20–700 700–900 900–1,000 1,000–1,200	7.1 14.0 93.0 12.0	20–700 700–900 900–1,230 1,230–1,430	7.2 10.7 13.9 2.2	7.2	7.6	−3.1	−3.2	None.
Indian chrome ore	1.5	5.5	21.6	-----	13.2	-----	-----	47.9	9.4	Cone 23 (1,580)	1,800	1,800	20–700 700–900 900–1,000 1,000–1,300	7.0 18.6 65.0 9.4	20–900 900–1,000 1,000–1,250 1,250–1,430	7.9 13.4 19.5 4.7	7.2	8.1	−3.1	−4.9	Very little, if any.
Turkish chrome ore	3.4	9.4	13.4	-----	15.6	-----	-----	40.0	16.8	1,400	1,555	-----	20–1,340	9.4	-----	-----	8.1	-----	−5.9	−13.6	Almost sheared.
Austrian magnesite	-----	3.9	-----	8.2	2.2	-----	2.5	-----	83.3	1,400	1,800	1,800	20–1,340	13.7	20–1,500	16.4	13.3	13.7	+2.3	−14.3	Great.
California magnesite	-----	4.4	-----	5.8	2.3	-----	3.0	-----	84.2	Cone 23 (1,580)	1,800	1,630	20–1,440	13.9	20–1,630	14.6	13.6	13.6	+.4	−2.3	Slight.
Electrically fused magnesite.	-----	-----	-----	-----	-----	-----	-----	-----	-----	Cone 23 (1,580)	1,800	1,800	20–1,355	14.0	20–1,800	13.8	13.4	13.4	+3.4	−3.9	Do.

Periclase brick, California.										As received and 1,000° C.	1,800	1,800	20–1,420	13.6	20–1,765	14.7	13.7	12.9		−4.6	Very little, if any.
Spinel											1,800	1,800	20–1,410	8.5	20–1,730	7.8	8.5	8.5	+1.0	−1.7	Do.
Fire clay brick "Q"[6]	.2	47.1		1.4	46.8	2.5	1.2		.5	As received	1,615	1,630	20–1,120	5.8	20–1,280	5.9	5.7	5.5	−.9	−5.0	Moderate.
Fire clay brick "F"[6]	.3	59.6		1.7	34.5	2.0	.5		.6		1,665	1,660	20–1,130	6.2	20–1,395	5.1	6.3	4.7	−.3	−5.6	Slight.
Fire clay "H-1"[6]	7.4	70.3		.9	19.5	2.0	.2		.03	1,155	1,575	1,585	20– 630 630–1,000 1,000–1,250	12.1 1.1 −3.3	20– 610 610–1,320 1,320–1,510	10.1 3.0 53.0			−.5	−14.4	Do.
										1,400	1,585		20– 610 610–1,020 1,020–1,425	11.4 2.1 −1.8							
Fire clay "M-1"[6]	13.7	44.6		1.1	38.2	2.2	.1		.1	1,155	1,660	1,600	20–1,120	4.9							
										1,400	1,670		20– 200 200–1,250	10.9 5.2	20–1,430	5.8	4.8	5.0	−.6	−10.8	Very little, if any.
Kentucky ball clay no. 4.	12.5	51.3		.8	31.2	1.5	.3			1,400	1,600		20– 200 200–1,400 1,400–1,490	10.8 5.2 47.2			6.1		−.1	−.3	Great (bloated).
Tennessee ball clay no. 5.	12.1	52.2		.8	31.2	1.1	.2			1,400	1,635	1,620	20–1,425	4.6	20–1,410	4.8	4.3	4.3	−.1	−.1	Slight (slightly bloated).
English ball clay "Dorset."	17.2	44.4		1.3	33.6	.8	.3		.5	1,400	1,650		20–1,430	4.6			4.4		−.5	−.3	Do.
Georgia kaolin[7]	13.7	45.3		.3	39.1	1.5	.1		.04	1,400	1,640	1,630	20– 210 210–1,335	14.0 5.4	20–1,570	4.7		4.4	−.9	−2.0	Very little (bloated).
English china clay[7]	12.4	47.0		1.0	37.7	.2	.2		.2	1,400	1,680	1,680	20–1,375	4.8	20–1,375	4.8	4.4	4.4	−.03	−.6	Do.
Firebrick "80 percent alumina."		15.0		1.9	80.5				.6	As received (cone 18–1485).	1,800	1,800	20–1,570	6.8	20–1,760	8.0	6.7	6.6	+.7	−3.9	None.
Corundum, artificial		1.9		.5	95.5		1.9			As received (cone 16–1425).	1,800	1,800	20–1,485	7.8	20–1,800	8.1	8.5	8.4	−.9	+.2	Do.
Diaspore											1,400	1,700	1,720	20–1,275	7.5	20–1,550	7.6	7.8	7.7	−.1	−17.4	Slight.
Bauxite (calcined)	.7	4.7		9.7	81.7	3.2					1,400	1,675	1,690	20–1,100	6.7	20–1,300	8.1	6.8	8.2	−2.3	−15.4	Great.
Mullite (Dumortierite).										As received cone 29½–1645).	1,670	1,730	20–1,410	5.2	20–1,530	5.1	5.2	5.2		−1.1	Very little, if any.
Mullite (Andalusite)										As received (cone 16–1450).	1,800	1,800	20–1,400 1,400–1,510 1,510–1,785	6.7 4.3 15.9	20–1,410 1,410–1,510 1,510–1,780	5.7 2.3 10.7	6.2	5.3		+.8	None (bloated).
Mullite (sintered)										As received	1,800	1,800	20–1,475 1,475–1,585 1,585–1,760	6.2 2.0 10.8	20–1,495 1,495–1,620 1,620–1,780	6.0 1.8 7.3	6.0	5.7	−.5	+.2	None.
Mullite (Indian cyanite).		36.2		.04	63.4	.7	.2			1,400	1,750	1,800	20–1,260	4.7	20–1,630	5.1	4.9	5.0			Slight.
Mullite (synthetic)										As received	1,750	1,735	20–1,430	5.5	20–1,600	5.3	5.4	5.0		−5.6	Do.

[6] These materials are referred to in Bureau of Standards Research Paper No. 114.
[7] Additional information relative to these materials may be found in Bureau of Standards Research Paper No. 410.

TABLE 1.—*Average coefficients of linear thermal expansion of refractories after different heat treatments*—Continued

Material	Chemical analyses									Original heat treatment	Maximum temperature reached in induction furnace		Linear thermal expansion in—						Total gain (+) or loss (−) after completion of tests, in —		Extent of deformation at end of tests
													Induction furnace				Resistance wire furnace				
													First test		Second test		Average coefficient of expansion between 20° and 1,000° C.—				
	Ignition loss	SiO_2	FeO	Fe_2O_3	Al_2O_3	TiO_2	CaO	Cr_2O_3	MgO		First test	Second test	Temperature range	Average coefficient of expansion	Temperature range	Average coefficient of expansion	Before first test in induction furnace	After first test in induction furnace	Weight	Length	
	Per-cent	*Per-cent*	*Per-cent*	*Per-cent*	*Per-cent*	*Per-cent*	*Per-cent*	*Per-cent*	*Per-cent*	°C.	°C.	°C.	°C.	$\times 10^{-6}$	°C.	$\times 10^{-6}$	$\times 10^{-6}$	$\times 10^{-6}$	*Per-cent*	*Per-cent*	
Zircon brick "A"										As received (1,700).	1,800	1,800	20–1,370	4.8	20– 900 900–1,200 1,200–1,615 1,615–1,715	5.0 −8.7 5.7 20.1	4.5	[1] 5.0	0	−5.6	Slight.
Zircon brick "B"										As received.	1,800	1,800	20–1,375	4.3	20– 900 900–1,140 1,140–1,315 1,315–1,725	5.7 −14.3 36.5 2.9	4.4	[1] 5.7	−.6	+.2	Do.
Zirconium silicate (98 percent zircon)										1,400	1,800	1,800	20–1,340	4.1	20– 930 930–1,225 1,225–1,655	4.6 −11.4 20.0	4.4	[1] 4.6	−.4	−10.1	Do.
Silicon carbide										1,400	1,700	1,690	20–1,525	4.9	20–1,470	4.5	5.2	4.3	------	1.1	Sheared.
Silica brick										As received.	1,670	1,670	20– 300 300–1,135 1,135–1,665	32.6 4.6 −1.1	20– 300 300–1,040 1,040–1,670	41.0 3.9 −3.3	------	------	−.3	−.04	None (very friable).
Insulating brick										As received.	1,330	------	20–1,330	4.2	----------	------	3.9	------	−.1	−.2	None.

[1] Average coefficient of expansion between 20° and 900° C.

The following generalizations may be made when comparing the different materials studied:

1. A comparison of the results obtained in oxidizing and reducing atmospheres showed that the expansions of the chrome ores were affected more by the reducing atmosphere than the other materials.
2. The magnesites showed the greatest total expansion of those materials which had nearly a uniform rate of expansion.
3. The expansion curves of the zircons in the second tests showed greater irregularities above 950° C. than the curves of the other materials. This was probably due to the decomposition of zirconium silicate into zirconium oxide and glass.
4. All materials showed some change in total expansion in the second test when compared with that obtained in the first test although in some instances the difference is small.
5. Nearly all the materials decreased in weight and length during the tests. The loss in weight was due to volatilization of one or more of the constituents. Such volatilized material condensed or sublimed in the upper tube of the set-up. In most cases this material was probably silica. Crystalline growths appeared on some of the specimens. At the end of the tests all chrome ores were covered with beads of metal, probably an alloy of iron and chromium.

2. PETROGRAPHIC ANALYSES[8]

Petrographic analyses were made on chips taken from the specimens of the materials before and after the various heat treatments in order to obtain information relative to the effect of the various heat treatments on their mineralogical constitution. The analyses follow:

AFRICAN CHROME SAND

As received.—Largely chromite. Grains mostly transparent. Index of refraction 2.07. Some hematite possibly present. Nonmagnetic.

Heated at 1,400° C.—Three major constituents present: (*a*) Red colored chromite, index 2.07, isotropic; (*b*) sharply delimited areas of opaque material in the chromite grains; (*c*) colorless, transparent grains, index slightly lower than 1.50.

Heated to 1,800° C.—Material has vitreous luster. Principal constituents present: (*a*) Chromite; (*b*) opaque material, less abundant than in previous samples; (*c*) interstitial material in spherulitic or needle-like forms, index about 1.65, intimately associated with an isotropic material of lower index, probably glass.

CUBAN CHROME ORE

As received.—Largely transparent chromite with some serpentine. Very little opaque material present.

Heated at 1,400° C.—Largely chromite with a few needle-like birefringent crystals.

Heated to 1,800° C.—Chromite changed very little. Many grains having the red color and high index of chromite show a slight double refraction, perhaps due to strain.

GRECIAN CHROME ORE

As received.—Largely brown transparent chromite with a small amount of serpentine and a few grains of opaque material.

Heated at 1,400° C.—Birefringent material, index higher than 1.70, and weak pleochroism, associated with chromite perhaps a pyroxene.

Heated to 1,800° C.—Chromite grains lighter in color. Opaque material present in distinct grains with sharp boundaries.

[8] Made by H. Insley.

FRIABLE AFRICAN CHROME ORE

As received.—Composed of (*a*) chromite, (*b*) much opaque material, (*c*) small aggregates of red colored particles having a high index and high birefringence (possibly hematite), (*d*) small amount of quartz.

Heated at 1,400° C.—Material not greatly different from that not heated.

Heated to 1,800° C.—Chromite grains lighter in color. Less opaque material present than originally. Occurs as distinct, rounded grains. Possibly some pyroxene and glass or cristobalite present.

RHODESIAN IMPERIAL CHROME ORE

As received and after heating at cone 23 (1,580° C.) and 1,800 °C.—None of the samples differ greatly. In addition to the chromite, a small amount of low index glass and opaque material, possibly hematite, present.

INDIAN CHROME ORE

As received.—Largely chromite, transparent and brown in thin pieces, and an opaque material.

Heated to cone 23 (1,580° C.).—Not greatly different from the "as received" material except the opaque grains are rounded and have sharp boundaries against the chromite. Needlelike inclusions in chromite may be rutile.

Heated to 1,800° C.—Chromite grains slightly lighter in color. Opaque grains not greatly changed. Crystalline grains of birefringent material, index about 1.70, have appeared in appreciable quantities.

TURKISH CHROME ORE

As received.—Largely deep red chromite grains and serpentine with a small amount of pyroxene.

Heated at 1,400° C.—Less opaque material. A spherulitic or fibrous crystalline material with a low birefringence and index of about 1.70, probably a pyroxene, was found to be intimately associated with and surrounded by a low index, isotropic material, probably glass.

Heated to 1,555° C.—Composed of: (*a*) Chromite usually brown in color, (*b*) high index almost opaque material which may be a spinel like hercynite, (*c*) birefringent grains (index 1.65–1.70) probably pyroxene, (*d*) lower index material, probably glass.

AUSTRIAN MAGNESITE

As received (calcined).—Material very heterogeneous. Isotropic material, periclase, index of refraction ranging from 1.735 to 1.76 composed approximately 85 percent of sample. The chief impurities are: (*a*) Forsterite, (*b*) aggregates of what is probably hematite, and (*c*) a small amount of low index material, probably glass.

Heated to 1,800° C.—Periclase grains large and rounded. Red, birefringent material (hematite) is almost absent. The grains of forsterite are large and very nearly pure $2MgO.SiO_2$.

CALIFORNIA MAGNESITE

As received (calcined).—Composed of: (*a*) More than 90 percent periclase, index 1.735, (*b*) forsterite as interstitial material.

Heated to cone 23 (1,580) and 1,800° C.—Periclase clear and colorless, either in rounded grains or faceted crystals. Forsterite crystals increased in size. Opaque material occurs as spherical inclusions in the periclase.

ELECTRICALLY FUSED MAGNESITE

As received, heated to cone 23 (1,580° C.) and 1,800° C.—Composed of: (*a*) Over 90 percent periclase, (*b*) less than 1 percent glass and, (*c*) forsterite. All constituents colorless. No noticeable change due to different heat treatments.

PERICLASE BRICK (CALIFORNIA)

As received.—Principally composed of periclase, small amounts of forsterite and probably glass, and a few scattered grains of what may be a spinel.

Heated to 1,800° C.—The size of the periclase grains and crystals of forsterite increased, otherwise little change from the "as received" material.

SPINEL BRICK

As received.—Composed of over 90 percent spinel (index 1.72). A small amount of glass and a crystalline birefractory material (probably clinoenstatite or forsterite) distributed along the boundaries of the spinel grains.

Heated to 1,800° C.—The spinel and glass grains increased in size and the birefractory material disappeared.

BRICK, FLINT CLAY, "BRAND Q"

As received.—Composed largely of glass and very small, poorly developed mullite crystals, with a few grains of quartz.

Heated to 1,630° C.—Mullite crystals increased in size, quartz dissolved. Apparently more glass present than mullite.

BRICK, SEMISILICEOUS, "BRAND F"

As received.—Composed principally of aggregates with a mean index of refraction of 1.56. These aggregates are probably glass or cristobalite and feebly developed needles of mullite. Some grains of quartz are visible.

Heated to 1,660° C.—Mullite needles well developed. Quartz completely disappeared. More glass (index 1.50) than mullite present.

FIRECLAY, HIGHLY SILICEOUS, "H-1"

Heated at 1,155° C.—Principally glass, quartz grains surrounded with cristobalite and poorly developed needles of mullite.

Heated to 1,585° C.—Not greatly different from preceding material.

FIRECLAY, M-1

Heated at 1,155° C.—Amorphous material (mean index 1.56) containing fibrous material with a lower index. Mullite not identifiable.

Heated to 1,670° C.—Small irregular needles of mullite and an interstitial material not identifiable.

KENTUCKY BALL CLAY

Raw.—Largely (*a*) platy clay mineral, often in vermicular growths, probably kaolinite; (*b*) quartz; (*c*) amorphous material (probably a clay mineral) with index about 1.55; (*d*) amorphous brown material; (*e*) a little rutile.

Heated at 1,400° C.—Largely poorly developed mullite needles embedded in a lower index matrix.

Heated to 1,600° C.—Principally mullite and glass.

TENNESSEE BALL CLAY

Raw.—Composition similar to that of the above Kentucky ball clay.

Heated at 1,400° C.—Wholly mullite and glass with apparently more glass than mullite.

Heated to 1,635° C.—Mullite crystals well developed with glass more abundant than mullite.

ENGLISH BALL CLAY

Raw.—Material extremely fine grained. Largely amorphous material and a platy clay mineral. Considerable organic matter, a little rutile, quartz, and muscovite also present.

Heated at 1,400° C.—A mass of poorly developed mullite crystals in a matrix of glass.

Heated at 1,650° C.—Considerably more glass than mullite present. Mullite grains show much evidence of solution.

GEORGIA KAOLIN

Raw.—Contains approximately 2 percent mica and less than 1 percent quartz. Remainder kaolinte.

Heated at 1,400° C.—Principally extremely small needles of mullite and an interstitial material.

Heated to 1,660° C.—Composed wholly of well developed crystals of mullite and glass.

ENGLISH CHINA CLAY

Raw.—Contains from 9 to 11 percent of muscovite, less than 1 percent of quartz, and less than 2 percent of feldspar. Remainder kaolinte.

Heated at 1,400° C.—Almost wholly well-developed needles of mullite and glass with the latter in preponderance.

Heated to 1,680° C.—The amount of glass increased, indicating the solution of the mullite.

FIREBRICK, 80 PERCENT ALUMINA

As received.—Largely corundum and mullite. A small amount of glass and a few grains high index, high birefringent material (rutile or zircon).

Heated to 1,800° C.—Mullite and corundum present in about equal proportions. A small amount of glass still present, but the high index material previously noted gone.

CORUNDUM, ARTIFICIAL

As received.—Largely corundum with small amounts of glass and a high index, high birefringent material (possibly rutile).

Heated to 1,800° C.—Not much change from the "as received" material.

DIASPORE

Raw.—Mainly diaspore with a very small amount of fine-grained clay mineral.

Heated at 1,400° C.—Almost wholly corundum and glass.

Heated to 1,720° C.—Corundum grains much larger. A small amount of mullite occurs as interstitial material associated with glass.

BAUXITE

Heated to 1,400° C.—Principally corundum, with lesser amounts of mullite, glass, and a compound of what is probably Fe_2O_3 and TiO_2.

Heated to 1,690° C.—Not greatly changed from preceding sample except that the size of the mullite crystals increased and the crystals of corundum show evidence of reaction with the fluxes present.

MULLITE (DUMORTIERITE)

Heated to 1,730° C.—Wholly mullite and glass, the latter composing 30 percent or more of the sample.

MULLITE (ANDALUSITE)

Heated to 1,800° C.—Mullite, corundum, and glass. The amount of corundum estimated at approximately 15 percent and the glass from 5 to 10 percent.

MULLITE (SINTERED)

Heated to 1,800° C.—Mullite, corundum, and glass. The amount of corundum estimated at approximately 25 percent and the glass between 15 and 20 percent.

MULLITE (INDIAN CYANITE)

Heated to 1,800° C.—Glass and corundum and well-developed crystals of mullite. The corundum present estimated at less than 15 percent.

MULLITE (SYNTHETIC)

Heated to 1,750° C.—Principally mullite, with very small percentages of corundum and glass.

ZIRCON BRICK A

As received.—Coarse-grained zircon with a small amount of glass.

Heated to 1,800° C.—Two phases present: (*a*) Aggregates of zirconium oxide, (*b*) brownish glass. The zirconium oxide crystals were identified by X-ray diffraction pattern.

ZIRCON BRICK B AND ZIRCONIUM SILICATE

Similar to zircon brick A.

SILICON CARBIDE

As received and heated to 1,715° C.—Wholly pure silicon carbide.

SILICA BRICK

As received.—Largely tridymite with a lesser amount of cristobalite. A few remnants of quartz grains observed as well as an interstitial material, present to the extent of approximately 5 percent.

Heated to 1,670° C.—Almost wholly cristobalite with a small amount of isotropic interstitial material (glass).

INSULATING BRICK

As received.—Only minute crystals of mullite embedded in a greater proportion of matrix material, probably glass.

Heated to 1,330° C.—No pronounced change.

VI. SUMMARY

With four exceptions linear thermal expension measurements were made of each of 36 refractory materials using the specimen throughout the following cycle: (1) Room temperature to 1,000° C. in an oxidizing atmosphere, (2) room temperature to some temperature above, 1,000° C. but not exceeding 1,800° C., in a reducing atmosphere, (3) room temperature to 1,000° C. in an oxidizing atmosphere, (4) room temperature to some temperature above 1,000° C. but not exceeding 1,800° C., in a reducing atmosphere. This procedure gave information relative to the effect on the expansion of the materials (1) when tested in an oxidizing or reducing atmosphere, and (2) when heated at a temperature higher than that which they received preliminary to the first test.

The petrographic analyses give information relative to the constitution of the materials before and after the several heat treatments.

It was noted that:

1. No apparent differences in expansion were obtained from room temperature to 1,000° C. when the materials were tested in either a reducing or oxidizing atmosphere except in the case of chrome ores which showed an exceptionally high expansion between 700° and 1,000° C. under reducing conditions.

2. The magnesites showed the greatest total expansion of the materials which had nearly a uniform rate of expansion.

3. The expansion curves of the zircons in the second tests showed greater irregularities above 950° C. than the curves of the other materials. This was probably due to the decomposition of zirconium silicate into zirconium oxide and glass.

4. All materials showed some changes in total expansion in the second test when compared with that obtained in the first test although in some instances the difference is small.

5. Nearly all of the materials decreased in weight and length during the tests. The loss in weight was due to the volatilization of one or more of the constituents. Such volatilized material condensed or sublimed in the upper tube of the set-up. In most cases this material was probably silica. Crystalline growths appeared on some of the specimens. At the end of the tests all chrome ores were covered with beads of metal, probably an alloy of iron and chromium.

WASHINGTON, January 12, 1933.

173145—33——3

RP563

FIRE TESTS OF COLUMNS PROTECTED WITH GYPSUM

By Nolan D. Mitchell

ABSTRACT

Fire tests of six building columns protected with gypsum have been made to supplement previous fire tests of columns similarly protected. These tests demonstrate the importance of some form of positive bond, such as steel cramps or ties, to hold unplastered block coverings in place. Block coverings with sanded gypsum plaster finish shrank less than the unplastered blocks and remained in place during the fire until the columns had failed. The plaster applied to block coverings increased the fire resistance in greater proportion than the ratio of the squares of resulting net thicknesses of covering outside of the steel.

CONTENTS

	Page
I. Introduction	737
II. Columns and protective coverings	738
1. Materials	738
2. Workmanship	738
3. Details of coverings	738
III. Method of testing	741
1. Testing equipment	741
2. Working loads, bearings, and restraint	741
IV. Results of fire tests	743
1. General results	743
2. Deformations	747
3. Fire effects on coverings	751
V. Summary and discussion	751
1. Comparison with results of previous tests	751
2. Fire effects on protective coverings	752
3. Anchorage of coverings	752
4. Effectiveness of plaster	752
5. Temperature at failure	753
6. Fire resistance of columns	753
VI. Acknowledgments	754

I. INTRODUCTION

The results of fire tests of six steel columns which had fire protective coverings of gypsum products are presented. One of the coverings was of monolithic construction, the others were built of blocks cut from gypsum partition tiles.

The information obtained supplements that derived from the tests of columns with gypsum block coverings included in the series of tests conducted jointly by the Associated Factory Mutual Fire Insurance Companies, the National Board of Fire Underwriters, and the Bureau of Standards, at Underwriters' Laboratories, Chicago, Ill., during the years 1917–18.[1] In those tests it was observed that

[1] Fire Tests of Building Columns, Underwriters' Laboratories, 1920, also published as B.S. Tech. Paper no. 184, 1921.

shrinkage of the unplastered blocks loosened the mortar until the metal ties imbedded in the horizontal mortar joints were no longer effective. As the fire progressed the blocks fell, exposing the steel, usually before its temperature exceeded 100° C. (212° F.).

In the present tests it was aimed to obtain more positive anchorage for the blocks and to determine the effect of plaster in decreasing the shrinkage from fire exposure and increasing the fire resistance of the protected column.

II. COLUMNS AND PROTECTIVE COVERINGS

1. MATERIALS

The six steel columns were fabricated from plates and angles in accordance with the details shown in figure 1. The tensile tests of the steel gave, yield point, 37,700 lb./in.^{2}; ultimate strength, 58,000 lbs./in.^{2}; and elongation, 32 percent in 8 inches.

The fibered gypsum concrete used in one test had a compressive strength of 760 lb./in.^{2} as tested in a 6 by 12 inch cylinder, the average of four 2-inch cubes was 790 lb./in.^{2}, and the average tensile strength of 3 standard briquettes was 180 lb./in.^{2}

The gypsum blocks used for the protective coverings in the other tests were cut from ordinary 2-inch solid and 3-inch hollow gypsum partition tiles having approximately 3 percent of wood fiber in the form of fine excelsior. These when tested for transverse breaking strength with a concentrated load at the center of a 28-inch span gave breaking loads of 230 and 420 pounds or moduli of rupture of 200 and 185 lb./in.^{2}, respectively, for the solid and hollow blocks. The modulus of rupture of the hollow blocks was computed on the gross section. Compressive strengths were determined on half-length blocks remaining from the transverse tests. The results for edge and end bearings, respectively, were for solid blocks, 920 and 810 lb./in.^{2}, and for hollow blocks, 760 and 770 lb./in.^{2} of net area.

The mortar used for setting the gypsum blocks had tensile and compressive strengths of 70 and 300 lb./in.^{2}, respectively. The sanded plaster as sampled during construction of the columns had tensile and compressive strengths of 50 and 670 lb./in.^{2}, respectively.

The gypsum plaster and the hydrated lime conformed with Federal specifications for the corresponding class of products and the hydrated lime also, except that 16 percent of the lime was retained on the no. 200 sieve where as 15 percent was the allowable limit.

2. WORKMANSHIP

The workmanship in the fabrication of the columns was in accordance with commercial practice. The construction of the coverings was superintended by a man having long experience in this class of work and the workmanship was of good commercial grade.

3. DETAILS OF COVERINGS

Details of the six coverings are given in table 1 and figures 2 and 3.

The gypsum concrete covering for column no. 1, composed of 7 parts gypsum cement, 1 part wood chips, and approximately 7 parts water, by weight, mixed to a semifluid consistency, was poured and puddled into the wooden form so as to flow through the wire mesh surrounding the column.

The mortar and plaster were proportioned by weight of dry materials in the ratio 1:3 gypsum plaster and sand. The amount of water used was varied slightly from batch to batch to compensate for conditions which cause variations in consistency or setting time, or both. The

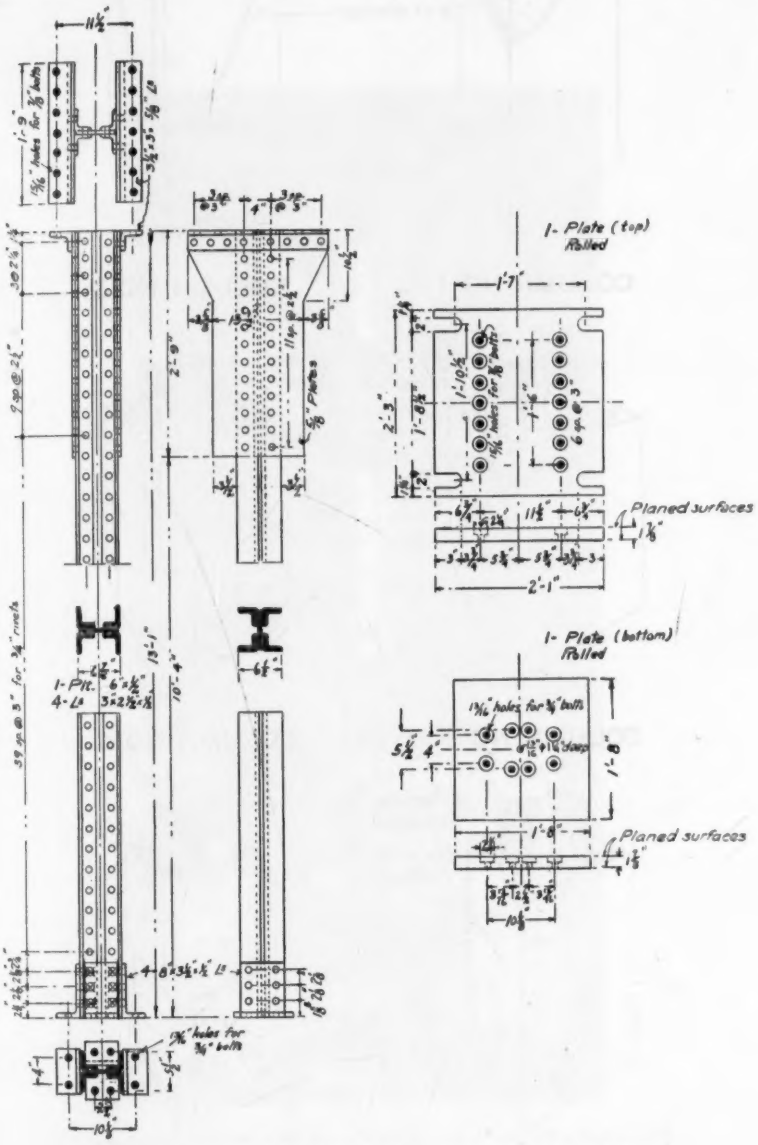

FIGURE 1.—*Details of test columns and bearing plates.*

plaster was applied by the double-up method and finished with lime and plaster of paris white coat.

The block coverings were dried from 1 to 2 weeks and the gypsum concrete for 1 month in the blast of a unit heater, with

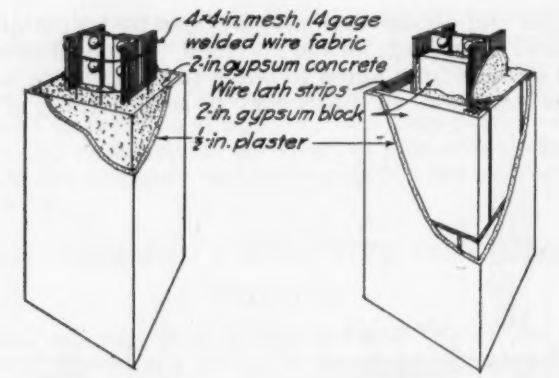

COLUMN NO. 1 COLUMN NO. 3

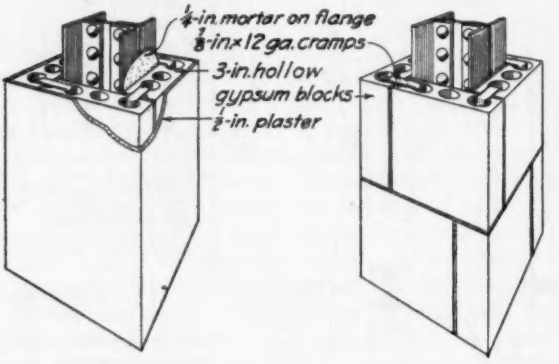

COLUMN NO. 2 COLUMN NO. 4

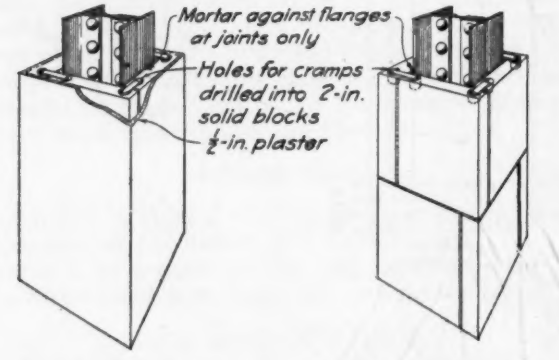

COLUMN NO. 5 COLUMN NO. 6

FIGURE 2.—*Details of column coverings.*

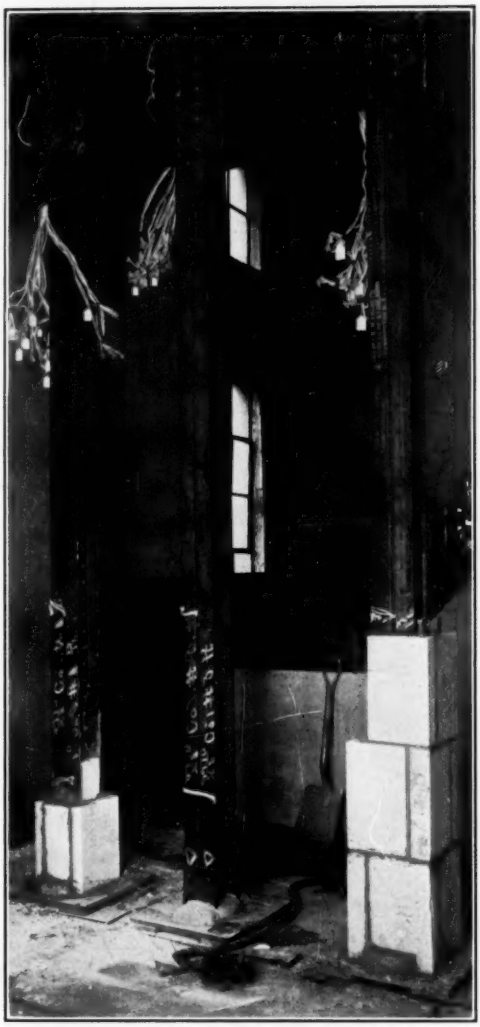

FIGURE 3.—*Columns nos. 3, 4, and 5 with block coverings started.*

temperatures ranging from 38° to 54° C. (100° to 130° F.) before the plaster was applied. Column no. 2. had the white-coat finish applied two days after the brown and scratch coats, but nos. 3 and 5 were dried for 2 weeks between the plastering and the application of the finish. The finished plaster on columns nos. 1, 2, 3, and 5 had seasoned 25, 25, 29, and 27 days, respectively, before being subjected to the fire test.

III. METHOD OF TESTING

1. TESTING EQUIPMENT

The tests were made in a gas-fired furnace which was equipped with a hydraulic jack for applying loads as shown in figure 4. The jack piston was raised by a hand pump and lowered by opening a needle valve, thus raising or lowering the movable furnace floor which rested on the spherical bearing block. Loads on the test columns corresponding to measured fluid pressures were determined by calibration of the system, including jack and connected fluid pressure scale.

The furnace was not designed for column tests and to accommodate a column of 10 feet 4 inches effective length an extension was built above the furnace roof slab. The temperatures at 12 locations in the furnace were indicated by chromel-alumel thermocouples, some protected by iron tubes and some by porcelain tubes. The temperature of the column at 10 points was indicated by iron-constantan thermocouples inserted into the steel column shaft.

The changes in length of the columns were obtained approximately by measuring the movements of the jack piston with micrometers and by observing the changes in elevation of the column heads through a telescope. As the furnace floor system was massive and had a protective covering of 5 inches of sand, gypsum, and fire bricks above the concrete, it can be assumed that the changes in length between the two observation points, which were 15 feet 6 inches apart, were mainly those of the steel column. No measurement of the lateral deflections of the columns was made.

2. WORKING LOADS, BEARINGS, AND RESTRAINT

The loadings (lb./in.^{2}) causing failure of the columns are shown in table 1. That for columns nos. 1 and 2 was about 14 percent in excess of allowable loads computed by the formula [2]

$$f = \frac{18{,}000}{1 + \frac{l^2}{18{,}000\, r^2}}$$

recommended by the American Institute of Steel Construction, and for columns nos. 3 to 6, inclusive, the excess was about 4 percent.

The average stresses imposed in these tests at the time of failure were for the first two columns 33 percent, and for the last four, 21 percent, more than would have been applied in the Chicago tests to columns of corresponding slenderness ratio.

The column was mounted in the furnace as shown in figure 4 with the top bolted and the bottom bearing plate bedded in quick-hardening

[2] In the formula f is the allowable stress, lb./in.^{2}, l, the effective length of the column, and r the least radius of gyration of the column section.

cement mortar. The condition of restraint of the columns during test was designed to be that of having the upper end fixed and the lower

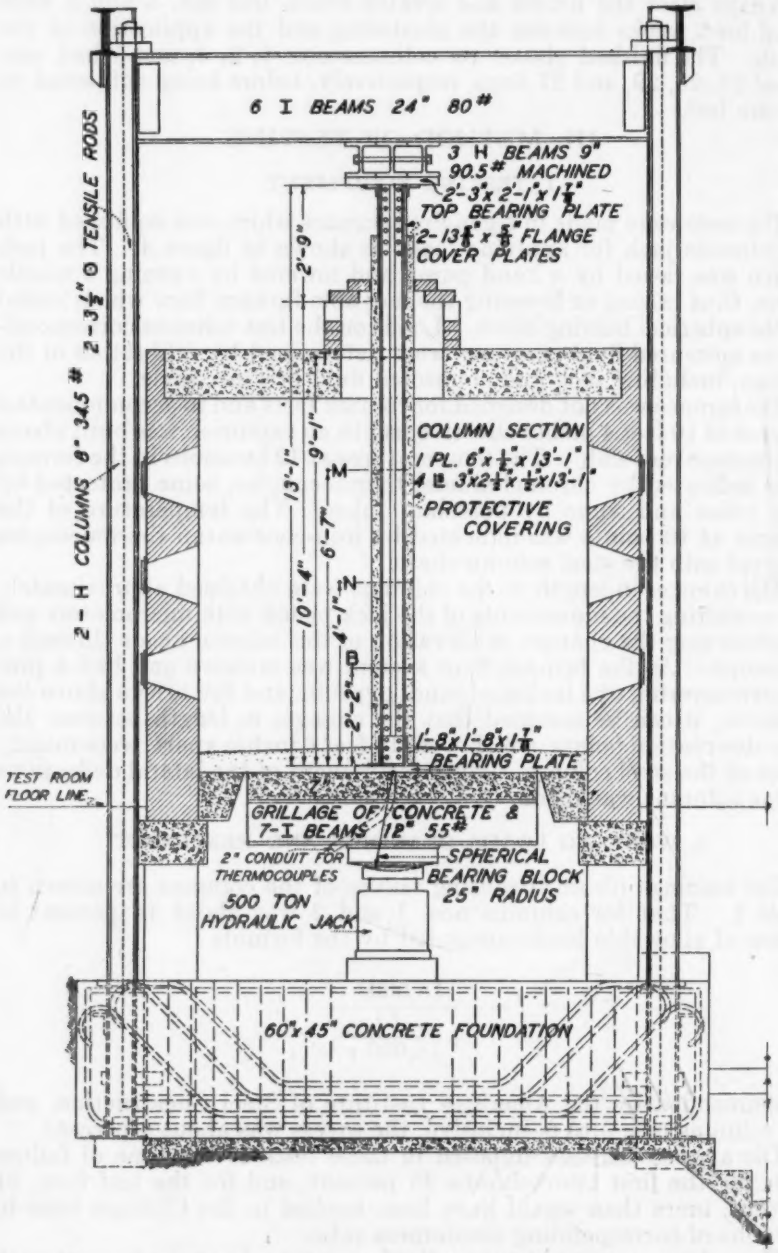

FIGURE 4.—*Furnace and loading equipment with column in place.*

end free except for friction at the spherical bearing and possible minor restraint at the edges of the movable floor section.

IV. RESULTS OF FIRE TESTS

1. GENERAL RESULTS

The results of the fire tests are summarized in table 1 and in table 2 results from the earlier series of fire tests of columns protected with

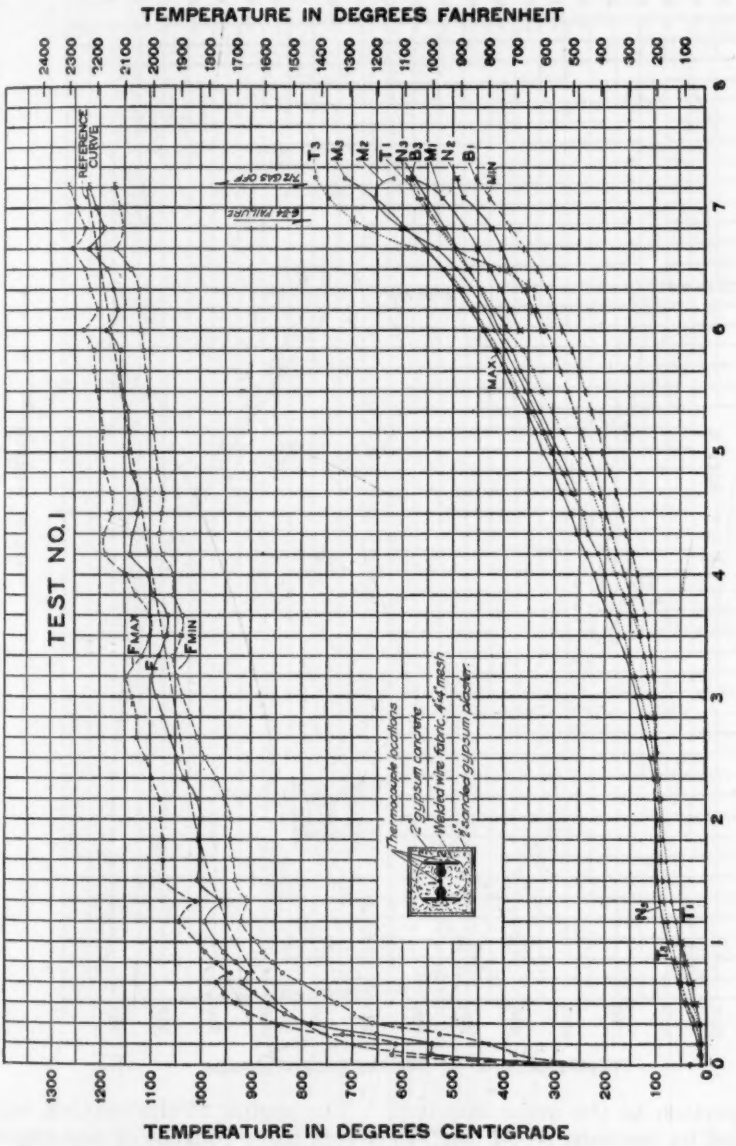

FIGURE 5.—*Temperature chart, test no. 1, column protected with 2-inch gypsum concrete and one half inch plaster.*

gypsum block coverings are given for comparison. The temperature charts, figures 5 to 8, inclusive, show temperatures of the furnace and at several points in the column steel. The locations of these points are shown in elevation in figure 4 by the letters *B*, *N*, *M*, and *T*, and

in plan by the numerals *1*, *2*, and *3*, on the detail sections (figs. 5 to 8). The temperature averages given in table 1 for the cross section were computed from the indications of the thermocouples weighted in

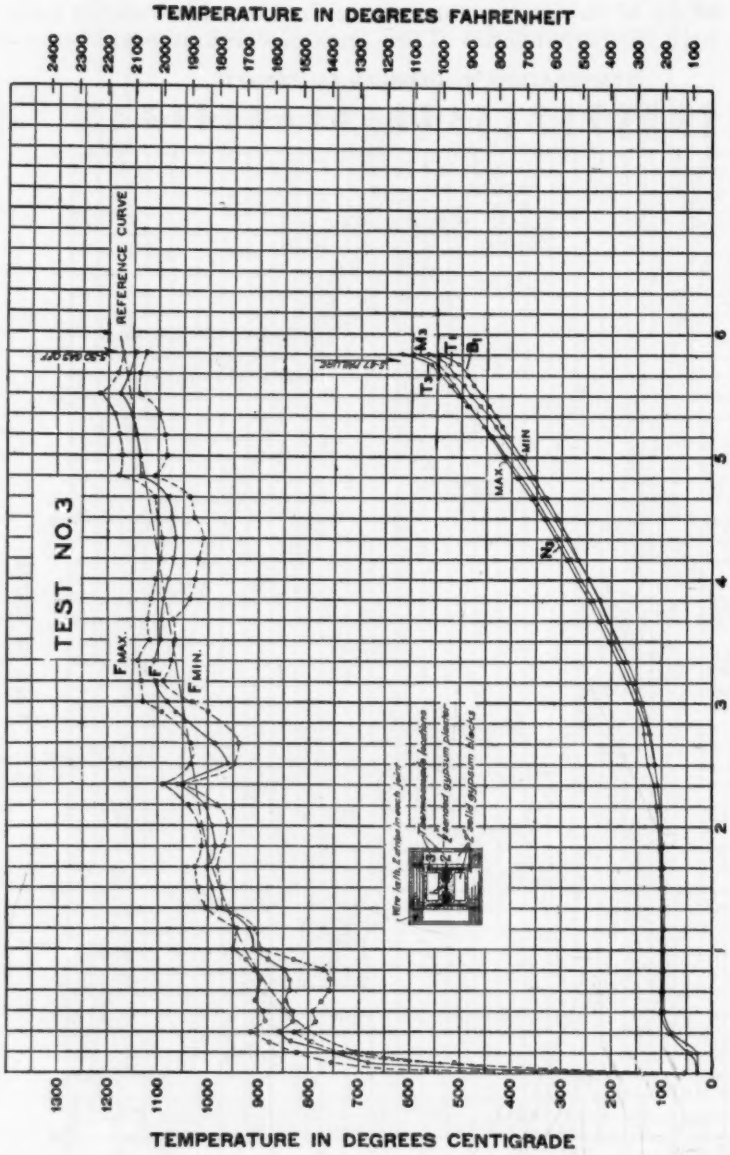

FIGURE 6.—*Temperature chart, test no. 3, column protected with 2-inch solid gypsum partition tile, filled solidly and plastered.*

proportion to the areas involved. The region of the column represented by sections *N*, *M*, and *T*, covers three fourths of the exposed length and comprises in each case the portion involved in the failure.

FIGURE 6.—*Temperature chart, test no. 3, column protected with 2-inch solid gypsum partition tile, filled solidly and plastered.*

TABLE 1.—*Fire resistance of columns with gypsum protective coverings*

[Tests conducted at the Bureau of Standards]

Column no.	Load [1]	Protective covering			Exposure, percent of standard	Period of expansion	Time to failure	Temperature at time of failure		
		Kind [2]	Thickness over flange of column, average	Net area of column and covering				Maximum indicated temperature in column flanges	Average at the hottest of 4 sections	Average for sections *N*, *M*, and *T*
	Lb./in.[2]		*Inches*	*Sq. inches*		*Hr. min.*	*Hr. min.*	*° C.*	*° C.*	*° C.*
1	14,100	Monolithic wood-fibered gypsum concrete, plastered	2½	130	100	6 30	6 54	700	620	554
2	14,100	Hollow gypsum block, plastered; no fill	[3] 2.9	123	100	5 00	5 10	[4]		
3	12,800	Solid gypsum block, plastered; filled	2.9	153	100	5 30	5 47	575	558	554
4	12,800	Hollow gypsum block; no fill; no plaster	[5] 2.2	94	101	2 52	2 52	558	546	514
5	12,800	Solid gypsum block, plastered; no fill	2½	107	100	4 05	4 21	574	565	543
6	12,800	Solid gypsum block; no fill; no plaster	2	84	103	2 32	2 33	587	559	508

[1] The allowable load computed by the American Institute of Steel Construction formula, based on an effective length of 124 inches and least radius of gyration of 1.36 inches (l/r=91.2) is 12,300 lbs./in.[2]

[2] See fig. 2 for details of construction.

[3] The gross thickness of covering of column no. 2 was 3¾ inches.

[4] The measurements of temperatures of column no. 2 were not reliable.

[5] The gross thickness of covering of column no. 4 was 3 inches.

TABLE 2.—*Fire resistance of columns with unplastered gypsum protective coverings*

[Tests conducted at Underwriters' Laboratories]

Column no.	Load [1]	Protective coverings			Exposure, percent of standard	Period of expansion	Time to failure
		Kind	Thickness over flange of column, average	Net area of column and covering			
	Lb./in.²		*Inches*	*Sq. inches*		*Hr. min.*	*Hr. min.*
64 [2]	11,750 (13,662)	4-inch solid gypsum block, corrugated wall ties in horizontal joints; fill of gypsum block and mortar.	4¾	303	104	4 32	4 43¼
65 [3]	12,670 (14,604)	2-inch solid gypsum block, corrugated wall ties in joints; fill of gypsum block and mortar	3	135	104	2 20	2 21½
66 [4]	14,270 (15,000)	2-inch solid gypsum block, wire lath strips in joints; fill of gypsum concrete [5]	3¼	240	101	2 32	2 36
67 [2]	11,750 (13,662)	4-inch solid gypsum block, wire lath strips in joints; fill of gypsum concrete [5]	4¾	303	101	5 01	5 31½
67A [2]	11,750 (13,662)	Same as no. 67	4¾	303	100	5 45	6 24½

[1] The allowable loads (lb./in. ²) computed by American Institute of Steel Construction formula are given in parentheses.
[2] Steel column, 8-inch H, 34.5 pounds; area 10.17 square inches; $l/r=75.6$.
[3] Steel column, two 6-inch channels, 8 pounds; two 8 by ¼ inch plates; area, 8.76 square inches; $l/r=64.7$.
[4] Steel column, two 9-inch channels, 13¼ pounds; area, 7.78 square inches; $l/r=44.0$.
[5] Concrete composed of 1 part gypsum cement, 1 part sand, and 4 parts broken gypsum block.

2. DEFORMATIONS

The average compressive deformation of three columns, including column, base plate, furnace floor, and bearing block, on applying the

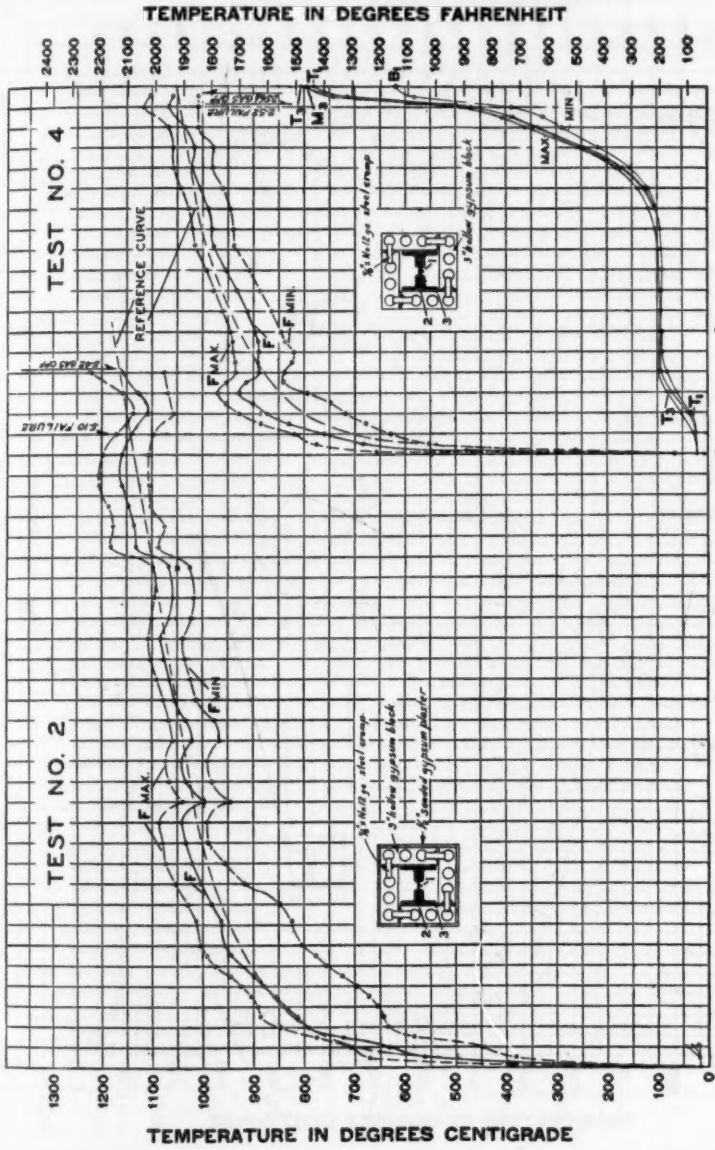

FIGURE 7.—*Temperature charts, tests nos. 2 and 4, columns protected with 3-inch gypsum partition tiles, no fill.*

load before test was 0.073 inch, approximately 60 percent of which was in the 124-inch effective length of the column, to judge from known stress-strain relations of steel. Changes in length of columns nos. 1, 2, and 3 during fire test, as determined by observation of movements

at the two gage points, located one on the lower bearing block and the other 6 inches from the upper bearing surface of the column, are shown by the curves in figure 9. A comparison of the expansion of column

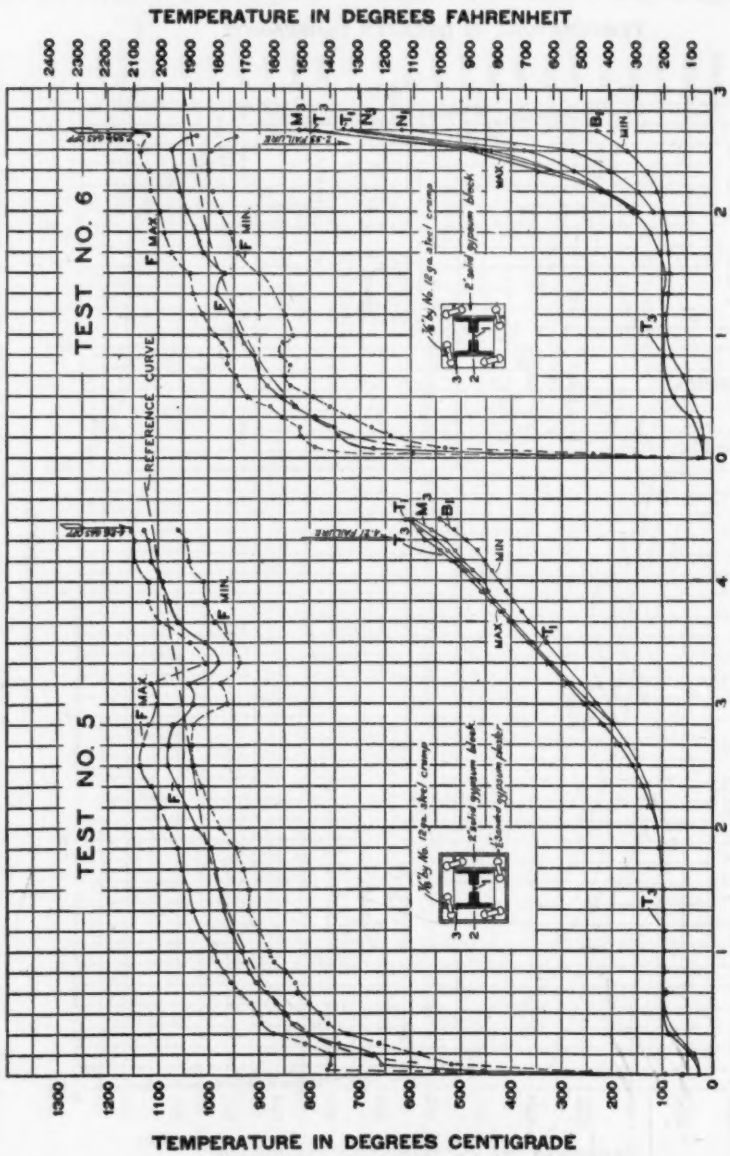

FIGURE 8.—*Temperature charts, tests nos. 5 and 6, columns protected with 2-inch solid gypsum partition tiles, no fill.*

no. 3 with steel of approximately the same quality expanding under load with rise of temperature is given by the curves in figure 10, in which the temperatures for the column are the averages computed

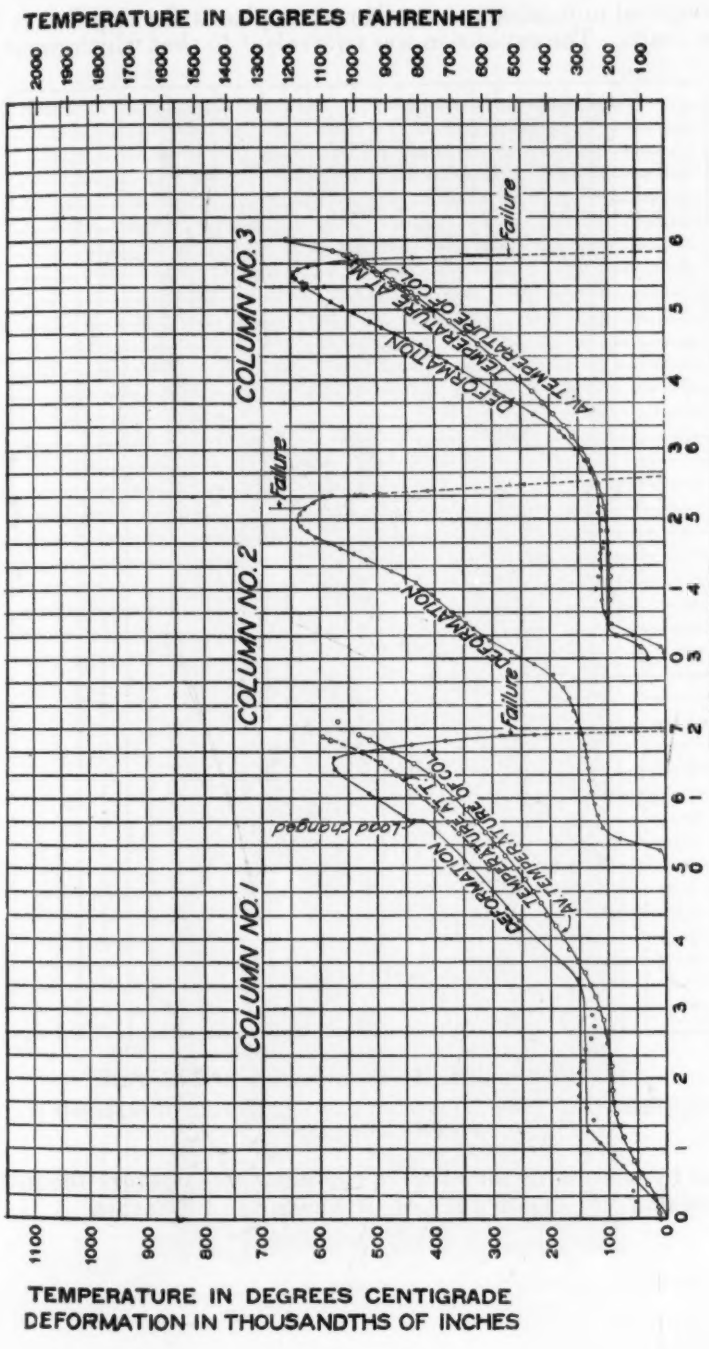

FIGURE 9.—*Average temperatures and measured deformations, tests nos. 1, 2, and 3.*

from weighted indications of the thermocouples at the 10 points in the column shaft. The expansion was equivalent to that which would be

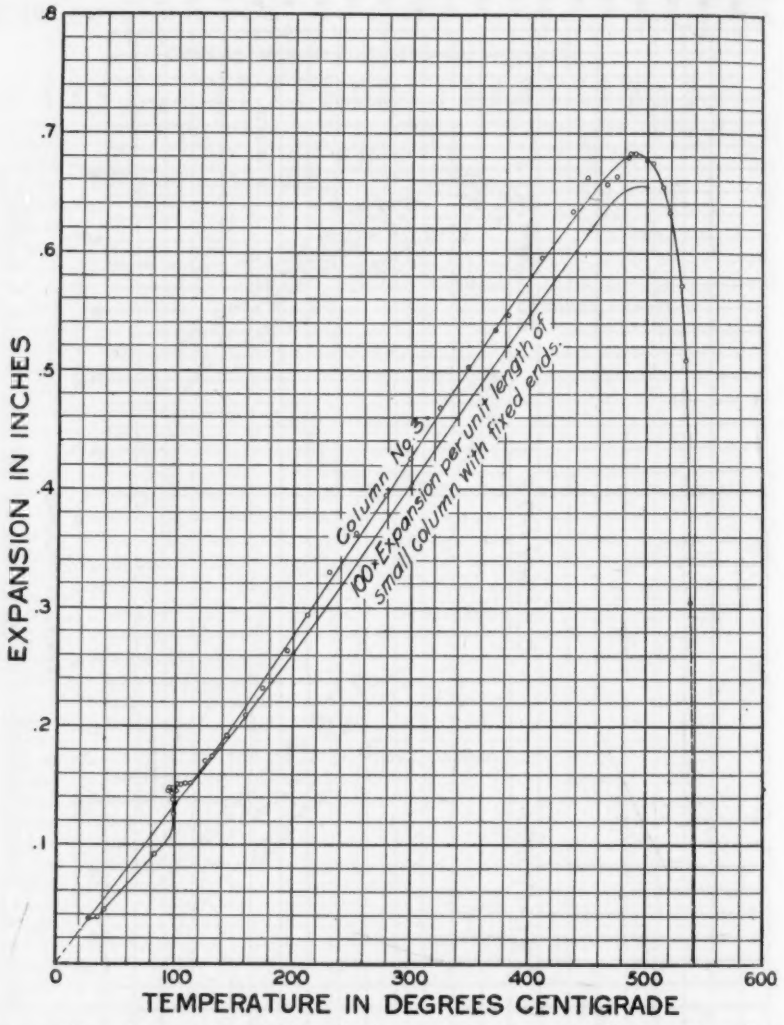

FIGURE 10.—*Measured expansion of column no. 3 compared with expansion of small loaded steel column.*

obtained by heating to the average measured temperature 105 inches of the column, the exposed length of which was 120 inches.

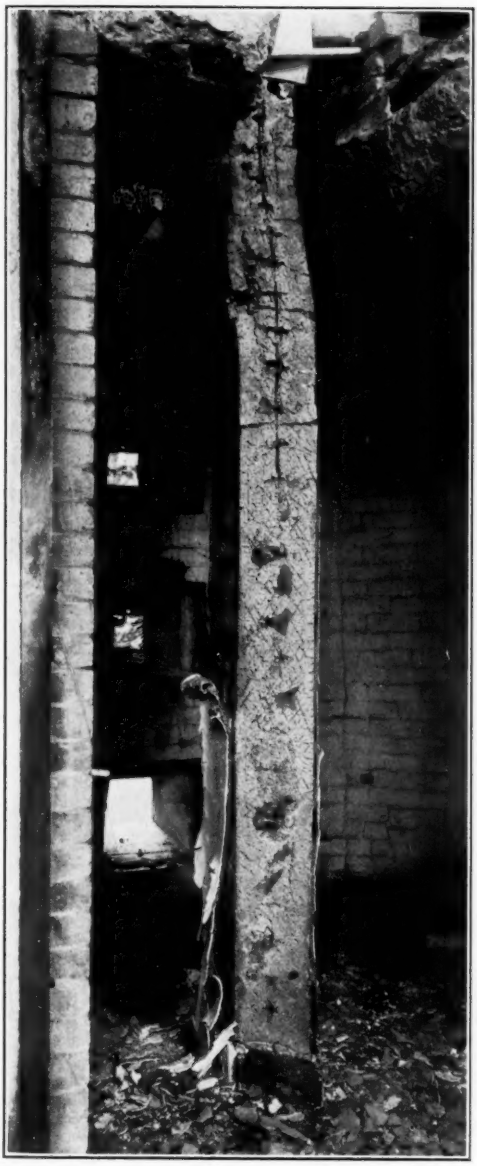

FIGURE 11.—*Column no. 1 after failure in fire test showing condition of fibered gypsum concrete after fire exposure.*

UNIV. OF MICH.

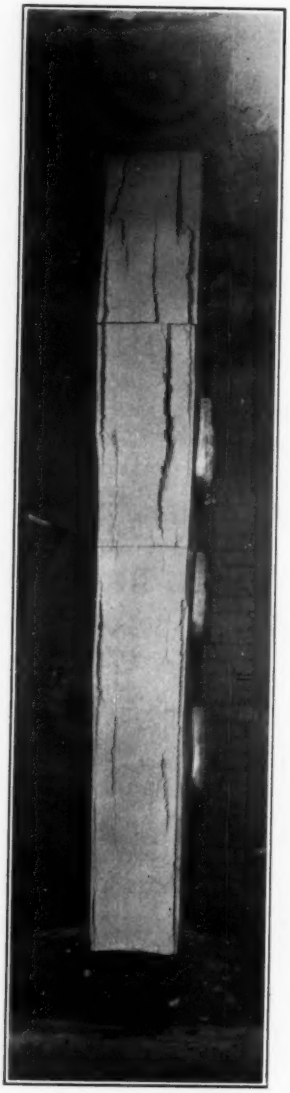

FIGURE 12.—*Column no. 5 after failure in fire test showing condition of covering after fire exposure.*

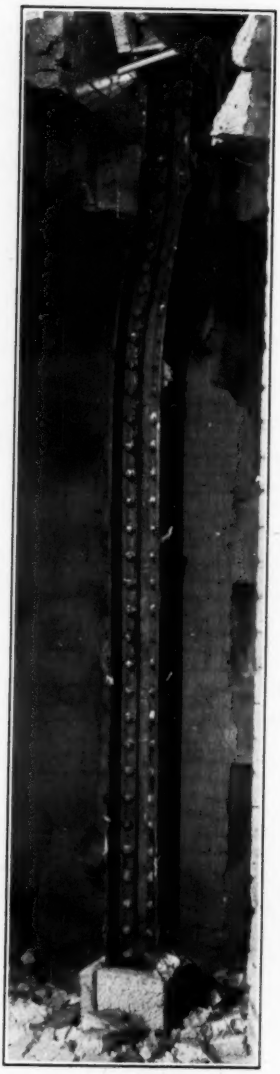

FIGURE 13.—*Column no. 6 after failure in fire test.*

3. FIRE EFFECTS ON COVERINGS

The photographs (figs. 11, 12, and 13) show columns nos. 1, 5, and 6 after completion of the fire tests, and are typical of all the tests. The plaster, it will be observed, has fallen from a large part of the exposed surface of column no. 1 but remained in place on the block covering of column no. 5.

Plaster began to fall from column no. 1 a few minutes after the fire was started. About two thirds of the plaster fell during the fire test, almost all of which took place during the first one and one half hours. The surface of the gypsum concrete, where exposed to the fire, was traversed by small cracks at intervals of 2 to 3 inches. One of these cracks, near where failure later occurred, had increased to five eighths inch in width at six and one half hours. The gypsum concrete shrank from 2 inches thickness to 1⅝ inches, but remained in place even after severe distortion of the column shaft.

Although cracks up to one half inch wide were observed in the covering of column no. 2 before failure, all plaster and blocks remained in place until removed after failure of the column. The plaster appeared to have prevented all serious cracking of the covering except opposite mortar joints. The other two plastered block-covered columns behaved in much the same manner as no. 2 except that the outside covering fell from column no. 3 after failure of the steel.

The block coverings of columns nos. 4 and 6, without plaster finish, began to crack early in the tests and before two hours had passed parts of the corners of some of the blocks had fallen, exposing ends of cramps. At 2 hours, 31 minutes, and 2 hours, 23 minutes, the steel of the respective columns was visible through cracks and from this time the cracks widened rapidly until at 2 hours, 49 minutes for no. 4 and 2 hours, 30 minutes for no. 6 some blocks fell. The column shafts, thus exposed, failed about 3 minutes later.

V. SUMMARY AND DISCUSSION

1. COMPARISON WITH RESULTS OF PREVIOUS TESTS

The fire tests of five steel columns with unplastered gypsum block coverings conducted in 1917–18,[3] give fire endurance limits from 2 hours 21½ minutes for a 2-inch block covering to 6 hours 24½ minutes maximum, for 4-inch block coverings. Failure in each test was hastened by exposure of the steel by falling of the blocks generally before the temperature of the steel exceeded 100° C. (212° F.). These columns had, in addition to the block coverings, layers of mortar three fourths inch or more in thickness between the steel and the blocks and all accessible reentrant parts were filled with gypsum blocks and mortar or a concrete made of gypsum cement and broken gypsum blocks.

The average stress from applied loads at failure in the recent tests, for columns having a slenderness ratio of 91.2, was 4 percent greater than for the columns of the previous tests, the slenderness ratios of which were 44.0, 64.7, and 75.6 for the three types employed. The degrees to which the performance was affected by the greater slenderness, greater stress, and different end restraint in the present tests

[3] See footnote 1, p. 737.

was not determined, but the effect of stress may be judged, at least qualitatively, from available information.[4]

2. FIRE EFFECTS ON PROTECTIVE COVERINGS

About two thirds of the plaster fell from column no. 1 during the test. This was the only column from which any considerable amount of plaster fell. The character of the concrete surface left by the oiled wooden form may have been a contributing cause.

The effect of fire on the block coverings without plaster was such as that described in the reports of previous tests [5 6 7]. Notwithstanding the iron cramps in the joints of these coverings, the blocks broke and fell before the temperature of the steel columns had reached a point high enough to cause failure of the steel. Even so, they remained in place relatively longer than the block coverings in the previous tests in which the metallic bond consisted of strips of wire lath or corrugated wall ties in the mortar of the horizontal joints. The plastered block coverings, on the other hand, remained in place throughout the test. The shrinkage and cracking of the sanded gypsum plaster was not as decided as that of the exposed surfaces of the unplastered gypsum blocks. Only a few cracks opened enough to be considered as particularly serious and there was no noticeable warping of the blocks during the test. After the failure of column no. 3, the covering fell, but neither of the other plastered coverings fell.

3. ANCHORAGE OF COVERINGS

The tests have clearly indicated that gypsum block coverings without plaster must have some means of positive anchorage to hold the units in place if they are to develop the full protection that can be given by the material. The cramps made of band iron and pushed down into holes to link adjacent blocks of the same course together served to hold the blocks in place for two and one-half hours or more, but did not enable the covering to develop its full fire protective properties. None of the block coverings with plaster finish fell from place before the fire endurance limit of the column had been reached irrespective of method of anchorage used. The collapse of the covering of column no. 3 when the column bent indicates that the anchorage of wire cloth strips in the horizontal joints was less effective than the cramps which held the coverings of columns nos. 2 and 5 in place through the period of failure of the column and the subsequent cooling.

4. EFFECTIVENESS OF PLASTER

Sanded gypsum plaster with the usual lime and plaster of paris white coat when applied over gypsum block coverings is apparently at least as effective as an equal thickness of block. Although the heat conductivity of the plaster may be greater than that of the block, its shrinkage under fire is less, and cracks do not open up to the same extent as when the blocks are exposed directly to the fire. The plaster also prevented the decided shrinkage and warping of the blocks

[4] S. H. Ingberg and P. D. Sale, Compressive Strength and Deformation of Structural Steel and Cast Iron Shapes at Temperatures up to 950° C. (1,742° F.) Proc. Am. Soc. Test. Materials, vol. 26, pt. 2, 1926.
[5] See footnote 1, p. 737.
[6] Hull, W. A., A Comparison of the Heat Insulating Properties of Some of the Materials used in Fire Resistive Construction. B.S. Tech. Paper No. 130, 1919.
[7] Hull, W. A., and Ingberg, S. H., Fire Resistance of Concrete Columns. B.S. Tech. Paper No. 272, 1925.

such as was experienced in fire tests of columns with unplastered block coverings.

5. TEMPERATURE AT FAILURE

The temperatures given in table 1, although the highest observed or the greatest average, were not necessarily the highest prevailing at the time of failure. However, for those columns on which the coverings remained in place it is improbable that the temperatures greatly exceeded those given.

Column no. 1 failed at higher local temperature than those tested later in spite of a greater applied load. The gypsum concrete covering may have augmented its load-carrying capacity by increasing its stability as a column and carrying at failure a minor portion of the load.

Columns nos. 3 to 6, inclusive, failed when the temperature of the cross section giving the highest average reached 546° to 565° C. (1,015° to 1,049° F.), or an average of 557° C. (1,035° F.) for the four. While the temperature at this section was, no doubt, a large factor in the cause of failure, it is believed that the maximum temperature and the general temperature over the region of failure were also significant.

6. FIRE RESISTANCE OF COLUMNS

Among the factors affecting the fire resistance of steel building columns are the size and slenderness of the columns, the intensity of loading, and the kind and thickness of protective covering. The slenderness ratio of all the columns in the recent tests was the same, but greater loads were applied to columns nos. 1 and 2 than the others. The principal variations in protection for the columns were in the manner of applying and anchoring the covering materials and in the thickness of the covering.

The tests were too few for the determination of the values of the various factors, but a consistent relation has been found for the fire tests on the basis of the thickness of covering and the method of its application and bonding. This relation is expressed by the formula, $t=c(d^2+b)$, in which t is the time to failure, c, a factor varying with the units of measurement employed and with the form and composition of the covering material and its method of application, d, the average net thickness of the covering material outside of the flange of the column shaft and b, a quantity depending on the size and properties of the column and its loading, also upon the effects of air spaces surrounding the steel or of fill in the reentrant spaces in the column shaft, and possibly other factors.

The test results have been plotted in figure 14 with average net thickness of covering on column flange and time to failure as coordinates. The relation for columns covered with gypsum blocks held in place by cramps or wire mesh ties, and plastered with one-half inch of sanded gypsum plaster is given by the formula, $t=35(d^2+1)$, where t is the time to failure in minutes and d is the average net thickness of covering over the column flange in inches. It is shown by curve A. This formula applies to results found in the tests with this type of covering for thicknesses from 2½ to 3 inches.

The time to failure in the tests of columns similarly protected, but without plaster finish, was 85 percent of that computed by the formula and is shown as curve B.

Similarly the time to failure in the earlier tests (table 2) as shown by curve *C*, was 40 percent of that computed by the formula. The time to failure for the 4¾-inch thickness of covering has been taken as the average of the three tests.

Only one test (no. 1) was made with gypsum concrete protection which contained about 35 percent by volume of wood shavings, or

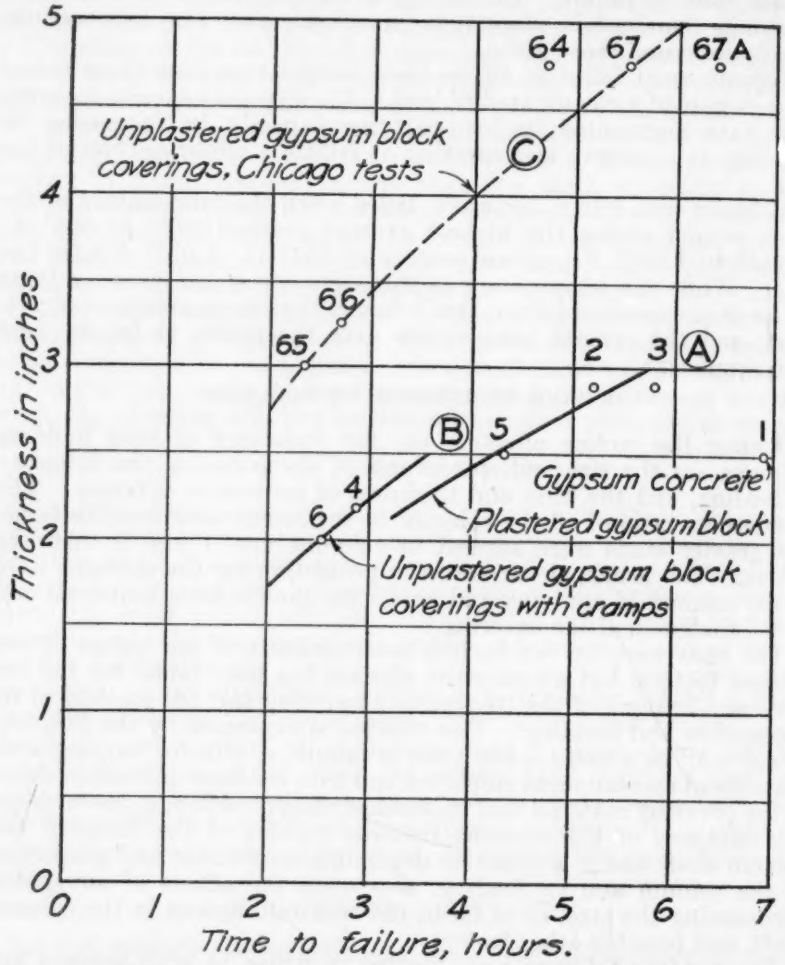

FIGURE 14.—*Relation of thickness of covering to time of failure of columns in fire tests.*

12½ percent of the dry mixture by weight. A considerable portion of the plaster finish fell off the 2-inch covering during the first part of the test, but, even so, a fire resistance of nearly 7 hours was developed. The principal differences between the covering of this column and those with solidly filled block coverings were its greater proportion of wood shavings, monolithic construction, and a well distributed reinforcement, but which of these or other factors contributed to its greater fire resistance is not known.

A summary of fire-resistance periods for small columns, unprotected and protected with gypsum coverings as derived from tests, together with data suitable for reference in designing fire-resistive buildings is given in table 3. A study of this summary will show striking advantages to be derived from the use of cramps or plaster with block coverings and still greater advantage from the use of the gypsum materials in reinforced monolithic coverings.

TABLE 3.—*Summary of ultimate fire resistance periods of steel columns with gypsum coverings*

Kind of covering	Surface finish	Thickness outside of column flange	Metal bond in horizontal joints	Internal construction	Minimum net area of column and covering	Ultimate fire resistance period
		Inches			*Square inches*	*Hours*
None		0		Bare column	13	¼
2-inch solid block	None	3	Corrugated wall ties.	Solid fill of gypsum block and mortar.	130	2¼
Do	do	3¼	Strips of wire lath.	Solid fill of gypsum concrete.	130	2½
4-inch solid block	do	4¾	Corrugated wall ties.	Filled with hollow block and mortar.	240	4½
Do	do	4¾	Strips of wire lath.	Filled with concrete of broken block and mortar.	240	6
2-inch solid block	do	2	Cramps	Air space surrounding steel. No fill.	85	2½
3-inch hollow block	do	[1] 2.2	do	do	95	2¾
2-inch solid block	Plaster	2½	do	do	105	4¼
3-inch hollow block	do	[1] 2.9	do	¼-inch of mortar on flange. No fill.	120	5
2-inch solid block	do	3	Strips of wire lath.	Solid fill of gypsum block and mortar.	150	5¾
			Reinforcement			
2-inch fibered gypsum concrete.	do	2½	4 by 4 inch mesh wire fabric.	Monolithic poured covering.	130	7

[1] Net average thickness outside column flange.

VI. ACKNOWLEDGMENTS

Acknowledgment is made to H. J. Schweim, chief engineer of the Gypsum Association, who arranged for the tests and to S. H. Ingberg, chief of the fire resistance section of the Bureau of Standards, who planned and supervised them. The author expresses appreciation for the assistance given by P. D. Sale and other members of the fire resistance section.

WASHINGTON, March 1, 1933.

THE INFRARED ARC SPECTRA OF MANGANESE AND RHENIUM

By William F. Meggers

ABSTRACT

New types of photographic plates sensitive to infrared radiation are employed to explore the long-wave portions of manganese and rhenium arc spectra from 7,200 to 11,000 A. The sources were metallic manganese in a copper arc and metallic rhenium in a silver arc. The spectrograms were made with large concave grating spectrographs, the first half of the range being investigated with a threefold increase in dispersion and resolution. Many new lines have been recorded in each spectrum and these in turn have disclosed new spectral terms or atomic energy levels. Lines in both spectra exhibit hyperfine structure.

CONTENTS

	Page
I. Introduction	757
II. Apparatus and methods	758
III. Results	759
1. Manganese	759
2. Rhenium	766

I. INTRODUCTION

Metallic manganese was first isolated in 1774 and for 151 years remained the only known metal with a maximum valence of 7. Nearly a century after its discovery, Mendeléeff predicted, on the basis of a periodic arrangement of the elements, that 2 homologues of manganese should exist. These hypothetical elements were referred to as eka-manganese and dwi-manganese, or more recently as atomic numbers 43 and 75, until they were finally captured in 1925 by Noddack and Tacke,[1] and renamed masurium and rhenium, respectively. At the present time the amount of concentrated masurium is probably still too small for the study of its optical spectra, so that manganese and rhenium are the only metals of Group VII available for spectroscopic study.

Although the spectra of manganese have been under investigation since 1864, they are still far from being in a satisfactory state, especially at their extremes. The longer wave portion of the manganese arc spectrum was investigated by Kiess and Meggers [2] in 1920 with dicyanin sensitized emulsions but even with 5-hour exposure only four lines beyond 9,000 A were detected.

The first extensive description and analysis of the rhenium arc spectrum was published by Meggers [3] in 1931, but the observations

[1] W. Noddack and I. Tacke, Naturwissenschaften, vol. 13, p. 567, 1925.
[2] C. C. Kiess and W. F. Meggers, B.S. Sci. Pap., vol. 16 (S372), p. 51, 1920.
[3] W. F. Meggers, B.S. Jour. Research, vol. 6 (RP322), p. 1027, 1931. See also W. Meidinger, Zeitschr. f. Phys., vol. 68, p. 331, 1931; H. Schober, Wiener Ber. IIa, vol. 140, pp. 79 and 629, 1931; vol. 141, p. 601, 1932; vol. 142, p. 35, 1933.

did not extend beyond 8,798 A in the infrared. The long-wave limit of these observations was imposed in part by the scarcity of rhenium, but mainly by the relatively low infrared sensitivity of the best photographic materials then at hand.

During the past year new types of photographic plates sensitive to infrared radiation have become available. These improved materials now permit the use of increased dispersion in the range formerly studied, and what is still more important they advance the long-wave limit of spectrographic observations to 11,000 A, or even beyond. Such superior photographic emulsions have recently been employed in a study of the arc spectra of manganese and rhenium, and the results form the contents of this paper. These observations constitute improved and extended descriptions of the characteristic emission spectra, and analyses of the new data give additional information as to the spectral and atomic structure of systems with 7 valence electrons.

II. APPARATUS AND METHODS

The spectra here described were obtained by dispersing and photographing the light from electric arcs at atmospheric pressure, the arcs being operated on a d.c. circuit with applied potential of 220 volts and current of 6 to 8 amperes.

Metallic manganese of high purity was fused on copper rods and thus used for the production of the manganese arc spectrum. The manganese, kindly supplied by Dr. F. M. Walters, Jr., was prepared in the Bureau of Metallurgical Research, Carnegie Institute of Technology. In the spectral range examined only one impurity line (Mg 8,806 A) was detected.

My former study of rhenium spectra (RP322) was executed with part of a gram of pure potassium perrhenate which was still very scarce early in 1930. However, in this same year, relatively large quantities of rhenium salts and metal were uncovered as a by-product of certain chemical industries [4] and pure metallic rhenium in larger quantity became available for the first time. A sample of metallic rhenium from Die Vereinigte Chemische Fabriken zu Leopoldshall, Germany, was used in the present investigation. This metal was in the form of fine powder or sponge, and when a small portion of it was fused on silver electrodes in the electric arc, it served very satisfactorily in producing an intense spectrum. The only impurities detected in the infrared range were two lines belonging to potassium (7,664 and 7,699 A), two characteristic of sodium (8,183 and 8,194 A); and three due to ionized calcium (8,498, 8,542, and 8,662 A).

The spectrograms were made with concave gratings of 21.7 feet radius of curvature, the gratings being mounted so as to give stigmatic slit images in the manner described elsewhere.[5] Two different gratings were used, one having 20,000 lines per inch and the other 7,500 lines per inch. The former covered the interval 7,200 to 9,000 A with a scale of 3.5 A/mm, while observations with the latter extended from 8,600 to 11,000 A with an average scale of 10.2 A/mm.

Several new types of photographic plates for spectrography developed by the Research Laboratory of the Eastman Kodak Co. were

[4] W. Feit, Zeitschr. Angew. Chem., vol. 43, p. 459, 1930.
[5] W. F. Meggers and Keivin Burns, B.S.Sci. Papers, vol. 18 (S441), p. 185, 1922.

described about a year ago.[6] Since that time still further improvements have been made by combining special types of emulsions with new photosensitizing dyes, so that the entire range of visible spectrum and an equal range of adjacent infrared is now easily recorded on commercial plates. From among various new types of plates now available three were chosen for the work in hand; they are identified as types I-R, I-P, and I-Q. The maximum sensitivities of these 3 plates occur at about 8,100, 8,600, and 9,700 A, respectively, but the 3 bands extend sufficiently to cover the entire range from 7,000 A to 12,000 A. Each plate just before use was hypersensitized in a dilute ammonia bath, and immediately after exposure was developed in Eastman X-ray developer at about 16° C.

The extraordinary sensitiveness of the R and P sensitized plates has permitted the use of a larger dispersion to 9,000 A than had ever been applied to these spectra before and the increased scale and resolution have revealed some new facts in addition to yielding improved wave lengths. Exposures of 10 to 30 minutes duration were made in the first-order spectrum, but the longer time always resulted in a severe over exposure in the region of maximum sensitiveness. In several such cases it was necessary to diminish the dense blackness of the spectrograms by chemical reduction until they became transparent enough for measurement.

Wave lengths of the infrared manganese and rhenium lines were derived from measurements relative to international standards in the iron arc spectrum which was recorded in the second order of the grating on each spectrogram. The adopted standards were doubled in value to serve as effective standards in the infrared. Each line was measured 4 or more times on 2 or more spectrograms. The probable error in wave length of a sharp line in the first range is estimated at about ± 0.01 A, but the uncertainty may be several times as large for the remainder.

III. RESULTS

1. MANGANESE (Mn, *Z*-25)

Kayser[7] has summarized all the spectroscopic data on manganese up to the year 1910, at which time the wave-length measurements did not extend beyond 6,022 A in the orange. A few years later the arc spectrum of manganese was remeasured on the international scale by Fuchs[8] who published a table of wave lengths extending from 2,289.93 to 7,069.855 A. In 1920 Kiess and Meggers[9] published a list of lines beginning at about the middle of the visible spectrum and running out into the near infrared. Relatively small dispersion and a low scale of intensities were used and it now appears that the last real line in this list has a wave length of 9,243 A. The long wave arc spectrum of manganese was investigated radiometrically by Randall and Barker[10] who found 20 lines in the interval 11,378 to 17,608 A. Furnace spectra of manganese were studied by King[11] in the range 2,795 to 8,200 A, but no lines were found beyond 6,500 A.

[6] C. E. K. Mees, J. Opt. Soc. Am., vol. 22, p. 204, 1932.
[7] H. Kayser, Handbuch der Spectroscopie, vol. 5, pp. 726–771, S. Hirzel, Leipzig, 1910.
[8] H. Fuchs, Zeitschr.f.w.Phot., vol. 14, pp. 239–248, 263–280, 1914.
[9] C. C. Kiess and W. F. Meggers, B.S.Sci.Papers, vol. 16 (S.372), p. 51, 1920.
[10] H. M. Randall and E. F. Barker, Astrophys.J., vol. 49, p. 57, 1919.
[11] A. S. King, Astrophys.J., vol. 53, p. 133, 1921.

Study of the atomic spectrum of manganese in the infrared is seriously handicapped by a molecular spectrum when the arc is operated at ordinary atmospheric pressure. Bands presumably due to oxides of manganese pervade the whole range of infrared which can be photographed and tend to obscure atomic lines of low intensity. Unfortunately the band heads are inconspicuous but the rotation structure of overlapping bands is so prominent and entangled that it is impossible to distinguish faint atomic lines from the background of fine lines due to bands. Consequently in the list presented below, many of the weaker lines may belong to bands and some true atomic lines may have been omitted. It will be worth while to reinvestigate this range of the manganese spectrum with a source in which the molecular spectrum is suppressed.

In spite of the troublesome presence of bands on my spectrograms, this investigation of the atmospheric arc spectrum of manganese has revealed some interesting features of the atomic spectrum and has led to some corrections and extensions of the spectral structure analysis.

The arc spectrum of manganese has played an important role in the development of a theoretical interpretation of complex spectra. Two series of triplets were recognized in this spectrum by Kayser and Runge [12] nearly 40 years ago, but no further progress was made until 1922 when Catalán [13] extended the analysis and drew attention to the existence of the certain groups of lines which he called multiplets. Up to this time only singlets, doublets, and triplets had been recognized in spectra, but now it appeared that spectral terms of higher multiplicity must also occur. This was indeed found to be the case and the discovery of quartet, quintet, sextet, etc., terms in other complex spectra soon led to a general interpretation of all atomic spectra.[14] The correlation of Zeeman effects with multiplet structure [15] showed that the two sets of threefold terms found in manganese in reality belonged to sextet and octet systems and thus removed an apparent violation of the alternation law. Manganese multiplets resulting from quartet terms were first pointed out by Russell [16] and some additions to these were published by McLennan and McLay,[17] who also gave the first comprehensive list of term values for the Mn I spectrum. This term table was copied by Bacher and Goudsmit [18] in a recent compilation of atomic energy states with modern notation added.

The main features of the infrared spectrum of manganese can be stated as follows: The most prominent group of lines in the investigated range is the y^6P°–b^6D multiplet lying between 8,670.92 and 8,740. 93 A. Each of the nine lines in this multiplet is now shown to be complex with hyperfine structure. The occurrence of hyperfine structure among manganese lines was first mentioned by Janicki [19] who also recognized the structures to be of the type since called "flag patterns" in which both intensities and intervals of components decrease in one direction. Hyperfine structure in neutral manganese

[12] H. Kayser and C. Runge, Abh.Berl.Akad.; 1894.
[13] M. A. Catalán, Phil.Trans., vol. 223, pp. 127–173, 1922.
[14] H. Hund, Linienspektren und Periodisches System der Elemente, Julius Springer, Berlin, 1927.
[15] E. Back and A. Landé, Zeemaneffekt und Multiplettstruktur der Spektrallinien, Julius Springer, Berlin, 1925.
[16] H. N. Russell, Astrophys.J., vol. 61, p. 223, 1925.
[17] J. C. McLennan and A. B. McLay, Trans.Roy. Soc. Canada, III, vol. 20, p. 15, 1926.
[18] R. F. Bacher and S. Goudsmit, Atomic Energy States, McGraw Hill Book Co., 1932.
[19] L. Janicki, Ann.d.Phys. (4), vol. 29, p. 833; 1909.

was further investigated by White and Ritschl,[20] who showed that this structure was determined primarily by the coupling between the $4s$ electron and the atomic nucleus. This $4s$ electron is present in both terms producing the $y^6P°$–b^6D multiplet, so that the complexity of the lines could have been predicted. Although the structures are not resolved in my grating spectrograms they are clearly of the flag-pattern type with a maximum spread of components of about 0.5 A.

Another prominent group of long-wave manganese lines is the $z^4F°$–b^4D multiplet ranging from 7,680.22 to 7,821.25 A. Superposed on this group is another one, $z^6F°$–c^6D, part of the latter term having been found by Russell [21] in his search for series in this spectrum. On account of the hazy character of the lines and rapid decline of intensity with quantum numbers, the weakest level $c^6D_{1/2}$ cannot be established with certainty. Combinations of the strongest level $c^6D_{4½}$ point to a correction which is necessary in the $z^6F°$ term. The level $z^6F_{5½}=16{,}624.24$ appears to have been derived on the assumption that a line at 3,806.866 A represents the combination $a^6D_{4½}$–$z^6F°_{5½}$, but the neighboring line at 3,806.724 A is the proper one so that $z^6F°_{5½}=16{,}623.30$.

McLennan and McLay [22] proposed a new ^6P term with levels at 6,668.12, 6,626.07, and 6,604.68, but were suspicious of it because the level separations violated the interval rule, and combinations with a^6D violated the intensity rule. The correct values for these levels are now found to be those given in table 1 for $v^6P°$.

The only remaining group of strong lines occurs between 9,084.27 and 9,243.29 A. It has been interpreted as the combination a^4F–$z^4D°$, thus establishing a new metastable term of the Mn I spectrum, and most likely arising from the $3d^7$ configuration.

My results for the Mn I spectrum are presented in tables 1 and 2. Table 1 lists the new terms which have been identified, the values being relative to the normal state $a^6S=59{,}937.47$.

TABLE 1.—*Energy levels of the manganese atom*

Symbol	J	Term value	Level separation
a^4F	4½	24,998.91	
	3½	24,896.20	102.71
	2½	24,822.66	73.54
	1½	24,772.57	50.09
$z^4F°$	5½	16,623.30	
$v^6P°$	3½	6,676.05	30.06
	2½	6,645.99	19.84
	1½	6,626.15	
c^6D	4½	3,748.01	166.76
	3½	3,581.25	134.5
	2½	3,446.7	77.2
	1½	3,369.5	97.0?
	½	3,271.5?	
^4P?	2½	3,475.46	

In table 2, estimated relative intensities, measured wave lengths, corresponding wave numbers in vacuum, and term combinations for the lines are shown in successive columns. Symbols accompanying

[20] H. E. White and R. Ritschl, Phys.Rev., vol. 35, p. 1146, 1930.
[21] H. N. Russell, Astrophys.J., vol. 66, p. 287, 1927.
[22] J. C. McLennan and A. B. McLay, Proc.Roy.Soc. Canada, III, vol. 20, p. 22, 1926.

the intensities have significance as follows: c = complex with hyperfine structure, h = hazy, H = very hazy, l = shaded to longer waves, v = shaded to violet, n = band head, p = part of band structure.

TABLE 2.—*Infrared arc spectrum of manganese*

Intensity	λ_{air} I.A.	ν_{vac} cm^{-1}	Level combination
2H	10, 622. 5	9, 411. 4	
2p?	10, 561. 0	9, 466. 2	
2p?	10, 537. 8	9, 487. 05	
2p?	10, 456. 6	9, 560. 7	$y^4P^2_{2½}$–$^4P_{2½}$?
3	10, 436. 7	9, 578. 95	
3h	10, 316. 0	9, 691. 0	$x^6P^1_{1½}$–$d^6D_{2½}$
4h	10, 300. 5	9, 705. 6	
8h	10, 212. 34	9, 789. 39	$x^6P^2_{2½}$–$d^6D_{3½}$
2	10, 102. 44	9, 895. 89	
20h	10, 052. 9	9, 944. 66	$x^6P^3_{3½}$–$d^6D_{4½}$
5h	10, 045. 04	9, 952. 44	$x^6P^3_{3½}$–$d^6D_{3½}$
3p?	9, 822. 68	10, 177. 74	
5p?	9, 761. 57	10, 241. 45	
5p?	9, 753. 24	10, 250. 20	
2p?	9, 727. 38	10, 277. 44	
2p?	9, 719. 17	10, 286. 13	
3p?	9, 706. 24	10, 299. 83	
2p?	9, 703. 56	10, 302. 67	
15	9, 686. 3	10, 321. 0	
15	9, 684. 9	10, 322. 5	$y^4P^1_{1½}$–$b^4D_{1½}$
40	9, 676. 50	10, 331. 49	$y^4P^1_{1½}$–$b^4D_{2½}$
4p?	9, 633. 02	10, 378. 12	$z^4D^1_{1½}$–$^4P_{2½}$?
6p?	9, 631. 02	10, 380. 27	
3p?	9, 628. 96	10, 382. 49	
3p?	9, 626. 10	10, 385. 58	
3p?	9, 624. 04	10, 387. 80	
100h	9, 608. 56	10, 404. 54	$y^4P^2_{2½}$–$b^4D_{3½}$
5h	9, 606. 71	10, 406. 54	$z^4D^1_{1½}$–$c^6D_{2½}$ $y^4P^2_{½}$ –$b^4D_{½}$
3p?	9, 598. 7	10, 415. 2	$z^4D^2_{2½}$–$c^6D_{3½}$
10h	9, 584. 0	10, 431. 2	
20h	9, 550. 80	10, 467. 46	$y^4P^1_{1½}$–$b^4D_{1½}$
10h	9, 542. 14	10, 476. 96	
5h	9, 535. 72	10, 484. 01	$z^4D^1_{1½}$–$c^6D_{1½}$
8h	9, 502. 12	10, 521. 08	$z^4D^3_{3½}$–$^4P_{2½}$?
4h	9, 476. 57	10, 549. 45	$z^4D^3_{3½}$–$c^6D_{2½}$
2p?	9, 474. 9	10, 551. 3	$y^4P^1_{1½}$–$b^4D_{½}$
40	9, 444. 90	10, 584. 82	$y^4P^2_{2½}$–$b^4D_{2½}$
30h	9, 429. 58	10, 602. 02	$z^4D^3_{3½}$–$c^6D_{3½}$
10h	9, 412. 78	10, 620. 94	
4h	9, 408. 38	10, 625. 91	
40h	9, 336. 47	10, 707. 75	$z^4D^3_{3½}$–$^4P_{2½}$?
20h	9, 331. 90	10, 712. 99	$a^4F_{3½}$–$z^4D^3_{3½}$
5	9, 325. 16	10, 720. 74	$y^4P^3_{3½}$–$b^4D_{1½}$
4h	9, 323. 76	10, 722. 35	
150	9, 243. 29	10, 815. 69	$a^4F_{4½}$–$z^4D^3_{3½}$

TABLE 2.—*Infrared arc spectrum of manganese*—Continued

Intensity	λ_{air} I.A.	ν_{vac} cm^{-1}	Level combination
4	9, 240. 81	10, 818. 60	
10	9, 234. 40	10, 826. 11	$a^4F_{3½}$–$z^4D^o_{2½}$
3p?	9, 220. 36	10, 842. 59	
100	9, 172. 09	10, 899. 66	$a^4F_{3½}$–$z^4D^o_{2½}$
2p?	9, 164. 77	10, 908. 36	
5	9, 155. 85	10, 918. 98	$a^4F_{1½}$–$z^4D^o_{1½}$
2p?	9, 128. 97	10, 951. 14	
2	9, 125. 0	10, 955. 9	
50	9, 114. 02	10, 969. 10	$a^4F_{2½}$–$zD^o_{1½}$
3hn?	9, 101. 2	10, 984. 6	
30	9, 084. 29	11, 005. 00	$a^4F_{1½}$–$z^4D^o_{½}$
2	9, 066. 50	11, 026. 59	
4h	9, 021. 80	11, 081. 22	
3dp?	8, 953. 2	11, 166. 1	
2	8, 932. 96	11, 191. 43	
60h	8, 929. 72	11, 195. 49	$x^6P^o_{3½}$–$c^6D_{4½}$
15h	8, 926. 06	11, 200. 08	$x^6P^o_{2½}$–$c^6D_{3½}$
2p?	8, 901. 0	11, 231. 6	$x^6P^o_{1½}$–$c^6D_{2½}$
4	8, 895. 36	11, 238. 72	
2h	8, 859. 08	11, 284. 76	
3h	8, 842. 48	11, 305. 94	$x^6P^o_{2½}$–$^4P_{2½}$?
2p?	8, 834. 70	11, 315. 90	
3	8, 827. 83	11, 324. 70	
4h	8, 820. 26	11, 334. 43	$x^6P^o_{3½}$–$c^6D_{2½}$
3h	8, 798. 66	11, 362. 25	$x^6P^o_{3½}$–$c^6D_{3½}$
6h	8, 796. 83	11, 364. 61	$z^4D^o_{2½}$–$b^4D_{3½}$
5h	8, 767. 96	11, 402. 03	$z^4D^o_{1½}$–$b^4D_{2½}$
1, 000cw	8, 740. 93	11, 437. 29	$y^6P^o_{3½}$–$b^6D_{4½}$
300c	8, 737. 32	11, 442. 02	$y^6P^o_{3½}$–$b^6D_{3½}$
30c	8, 734. 60	11, 445. 58	$y^6P^o_{3½}$–$b^6D_{2½}$
2h	8, 729. 80	11, 451. 87	$z^4D^o_{½}$–$b^4D_{1½}$
2h	8, 717. 29	11, 468. 31	$x^6P^o_{3½}$–$^4P_{2½}$?
10	8, 710. 21	11, 477. 63	
500cw	8, 703. 76	11, 486. 14	$y^6P^o_{2½}$–$b^6D_{3½}$
300c	8, 701. 05	11, 489. 71	$y^6P^o_{2½}$–$b^6D_{2½}$
100c	8, 699. 13	11, 492. 25	$y^6P^o_{2½}$–$b^6D_{1½}$
2h	8, 680. 24	11, 517. 26	$z^6F^o_{3½}$–$d^6D_{3½}$
200c	8, 673. 97	11, 525. 58	$y^6P^o_{1½}$–$b^6D_{2½}$
300c	8, 672. 06	11, 528. 12	$y^6P^o_{1½}$–$b^6D_{1½}$
200c	8, 670. 92	11, 529. 64	$y^6P^o_{1½}$–$b^6D_{½}$
2h	8, 666. 3	11, 535. 8	$z^4D_{½}$–$b^4D_{½}$
2h	8, 664. 6	11, 538. 0	$z^4D^o_{1½}$–$b^4D_{1½}$
10h	8, 659. 38	11, 545. 00	$z^4D^o_{2½}$–$b^4D_{2½}$
40h	8, 654. 63	11, 551. 34	$z^4D^o_{3½}$–$b^4D_{3½}$
5	8, 603. 03	11, 620. 62	
2H	8, 602. 1	11, 621. 9	$z^4D^o_{1½}$–$b^4D_{½}$
5H	8, 600. 34	11, 624. 26	$z^6F^o_{3½}$–$d^6D_{4½}$
8h	8, 558. 63	11, 680. 91	$z^4D^o_{3½}$–$b^4D_{1½}$
10h	8, 521. 57	11, 731. 71	$z^4D^o_{3½}$–$b^4D_{2½}$
1H	8, 506. 0	11, 753. 2	$z^4F^o_{1½}$–$c^6D_{1½}$

TABLE 2.—*Infrared arc spectrum of manganese*—Continued

Intensity	λ_{air} I.A.	ν_{vac} cm^{-1}	Level combination
3	8, 481. 70	11, 786. 85	
1H	8, 476. 3	11, 794. 4	$z^4F^2_{2½}$–$c^6D_{2½}$
20Hv	8, 431. 20	11, 857. 45	$b^6S_{2½}$–$v^6P^3_{3½}$
2H	8, 421. 12	11, 871. 65	$z^4F^3_{3½}$–$c^6D_{1½}$
15Hv	8, 409. 88	11, 887. 51	$b^6S_{2½}$–$v^6P^2_{2½}$
10Hv	8, 395. 87	11, 907. 35	$b^6S_{2½}$–$v^6P^1_{1½}$
40	8, 380. 77	11, 928. 80	
4h	8, 373. 93	11, 938. 54	
2H	8, 353. 79	11, 967. 33	$z^4F^3_{3½}$–$c^6D_{2½}$
2	8, 344. 80	11, 980. 22	
5Hl	8, 304. 42	12, 038. 48	
4h	8, 284. 48	12, 067. 45	$z^4F^4_{4½}$–$c^6D_{3½}$
5h	8, 251. 64	12, 115. 48	
1	8, 237. 87	12, 135. 73	
1	8, 234. 43	12, 140. 80	$a^4D_{2½}$–$y^6P°_{½}$
2	8, 229. 99	12, 147. 35	
40hl	8, 212. 43	12, 173. 32	
2	8, 210. 16	12, 176. 69	$a^4D_{2½}$–$y^6P^2_{2½}$
2	8, 204. 50	12, 185. 09	
1	8, 194. 06	12, 200. 61	
2	8, 148. 78	12, 268. 41	
2	8, 119. 36	12, 312. 86	
3	8, 110. 51	12, 326. 30	
2	8, 105. 89	12, 333. 32	
3	8, 079. 46	12, 373. 67	
8	8, 043. 37	12, 429. 18	$a^4D_{3½}$–$y^6P^2_{2½}$
5	8, 032. 54	12, 445. 94	
2	8, 026. 23	12, 455. 73	
1h	8, 021. 69	12, 462. 78	
4	7, 948. 10	12, 578. 17	
25	7, 942. 91	12, 586. 39	
2	7, 938. 52	12, 593. 35	
4	7, 928. 45	12, 609. 34	$z^4F^2_{2½}$–$b^4D_{3½}$
2	7, 920. 44	12, 622. 10	
1h	7, 916. 31	12, 628. 68	
2	7, 911. 68	12, 636. 07	
1h	7, 889. 61	12, 671. 42	$z^4F^1_{1½}$–$b^4D_{2½}$
2	7, 871. 58	12, 700. 44	
2	7, 865. 36	12, 710. 48	
3	7, 854. 24	12, 728. 48	
10h	7, 834. 34	12, 760. 81	$z^6F^4_{4½}$–$c^6D_{4½}$ $z^6F^3_{3½}$–$c^6D_{3½}$
20	7, 821. 25	12, 782. 17	$z^4F^4_{4½}$–$b^4D_{3½}$
30h	7, 816. 61	12, 789. 76	$z^4F^3_{3½}$–$b^4D_{2½}$
8hd?	7, 806. 00	12, 807. 14	$z^4F^2_{2½}$–$b^4D_{1½}$
15h	7, 790. 82	12, 832. 10	$z^6F^3_{3½}$–$c^6D_{3½}$
1h	7, 782. 2	12, 846. 3	$z^6F^1_{1½}$–$c^6D_{2½}$
250hl	7, 764. 72	12, 875. 23	$z^6F^5_{5½}$–$c^6D_{4½}$
20Hl	7, 755. 15	12, 891. 11	$z^4F^1_{1½}$–$b^4D_{½}$
9Hl	7, 752. 67	12, 895. 24	$z^6F^2_{2½}$–$c^6D_{2½}$
4	7, 737. 16	12, 921. 09	

TABLE 2.—*Infrared arc spectrum of manganese*—Continued

Intensity	λ_{air} I.A.	ν_{vac} cm^{-1}	Level combination
2h	7, 735. 77	12, 923. 41	$z^6F^0_{1\frac{1}{2}}$–$c^6D_{1\frac{1}{2}}$
50h	7, 734. 43	12, 925. 66	$z^4F^0_{2\frac{1}{2}}$–$b^4D_{1\frac{1}{2}}$
150hl	7, 733. 24	12, 927. 64	$z^6F^0_{4\frac{1}{2}}$–$c^6D_{3\frac{1}{2}}$
3h	7, 727. 07	12, 937. 96	
3	7, 721. 57	12, 947. 18	
100h	7, 712. 42	12, 962. 54	$z^4F^0_{3\frac{1}{2}}$–$b^4D_{2\frac{1}{2}}$
40Hl	7, 709. 98	12, 966. 64	$z^6F^0_{3\frac{1}{2}}$–$c^6D_{2\frac{1}{2}}$
10Hl	7, 706. 52	12, 972. 46	$z^6F^0_{2\frac{1}{2}}$–$c^6D_{1\frac{1}{2}}$
200	7, 680. 22	13, 016. 88	$z^4F^0_{4\frac{1}{2}}$–$b^4D_{3\frac{1}{2}}$
2Hl	7, 677. 46	13, 021. 56	$z^6F^0_{1\frac{1}{2}}$–$c^6D_{\frac{1}{2}}$?
10h	7, 670. 42	13, 033. 51	
6h	7, 667. 89	13, 037. 81	
5Hl	7, 655. 99	13, 058. 08	$a^8S_{3\frac{1}{2}}$–$a^8P^0_{2\frac{1}{2}}$
7Hl	7, 651. 62	13, 065. 54	$a^8S_{3\frac{1}{2}}$–$a^8P^0_{3\frac{1}{2}}$
10Hl	7, 646. 02	13, 075. 11	$a^8S_{3\frac{1}{2}}$–$a^8P^0_{1\frac{1}{2}}$
3	7, 603. 43	13, 148. 34	
1	7, 552. 10	13, 237. 71	
2	7, 534. 82	13, 268. 07	
4	7, 515. 74	13, 301. 65	
3h	7, 483. 42	13, 359. 20	
1h	7, 477. 38	13, 370. 00	
1?	7, 453. 88	13, 412. 14	
1?	7, 453. 56	13, 412. 72	
1	7, 446. 16	13, 426. 05	
3	7, 443. 50	13, 430. 85	
1	7, 432. 27	13, 451. 14	
2	7, 425. 52	13, 463. 37	
3	7, 415. 81	13, 481. 00	
2	7, 404. 24	13, 502. 06	
1	7, 391. 73	13, 524. 91	
1	7, 390. 04	13, 528. 01	
1	7, 387. 15	13, 533. 30	
2	7, 383. 52	13, 539. 95	
1	7, 380. 88	13, 544. 79	
1	7, 378. 98	13, 548. 28	
3	7, 376. 85	13, 552. 19	
3	7, 342. 80	13, 615. 04	
400l	7, 326. 51	13, 645. 31	$y^6P^0_{3\frac{1}{2}}$–a^6D?
1	7, 322. 22	13, 653. 30	
2	7, 304. 98	13, 685. 53	
300l	7, 302. 89	13, 689. 44	$y^6P^0_{2\frac{1}{2}}$–a^6D?
3h	7, 301. 38	13, 692. 27	
1	7, 293. 85	13, 706. 41	
2h	7, 287. 10	13, 719. 10	
250l	7, 283. 80	13, 725. 32	$y^6P^0_{1\frac{1}{2}}$–a^6D?
2	7, 275. 66	13, 740. 68	
15	7, 247. 82	13, 793. 46	
3	7, 239. 61	13, 809. 10	

2. RHENIUM (Re, Z=75)

My former description of the rhenium arc spectrum [23] gave the wave lengths and estimated intensities of about 2,000 lines from 2,500.59 in the ultraviolet to 8,797.6 in the infrared. About 500 of these lines, including nearly all of the stronger ones, were classified as combinations of established energy levels but relatively few of these levels could be grouped into identifiable terms. Now in this supplementary investigation of the the infrared, the data between 7,200 A and the former limit have been greatly improved and lines have been recorded out 10,639.44 A. Several hundred new lines have thus been added to the number characteristic of neutral rhenium atoms and additional spectral features of interest have been disclosed.

The use of higher dispersion and resolving power in the interval 7,200 to 9,000 A has given new data on hyperfine structure which is such a prominent feature of rhenium lines. Whereas the widest manganese lines cover an interval of only 0.5 A, some of the infrared rhenium lines are nearly 2.0 A broad and are resolved into 5 or 6 components in the first order of our Rowland grating. Details of this hyperfine structure are reserved for another publication, but some qualitative information is shown here with the same symbols that were employed in Research Paper No. 322.

A brief analysis of the new infrared data disclosed five additional metastable levels in the Re I spectrum. These are presented in table 3, the values being relative to the normal state $a^6S=0.00$.

TABLE 3.—*Energy levels of the rhenium atom*

Level no.	J	Value
17.1	2½	19,457.76
19.1	2½	23,154.75
20.1	3½	24,724.12
20.2	2½	26,131.46
20.3	3½	27,141.00

Combinations of these levels with those previously described (RP 322) account for nearly all of the stronger lines in the infrared as well as many others in the remainder of the spectrum. No further attempts to establish middle or high levels have been made, this being postponed until the spectrum has been accurately described in the ultraviolet between 2,000 and 2,500 A. Furthermore, additional efforts to group levels into terms is regarded as premature until the Zeeman effect of rhenium lines has been extensively studied. It is obvious that the Re I spectrum exhibits a considerable number of wide-spreading, overlapping terms, and lacking confidence in the interval or intensity rules as criteria for grouping levels in such a case it may be hoped that the Zeeman effect and g-sum rule will really serve as a guide out of this wilderness. Comparison of the two spectra, Mn I and Re I, shows that the normal state (zero energy) is represented by a sextet S term in each and that both exhibit excited states belonging to quartet, sextet, and octet systems, but it would be presumptious to go beyond this at the present time.

[23] W. F. Meggers, B.S. Jour. Research, vol. 6 (RP322), p. 1027, 1931.

The new data for the infrared spectrum of rhenium are displayed in table 4 in which estimated relative intensities, measured wave lengths, vacuum wave numbers, and level combinations appear in successive columns. Fortunately molecular bands which are so troublesome in the Mn I spectrum are almost entirely absent from the Re I spectrum and it has, therefore, been possible to give a more satisfactory description of the latter.

TABLE 4.—*Infrared arc spectrum of rhenium*

Intensity	λ air I.A.	ν vac cm^{-1}	Level combination	Intensity	λ air I.A.	ν vac cm^{-1}	Level combination
10cW	10,639.44	9,396.42	17.1–21	20	9,762.65	10,240.31	20.3–38
3	10,625.57	9,408.68		4	9,752.07	10,251.43	
5	10,618.40	9,415.03	6–20	6	9,749.67	10,253.95	19.1–26
1	10,609.28	9,423.13		3	9,748.60	10,255.07	
1cw	10,599.4	9,431.92	17.1–22	1cw?	9,725.6	10,279.3	
4cw	10,556.52	9,470.23		4	9,722.76	10,282.33	
4	10,464.23	9,553.74		50	9,710.52	10,295.29	
1	10,440.92	9,575.08		3	9,704.94	10,301.21	
3c	10,348.94	9,660.18		1	9,685.69	10,321.68	
10cW	10,332.57	9,675.48	61–111	5c	9,635.30	10,375.66	
4cw	10,287.58	9,717.80	61–113	2ln?	9,617.78	10,394.56	
5cw	10,282.46	9,722.63		1	9,600.98	10,412.75	
2	10,262.77	9,741.29		3cw	9,591.32	10,423.24	
1?	10,258.42	9,745.42		2ln?	9,587.0	10,427.9	
1	10,242.68	9,760.40		8c	9,581.12	10,434.33	19.1–28
4	10,238.26	9,764.61		6cw	9,571.75	10,444.55	
20	10,206.32	9,795.17		1	9,564.06	10,452.94	
2cW	10,201.86	9,799.45		6cW	9,523.40	10,497.58	
1c?	10,197.58	9,803.57		3	9,504.34	10,518.62	
1c?	10,191.57	9,809.35		8	9,500.49	10,522.89	
4c	10,183.32	9,817.29		1cW	9,481.6	10,543.9	20.1–34
20w	10,175.68	9,824.66	60–111	30	9,470.14	10,556.61	20.3–39
100cW	10,169.85	9,830.30	60–112	1	9,468.38	10,558.57	
1	10,162.75	9,837.16		3	9,427.53	10,604.33	
1?	10,146.84	9,852.59		15	9,423.44	10,608.93	
2	10,138.24	9,860.94		2ln?	9,400.27	10,635.08	
15	10,128.78	9,870.16		2	9,391.12	10,645.44	26–75
1	10,127.21	9,871.68		40	9,383.74	10,653.81	
10cW	10,064.02	9,933.66		10c	9,380.24	10,657.79	
2cw	10,059.56	9,938.08		1	9,377.02	10,661.45	
1	10,056.81	9,940.79		2	9,370.87	10,668.43	
5c	10,026.96	9,970.38		1	9,367.59	10,672.18	
7cW	10,019.21	9,978.10		20c	9,363.13	10,677.26	
1cW	10,010.29	9,986.99		2H?	9,340.8	10,702.8	
1c?	10,006.4	9,990.9	59–111	2cW	9,337.73	10,706.31	
1c?	9,980.9	10,016.4		2cw	9,332.47	10,712.34	
4	9,976.45	10,020.86		1	9,328.36	10,717.06	
1c	9,970.87	10,026.47		3	9,325.90	10,719.89	
2	9,964.90	10,032.47		5	9,311.59	10,736.36	
60cW	9,955.45	10,042.00	58–111	1	9,307.72	10,740.82	
3cw	9,953.02	10,044.45		1	9,298.07	10,751.97	
200cW	9,949.90	10,047.60	58–112	1cW	9,278.3	10,774.9	
20	9,943.70	10,053.86		15cw	9,268.46	10,786.32	
1	9,937.8	10,059.8		4	9,262.28	10,793.52	
1cW?	9,921.7	10,076.2		2cw	9,255.71	10,801.18	
5c	9,908.97	10,089.10		1	9,253.71	10,803.52	
6	9,903.30	10,094.88		10	9,250.02	10,807.82	
1	9,901.72	10,096.49		4	9,236.50	10,823.65	
2cw	9,884.10	10,114.49		1	9,220.40	10,842.54	
15vd?	9,872.38	10,126.50		2	9,213.58	10,850.57	
1	9,851.88	10,147.57		2cw	9,209.66	10,855.19	
20cW	9,842.63	10,157.10		2cw	9,205.12	10,860.54	
9	9,831.35	10,168.76		1	9,198.04	10,868.90	
2	9,813.75	10,186.99		1	9,192.18	10,875.83	
1	9,790.20	10,211.50		1cW	9,171.35	10,900.53	

TABLE 4.—*Infrared arc spectrum of rhenium*—Continued

Intensity	λ_{air} I.A.	ν_{vac} cm^{-1}	Level combination	Intensity	λ_{air} I.A.	ν_{vac} cm^{-1}	Level combination
2	9,165.38	10,907.63		2p?	8,513.44	11,742.90	
1	9,154.52	10,920.57		6cv	8,507.72	11,750.80	
6cw	9,144.86	10,932.11	20.2–37	1	8,503.83	11,756.18	
2cW	9,132.08	10,947.40		3c	8,503.35	11,756.85	
1c?	9,123.76	10,957.39		4cW	8,433.90	11,853.66	20.3–46
1	9,102.47	10,983.02		2dp?	8,430.87	11,857.92	
2	9,083.03	11,006.52		300	8,417.14	11,877.26	3–20
4	9,081.45	11,008.44		3	8,403.58	11,896.42	
5	9,070.74	11,021.44		8cw	8,399.79	11,901.79	
2cW	9,066.6	11,026.5		1p?	8,379.88	11,930.07	
2	9,063.31	11,030.47		25	8,357.59	11,961.89	
4	9,059.85	11,034.68		1	8,356.36	11,963.65	
3	9,058.53	11,036.29		2	8,354.00	11,967.03	
6	9,044.38	11,053.56		2p?	8,352.73	11,968.85	
3	9,032.46	11,068.14		5cW	8,313.02	12,026.02	
1	9,018.9	11,084.8		20cw	8,301.01	12,043.42	
2cw	9,009.15	11,096.78		2p?	8,296.28	12,050.29	
1	9,003.24	11,104.07		20	8,293.73	12,053.99	
1	8,995.26	11,113.92		3cWv	8,285.13	12,066.50	
1	8,992.91	11,116.82		6cw	8,262.87	12,099.01	
2	8,988.40	11,122.40		3cw	8,256.25	12,108.71	
1	8,983.55	11,128.40		4cWl	8,254.0	12,112.0	25–78
2	8,971.14	11,143.80	52–111	1	8,253.26	12,113.10	19.1–34
4	8,969.21	11,146.20		2	8,246.93	12,122.40	
7cw	8,966.63	11,149.40	52–112	1p?	8,231.59	12,144.98	
2	8,962.07	11,155.08		2c	8,224.30	12,155.75	
2	8,944.56	11,176.91		2h	8,190.75	12,205.54	
5	8,927.28	11,198.55		8cw	8,166.63	12,241.59	
3cW	8,901.36	11,231.16		1c?	8,141.2	12,279.8	
2c	8,899.2	11,233.9		15	8,088.25	12,360.22	
15c	8,886.58	11,249.83	20.2–38	1c?	8,064.18	12,397.12	
15cwv	8,882.95	11,254.43		30	8,060.03	12,403.50	
1	8,871.82	11,268.55		4	8,055.98	12,409.73	
3cWl	8,851.32	11,294.65	26–78	10cWv	8,052.11	12,415.70	
3cW	8,845.23	11,302.43		3	8,027.53	12,453.71	
2cv?	8,844.57	11,303.27		3	8,004.63	12,489.34	
30cWl	8,797.70	11,363.49		4	7,985.28	12,519.59	
2h	8,792.0	11,370.9		300cWl	7,980.75	12,526.71	12–21
40cWl	8,786.77	11,377.62		20	7,979.04	12,529.39	20.3–51
2c?	8,772.49	11,396.15		20\ 15/ c?	7,971.26 7,970.87	12,541.62 12,542.24	
3c	8,750.45	11,424.85					
6cW	8,721.64	11,462.59		8	7,938.57	12,593.27	
2cW	8,715.7	11,470.4		400cWl	7,912.94	12,634.06	12–23
1c?	8,699.16	11,492.21		40	7,898.47	12,657.20	10.1–38
20cw	8,697.26	11,494.72		7	7,888.93	12,672.51	
				25cWl	7,882.09	12,683.51	
1	8,686.94	11,508.37					
8	8,683.75	11,512.60		8c	7,880.72	12,685.71	
3	8,680.33	11,517.14		2c?	7,872.09	12,699.62	
50cWl	8,675.65	11,523.35	15–21	100cWl	7,869.60	12,703.63	20.3–52
30cWl	8,648.97	11,558.90	15–22	5	7,861.85	12,716.16	
				10c	7,844.14	12,744.87	19–31
15	8,643.61	11,566.07	20.2–39	1	7,838.43	12,754.15	
3cWl	8,633.10	11,580.15		8	7,828.13	12,770.94	
8c	8,630.66	11,583.42		10	7,825.85	12,774.65	
5c	8,628.44	11,586.40		4c	7,801.05	12,815.27	
6	8,603.88	11,619.48		3	7,799.58	12,817.68	
3	8,593.62	11,633.35		4	7,794.67	12,825.76	
3c	8,588.52	11,640.25		8c	7,789.88	12,833.64	
15	8,570.71	11,664.44		2cp?	7,781.21	12,847.94	
1h	8,562.17	11,676.08		2cp?	7,763.9	12,876.6	
2c?	8,557.50	11,682.45		15cw	7,743.15	12,911.09	
4c?	8,554.61	11,686.40		2p?	7,741.14	12,914.45	
2	8,537.38	11,709.98		2p?	7,738.92	12,918.15	
3cW	8,534.99	11,713.26		25	7,733.62	12,927.00	
300cWl	8,527.73	11,723.23	14–23	1p?	7,716.52	12,955.65	
1	8,524.64	11,727.48		2c	7,712.58	12,962.27	

TABLE 4.—*Infrared arc spectrum of rhenium*—Continued

Intensity	λ air I.A.	ν vac cm⁻¹	Level combination	Intensity	λ air I.A.	ν vac cm⁻¹	Level combination
25c	7,705.92	12,973.47	20.1–39	4	7,447.58	13,423.49	
20c	7,693.63	12,994.19		1p?	7,446.97	13,424.59	
3	7,684.83	13,009.07		1	7,442.75	13,432.20	
2	7,683.45	13,011.41		3	7,440.71	13,435.88	
5?	7,656.81	13,056.68		2	7,437.78	13,441.20	
2c	7,652.49	13,064.05		2	7,431.93	13,451.76	
400cWl	7,640.93	13,083.82	10–21	3c	7,416.44	13,479.85	
200 cWl	7,620.25	13,119.32	10–22	2c	7,413.41	13,485.37	
3c	7,618.32	13,122.65		15	7,409.47	13,492.53	19–34
100	7,611.90	13,133.71	17.1–25	3	7,404.27	13,502.01	
2	7,596.30	13,160.69		2c	7,396.04	13,517.03	
2c	7,587.66	13,175.67		4cWv	7,390.71	13,526.78	
6cWl	7,583.26	13,183.32		15	7,386.35	13,534.76	
200cw	7,578.72	13,191.21	101–23	1	7,384.07	13,538.94	20.2–51
2c?	7,573.47	13,200.36		2	7,382.68	13,541.49	
1p?	7,569.66	13,207.00		2c	7,362.12	13,579.31	
6	7,567.82	13,210.21		2	7,360.95	13,581.47	
30	7,548.71	13,243.65		30cWl	7,352.03	13,597.95	
5cWl	7,545.37	13,249.52		1	7,346.88	13,607.48	
1p?	7,543.22	13,253.29		5	7,329.37	13,639.98	
1p?	7,539.73	13,259.43		6	7,324.20	13,649.61	
2	7,536.42	13,265.25		2	7,318.02	13,661.14	
3	7,526.50	13,282.73		4cw	7,316.1	13,664.7	
20cW	7,524.48	13,286.30		4c	7,307.55	13,680.72	20.3–57
2	7,494.04	13,340.27		250cWl?	7,292.67	13,708.63	22–67
				100cWl	7,273.84	13,744.12	21–67
2	7,489.13	13,349.02		3	7,265.45	13,759.99	
5cw	7,488.12	13,350.82		4	7,263.87	13,762.98	
1p?	7,482.62	13,360.63		200cWl	7,246.67	13,795.64	9–21
6	7,481.15	13,363.25		3	7,237.28	13,813.54	
4	7,478.63	13,367.76		20	7,228.03	13,831.22	9–22

WASHINGTON, April 5, 1933.

RECOMBINATION RADIATION IN THE CESIUM POSITIVE COLUMN

By F. L. Mohler

ABSTRACT

The radiation emitted along the axis of a positive column has been measured by spectrophotometric methods and electrical measurements have been made with small probe surfaces near the line of sight.

The continuous spectrum near the 6^2P limit was measured with pressures ranging from 0.8μ to 290μ and with a 50-fold range of electron concentration, N_e. At low pressures the intensity varies as N^2_e and is nearly a linear function of pressure with about twice the zero pressure value at 9μ for $N_e = 10^{12}$ or less. At higher pressures and high values of N_e the increase in intensity is less than N^2_e.

The intensity near the 5^2D limit remains nearly equal to that at 6^2P for pressures above 3μ. At high pressures the subordinate and fundamental series lines change in the same way as the continuous spectrum.

The low-pressure measurements give a basis for evaluating the probability of spontaneous recombination of an ion and an electron into the 6^2P level. The effective collision area for 0.3 volt electrons is 1.7×10^{-21} cm^2.

The effect of vapor density is to increase the probability of transition. Expressed as a 3-body collision, recombination takes place if an electron and an atom are simultaneously within 6×10^{-8} cm of an ion.

With high electron concentration radiation is suppressed in a process which is probably the converse of ionization by collision. This quenching process takes place when two electrons are simultaneously within a distance of about 10^{-7} cm of an ion but the distance increases with vapor density.

CONTENTS

	Page
I. Introduction	771
II. Experimental procedure	773
III. Results	774
1. Intensity of the 6P band	774
2. Intensity of other bands and lines	776
IV. Discussion	777
1. Spontaneous recombination	777
2. Vapor density effect	778
3. Quenching of recombination by electron collisions	779
4. Conclusions	780

I. INTRODUCTION

This is one of a series of papers giving measurements of the atomic constants which determine the rate of interaction of electrons, ions, and atoms in an electric discharge.[1] The uniform glow which fills most of the tube in the familiar type of electric discharge is a mixture of atoms, positive ions, and negative electrons. The electrons collide with the atoms and ions and produce ionization and radiation. The

[1] Mohler, B.S. Jour. Research, vol. 9 (RP455), p. 25, 1932; (RP485), p. 493, 1932. Boeckner and Mohler, B.S. Jour. Research, vol. 10 (RP536), p. 357, 1933.

chance of producing any given effect can be expressed in terms of an area around each atom through which an electron must pass to produce the effect. These collision areas are evaluated by measuring the number of atoms or ions, the number of electrons and the total effect produced in a given volume. This paper deals with collisions in which an electron becomes attached to an ion to form a neutral atom and the effect measured is the continuous spectrum radiation emitted in this recombination process. Results show that this effect which is negligible in low-pressure discharges can become an important factor in high-pressure high-current discharges.

When a positive ion and an electron recombine spontaneously, that is, in a 2-body collision, the energy will be radiated in a single quantum of energy

$$h\nu = h\nu_i + 1/2mv^2 \tag{1}$$

where ν_i is the frequency of a series limit and v is the electron velocity. With electrons of random velocity there is a continuous band extending beyond each series limit and the intensity at any frequency measures the rate of recombination of electrons of the corresponding speed into a particular level, provided the continuous bands do not overlap. The rate of recombination will be expressed as an effective area $q(\nu_i v)$ characteristic of the limit ν_i and the electron speed. The number of collisions within this area gives the number of quanta radiated

$$\frac{J(\nu)\,d\nu}{h\nu} = q(\nu_i v)\, N^+ N_e v f(v)\, dv$$

where the N's are the number of ions and electrons per cubic centimeter and $f(v)\,dv$ is the fraction of electrons having a range of speed dv corresponding to dv. The electrons in a plasma have a Maxwell distribution of velocity and N^+ and N_e are very nearly equal

$$\frac{J(\nu)\,d\nu}{h\nu} = q(\nu_i, v)\, N^2{}_e \frac{4\pi^{-1/2}}{\sqrt{2me}} \frac{V}{V^{3/2}{}_0} \exp.\,(-V/V_0)\, d\nu \tag{2}$$

where V and V_0 are the electron energy and the most probable energy in electron volts.

About five years ago Boeckner and the author made a quantitative study of the continuous bands emitted by a cesium discharge.[2] Results indicated that the intensity distribution depended on the electron velocity distribution in a manner consistent with equation (2) and for the 6^2P and 5^2D bands q was inversely proportional to $\nu^2 V$.[3] The intensity distribution[4] then has the form

$$\lambda J(\lambda) = bN^2{}_e \exp.\,(-V/V_0)/V^{3/2}{}_0 \tag{3}$$

where b is a constant characterisitc of the limit. As concerns the absolute magnitude of the effect, the results indicated complications in the theory. The variation of intensity was less than $N^2{}_e$ for high values of N_e and there was a marked increase in intensity with vapor pressure. The vapor pressure does not enter explicitly in equation (2) and the only predicted effect would be a slow variation resulting from the small change in V_0. Nevertheless the importance of vapor pres-

---

[2] Mohler and Boeckner, B.S.Jour. Research, vol 2 (RP46), p. 489, 1929.

[3] We here use total quantum numbers instead of the Paschen notation used in other papers of this series. 6P and 5D are the first P and D terms of cesium.

[4] Boeckner, B.S.Jour. Reaserch, vol. 6 (RP274), p. 277, 1931.

sure has been emphasized in numerous qualtitative studies of recombination spectra.[5]

Recently Webb and Sinclair [6] have studied the afterglow of a mercury discharge as a function of electron concentration and electron temperature. The intensity was proportional to the first power of N_e and decreased very rapidly with increasing electron temperature. The results could be accounted for by assuming that recombination proportional to N^2_e was quenched by collisions of electrons with energy exceeding about 1 volt. They also found a rapid increase in intensity with pressure.

II. EXPERIMENTAL PROCEDURE

Mohler and Boeckner used the negative glow and dark space between a hot wire cathode and surrounding anode as a source of radiation but the positive column is better adapted to the purpose. The radiation per unit volume is somewhat less but the volume can be made as large as desired and is not a function of the pressure. The procedure was to measure the intensity sighting along the axis of the column and to measure the electron concentration with small probe surfaces at the axis.

The discharge tube was 1.8 cm in diameter and the length of the column was about 24 cm along the line of sight. The thermionic cathode and anode were in side tubes. The cesium was in an appendix and the vapor pressure was controlled by a separate heater around it. The probe surfaces were the ends of platinum wires covered except at the end with glass. Commonly there were two probes 0.4 and 1 mm in diameter.

The technique of the electrical measurements has been described before [7] but will be repeated in part as these measurements offer the chief source of uncertainty. The electron current reaches a nearly constant value at potentials positive to the space. The current per unit collecting area I is then related to the electron concentration by the equation

$$N_e = 3.75 \times 10^{11} I/\sqrt{V_0}$$

and the electron energy V_0 is obtained in the usual manner from the slope of the linear log I vs. V curve for values of V negative to the space potential. The difficulty is that, while the random space current may be as high as 40 amperes per square centimeter, the probe current should not exceed 0.1 ampere which necessitates a small area. In cesium vapor it is necessary to avoid a close fit of the insulator around the probe to reduce leakage, and in use the probe is heated enough to cause a gradual change in the exposed area. The use of probes of two sizes reduces the uncertainty, as the effective area of the smaller one can be found by comparison. Absolute values are based on the mean results obtained with several tubes. An upper limit of pressure and current is set by the probe limitations; the lower limit is determined largely by intensity considerations.

Intensity was measured by direct comparison of the spectra of the discharge and of a calibrated tungsten strip lamp. The discharge was

[5] Krefft, Zeits. f. Phys. ,vol. 77, p. 752, 1932.
[6] Webb and Sinclair, Phys. Rev., vol. 37, p. 182, 1931.
[7] Mohler, F. L., Collisions of the First and Second Kind in the Positive Column of Cesium Discharge, B.S.Jour. Research, vol. 9 (RP485), p. 493, October 1932.

focussed on the strip and the superposed images of the strip and discharge were focussed on the spectrograph slit. Visual measurements were made by varying the strip lamp current to match the discharge. Photographic measurements were based on densitometer measurements with the strip and discharge nearly matched and were always more accurate than my visual measurements. A correction for transmission of the tube and furnace windows and first lens is included. The accurate collimation of points extending 24 cm along the line of sight would require a very small aperture and the actual aperture ratio of about one thirtieth is necessarily a compromise.

A troublesome source of error in the continuous spectrum measurements is the scattered light from the line spectrum. At 4,950 A the photographic fogging comes largely from the doublet at 4,555 and 4,593 A. This is an absorption doublet and a bulb of dense cesium vapor in front of the discharge, combined with a mask over the plate, seemed to eliminate the trouble. Repeated runs were vitiated before the need of extreme precaution was realized.

III. RESULTS

1. INTENSITY OF THE 6P BAND

Figure 1 gives plots of the log of the intensity at 4,950 A, near the 6P limit, versus the log of the electron concentration at nine different vapor pressures. A correction of 0.23 must be added to give the intensity in the tube. Circles give a single set of measurements, judged to be the most reliable; but the interpolation and extrapolation are based on several other series of measurements. At low pressures the curves are straight lines of slope two, which means that the intensity is proportional to N^2_e. Except at the highest pressures the curves start with a slope of two. At the lowest pressures the intensity is nearly independent of pressure while above 6μ the intensity is roughly proportional to the pressure at constant N_e.

Probably the intensity depends on the vapor density or number of atoms per cubic centimeter rather than on the pressure. A rough measurement with tube temperatures of 240° and 440° C., and a vapor pressure of 12.5μ showed that the intensity was about 35 percent less at the higher temperature. The density change would account for a 25 percent change and the discrepancy can be ascribed to inadequate control of the cesium temperature. An effect depending on collisions between atoms and relatively high-speed ions would vary with the density rather than the pressure.

The intensity distribution in the 6P band has been checked at two extreme pressures by intensity measurements at two wave lengths. From equation (3) the intensities at two wave lengths, λ_1 and λ_2, separated by an interval corresponding to $V_2 - V_1$ electron volts, are related to the electron energy V_e as follows

$$\frac{(V_2 - V_1) \log \epsilon}{\log \lambda_1 J(\lambda_1) - \log \lambda_2 J(\lambda_2)} = V_e$$

At a pressure of 290μ with a 2-ampere discharge, $V_e = 0.187$ volts. Measurements of the reversal temperature of the resonance line give $V_e = 0.195$ volts. At a pressure of 6μ measurements on a 3-ampere discharge gave $V_e = 0.255$ volts while electrical measurements and

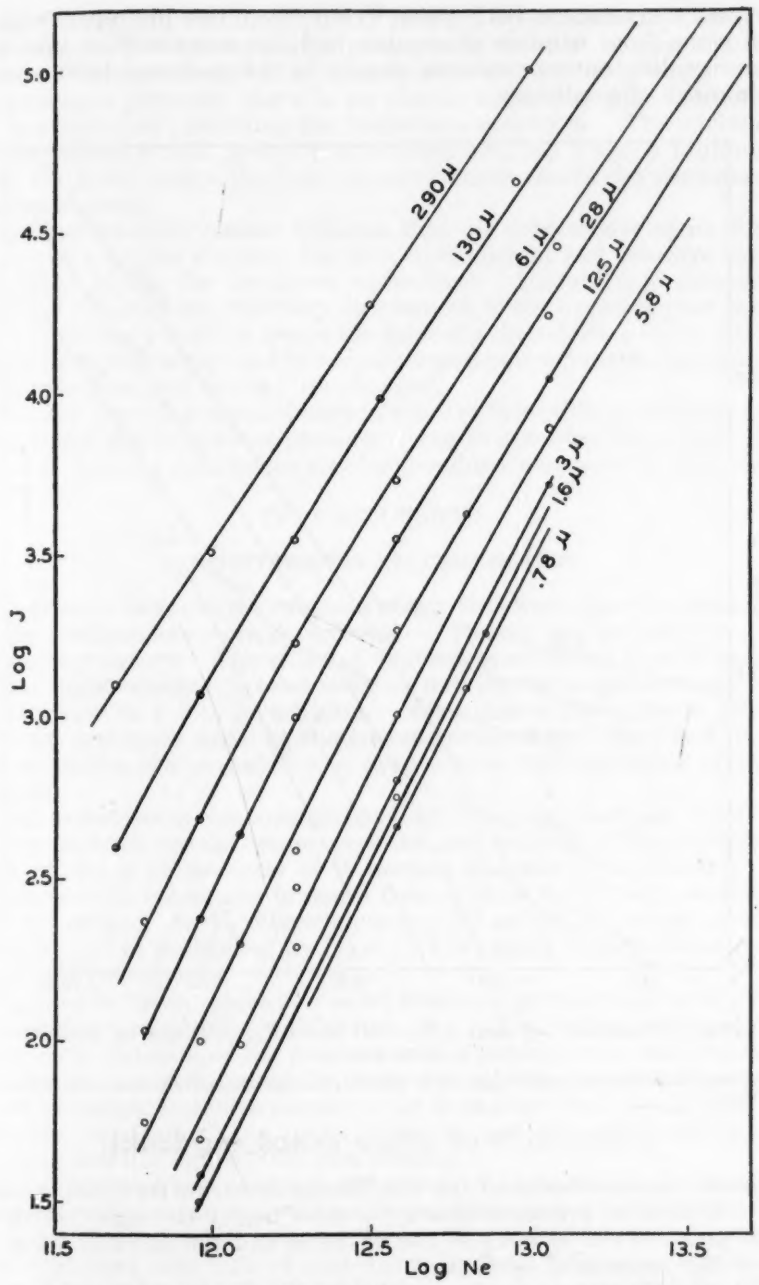

FIGURE 1.—*Intensity of the continuous spectrum near the 6P limit.*

Log J (4,950) versus the log of the electron concentration at nine pressures. J is radiation flux in ergs in a wave length range of 1 μ in an angle 2π.

reversal temperature both gave $V_e = 0.283$. The discrepancy may well come from window absorption and the conclusion is that the intensity distribution conforms closely to the predicted form over a wide range of conditions.

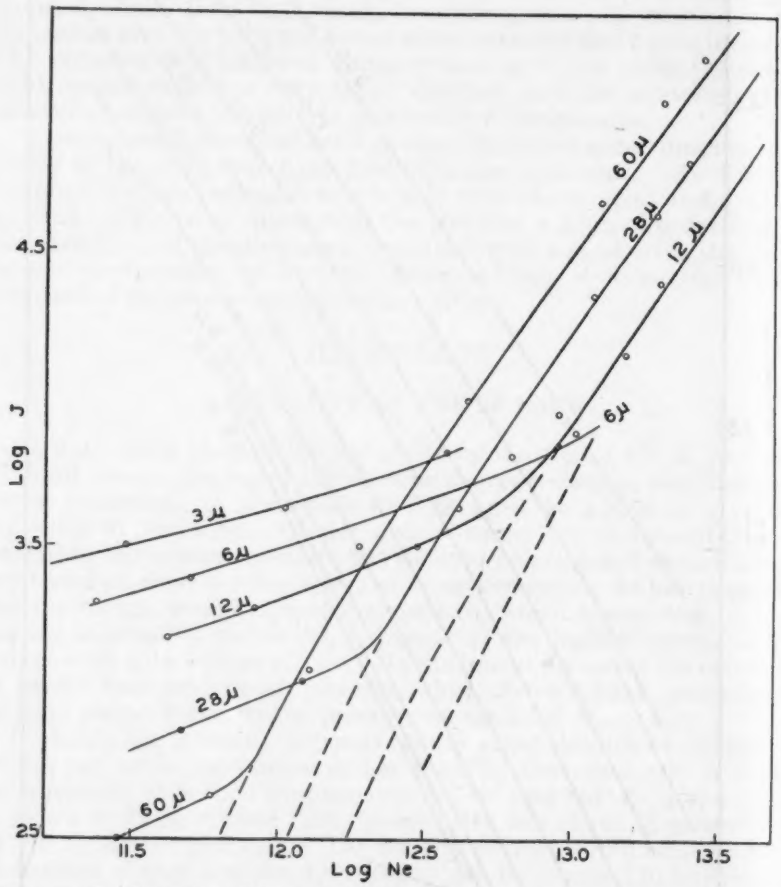

FIGURE 2.—*Intensity of lines $6P_{1/2}$–10D and $6P_{3/2}$–11D and of continuous spectrum.*

The steep, smooth curves give the continuous intensity, the dots and nearly horizontal curves the line intensity.

2. INTENSITY OF OTHER BANDS AND LINES

Visual measurements of the continuous spectrum at 5,925 A near the 5^2D limit at pressures above 3 μ show nearly the same variation with pressure and current as the 6P band and the absolute value is about the same as at 4,950 A.

Visual settings were made on the superposed pair of lines $6P_{1/2}$–10D at 5,466 A and $6P_{3/2}$–10D at 5,503 A. At pressures above 80 μ the variation of intensity with pressure and current is the same as for the continuous spectrum. Figure 2 shows the results at lower pressures. The smooth steep curves give the intensity of the 6P band; the dots

and full lines give the line intensity reduced by an arbitrary factor to the same scale. At the lowest pressures there is no correspondence between the variation of line intensity and continuous intensity. At intermediate pressures there is an abrupt transition with increasing N_e to a variation paralleling the continuous spectrum. The variation of line intensity with pressure at constant N_e has a sharp minimum near the point where the line intensity curve meets the continuous spectrum curve.

Qualitative observations indicate that all subordinate series lines change in a similar manner, the transition current and pressure being somewhat higher for the lower series lines. Unpublished measurements of the spectrum intensity distribution in the negative glow show that above the transition range the intensity distribution in the whole visible spectrum except the principal series doublet remains unchanged as the pressure and current are changed.

Because there is a rapid change in relative intensity of continua and lines below the transition pressure there is a misleading visual impression that the continuous spectrum suddenly appears in this pressure range.

IV. DISCUSSION

1. SPONTANEOUS RECOMBINATION

The results bear out the evidence of previous work that the intensity of the continuous spectrum depends on factors not included in the elementary theory. The effect of vapor density shows that recombination under discharge conditions is not purely a spontaneous recombination in a 2-body collision. Nevertheless the pressure effect becomes extremely small at the lowest pressures and there is a basis for evaluating the probability of spontaneous recombination at zero pressure.

The experiments are complicated by the fact that the electron energy depends on the vapor pressure and current. The variation with current is of the order of 10 percent and will be neglected. V_0 decreases with increasing pressure from 0.38 to 0.195 volts over the extreme range. As V_0 enters equation (2) as $1/V_0^{3/2}$, values of the intensity will be multiplied by $(V_0/0.3)^{3/2}$ to reduce them to a standard value of $V_0=0.3$ volts.

Figure 3 includes values of J as a function of pressure up to 61 μ for $N_e=10^{12}$ and values of $J/100$ for $N_e=10^{13}$. The values for $N_e=10^{12}$ are a linear function of the pressure within experimental uncertainty. The two curves have nearly the same intercept at $p=0$ and the separation at higher pressures measures the departure from the N_e^2 law of intensity variation. The mean value of the two intercepts gives $J=43$ in units of figure 1 for zero pressure.

It is convenient to evaluate the effective cross section for recombination $q(6P)$ at an interval corresponding to 0.3 volts from the limit, viz, 4,400 A, and, from equation (3), $J(4,400)=0.415\ J(4,950)$. It is estimated that 0.28 of this comes from the 5D band. On this basis the number of quanta emitted in a cubic centimeter in unit frequency range is 0.66×10^{-5} times the plotted values. The effective collision area $q(6P, 0.3\text{ volts})$, is by equation (2), 1.7×10^{-21} cm^2. As cesium 6P has an effectivc quantum number of 2.35 it should be compared with a hydrogenic 2 quantum level. The theoretical value

for recombination of 0.3 volt electrons into the hydrogen 2_2 level is 3.66×10^{-21} cm^2.[8]

2. VAPOR DENSITY EFFECT

The increase in the rate of recombination with vapor density can be expressed as an increase in q with the number of atoms per cubic centimeter N_a. The upper curve of figure 3 gives the relation

$$q-q_0=0.71\times10^{-14}N_aq_0 \tag{4}$$

where q_0 is the value at zero pressure, 1.7×10^{-21} cm^2. The transition probability is doubled at a pressure of 9 μ or when the average distance

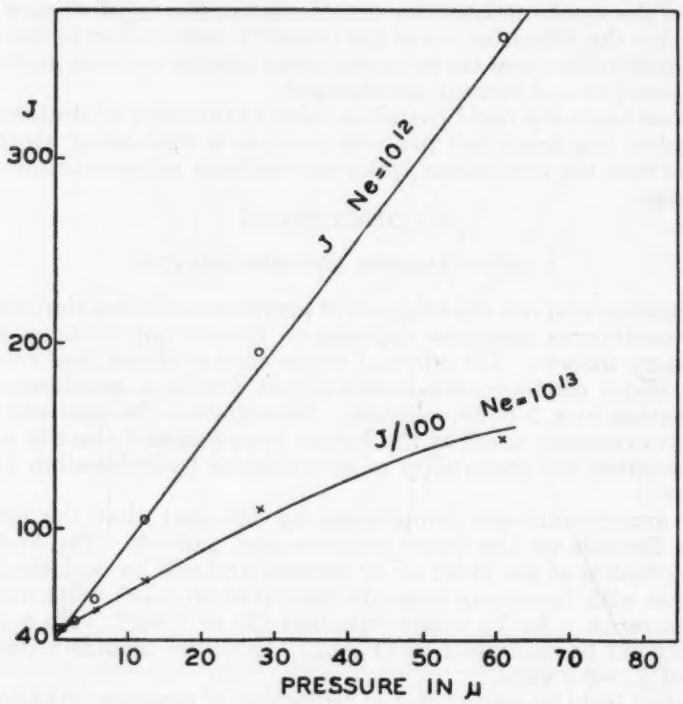

FIGURE 3.—*Intensity of continuous spectrum at 4,950 A versus pressure.*
Intensity is reduced to V_0=0.3 volts.

between atoms is about 2×10^{-5} cm. The interaction can be described as follows: For an electron and ion to recombine spontaneously the electron path must have a narrowly restricted value of angular momentum relative to the ion. With the presence of another atom near the ion there is the possibility of the transfer of some of the momentum to that atom and the range of electron paths which can recombine is extended. The magnitude of the interaction is, however, surprisingly great.

As the interaction involves three bodies, one can express the probability of induced radiation as the probability of an atom and an electron being simultaneously within a distance r_a of an ion. With

[8] Steuckelberg and Morse, Phys. Rev., vol. 36, p. 16, 1932.

N_a atoms per cubic centimeter the number of atoms within a distance r_a of N^+ ions is $\frac{4}{3}\pi r_a^3 N^+ N_a$ and the number of electron collisions with these ions is $\frac{4}{3}\pi^2 r^5 N^+ N_e N_a v_e$. At a pressure of 9 μ, $N_a = 1.4 \times 10^{14}$, the number of induced collisions equals the number of spontaneous collisions.

$$\frac{4}{3}\pi^2 r_a^5 N^+ N_e N_a v_e = 1.7 \times 10^{-21} N^+ N_e v_e \qquad (5)$$
$$r_a^5 = 0.92 \times 10^{-36} \quad r_a = 6.2 \times 10^{-8} \text{ cm}$$

This interaction distance r_a bears no simple relation to the q of equation (4), for equations (4) and (5) express two different interpretations of the phenomenon.

3. QUENCHING OF RECOMBINATION BY ELECTRON COLLISIONS

The continuous spectrum intensity increases less rapidly than the square of the electron concentration at high pressure and currents. This can be ascribed to an interaction between the recombining electron and a second electron in which the energy of recombination is given to the second electron. This process is the converse of ionization by electron collision except for the complicating effect of vapor density considered above. This quenching process is a 3-body collision and the number of collisions per cubic centimeter per second can be expressed in terms of the probability of two electrons being within a distance r_e of an ion. The number of quenching collisions is proportional to $J_0 - J$, where J is the actual intensity and J_0 is the value that would be observed if J were proportional to N_e^2. The absolute value can be expressed in terms of $q(6P)$ of equation (4).

$$\frac{4}{3}\pi^2 r_e^5 N^+ N_e^2 v_e = \frac{J_0 - J}{J_0} q(6P) N_e^2 v_e \qquad (6)$$

$$\frac{4}{3}\pi^2 r_e^5 N_e = \frac{J_0 - J}{J_0} q(6P) \qquad (7)$$

Table 1 gives values computed for all curves where the departure from the N_e^2 relation was measurable. The interaction radius is of the same magnitude as was found by equation (5) for radiation induced by atomic collision.

TABLE 1.—*Quenching of recombination by electron collisions*

Pressure (in μ)	q (6P 0.3 volts)	$\frac{J_0 - J}{J_0}$ at $N_e = 10^{13}$	$\frac{4}{3}\pi^2 r_e^5 v_e$	r_e	$q_e \tau$
	$\times 10^{-21}$		$\times 10^{-41}$	$\times 10^{-7}$	$\times 10^{-21}$
289	107	0.77	23	2.3	2.1
130	38	.71	7.2	1.8	1.9
61	14	.58	2.2	1.4	1.6
28	8	.44	.96	1.2	1.2
12.5	4.2	.31	.36	1	.85
5.8	2.5	(.18, fig. 3)	.125	.77	.5
0	1.73				

One can alternatively express the quenching in terms of the chance of a quenching collision during the recombination process by assuming a time interval τ and an effective area q_e in which the collision of a second electron will be effective. There are $q_e N_e v_e$ collisions per second with a recombining atom and $q_e N_e v_e \tau$ is the chance of a collision given by $\frac{J_o - J}{J_o}$. From equation (6)

$$q(6P) q_e \tau = \frac{4}{3} \pi^2 r_e^5 / v_e \tag{8}$$

The effective area q_e can be expressed in terms of an effective radius r' and τ is naturally identified with the time it takes for an electron to cross this area. In conformity with the right side of equation (8) we can take $\tau = \frac{4}{3} r'/v_e$. The radius r' is much larger than r_e (at a pressure of 61 μ it is 2.4 μ 10^{-5} cm). The difference is the same as appeared in the two views of the pressure effect. The right side of equation (8) expresses the chance of two electrons being within equal distances r_e of the ion. The left side gives one electron the very much smaller distance corresponding to q (6P) so that q_e must be proportionately larger. It is the product that is measured and there is nothing in the experiment to distinguish the two viewpoints. The values listed in the table are subject to a large experimental uncertainty for the effect is small except at pressures where the measurements of N_e become inaccurate.

4. CONCLUSIONS

Recombination in a cesium discharge is in general not a spontaneous 2-body collision but is influenced by the presence of atoms and other electrons. From measurements at sufficiently low pressures one can evaluate the probability of spontaneous recombination. For 0.3 volt electrons recombining into 2^2P the collision area is 1.7×10^{-21} cm.[2] The effect of pressure is to increase greatly the probability of radiation. The effect of electron concentration is to quench the radiation. The interaction radii for the induced radiation resulting from atomic collisions and for the quenching by electron collisions are both of the same magnitude, 10^{-7} cm, when expressed in terms of finding three bodies in a volume of radius r.

I am indebted to Dr. C. Boeckner for helpful suggestions concerning the interpretation of these results.

WASHINGTON, March 29, 1933.

THE VISCOSITY OF SULPHURIC-ACID SOLUTIONS USED FOR BATTERY ELECTROLYTES

By G. W. Vinal and D. N. Craig

ABSTRACT

The viscosity of sulphuric-acid solutions used for the elecrolyte in lead-acid storage batteries is a factor affecting the diffusion of the electrolyte through the porous material of the plates and separators. The decreased capacity of batteries at low temperatures is attributable in part to increase in viscosity of the electrolyte. Storage batteries are commonly used under widely different conditions of temperature, but data for the viscosity of the electrolyte at temperatuers below 0° C. have not been previously available. The viscosity of sulphuric-acid solutions containing 10 to 50 per cent acid has now been measured over a temperature range from +30° C. to −50° C., the measurements for some solutions being limited, however, by their freezing points. Below 0° C. the viscosity of the solutions increases rapidly as the temperature is diminished.

CONTENTS

	Page
I. Introduction	781
II. The apparatus	782
1. Description of apparatus	782
2. Calibration of the viscometer	784
III. Experimental results	785
IV. Discussion of the results	790
1. Accuracy of the measurements	790
2. Comparison with previous determinations	791
V. Summary	792
VI. Acknowledgements	793

I. INTRODUCTION

Storage batteries of the lead-acid type are now used under such widely differing conditions of temperature and rate of discharge that an extension of our knowledge of the basic properties of sulphuric-acid solutions which are employed for the electrolyte is desirable. Resistivity and viscosity of the solutions are two of the more important properties of the electrolyte which affect the performance of batteries. The useful voltage of a battery is decreased as the resistivity of the electrolyte increases. The viscosity affects the rate of diffusion of the electrolyte through the porous material of the plates and separators. Increase in viscosity results in decreased capacity of a battery. Both resistivity and viscosity are, therefore, factors determining the amount of electrical energy which a battery can deliver under specified conditions of temperature and rate of discharge. As a part of a comprehensive investigation of the properties and behavior of battery electrolytes and separators the viscosity of sulphuric-acid

solutions from 10 to 50 percent H_2SO_4 have been measured. The viscosity measurements have been made over a temperature range from +30° C. to −50° C. insofar as the temperatures were above the freezing points of the solutions. In the present paper the results of these viscosity measurements are given, and in a later paper we expect to give the results of our work on the resistance of battery separators and the resistivity of sulphuric-acid solutions.

Although several authors have published values for the viscosity of sulphuric-acid solutions at ordinary temperatures and above, data are not available in the literature for temperatures below 0° C. Wagner [1] measured the viscosity of dilute solutions, 1.0035 to 1.2003 specific gravity, at temperatures of 15° to 45° C. Dunstan and Wilson [2] measured the viscosity of a large number of solutions ranging from dilute to concentrated acid at 25° C.

Rhodes and Barbour [3] also measured the viscosity of a large number of solutions ranging from dilute to concentrated acid. Their measurements were made at 0°, 25°, 50°, and 75° C. Their paper is the only one, which we have found, giving viscosities at temperatures as low as 0° C. In the same year Bingham and Stone [4] published the results of their measurements on solutions from 11 to 97 percent acid at 10°, 20°, and 40° C.

Grunert [5] measured the viscosity of sulphuric-acid solutions from 0.4344 to 3.475 molar at temperatures of 20°, 40°, 60°, and 80° C.

In a later section of this paper the values reported by the above authors are compared with the present determinations. Such a comparison, however, is necessarily limited to few values since our work extended to low temperatures while previous work was mostly confined to measurements at higher temperatures.

II. THE APPARATUS

1. DESCRIPTION OF APPARATUS

The viscosity measurements were made by timing the discharge of a fixed volume of solution through the capillary tube of a viscometer made of Pyrex glass. The ratio of the length of the capillary to its diameter was approximately 100. A diagram of the apparatus which was employed is shown in figure 1. The liquid was drawn up in the viscometer above index A and then released. The passage of the miniscus from A to B was timed.

The viscometer and the tube surrounding it, containing one of the sulphuric-acid solutions, or a liquid used for calibrating the instrument, were placed in a temperature-controlled bath in a Dewar flask of clear glass. This was provided with a stirrer. For measurements at 20° C. and above, the temperature was regulated and held constant by the addition of small portions of warm or cold water to the water in the Dewar flask. At temperatures below 20° C. the water in the Dewar flask was replaced by alcohol and the temperature was adjusted and held constant during each experiment by adding small portions of solid carbon dioxide.

---

[1] Ann. d Phys., vol. 254, p. 259, 1883, and Zeit. Phys. Chem., vol. 5, p. 31, 1890.
[2] J. Chem. Soc., vol. 91, p. 83, 1907. An important correction to all of their results was published in Proc. Chem. Soc., vol. 30, p. 104, 1914.
[3] Ind. and Eng. Chem., vol. 15, p. 850, 1923.
[4] J. Phys. Chem., vol. 27, p. 701, 1923.
[5] Zeit. Anorg. Chem., vol. 145, p. 394, 1925.

Reference lines etched on the viscometer and on the tube surrounding it served to fix the position of the viscometer relative to the tube. The level of liquid in the tube was adjusted for each experiment to an etched line on the tube (*C* in the diagram) before drawing the liquid up into the viscometer. Slight adjustments in level of the liquid were accomplished by raising or lowering the thermometer to

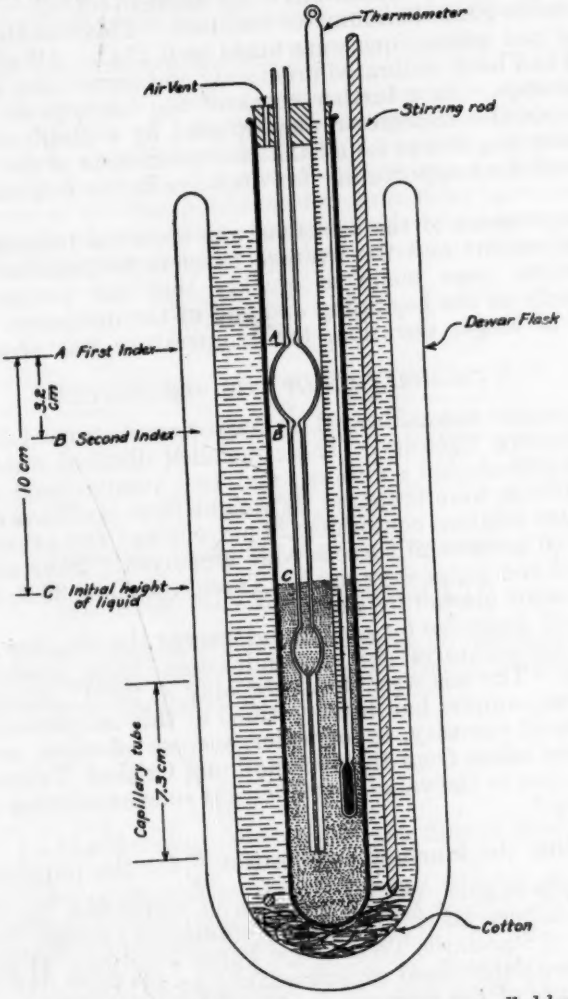

FIGURE 1.—*Viscometer and temperature-controlled bath.*

compensate for the expansion or contraction of the liquid as the temperature was changed. The same head of the liquid was thereby obtained at the beginning of each discharge. The viscometer was provided with two bulbs, the lower bulb always being immersed in the liquid. This aided materially in equalizing temperatures before the liquid passed through the capillary tube.

The temperature was read on a thermometer which was placed directly in the solutions to be measured and adjacent to the capillary of the viscometer. The thermometer employed for temperatures above −1° C. was a mercury-in-glass type graduated in tenth degrees, and estimations were made to 0.01° C. Below −1° C. and above −20° C. a mercury-in-glass thermometer was also used. This was graduated in degrees, estimations being made to 0.1° C. Below −20° C. a toluene-in-glass thermometer was used. This was also graduated in degrees and estimations were made to 0.1° C. All of these thermometers had been calibrated previously and corrections were applied to the readings. As a further check of the readings of the toluene thermometer, the viscometer was replaced by a platinum resistance thermometer and it was found that the conditions of the experiment afforded sufficient opportunity for drainage in the toluene thermometer.

The temperature of the solutions was observed frequently during each measurement and the average temperature calculated. Some determinations were made so quickly that the temperature was observed only at the beginning and end of the discharge. In determinations of longer duration, the temperature was observed 6 or 8 times.

2. CALIBRATION OF THE VISCOMETER

The viscometer was calibrated by measuring the time of discharge of liquids of known viscosity. These included distilled water, sucrose solutions, ethyl-alcohol solutions, and two standardized oils. The sucrose solutions were prepared by weight from standard samples of sucrose. One solution containing 20 percent and two other solutions containing 40 percent of sucrose were employed. Four solutions of ethyl alcohol and water were used. These contained 39.2, 46.4, 49.7, and 50.5 percent alcohol by weight.

The time of discharge for each liquid, except the oils, was measured at several temperatures, six determinations being made at each temperature. The oils were measured only at 25° C., since the viscosity of these samples had been certified at this temperature.

The values of viscosity, μ, for water, sucrose solutions, and alcohol solutions were taken from the International Critical Tables[6] except that a correction to the value for 40 percent sucrose solution at 10° C. was necessary.[7]

In computing the kinematic viscosities, $\frac{\mu}{\rho}$, for the purpose of calibrating the viscometer, the densities, ρ, of water and the solutions employed have been taken from the International Critical Tables and from Bureau of Standards Technologic Paper No. 100. The densities of the oils were determined experimentally at 25° C.

The constants of the viscometer, A and B, were evaluated graphically[8] by plotting the computed ratios of kinematic viscosities to time of discharge $\left(\frac{\mu}{\rho t}\right)$ of the calibrating liquids as ordinates against $\frac{1}{t^2}$ (t = measured time of discharge in seconds). The results of the calibration measurements are shown in figure 2. The value of A (the inter-

[6] Vol. 5, pp. 10, 22, and 23.
[7] J. Rheology, vol. 3, p. 500, 1932.
[8] Higgins, Collected Researches, National Physical Laboratory, vol. 11, p. 12, 1914.

cept of the straight line on the y-axis) and the value of B (the slope of the straight line) were found to be 0.02365 and 2.333, respectively. Calibration of the viscometer was necessarily extended over a wide range because of the large variation in viscosity of sulphuric-acid solutions from $+30°$ to $-50°$ C. The calibration curve, however, shows no evidence of turbulent flow within the range for which this viscometer was actually used.

With the exception of the alcohol solutions, the maximum deviation of any value of $\frac{\mu}{\rho t}$ from the calibration line as drawn (fig. 2) is less than 1 percent and 15 out of 16 points for sucrose solutions, water and the oils are within one half of 1 percent of corresponding points on the line. The values obtained with alcohol solutions are, with one exception, above the line. Six out of ten of the alcohol points lie within 1 percent of the line, but these determinations have been given less weight in drawing the line, because values for the viscosity of alcohol solutions appear to be known less accurately than the others.

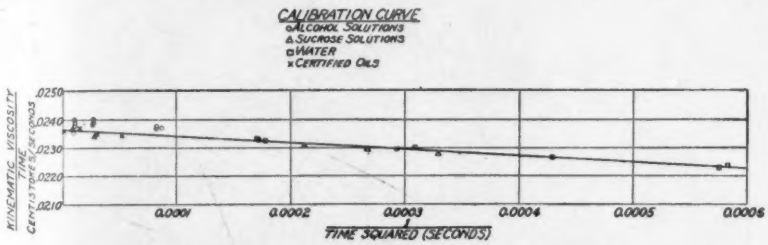

FIGURE 2.—*Calibration curve of the viscometer*

III. EXPERIMENTAL RESULTS

The time of discharge of a specified volume of solution under test having been measured at a temperature $T°$, the kinematic viscosity was calculated from the equation

$$\left(\frac{\mu}{\rho}\right)_{T°} = At - \frac{B}{t}$$

in which $\left(\frac{\mu}{\rho}\right)$ is the kinematic viscosity, t the time of flow in seconds and A and B are constants for the instrument which was used. The values of A and B were determined by the method described in a previous section. Eight different solutions of sulphuric acid ranging in composition from 10.1 to 49.1 percent by weight of H_2SO_4 were measured at temperatures between $-50°$ and $+25°$ C. ($-58°$ and $+77°$ F.). These solutions were prepared from "Cp" acid and distilled water. They did not contain lead sulphate which is normally present in small amounts in battery electrolytes.

The composition of these solutions, expressed as percent H_2SO_4. was determined by titrating two weighed portions of each solution,

The percentages so obtained were 10.13, 14.68, 21.41, 28.13, 33.89, 40.17, 45.45, and 49.1. As a check on these determinations the specific gravity at $\frac{25° \text{ C.}}{25° \text{ C.}}$ of each solution was measured by calibrated hydrometers which could be read to 0.0005. The densities at 25° C. were then calculated and converted to percentages by using data in the International Critical Tables. The average difference between the measurements by titration and specific gravity was less than 0.1

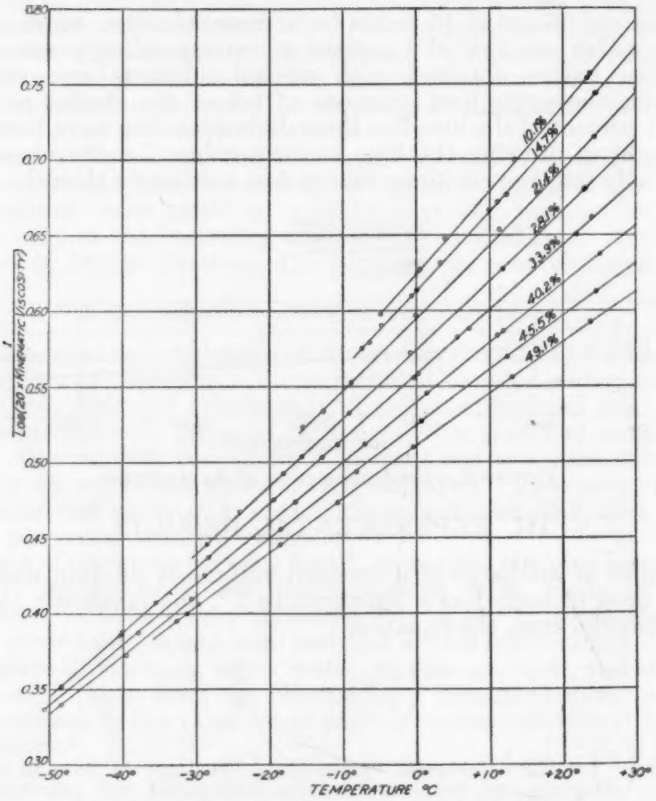

FIGURE 3.—*Plot of the experimental determinations.*

percent. The results given in this paper are based upon the values determined by titration.

The experimental results are shown in figure 3. In plotting these curves we have followed a suggestion, made by C. S. Cragoe, of this Bureau, that the reciprocal of log (20 × kinematic viscosity in centistokes) be plotted against temperature. Mr. Cragoe had found previously in the case of oils that an approximately linear relationship exists between this function and the temperature. The present work indicates that a similar relationship may exist for electrolytes.

The individual points shown in figure 3 are, for the most part, average results of 6 or 8 independent determinations. Some experi-

ments were repeated at slightly different temperatures. These are shown in this figure by closely adjacent points.

Since the experimental results could be plotted as nearly straight lines on a large scale, interpolation and extrapolation (over a few degrees) could be made easily and accurately. The values of the function

$$\frac{1}{\log (20 \times \text{kinematic viscosity})}$$

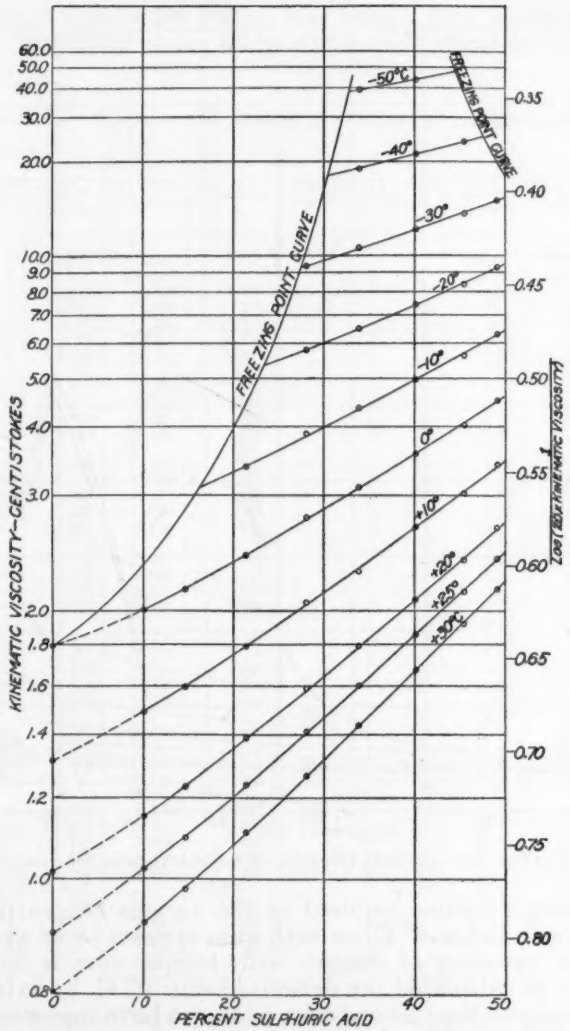

FIGURE 4.—*Kinematic viscosity of sulphuric-acid solutions.*

were read for each 10° of temperature and these values replotted as isothermal lines having percent composition of the solutions as the abscissas (fig. 4). The scale of kinematic viscosity, expressed in

centistokes at the left of the diagram, has been calculated to correspond with the scale at the right. The figure shows two branches of the freezing point curve which limit the isothermals at the lower temperatures. Values for water taken from the International Critical Tables are plotted at 0 percent in this figure.

In order to compute the viscosity of these solutions from the kinematic viscosity it is necessary to know the density of each solution at each temperature. We have employed existing data as given in the International Critical Tables for temperatures above 0° C. as a basis

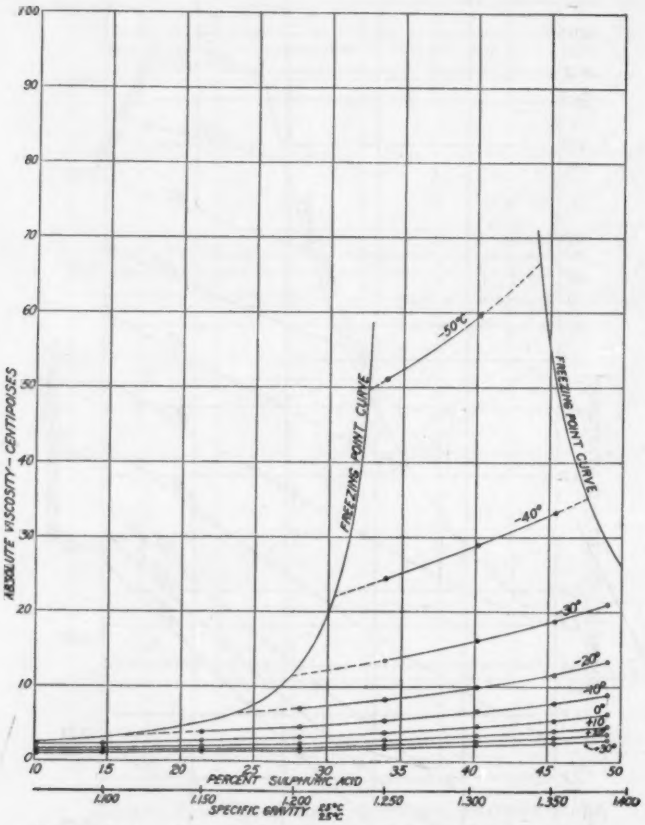

FIGURE 5.—*Absolute viscosity of sulphuric-acid solutions.*

for computing densities required at the various concentrations and temperatures. Below 0° C. no such data appears to be available.

Since the variation of density with temperature is linear above 0° C., we have calculated the densities below 0° C. by extrapolation. In order to check the values below 0° C. we have measured the contraction in volume of one solution as the temperature was decreased and found that the linear relation proved to be true. A pycnometer of Pyrex glass with graduated stem was used for this purpose. On the basis of the density of this solution at 0° C., as given by the International Critical Tables and the observed contraction in volume, the density of this solution at −50° C. was calculated to be 1.3550 and the

extrapolated value was 1.3548. The difference between these values is negligible in calculating the absolute viscosities.

The viscosity expressed in centipoises is given in figure 5. To this figure has been added a scale of specific gravities at 25° C. corresponding to the scale of percentages, in order to indicate more clearly the range of solutions which are customarily used in storage batteries.

Table 1 gives the numerical values for the kinematic viscosity, the absolute viscosity, and the fluidity (reciprocal of absolute viscosity) for sulphuric-acid solutions. In this table the viscosities are given to four significant figures for values less than 2.500, which are above 0° C. The remainder of the table is uniformly given to three significant figures.

TABLE 1.—*Viscosity and fluidity of solutions of sulphuric acid*

Temperature (° C.)	Percent H_2SO_4	Kinematic viscosity	Absolute viscosity	Fluidity	Temperature (° C.)	Percent H_2SO_4	Kinematic viscosity	Absolute viscosity	Fluidity
		Centistokes	*Centipoises*				*Centistokes*	*Centipoises*	
30	10	0.919	0.976	1.026	0	10	2.01	2.16	0.464
	15	.992	1.088	.919		15	2.16	2.41	.416
	20	1.081	1.225	.816		20	2.35	2.71	.369
	25	1.188	1.392	.718		25	2.58	3.08	.325
	30	1.318	1.596	.626		30	2.85	3.52	.284
	35	1.477	1.850	.541		35	3.17	4.04	.247
	40	1.670	2.163	.462		40	3.56	4.70	.213
	45	1.909	2.56	.391		45	4.03	5.49	.182
	50	2.214	3.07	.326		50	4.62	6.52	.153
25	10	1.026	1.091	.917	−10	20	3.30	3.82	.262
	15	1.108	1.218	.821		25	3.62	4.33	.231
	20	1.207	1.371	.729		30	4.00	4.95	.202
	25	1.327	1.559	.641		35	4.45	5.70	.175
	30	1.468	1.784	.561		40	4.98	6.60	.152
	35	1.645	2.067	.484		45	5.64	7.72	.129
	40	1.854	2.409	.415		50	6.45	9.15	.109
	45	2.120	2.85	.351	−20	25	5.50	6.63	.151
	50	2.447	3.40	.294		30	6.01	7.49	.133
20	10	1.152	1.228	.814		35	6.64	8.56	.117
	15	1.245	1.372	.729		40	7.42	9.89	.101
	20	1.356	1.545	.647		45	8.36	11.5	.0868
	25	1.490	1.755	.570		50	9.51	13.6	.0737
	30	1.646	2.006	.499	−30	30	9.73	12.2	.0820
	35	1.841	2.319	.431		35	10.7	13.9	.0718
	40	2.072	2.70	.370		40	11.9	16.0	.0626
	45	2.368	3.19	.313		45	13.4	18.6	.0539
	50	2.72	3.79	.264		50	15.1	21.7	.0460
10	10	1.490	1.595	.627	−40	35	19.4	25.3	.0395
	15	1.612	1.784	.561		40	21.4	28.8	.0347
	20	1.755	2.010	.498		45	23.7	33.0	.0303
	25	1.919	2.274	.440					
	30	2.124	2.60	.384	−50	35	40.2	52.6	.0190
	35	2.359	2.99	.335		40	43.9	59.5	.0168
	40	2.66	3.48	.287					
	45	3.02	4.09	.245					
	50	3.47	4.86	.206					

In dealing with storage batteries it is convenient to employ the values for fluidity, since the capacity of the battery and the fluidity of the solution vary together and inverse relationships are thereby avoided. An analysis of the data in table 1 shows that the percentage change in fluidity of sulphuric-acid solutions with change in temperature is practically the same for a specified temperature interval, irrespective of the concentration of the acid. That is, if some tempera-

ture, such as 25° C., be chosen as standard and the fluidity of each solution at that temperature called 100 percent, the fluidity of each solution at other temperatures will increase or decrease in the same proportion. This is shown in table 2. If the fluidity of any sulphuric-acid solution within the range covered by this paper is known at 25° C., the approximate fluidity at any other temperature may be calculated. The application of this simple relation, which is the same for the sulphuric-acid solutions as for water, is probably limited to solutions whose so-called "specific viscosity" at various concentrations is a constant or nearly constant quantity with change in temperature. The term specific viscosity is applied to the ratio of the absolute viscosity of the solution to the absolute viscosity of water at the same temperature.

TABLE 2.—*Percent change in fluidity with temperature*

Temperature (° C.)	Water		10 percent H_2SO_4		20 percent H_2SO_4		30 percent H_2SO_4		40 percent H_2SO_4		50 percent H_2SO_4	
	Fluidity	Percent fluidity	Fluidity	Percent fluidity	Fluidity	Percent fluidity	Fluidity	Percent fluidity	Fluidity	Percent fluidity	Fluidity	Percent fluidity
30	1.248	112	1.026	112	0.816	112	0.626	112	0.462	111	0.326	111
25	1.119	100	.917	100	.729	100	.561	100	.415	100	.294	100
20	.995	89	.814	89	.647	89	.499	89	.370	89	.264	90
10	.765	68	.627	68	.498	68	.384	68	.287	69	.206	70
0	.558	50	.464	51	.369	51	.284	51	.213	51	.153	52
−10					.262	36	.202	36	.152	37	.109	37
−20							.133	24	.101	24	.074	25
−30							.082	15	.062	15	.046	16
−40									.035	8.4		
−50									.017	4.1		

IV. DISCUSSION OF THE RESULTS

1. ACCURACY OF THE MEASUREMENTS

The experimental determinations plotted in figure 3 are mostly averages of repeated measurements, in some cases as many as 6 or 8 repetitions having been made. The average deviation of any point from its curve as drawn in figure 3 does not exceed 0.4 percent above −1° C., or 0.5 percent below −1° C. The number of points exceeding a deviation of 1 percent from the curve is 4 for the temperatures above −1° C. and 6 below this temperature out of a total of 70 points. The drawing of curves for figure 4 from which the values given in table 1 have been calculated has reduced deviations to a smaller percentage.

The measurements are subject to systematic errors from several sources. We have endeavored to avoid systematic errors in calibrating the instrument by using a variety of solutions and oils for which the viscosity is known. Since the time of discharge of the oils at 25° C. was equal to the longer periods required at the lowest temperatures for the sulphuric-acid solutions, drainage errors at the low temperatures are believed to be negligible. Referring to figure 2, it seems probable that any systematic errors in the constants of the instrument do not exceed 0.5 percent. The error caused by change in dimensions of the glass was calculated to be negligible.

Systematic errors in determining the composition of the solution have been avoided as far as possible by checking the results of titrations by measurements of specific gravity. The final results given in this paper are based on the titrations alone, but the difference between the two methods of standardizing the solutions would not change the viscosities by as much as 0.3 percent.

Accidental errors in measuring the temperature of the solutions were minimized by repetitions of the discharges. At temperatures above $-1°$ C. the error in temperature of a single determination did not exceed 0.05°. This would correspond to 0.1 percent error in the viscosity at 25° C. Below $-1°$ C. the viscosity increases rapidly with decreasing temperatures. At these temperatures the thermometer readings were estimated to tenth degrees and the average of 6 or 8 determinations were probably correct to 0.2° which corresponds to 2 percent of the viscosity at $-40°$ C. The errors arising from the temperature measurements are therefore somewhat variable with the temperature, but are estimated to be 0.1 percent at 25° C., 0.3 percent at 0° C., and 2.0 percent at $-40°$ C.

The errors in timing the discharges were minimized also by repetitions of the experiment. For a few of the fastest discharges the error in timing may have amounted to 0.5 percent. For most of the determinations, however, the error in timing probably did not exceed 0.2 percent and at the low temperatures 0.1 percent.

The last of the accidental sources of error to be mentioned is the adjustment of the head of the solution. The head was 10 cm so that an error of 0.5 mm would correspond to 0.5 percent in the viscosity measurement. The actual error from this source in the final results was probably not more than 0.2 percent.

In view of the estimated magnitude of the possible errors given above, it is believed that the values above $-1°$ C. are not in error by more than 1 percent. The values below $-1°$ C. vary somewhat in accuracy according to the temperature, the uncertainty being from 1 to 3 percent. These statements are based, however, on the assumption that the viscosities for the liquids used in calibrating the viscometer, as given in the International Critical Tables, are sufficiently accurate for the purpose.

2. COMPARISONS WITH PREVIOUS DETERMINATIONS

Comparisons have been made with the results obtained by others who have been mentioned in the introductory paragraphs. Since these earlier results cannot be calculated readily to the same percentages and temperatures, the comparison has been made graphically in figure 6. The curves have been drawn through the points plotted for the present results as given in table 1. The results of other workers have been plotted by distinctive characters. Excellent agreement between the results of Grunert, Wagner, Bingham, and Stone (except near 12 percent) and the results of the present investigation has been found. In figure 6 we have plotted also the values for sulphuric-acid solutions selected for the International Critical Tables.[9]

[9] Vol. 5, p. 12.

V. SUMMARY

Measurements of the viscosity of sulphuric-acid solutions containing 10 to 50 percent acid have been made over a temperature range from +30° to −50° C., except as the measurements were limited by freezing points.

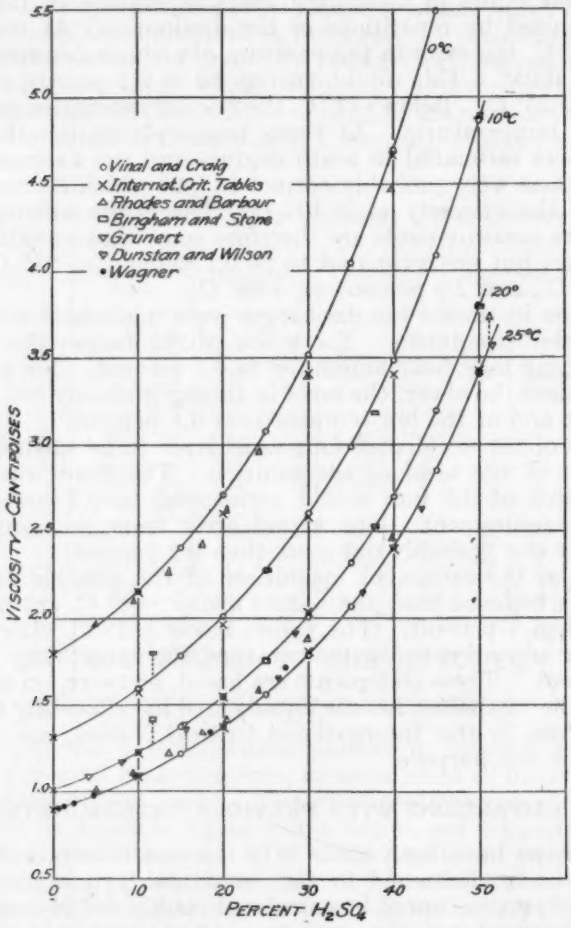

FIGURE 6.—*Comparison of values for the viscosity of sulphuric-acid solutions.*

The viscosity of these solutions at 0° C. is about 2.2 times as great as at +30° C., but at −50° C. the viscosity is 28 times as great.

Fluidities of the solutions have been calculated, since these are more simply related to changes in storage-battery capacity than the absolute viscosity.

The percentage change in fluidity of these solutions with temperature is very nearly the same irrespective of the percentage of acid contained in the solution.

VI. ACKNOWLEDGMENTS

The authors wish to thank C. S. Cragoe for permission to use his linear method of calculating the results in advance of his own publication describing it. They are also indebted for helpful advice to Dr. N. E. Dorsey and W. H. Herschel and R. C. Hardy. E. L. Peffer kindly calibrated the pycnometer used for checking the densities.

WASHINGTON, March 11, 1933.

COMPOSITION OF GRIDS FOR POSITIVE PLATES OF STORAGE BATTERIES AS A FACTOR INFLUENCING THE SULPHATION OF NEGATIVE PLATES

By G. W. Vinal, D. N. Craig, and C. L. Snyder

ABSTRACT

The conditions under which antimony, a constituent of battery grids, may produce detrimental effects in the operation of storage batteries have generally been regarded as exceptional. Recent experiments at the Bureau and elsewhere have shown, however, that the corrosion of the grids of positive plates, under normal operating conditions, may liberate antimony from the alloy in sufficient amounts to affect the operation and life of the negative plates. Two series of cells were prepared and operated in the laboratory to study the effect of varying the composition of the grids for positive plates. The first series included all cells having lead-antimony grids and the second included cells having positive grids containing various percentages of cadmium. Data on the capacity of these cells during 115 cycles are given, together with measurements of plate potentials, rate of sulphation, and the chemical analysis of the active material of negative plates for antimony.

CONTENTS

	Page
I. Introduction	795
II. Preparation of experimental plates	798
1. Grids	798
2. Pasting the plates	798
3. Formation of the plates	799
III. Apparatus for charging and discharging the batteries	799
IV. Antimony series of experiments	800
1. Capacity determinations	800
2. Loss of capacity on open circuit	801
3. Changes in plate potentials	802
4. Determination of antimony in the plates	803
5. Rate of sulphation of negative plates	804
V. Cadmium series of experiments	806
1. Capacity determinations	806
2. Rate of sulphation of negative plates	807
VI. Discussion of results	807
VII. Summary	807
VIII. Acknowledgment	808

I. INTRODUCTION

Antimony, when present in the active material of negative plates of storage batteries, is a cause of local action which results in the formation of lead sulphate and the liberation of hydrogen. Jumau [1] mentioned antimony as a cause of excessive sulphation of negative plates in a paper published in 1898 and 2 years later Strasser and Gahl [2] showed that hydrogen is liberated more easily on antimony

[1] Ecl. Electr., vol. 16, p. 133, 1898.
[2] Zs. Elektrochemie, vol. 7, p. 11, 1900.

than on lead. The rapid local action which is produced when freshly charged negative plates are immersed in electrolyte containing as little as 0.001 percent of antimony sulphate was measured quantitatively by Vinal and Schramm.[3]

Lead alloyed with antimony has been used for making the grids of pasted plates since Sellon [4] patented a grid of such material for storage batteries more than 50 years ago. His invention proved to be an important step in the development of storage batteries, since this alloy has good casting qualities and is stronger and less subject to corrosion than pure lead. Because of these and other desirable qualities, lead-antimony alloys have been used almost exclusively for making grids.

The antimony in the grid metal is not a source of serious local action at the negative plates, provided the antimony remains in the grids and is not deposited on the active material. Any antimony in the electrolyte, whether it comes from the grids or is present as an impurity from some other source, has been found to deposit on the active material of the negative plates. Analyses of electrolyte from batteries which have been in service seldom reveal appreciable amount of antimony, but analyses of the active material of the negative plates have shown one half percent or more of antimony in the surface layers. Jumau [5] found 40 percent of the antimony to have been deposited within 0.1 mm from the surface of the plate and 99 percent of the total in a layer of active material 1 mm deep. More recently Barrett,[6] who used the X-ray spectrograph to study the crystalline structure of lead sulphate, reported finding numerous lines from antimony and other unidentified crystals in the active material of discarded battery plates.

Conditions under which antimony may produce detrimental effects have generally been regarded as exceptional, but recent experiments by Crennell and Milligan [7] and by Schubert [8] as well as tests made at the Bureau of Standards have demonstrated that corrosion of the grid structure of positive plates, even in normal operation, may supply antimony to the negative plates in sufficient amounts to affect seriously their performance. During each period of charge, antimony from the positive grids is deposited in minute amounts upon the negative plates. It accumulates there and increases the rate of sulphation of these plates.

Crennell and Milligan have stated that there is no relation between the amount of antimony which is present in the active material and the rate of sulphation produced, because successive charges and discharges of the battery cover the antimony with lead or lead sulphate and thereby decrease its effect. Freshly deposited antimony is, however, very active, as the results of Vinal and Schramm have shown. This is to be expected because the overvoltage for hydrogen discharge on antimony is lower than on lead by 0.11 volt [9] or more.[10]

Other alloys of lead have been proposed at various times and some of these have been used in storage batteries to a limited extent. The

---

[3] J. Am. Inst. Elec. Eng., vol. 44, p. 128, 1925.
[4] British patent 3987 of 1881, French patent 147831 of 1882.
[5] Les accumulateurs Electriques, p. 350, 1907.
[6] J. Ind. & Eng. Chem., vol. 25, p. 298, 1933.
[7] Trans. Faraday Soc., vol. 27, p. 103, 1931.
[8] Paper read before National Battery Manufacturers Association Apr. 24, 1931.
[9] See footnote 7.
[10] See footnote 2, p. 795.

James [11] form of storage battery made use of an alloy containing 1 percent cadmium for the positive grids and 2 percent antimony for the negative grids. The Knowles [12] battery employed an alloy of 82 percent lead, 16 percent tin, 1.9 percent antimony, and 0.1 percent arsenic. The Worms [12] battery, 1892, used an alloy of 96.5 percent lead, 2.2 percent antimony, and 1.3 percent mercury. Grids for Julien [12] plates were made of 92 percent lead, 4.5 percent mercury, and 3.5 percent antimony. More recently patents have been issued for other compositions. An alloy of lead and barium was patented [13] in Germany in 1917. In 1923 Heil patented [14] a lead-cadmium alloy containing 2½ percent cadmium. Hagen [15] also patented a lead-cadmium alloy. LaRoche [16] patented an alloy of lead, nickel, silver, and cadmium, and Heil [17] patented a composition of lead with 0.5 per cent cadmium and 1 percent mercury. Gardner [18] patented a composition of lead and molybdenum and Kawakami [19] patented a composition of lead, antimony, and mercury. Alloys of lead and bismuth have been tried at the Bureau of Standards and by Schubert.[20]

Few data are available about the performance of grids made from these alloys. Obviously there is little to tempt the manufacturer to change from the established alloys of lead and antimony except as some other composition may be shown to be definitely superior.

It is not the purpose of this paper to advance claims for unusual compositions or new alloys, but rather to report the results of tests which have been made, showing the limitations imposed on the negative plates by antimony coming from the positive grids. Corrosion of the positive grids occurs slowly in the normal operation of a battery, and the service of the battery may extend over a long period of years. The Bureau has been called upon, however, to examine batteries in which more severe corrosion of the grid structure of the positive plates has caused the failure not only of these but the failure of the negative plates as well by excessive sulphation.

The experiments reported in this paper deal with batteries containing positive plates having grids made of lead-antimony alloys of varying composition and other batteries containing positive plates having grids of lead-cadmium alloys. The capacity of the individual cells was measured during 115 cycles of charge and discharge following which tests for the retention of charge were made. The rate of sulphation of the negative plates was determined by a method which has been described [21] previously. Significant changes in the charging potential of the negative plates were observed during the course of the work and these are compared with measurements on experimental cells to which portions of antimony were added. Analytical determinations of the amount of antimony present in the negative active material were made at the conclusion of the work.

---

[11] Electrician, vol 26, p. 751, 1891.
[12] The Storage Battery, by Treadwell, p. 51.
[13] German patent, 301380 of 1917.
[14] German patent, 385651 of 1923.
[15] German patent, 482061 of 1928.
[16] British patent, 119100 of 1918.
[17] British patent, 209749 of 1924.
[18] U.S. Patent, 938312 of 1909.
[19] U.S. Patent 1575167 of 1926.
[20] See footnote 8, p. 796.
[21] B.S.Tech. Paper no. 225, 1922.

II. PREPARATION OF THE EXPERIMENTAL PLATES

1. GRIDS

Grids of various alloy compositions were used in making the positive plates. Since most of the desired compositions were not available commercially, it was necessary to prepare these alloys and cast the grids in the laboratory. A few commercial grids were included in the experiments for comparison with the laboratory product. All of the grids were 5⅝ inches wide, 4⅞ inches high, and ⅛ inch thick. The grids cast in the laboratory differed in design from the commercial grids in having 27 horizontal crossbars (exclusive of the frame), while the commercial grids had 36 horizontal crossbars. This difference may explain some of the variations in performance of the cells as will appear in later paragraphs.

Grids for negative plates were all commercial grids of the same composition, since no question of the corrosion of these grids is involved.

The results of the work have been divided into two series of experiments. The first, called the antimony series, includes measurements on cells for which the positive grids were of lead alloyed with antimony in amounts ranging from 0 to 12 percent of antimony. The second series, called the cadmium series, includes results on all cells whose positive grids contained cadmium. The percentages of cadmium varied from 0.25 to 2 percent and several of these alloys also contained small percentages of antimony, since the casting qualities of the lead-cadmium alloys appeared to be improved by the addition of the antimony. The compositions of the various alloys is shown in tables 1 and 7. The materials used were refined grades of lead and antimony. The cadmium was part of the supply used for making standard cells.

2. PASTING THE PLATES

The grids were pasted in the laboratory, using nearly identical formulas for both positive and negative plates. This was done in order to avoid unnecessary variations in the materials employed. For the positives, litharge, having properties described below, was mixed with sulphuric acid, 1.100 specific gravity, in the proportion of 100 ml of solution per kilogram of oxide, and to the mix a small quantity of water was added to control the consistency of the paste. The same formula was employed for the negative plates with the addition of three eighths percent of lampblack. Mixing was done in a lead-lined mixing machine.

The properties of the oxide, determined by methods previously described,[22] were as follows:

Apparent density (Scott volumeter figure)		32.5
True density		9.54
Red lead content	percent	.8
Acid absorption	mg/g	80
Fineness:		
Cone 1 (Thompson classifier)	percent	29
Cone 2	do	17
Cone 3	do	15
Cone 4	do	12
Cone 5	do	27

[22] Vinal, Storage Batteries, 2d ed., pp. 20–21.

FIGURE 1.—*Life-test rack for the automatic control of charging and discharging storage batteries.*

UNIV. OF MICH.

After pasting, the plates were pickled for 20 hours in sulphuric acid having an initial specific gravity of 1.150 at 25° C.

3. FORMATION OF THE PLATES

Because of the various compositions of the grid metal, it was not advisable to form all the plates together. The plates were assembled, therefore, into groups according to the kind of grids. Separators of Port Orford cedar were inserted and the elements placed in individual jars. Each cell contained 5 positive plates and 6 negative plates.

Formation proceeded nearly uniformly in all cells, and no significant differences in the potentials of the positive plates were observed as a result of the differences in composition of the grids in these plates. At the conclusion of formation the cadmium readings on the positive plates were all within 0.01 volt of the value 2.45 volts, the current at this time being 2.1 amperes. Cadmium potentials of negative plates ranged from −0.13 to −0.09 volts. The more negative readings were obtained for plates in the cells whose positive grids contained the least amount of antimony.

III. APPARATUS FOR CHARGING AND DISCHARGING THE CELLS

The cells were charged and discharged automatically during 115 cycles except as the automatic control was omitted at intervals in order to determine the capacity of the individual cells to a final voltage of 1.75 volts per cell at the 5-hour rate.

The automatic control for making life tests of storage batteries has been in operation at the Bureau since 1930. This equipment, part of which is shown in figure 1, has not been described previously.

The essential parts of the equipment are:

1. *Time-controlled programs of charge and discharge.*—The clocks employed for these tests are the same as for the automatic testing of dry cells.[23] An additional program machine was provided for the storage-battery tests and the following schedule adopted:

4 p.m. charging begins.
7 a.m. charging ends.
10 a.m. discharging begins.
3 p.m. discharging ends.

When the program machine made contact at the time for charging to begin a latching relay was closed and this in turn closed the switch of the charging circuit and held it closed for a period of 15 hours when a second contact on the program machine unlatched the relay and terminated the charge. The discharge circuit for the batteries was operated as a separate circuit in a similar manner.

2. *Regulation of the current during charge and discharge.*—The current was adjusted initially to the proper value by inclosed carbon rheostats, one being provided for the charging circuit and a separate rheostat for the discharging circuit. The current for discharge was held constant automatically by the use of ballast resistance tubes consisting of iron filaments in an atmosphere of hydrogen. The particular tubes were rated for 6½ amperes so that two in parallel main-

[23] Commercial Standards Monthly, vol. 7, p. 37, 1930.

tained a current of 13 amperes, which is about the 5-hour rate for these batteries. The essential characteristic of these ballast tubes is their ability to maintain a constant current, although the voltage at the terminals of the tubes may vary from 10 to 30 volts. This allowed for variations in the voltage of the batteries during discharge, and no manual regulation was required. The current was held constant to within about 1 percent. Similar arrangements were available for charging the batteries, but the ballast tubes were not always used in the charging circuit because the cells could be charged satisfactorily without them.

3. *Recording meters.*—The electrical input and the output of the batteries were measured by ampere-hour meters mounted on the panels of each test rack. These can be seen in figure 1 to the right and left of the recording ampere-hour meter which is in the center of the panel. When measured discharges were made the current was indicated by an ammeter. The voltages of the individual cells were recorded and in addition the potentials of the positive and negative plates were measured with the cadmium electrode. The algebraic difference of the cadmium potentials of the positive and negative plates agreed with the measured cell voltage to within 0.01 volt in nearly all determinations. However, the presence of cadmium in the electrolyte of some of the cells as a result of corrosion of grids containing cadmium makes the readings with the cadmium electrode on such cells of doubtful value. We have given in this paper the cadmium potentials of the negative plates for the antimony series of experiments only.

IV. ANTIMONY SERIES OF EXPERIMENTS

1. CAPACITY DETERMINATIONS

The cells were connected in series and their capacities, voltages, and plate potentials were observed during 115 cycles of charge and discharge. Table 1 gives the results of measurements for 6 cycles at intervals during the course of the work, together with the composition of the grids of the positive plates in each cell. The capacity of each cell increased slowly. Cells A, B, and C, which contained grids having the least antimony, were not in as good condition as the others when the plates were examined at the end of the hundredth cycle. The pure-lead grids of the positive plates, cell A, were badly corroded and expanded and a short circuit was removed. Cell B was in about the same condition. Cell C had positive plates that were definitely better than in cells A and B, but one grid was cracked. All the other cells were in satisfactory condition.

TABLE 1.—*Capacity during 113 cycles of charge and discharge*

[Ampere-hours at the 5-hour rate]

Cell	Composition of positive grids		Cycle no. 2	Cycle no. 23	Cycle no. 49	Cycle no. 78	Cycle no. 91	Cycle no. 113	Condition of positive plates
	Lead	Antimony							
	Percent	*Percent*							
A	100	0	40	63	68	69	70	72	Corroded, expanded, and cracked.
B	99	1	47	65	68	74	75	68	Do.
C	97	3	53	63	66	72	70	74	1 grid cracked.
D	93	7	49	64	68	70	72	74	Good.
E	91	9	49	64	68	72	74	76	Do.
F	88	12	42	64	70	72	74	76	Do.
T	90	10	49	66	70	74	75	76	Do.
U	90	10	56	66	70	74	77	76	Do.
V	90	10	44	66	70	73	77	76	Do.

The table shows that the three cells, T, U, and V, which contained the commercial grids exceeded most of the others in capacity. This may have been the result of slightly greater amount of active material in these plates compared with the others. The general conclusion to be drawn from the results in table 1 is that no large differences in capacity resulted from variations in the antimony content of the positive grids.

2. LOSS OF CAPACITY ON OPEN CIRCUIT

Following the capacity measurements the cells were tested for loss of charge during 114 days. They remained on open circuit for this period at room temperature. The results are given in table 2. Cell B failed completely. The other cells, from A to F, showed increasing loss of charge as the percentage of antimony in the positive grids was increased. The capacity of the cells, however, was limited by the negative plates (except for cell A whose positives were badly corroded and expanded). The cells T, U, and V, containing the commercial grids, suffered a greater loss of charge than the others. It will be shown in table 5 that more antimony had been deposited on the negative plates of these cells.

TABLE 2.—*Retention of charge during standing test of 114 days*

Cell	Composition of positive grids		Loss of charge during 114 days	Remarks
	Lead	Antimony		
	Percent	*Percent*	*Percent*	
A	100	0	46	Positives limited capacity.
C	97	3	46	Negatives limited capacity.
D	93	7	54	Do.
E	91	9	59	Positives and negatives equal.
F	88	12	62	Negatives limited capacity.
T	90	10	70	Do.
U	90	10	72	Do.
V	90	10	70	Do.

3. CHANGES IN PLATE POTENTIALS

In table 3 the charging voltages and cadmium potentials of the negative plates are given. With few exceptions, the cell voltage was found to be lower and the negative plates less polarized in cells having the larger amounts of antimony in the positive grids. The high value of voltage for cell A (in which no antimony was present in the positive grids) is attributable to the high polarization of the negative plates. This is in marked contrast to cell F. The cadmium potential measurements on the positive plates of these two cells were the same within 0.01 volt. The results in table 3 show a decrease in the polarization of negatives for all cells having positive plates containing antimony.

TABLE 3.—*Changes in potential of the plates during 115 cycles*

[Values in volts at end of charging periods]

Cell	Composition of positive grid		Cycle 1		Cycle 23		Cycle 50		Cycle 115	
	Lead	Antimony	Cell	Negative Cd	Cell	Negative Cd	Cell	Negative Cd	Cell	Negative Cd
	Percent	*Percent*								
A	100	0	2.61	−0.15	2.74	−0.24	2.79	−0.24	2.82	−0.25
B	99	1	2.62	−.14	2.72	−.23	2.75	−.23		
C	97	3	2.63	−.13	2.73	−.22	2.76	−.24	2.60	−.10
D	93	7	2.61	−.13	2.71	−.22	2.73	−.22	2.59	−.06
E	91	9	2.60	−.12	2.69	−.20	2.73	−.21	2.53	−.02
F	88	12	2.57	−.11	2.67	−.19	2.71	−.19	2.56	−.02
T	90	10	2.60	−.13	2.69	−.19	2.70	−.16	2.52	.00
U	90	10	2.60	−.12	2.69	−.19	2.69	−.16	2.52	−.02
V	90	10	2.60	−.14	2.69	−.19	2.70	−.17	2.54	−.02

As a further test of the effect of antimony on the polarization of the negative plates, four negative plates were placed in separate containers with pure-lead positives and subjected to a prolonged charge (table 4). Two of the negative plates had been in active service 2 years; the others were previously unused. Cadmium readings on the positive plates all show a remarkable uniformity, but quite the contrary is true for the negative plates. Plates which had been in service previously did not reverse in potential to the cadmium electrode, as was observed in the case of unused plates.

TABLE 4.—*Effect of antimony on charging voltages and cadmium potentials*

[Specific gravity of electrolyte 1.190 at 25° C.]

[Negative plates of same make and type charged against pure-lead positives]

No.	Condition of cell	Voltage of cell	Positive cadmium potentials	Negative cadmium potentials
		Volts	*Volts*	*Volts*
1	Negative plates after 2 years' service	2.51	2.49	0.00
2	do	2.49	2.50	+.02
3	Unused negative plate	2.64	2.49	−.13
4	do	2.63	2.49	−.16
4	Unused negative plate, first portion of antimony added	2.51	2.49	−.05
4	Unused negative plate, second portion of antimony added			−.03
4	Unused negative plate, third portion of antimony added	2.54	2.50	−.01
4	Unused negative plate, fourth portion of antimony added	2.53	2.50	.00

After steady readings had been obtained, four portions of antimony were added to one of the cells (no. 4), and a decrease in polarization of the negative plates in this cell was observed while the charging current was maintained at its previous value. The antimony was added in the following manner: 100 ml of electrolyte was withdrawn from the cell, which contained a total of 700 ml of electrolyte. The portion withdrawn was saturated with antimony sulphate, $Sb_2(SO_4)_3$, filtered and returned to the cell. The three remaining portions were added, similarly, at intervals of one half hour, except that 50-ml portions were employed. The total amount of antimony added was small. Determination of the antimony, Sb, in solutions similarly treated indicated that the total amount added to the cell was probably less than ¼ g.

The cell voltage and cadmium potentials of plates in the cell to which antimony was added were unchanged on the following day. This was true also of the other cells to which antimony had not been added.

4. DETERMINATION OF ANTIMONY IN THE PLATES

Analytical determinations of antimony in the surface layers of active material of the negative plates were made after the completion of the sulphation tests reported in the next section. It is desirable, however, to present the analytical determinations before giving the results of the sulphation measurements.

After removing the negative plates from their respective solutions in the sulphation apparatus they were allowed to dry without washing. Samples of the surface material, which was largely lead sulphate, were removed with particular care to avoid including in the sample any portion of the grid material. Samples of about the same weight were removed from the same surface area of each plate in order that the depth of the removed layer should be approximately the same for each plate. The weight of each sample is given in table 5.

TABLE 5.—*Determination of antimony in active material of negative plates after 115 cycles against positive plates having grids containing various percentages of antimony*

Cell	Composition of positive grids		Weight of sample negative active material	Antimony found in active material	Average
	Lead	Antimony			
	Percent	*Percent*	*g*	*Percent*	*Percent*
A	100	0	1.08	0.04	0.04
			1.17	.04	
C	97	3	1.04	.12	.11
			1.20	.11	
			.91	.09	
D	93	7	.98	.25	.24
			1.15	.23	
E	91	9	1.47	.25	.26
			.97	.27	
			1.07	.26	
F	88	12	.99	.33	.32
			1.09	.31	
T	90	10	1.11	.50	.46
			1.21	.42	
V	90	10	1.22	.41	.41

The analytical procedure was as follows: 12 ml of concentrated sulphuric acid and about 5 g of potassium sulphate were added to the samples which had been placed in 500-ml flasks. Funnels with short stems partially closed the flasks. The contents of each flask was heated to the boiling point for 20 minutes. To each flask was then added 250 ml of water and 20 ml of hydrochloric acid and the solution boiled 5 minutes. The contents of each flask was then cooled to 10° C. and titrated with a permanganate solution which had an antimony titre of 0.00340 g. The volumes of permanganate used in the titrations were corrected for the "blank" determinations which required an average volume of 0.08 ml. As a check on the antimony determinations, a number of 0.1 g portions of the Bureau's standard sample of lead-base bearing metal were analyzed and the amounts of antimony found in each determination agreed well with the calculated amounts.

The results in table 5 show that the percentage of antimony found in the active material of the negative plates of cells A to F increased as the antimony content of the positive grids was increased. The commercial grids in cells T, U, and V, however, deposited greater amounts of antimony upon the negative plates. The reason for this is not altogether apparent, but a possible explanation is the fact that these grids had 36 crossbars compared with 27 for the grids in cells A to F. The 36 crossbars were finer in structure than the others, but the corrosion of the grids is probably localized at the surface of the plates and the number is of more significance therefore than the actual area or amount of the metal. Another possible explanation is found in the fact that the outer edges of the crossbars of the commercial grids were much sharper than the others. A nonuniform current distribution between grid and active material would result in an increased current density at the outer edges of these grid bars. This would accelerate the corrosion of these bars.

Although table 5 shows clearly that positive grids containing 9 and 12 percent antimony have deposited appreciably more antimony on the negative plates than those containing 3 and 7 percent of antimony, there is no exact proportionality between the composition of the positive grids and the antimony found in the negative active material after 115 cycles of charge and discharge.

5. RATE OF SULPHATION OF NEGATIVE PLATES

The "local action" produced at the surface of the plates when immersed in solutions of sulphuric acid results in the formation of lead sulphate and consequently a gain in weight of the plates. We have employed an apparatus, referred to previously, to determine the rate of local action when the plates were suspended in solutions of 1.250 specific gravity and maintained at 25° C. The results corrected for buoyancy are given in table 6.

TABLE 6.—*Rate of sulphation of negative plates in sulphuric acid solutions of 1.250 specific gravity at 25° C.*

Cell	Antimony in active material	Final charge		Increase in weight of negative plates—			
		Cell	Negative Cd	5 days	10 days	15 days	25 days
	Percent	*Volts*	*Volts*	*g*	*g*	*g*	*g*
A	0.0$_4$	2.82	−0.25	0.8	1.5	2.0	3.0
C	.1$_1$	2.60	−.10	1.0	1.9	2.7	4.2
D	.2$_4$	2.59	−.06	1.6	3.0	4.2	6.6
E	.2$_6$	2.53	−.02	1.8	3.3	4.7	7.4
F	.3$_2$	2.56	−.02	2.4	4.3	6.1	9.5
V	.4$_1$	2.54	−.02	2.7	4.8	6.9	10.7
U		2.52	−.02	3.3	6.1	8.7	13.5
T	.4$_8$	2.52	.00	3.4	6.5	9.1	13.6

The chemical reaction is believed to take place according to the equation

$$Pb + H_2SO_4 \rightarrow PbSO_4 + H_2$$

This reaction might also be measured by determining the volume of hydrogen liberated as a result of the reaction. Crennell and Milligan,[24] and others have used such a method. Since the overvoltage for hydrogen discharge on antimony is less than on lead, this reaction will proceed more rapidly when antimony is present in the active material of the plate, provided the antimony is not covered by lead or lead sulphate and thereby rendered ineffective.

The results in table 6 show increased rates of sulphation as the amount of antimony in the active material increased. An exact proportionality between all values does not exist. Grids of similar design but varying in percentages of antimony will liberate antimony in the electrolyte in proportion to the antimony which they contain, provided there is no appreciable difference in the relative rate of corrosion. Antimony will deposit on the negative plates in the same proportion as the amounts set free in the electrolyte. The freshly deposited antimony is therefore proportionately greater on those plates operating in the cells with positives of high antimony content, and the total amount of antimony in the active material of the negative plates is also proportionately greater as was observed in the case of cells D, E, and F. In cell C, however, where the grid corrosion exceeded that in D, E, and F the antimony found in the active material and the rate of sulphation are both more than proportionately greater. It does not follow necessarily that the rate of sulphation is proportional to the total amount of antimony present except as the freshly deposited antimony is also proportional to the total amount.

The results in table 6 show that the rate of sulphation for plates from cell A (which contained positive grids of pure lead) was very small. A gain in weight of 3 g per plate is equivalent to a discharge of 1.68 ampere-hours by local action in 25 days or one fourth the loss in cells T, U, and V which contained plates with the ordinary commercial grids.

Local action on negative plates has been attributed sometimes to certain materials used as expanders. In the present experiments

[24] World Power, vol. 17, p. 406, 1932.

all of the negative plates were pasted with the same materials and the results are comparable. It is evident that local action caused by the expander is small compared with that caused by antimony.

V. CADMIUM SERIES OF EXPERIMENTS

1. CAPACITY DETERMINATIONS

The cells containing positive grids consisting of alloys of lead and cadmium were made and operated in a similar manner to that described in the preceding antimony series of experiments. The composition of the positive grids for these cells is shown in table 7. Most of these cells compared favorably in capacity with the cells of the antimony series until near the end of the experiment. Examination of the plates was made after the hundredth cycle and the condition of the positive plates is described in the last column. The positive grids were all corroded and expanded, except in cells O, P, and S. The negative plates in all cells were in good condition, however. One of the most striking features revealed by the examination of the plates was the formation of compact and adherent moss on the lower part and sides of the elements. This was found in nearly all cells containing cadmium. The moss was removed before continuing the test of these cells.

TABLE 7.—*Capacity of cells having cadmium in positive grids*

Cell	Composition of positive grids			Cycle no. 2	Cycle no. 23	Cycle no. 49	Cycle no. 78	Cycle no. 91	Cycle no. 113	Condition of positive plates
	Lead	Antimony	Cadmium							
	Percent	*Percent*	*Percent*	*Amp.-hr.*	*Amp.-hr.*	*Amp.-hr.*	*Amp.-hr.*	*Amp.-hr.*	*Amp.-hr.*	
A	100	0	0	40	63	68	69	70	72	Corroded, expanded, and cracked.
G	99	0	1	42	63	64	72	65	64	Corroded, expanded, moss.
H	98	0	2	42	63	67	70	74	68	Do.
I	98.75	.25	1	49	63	64	68	62	62	Do.
J	97.75	.25	2	49	63	65	68	72	75	Do.
K	99	.5	.5	51	62	63	70	72	69	Do.
L	98.5	.5	1	42	61	64	66	72	69	Do.
M	97.5	.5	2	51	65	64	69	66	65	Do.
N	98.5	1	.5	40	62	65	74	66	72	Do.
O	97	1	2	42	62	62	64	66	64	Better condition, no moss.
P	97	2	1	42	61	62	62	68	72	Do.
S	96	2	2	42	61	63	66	62	72	Good condition, some moss.

The grids containing cadmium did not give as good service as those containing antimony in the usual amounts. They were distinctly better, however, than grids of lead-bismuth alloys which were tested previously. With improved technic for casting the lead-cadmium alloys, it is possible that such grids could be improved. Corrosion may have been accelerated by slight porosity of the metal. The fact that the plates were formed with the separators present in the element may have been a factor in causing corrosion. Corrosion of grids has been found to be serious when minute amounts of volatile organic acids have direct access to the bare metal during charge. Lead sul-

phate affords little protection to lead against the attack of such acids, but lead dioxide, when formed, is a much more effective covering.

2. RATE OF SULPHATION OF NEGATIVE PLATES

Experiments on the rate of sulphation of the negative plates after 115 cycles were made similarly to those reported for the antimony series. The results are given in table 8. The contrast between the results in this table and those in table 6 for the cells containing antimony grids is very marked. The increase in weight of the plates (table 8) because of the formation of lead sulphate is less in every case than for any cell in table 6 with the single exception of cell A, which contained no antimony. At the same rate of local action some of these plates could have stood for a year without being completely discharged.

TABLE 8.—*Rate of sulphation of negative plates in sulphuric-acid solutions of 1.250 specific gravity at 25° C.*

Cell	Increase in weight of negative plates				Cell	Increase in weight of negative plates			
	5 days	10 days	15 days	25 days		5 days	10 days	15 days	25 days
	g	g	g	g		g	g	g	g
A	0.8	1.5	2.0	3.0	M	0.6	1.1	1.7	2.5
G	.7	1.4	1.9	2.9	P	.8	1.4	1.8	2.7
H	.6	1.1	1.5	2.4	S	.9	1.7	2.3	3.5
L	.7	1.3	1.8	2.8					

VI. DISCUSSION OF RESULTS

The higher rate of sulphation of negative plates previously cycled with positives whose grids contain antimony in customary amounts, compared with the negligible rate of sulphation of similar plates cycled with pure-lead positives or those containing little or no antimony, is convincing evidence that the composition of the positive grids is an important factor influencing the operation of the negative plates. The effects of antimony on the negative plates are not the result of exceptional conditions, but may be expected in the ordinary conditions of operation of batteries.

Some of the advantages to be gained in the operation of negative plates by curtailing the use of antimony in the positive plates are: (*a*) Longer life of the negative plates in service; (*b*) more uniform cell voltages and plate potentials during the life of the cell; (*c*) less local action at the negative plates when battery is inactive; (*d*) less occasion for overcharging batteries, because of less sulphation of the negatives; and (*e*) less possibility for the formation of stibine when hydrogen is discharged on antimony.

To gain such advantages for the negative plates, however, requires the solution of difficult problems regarding the construction of the positive plates.

VII. SUMMARY

The effect of antimony in producing excessive sulphation of negative plates in storage batteries has been known previously, but recent experiments at the Bureau of Standards and elsewhere have shown that the small amounts of antimony released from the positive grids

in the course of normal operation of batteries are sufficient to affect the negative plates.

Batteries have been made and operated in the laboratory to test the effect of varying the composition of the grids for positive plates. The alloys, which were employed in this work, included a series of lead-antimony and lead-cadmium compositions.

The operation of the batteries was observed during 115 cycles of charge and discharge. For the most part, the cycling of the batteries was controlled automatically, but measurements of capacity and plate potentials were made at intervals during the course of the tests.

No large differences in capacity resulted from variations in the antimony content of the positive grids, but grids containing 3 percent or less of antimony were not as durable as those of customary compositions.

Tests for loss of charge on standing for a period of 114 days showed the loss to be greater in those cells containing the higher percentages of antimony in the positive grids. The capacity of the cells, with one exception, was limited by the negative plates, however, and these were found to contain measurable quantities of antimony in the active material after completing 115 cycles of charge and discharge.

The percentage of antimony found by analysis in the active material of the negative plates was greater in those cells whose positive grids contained the greater percentages of antimony. The analysis for antimony was made at the conclusion of 115 cycles of charge and discharge.

Local action produced at the surface of the negative plates was measured by weighing the plates at intervals while they were suspended in solutions of sulphuric acid and maintained at a constant temperature. The plates having the greatest amount of antimony in the active material sulphated the most rapidly. The negative plates from cells whose positive grids were made of pure lead or the lead-cadmium alloys sulphated less than the others.

Positive grids of lead-cadmium alloys did not prove to be as durable as the lead-antimony alloys in these experiments. The operation of negative plates was improved, however, by the absence of antimony from the positive grids. Part of the difficulty with the lead-cadmium alloys may have been caused by insufficient experience in using such material in batteries.

VIII. ACKNOWLEDGMENT

The authors are indebted to J. A. Scherrer for assistance in the chemical analysis for antimony in the active material of the negative plates.

WASHINGTON, April 6, 1933.

THE FREEZING POINT OF IRIDIUM

By F. Henning[1] and H. T. Wensel[2]

ABSTRACT

The ratio of brightness for red light of a black body immersed in freezing iridium to that of a similar black body immersed in freezing gold was measured both directly and indirectly. The indirect method consisted in determining the ratio of brightness at the iridium and platinum freezing points and calculating the result from the previously determined platinum to gold ratio. The two methods, agreeing with each other within experimental errors, yielded a value for the iridium to gold ratio of 4,380 at wave length 0.652 μ. This fixes the freezing point of iridium on the International Temperature Scale as 2,454° C.

CONTENTS

		Page
I.	Introduction	809
II.	Previous work	810
III.	Present work	813
	1. The iridium	813
	2. The furnace and crucible	814
	3. Method of observation	814
	4. Determination of effective wave length	814
IV.	Results	817
V.	Summary	819
VI.	Acknowledgments	819
VII.	Appendix. Preparation and purity of iridium	819

I. INTRODUCTION

In making an accurate determination of the freezing or melting temperature of a pure metal, one of the objects is usually a more accurate establishment of the temperature scale in practical use by providing an additional known fixed point at which temperature measuring equipment may be checked. In the present work, however, this item was of comparatively small importance. The extremely high cost of the metal, the difficulty of purifying it to the required degree, and the difficulties encountered in melting the metal under suitable conditions prohibit its use as a secondary thermometric fixed point except in very unusual cases. Indeed these factors would have rendered the result obtained in the present work scarcely worth the effort put forth were it not for the fact that data were obtained which are greatly needed in connection with standards in other fields.

The color temperature scales used by various laboratories are not on a very satisfactory basis. Not much is known concerning the agreement of these scales and in some cases even the basis for the

[1] Chief of the Division of Heat and Pressure, Physikalisch-Technische Reichsanstalt. This investigation was carried out at the Bureau of Standards under an arrangement for an exchange of personnel between these institutions.

[2] Chief of the Pyrometry Section, Bureau of Standards.

scale is not definitely set forth. A project is under way at the Bureau of Standards to establish a color temperature scale based on the colors of black bodies maintained at the freezing points of platinum, rhodium, and iridium. For this, accurate values for the temperatures of these fixed points are essential.

The primary purpose, however, for which this work was undertaken was to secure data bearing upon the basic standards in the field of photometry. If a carbon filament electric lamp operating at the color temperature of the platinum point be photometered against a black body immersed in freezing platinum [3] and a tungsten electric lamp operating at the color temperature of the iridium point be photometered against a black body immersed in freezing iridium, then the relative candlepowers of these two lamps can be calculated from the temperatures of the two black bodies employed. This provides a method for comparing two photometric standard lamps differing widely in color which avoids the difficulties met with in heterochromatic photometry.

These two applications of the black body immersed in freezing iridium will be reported in subsequent papers and have been mentioned here merely to explain why extreme accuracy was sought in this determination of the freezing temperature.

II. PREVIOUS WORK

For the past 25 years the value 2,350° C. has been almost universally accepted as the melting point of iridium. It appears in practically all the tables of melting points, such as those of Landolt and Börnstein, and is listed in the International Critical Tables as 23_{50}, indicating that this value is uncertain by at least 100°. After the present work had yielded a value some 100° C. higher than this, a critical analysis of the literature led to the conclusion that previous work alone indicated the freezing point of iridium to be 2,435° C. with an uncertainty of perhaps 25° or 30° C. In view of this condition it was thought advisable to discuss the published work in greater detail than would otherwise seem warranted.

The high temperature scale is defined by the equation

$$\frac{1}{t+273}=\frac{1}{t_{Au}+273}-\frac{\lambda \log_e \frac{J}{J_{Au}}}{C_2} \qquad (1)$$

in which t is the temperature in degrees centigrade, t_{Au} is the temperature of freezing or melting gold, $\frac{J}{J_{Au}}$ is the ratio of the intensities of the radiation at wave length λ emitted by black bodies at the above two temperatures, and C_2 is a constant. A measurement of $\frac{J}{J_{Au}}$, together with a determination of the corresponding λ, obviously determines t, once t_{Au} and C_2 are fixed. It is equally obvious that a change in the value assigned to either C_2 or the gold point will produce a change in the numerical value of t. During the past 30 years some 10 or 12 different values have at some time or other been assigned

[3] The Waidner-Burgess Standard of Light, B.S.Jour. Research, vol. 6, p. 1103, 1931.

to C_2, the value on the present International Temperature Scale[4] being 1.432 cm degrees. The gold point on this scale is defined as 1,063° C.

The utility of a temperature determination which has been made by measuring λ and the ratio of brightness is not affected when a new scale is adopted, since the numerical value of the temperature may be equally well calculated on the new scale. It is essential, however, to reduce such values to a common scale for purposes of comparison.

The earliest experiments of any consequence on the temperature of the iridium point are those of Nernst,[5] who measured the brightness of black bodies at the platinum and iridium points in terms of the Hefner Kerze. The values first reported were, respectively, 91 and 1,210 H.K. per cm^2. Light of the whole spectrum was used instead of monochromatic light, so that equation (1) cannot be applied. Nernst calculated the temperature of the iridium point as 2,203° C. on the assumption that the brightness of a black body is 47 H.K. per cm^2 at 1,690° C. and varies as the fourteenth power of the absolute temperature. On the basis of our present knowledge of the relation between the photometric brightness and temperature it is possible to calculate the iridium point from the ratio 1,210 to 91 obtained by Nernst at the iridium and platinum points. Nernst [6] himself, however, showed later that due to contamination of his platinum specimens with iridium, the temperature of the furnace in his first work had been about 50° C. above the platinum point when the brightness was measured as 91 H.K. per cm^2. Taking precautions to avoid this contamination in his later work, he obtained a value of 63.4 H.K. per cm^2.

Nernst made an attempt to express his 1906 results in terms of the Reichsanstalt scale and obtained the value 2,348°, which is equivalent to 2,394° C. on the present scale. However, this value is dependent on the degree of success which Nernst met with in making the transfer, and a more reliable value can be deduced directly from the measured ratio of brightness 1,210/63.4.

Calculation based on the I.C.I.[7] visibility factors shows that two black bodies, one at 2,428° C. and the other at the platinum point, taken as 1,773.5° C.[8] will have a ratio of brightness 1,210/63.4 for a normal observer. The ratio measured by Nernst, therefore, leads directly to a value of 2,428° C. (Int.) for the iridium point, which is probably the best one to be found in the literature, since it is independent of the photometric unit used and depends only on the purity of the metals and the accuracy with which the ratio determined corresponds to that for a normal observer.

Mendenhall and Ingersoll [9] determined the melting point of minute bits of iridium placed on top of a Nernst glower. The temperature

[4] Proc. Seventh Gen. Conf. of Weights and Measures, p. 56, 1927; Text in annex 4, p. 94; B.S.Jour. Research, vol. 1, p. 635, 1928; Zs. f. Phys., vol. 49, p. 742, 1928.
[5] Phys. Zeits., vol. 4, p. 733, 1903.
[6] Phys. Zeits., vol. 7, p. 380, 1906.
[7] Recueil des Travaux, I.C.I., 16th session (Geneva), p. 67, 1924. See also B.S.Sci. Papers, vol. 16, p. 131, 1923–24.
[8] B.S.Jour. Research, vol. 6, p. 1119, 1931.
[9] Phys. Rev., vol. 25, p. 1, 1907.

of the glower was obtained by extrapolation of the empirical isochromatic radiation formula

$$\log E = K_1 + \frac{K_2}{t+273} \tag{2}$$

The gold point, taken as 1,065° C. and the platinum point, taken as 1,745° or 1,789° C., were used to determine the necessary constants. The iridium point was reported as 2,292° or 2,388° C., according to the value accepted for the platinum point.

The paper does not mention the values obtained for either the E's or the K's in equation (2). From the two values of the iridium point calculated from the two corresponding platinum points, however, it is possible to solve for the K's in equation (2) and deduce a value of 2,360° C. on the basis of the gold point being 1,063° and the platinum point 1,773.5° C. However, the results are stated to be consistent with a value of $C_2 = 1.65$ cm degrees. If their mean values for platinum, iridium, and C_2 are used, a recalculation on the basis of present data ($C_2 = 1.432$ and $Pt = 1{,}773.5$° C.) yields the value 2,468° C. for the iridium point. Neither of these methods of calculation is free from objection and we can only conclude that the result corresponds to a value between 2,360° and 2,468° C., the mean of which is 2,414° C.

In 1905 Holborn and Henning [10] reported a value of 2,000° C. for the apparent temperature of melting iridium measured at wave length 0.643 μ and using 1.45 cm degrees for C_2. No attempt was made to convert the value obtained to true temperature while the fact that the reported value was rounded to the nearest 100° indicates its approximate nature. However, five years later H. von Wartenberg [11] determined the reflection factors for a number of metals and used the value 0.752 (emissivity 0.248) obtained for iridium to convert the value of Holborn and Henning to true temperature. The value there calculated reduces to 2,407° C. (Int.).

Von Wartenberg [11] also reported a value of 2,360° C. measured by himself on the basis of 1,745° C. for the platinum point and 1.46 cm degrees for C_2. This value becomes 2,425° C. on the present scale ($C_2 = 1.432$ cm degrees) if the platinum point be taken as 1,773.5.

In 1916, Burgess [12] reported a value of 2,400° C. which reduces to 2,418° C. (Int.), but the value was reported as doubtful.

An accurate value for the apparent temperature of the iridium point was obtained by Henning and Heuse [13] in 1924. The value, 2,068° C. was found for wave length 0.622 μ. Using v. Wartenberg's value of 0.248 for the emissivity, this reduces to 2,458° C. (Int.).

A change of 10 percent in the value of the emissivity used, however, will result in a change of about 30° in the result. If, therefore, the temperature be calculated on the basis of an emissivity of 0.3 as found by Burgess and Waltenberg [14] the value, 2,395° C. is obtained for the melting point.

Since the presentation of the present work [15] before the Optical Society of America, October 22, 1931, von Wartenberg, Werth, and

[10] Berl. Ber., p. 317, 1905.
[11] Verh. Deut. Phys. Gesell., vol. 12, p. 105, 1910; and vol. 12, p. 121, 1910.
[12] J. Frank. Inst., vol. 182 p. 19, 1916.
[13] Zeits. f. Physik., vol. 29, p. 157, 1924.
[14] B.S. Bull., vol. 11, p. 591, 1915.
[15] J. Opt. Soc. Am., vol. 22, 1, p. 7, January 1932.

Reusch [16] have reported a value of 2,440° ± 25° C. The values obtained, however, ranged from 2,390° to 2,470° C.

The mean of the seven determinations listed in table 1 is 2,424° C. with an uncertainty of perhaps 40°. A weighted mean of the above values would undoubtedly be subject to a lesser uncertainty, but, instead of assigning weights, three values obtained by three different methods have been starred in table 1. Each of these starred values is, in our opinion, the best one for a particular method. The average of these three values is 2,442° C. with an uncertainty of perhaps 25° C.

TABLE 1.—*Summary of values previously reported for the melting point of iridium*

Observers	Year	Scale used	Temperature			Remarks
			Reported		International scale	
			Apparent	True		
			° C.	° C.	° C.	
Nernst	1903	$B=63.4\left(\frac{t+273}{1,690}\right)^{14}$		2,203	(?)	Scale indefinite.
Do	1906	Gold point, 1,064; C_2=1.46 cm degrees.		2,348	2,428*	Calculated directly from Nernst's measurements.
Mendenhall and Ingersoll.	1907	Gold point, 1,065; platinum point, 1,789; C_2=1.65 cm degrees.		2,388	2,414?	Conversion to International scale very uncertain.
Holborn and Henning.	1905	Gold point, 1,064; C_2=1.46 cm degrees.	2,000			[True temperature calculated by v. Wartenberg from work of Holborn and Henning taking emissivity as 0.248.
v. Wartenberg	1910	Computed value from work of Holborn and Henning.		2,348	2,394	
Do	1910	Platinum point, 1,745; C_2 =1.46 cm degrees.		2,360	2,425	Emissivity taken as 0.248.
Burgess	1916	Gold point, 1,063; C_2= 1.445 cm degrees.		2,400	2,418	Value reported as doubtful.
Henning and Heuse.	1924	Gold point, 1,063; C_2=1.43 cm degrees.	2,068		2,458*	Emissivity taken as 0.248.
v. Wartenberg, Werth, and Reusch.	1932	International		2,440	2,440*	Range of values 2,390 to 2,470.

	° C.
Unweighted mean of all values	2,424
Mean of 3 best values (*)	2,442

III. PRESENT WORK

1. THE IRIDIUM

The iridium used in this work is believed to have contained less than 0.01 percent of metallic impurities, undoubtedly the first iridium that has been prepared in a state of purity even approaching this. The production of iridium of this purity is considered to be of such significance that we have requested Dr. E. Wichers to describe, in the appendix, the special methods which were used in preparing the sponge.

The melting of the sponge and the preparation of an ingot which would fit into the crucible and into which a sight tube or black body could be inserted was not by any means a simple matter. Because of the high melting point, it was not considered advisable to attempt the casting of an ingot as can so easily be done with platinum.

[16] Zs. f. Elektrochem., vol. 38, p. 50, 1932.

The sponge was compressed to a specific gravity of about 12 or 14 and several compressed pellets placed in a crucible of the kind used in the actual observations. The compressed sponge suffered considerable shrinkage in the melting and additional pellets were added after each melting until an ingot of approximately 200 g and specific gravity of 22.5 was obtained.

After the ingot was removed from the crucible it was found that distortion of the crucible caused sufficient change in the shape of the ingot to prevent its fitting a new crucible. The ingot was therefore hot swaged by hand until it fitted loosely into a new crucible.

Iridium of high purity is extremely difficult to drill. It was found that a hole 3.5 mm in diameter could be laboriously drilled along the axis with drills tipped with tungsten carbide.

After swaging and drilling, the ingot was immersed for about 30 minutes in molten potassium pyrosulphate to remove surface contamination.

2. THE FURNACE AND CRUCIBLE

The arrangement of crucible, immersed black body or sight tube, insulation, and metal was identical with that used in the work on the Waidner-Burgess Standard of Light [17] and shown there in figures 1 and 2. The advantages to be gained from the use of the induction furnace are likewise described there.

The only difference between the work on platinum and iridium, aside from the metals used, lay in the fact that in the latter case the crucibles and sight tubes were fired to a temperature of about 2,500° C. before use. This was done in the induction furnace by placing the crucibles inside a graphite cylinder with zirconium oxide packed between the crucible and the graphite cylinder. In firing the crucibles in this way a layer of the zirconium oxide packing next to the graphite was contaminated with carbon, but the crucibles were not affected.

3. METHOD OF OBSERVATION

The method of observation and the pyrometer used were the same as were used in determining the freezing point of platinum [18] and the measurement of the ratio of brightness from gold to iridium was made in two steps as there described. The observations on the black body immersed in iridium were taken through a sector disk with an opening of 2°44′38″ (transmission 0.7622 percent). The lamp was consequently operated at a temperature of about 1,425° C. The exact value of this temperature was determined by means of a second sector with an opening of 9°27′16″ (transmission 2.626 percent). The combination of the two sectors corresponded to the ratio of brightness from the iridium point to a temperature within about 10° of the gold point. Four observers participated in determining the ratio of brightness at the iridium point to that at the gold point.

After making a series of nine freezes, the iridium was allowed to cool to room temperature. Upon melting the iridium again, it was found that the sight tube was broken and it was therefore necessary to again swage, drill, and treat with molten potassium pyrosulphate. We have found it necessary to mount the iridium ingot in a new crucible each time it has been cooled to room temperature after a series of observations.

---

[17] B.S.Jour. Research, 6, p. 1103, 1931.
[18] B.S.Jour. Research, vol. 6, p. 1119, 1931.

Additional data for calculating the iridium point in terms of the platinum point were obtained by measuring the ratio of brightness—iridium to platinum. This was done by operating the pyrometer lamp at the platinum point and making observations on the black body immersed in freezing platinum and, through a sector of 6.96 percent transmission, on the black body immersed in freezing iridium.

This operating temperature is above the range in which pyrometer lamps are customarily operated. By taking readings on platinum before and after the readings on iridium, however, the effect of any change in the lamp, if not too large, will be eliminated. As a matter of fact it was found that the total change in the lamp during this phase of the work corresponded to a difference of only 0.3° C. in the value of the iridium point.

In this part of the work only three observers participated as the work could not be completed during the two months' exchange of personnel.

4. DETERMINATION OF EFFECTIVE WAVE LENGTH

Due to the large temperature step from the gold point to the iridium point the individual characteristics of the observers' eyes produce a noticeable effect. For this reason it was decided not to use the same effective wave length; that is, the average for all the observers, in calculating the results as was done in the determination of the platinum point.[19] Moreover, it was necessary to know the effective wave length very accurately. For this reason the following investigation was carried out.

A reflecting test plate of milk glass smoked with magnesium oxide was illuminated by a tungsten lamp operating at a color temperature of approximately 2,600° K. The distance between this lamp which will be called the source and the test plate was adjusted until the optical pyrometer indicated about 1,300° K. when sighted upon this test plate with no absorption device interposed. The observer matched the brightness of the lamp filament, whose color temperature was near the gold point, with that of the test plate, whose color temperature was near the iridium point.

Eight men from other sections of the Bureau, whose visual characteristics had been determined by Gibson and Tyndall [20] so that the effective wave length of the red screen used could be calculated for each of the eight, were compared with the men who made the observations on the freezing point of iridium. The method of making the comparisons was as follows: Four settings were made by observer A, then four by observer B, four more by observer A, four more by observer B, and finally four by observer A.

Let the effective wave length of the red screen for the temperature interval in question, calculated on the basis of A's visibility, be λ_A and let that for observer B, which is to be determined, be λ_B. Further let θ_s be the color temperature of the source, θ_A the apparent brightness temperature of the test plate determined from the pyrometer settings of A, and let $\theta_A + \Delta\theta_A$ be the corresponding value determined from the pyrometer settings of observer B.

[19] See footnote 18 p. 814.
[20] B.S. Bull., vol. 19, p. 131, 1923.

$$\frac{1}{\theta_s}-\frac{1}{\theta_A}=\frac{\lambda_A \log_e R}{C_2} \tag{3}$$

and

$$\frac{1}{\theta_s}-\frac{1}{\theta_A+\Delta\theta_A}=\frac{\lambda_B \log_e R}{C_2} \tag{4}$$

Hence

$$\frac{\frac{1}{\theta_s}-\frac{1}{\theta_A}}{\frac{1}{\theta_s}-\frac{1}{\theta_A+\Delta\theta_A}}=\frac{\lambda_A}{\lambda_B} \tag{5}$$

$$1+\frac{\theta_s\Delta\theta_A}{\theta_s\theta_A-\theta_A{}^2-\theta_A\Delta\theta_A}=1-\frac{\lambda_B-\lambda_A}{\lambda_B}$$

or

$$\lambda_B-\lambda_A=-\lambda_B\frac{\theta_s\Delta\theta_A}{\theta_s\theta_A-\theta_A{}^2-\theta_A\Delta\theta_A} \tag{7}$$

Now since $\lambda_B-\lambda_A$ need never be known to better than about 10 percent, it is evident for the case in question, where $\theta_s=2\theta_A=2{,}600°$ K., that θ_s and θ_A need be known only approximately, say to the nearest 100° or 200° K., and that the term $\theta_A\Delta\theta_A$ may be neglected. λ_B is approximately 0.65 μ and consequently

$$\frac{\lambda_B-\lambda_A}{\Delta\theta_A}=-0.001\ \mu/\text{degree} \tag{8}$$

The minus sign means that the effective wave length is greater for the observer whose setting of the pyrometer is the lower. The result of this determination is shown in the following table for one observer:

TABLE 2.—*Effective wave length of observer H.T.W.*

Observer A	λ_A	$\lambda_{H.T.W.}-\lambda_A$	$\lambda_{H.T.W.}$
	μ	μ	μ
E.C.C.	0.6522	0.0000	0.6522
G.E.M.	.6519	+.0001	.6520
R.F.J.	.6526	−.0001	.6525
C.F.S.	.6522	.0000	.6522
A.Q.T.	.6516	+.0002	.6518
K.S.G.	.6515	+.0003	.6518
F.P.P.	.6521	−.0003	.6518
I.C.G.	.6521	+.0003	.6524
	.6520$_3$		.6520$_9$

This indirectly obtained value, since it is based on the visibility data of eight observers, is unquestionably more accurate than the value 0.6522 previously used for the observer in question, but the difference is small enough to be neglected.

The effective wave lengths for the four observers are given in table 3.

TABLE 3.—*Effective wave length for the observers used in this investigation*

Observer	λ
F.H.	0.6530
H.T.W.	.6521
W.F.R.	.6522
F.R.C.	.6526
Mean	.6525

IV. RESULTS

The method of calculating the temperatures from the observed ratio of brightness and the effective wave length is described in previous work on the freezing point of platinum.[21] When the average effective wave length for the four observers is used to calculate the results (based on the gold point) of the individual freezes, the mean values for the individual observers range from 2,451° to 2,455° C. When, however, each freeze is calculated on the basis of the effective wave length for the man who observed that freeze, the values shown in the left half of table 4 are obtained. The values based on platinum are not greatly affected by the value of the effective wave length used. In this latter work, the illumination of the photometric field of the pyrometer was somewhat too high for precise matching and accounts for the larger scatter of the results obtained. These variations, however, are random in nature and the mean value is nearly as good as the one based on gold.

TABLE 4.—*Summary of determinations of the freezing point of iridium*

Values based on gold point, 1,063° C.					Values based on platinum point, 1,773.5° C.			
Freeze nos.[1]	F.H.	H.T.W.	W.F.R.	F.R.C.	Freeze nos.	H.T.W.	W.F.R.	F.R.C.
	°C.	°C.	°C.	°C.		°C.	°C.	°C.
1, 2, 3, 5	2,452.5	2,453.2	2,453.5	2,452.3	1, 2, 3	2,458.2	2,454.4	2,456.6
4, 6, 7, 9	2,452.4	2,452.9	2,452.5	2,454.9	4, 5, 6	2,455.8	2,451.8	2,455.4
8	2,452.9				7, 8, 9	2,455.0	2,453.9	2,455.1
					10, 11, 12	2,454.1	2,453.7	2,455.5
Mean	2,452.6	2,453.0	2,453.0	2,453.6	Mean	2,455.8	2,453.7	2,455.5
Mean of values based on gold, 2,453° C.					Mean of values based on platinum, 2,455° C.			

[1] The observers of the freezes are listed in the columns of the table in the same order as the freeze numbers are given in this column, thus freeze no. 3 goes with W.F.R.

The difference of 2° C. between the freezing point value based upon the gold point and that based upon the platinum point is not surprising in view of the fact that each of these separate values is considered to be accurate only to ±3° C. The consistently higher values obtained in the latter case indicate that the difference is not due solely to accidental errors in making the pyrometric settings.

In column 2 of table 5 are listed three ratios of brightness, all measured with black bodies immersed in freezing metals. In measuring such ratios, the greatest ratio is most sensitive to errors in the effective wave length and in the measured sector disk openings. The iridium to platinum ratio should therefore be the most accurately

[21] See footnote 18, p. 814.

known of the three. The value for the iridium point based on this ratio, however, is not necessarily the best one since the uncertainty in the platinum point enters directly into this and moreover the observations are not as precise.

TABLE 5.—*Summary of ratios of brightness and corresponding temperatures of fixed points*

Fixed points	Measured		Adjusted	
	Ratio of brightness $\lambda=0.652\ \mu$	Temperature	Ratio of brightness $\lambda=0.652\ \mu$	Temperature
		°C.		°C.
Iridium/platinum	14.60±0.1	2,455±3	14.57	2,453.8
Platinum/gold	301.0±1.5	1,773.5±1.0	300.6	1,773.2
Iridium/gold	4,366±43	2,453±3	4,380	2,453.8
Iridium/gold / Platinum/gold	(14.50±0.15)		(14.57)	

The three ratios in table 5 have been adjusted by the usual method for the adjustment of conditioned observations. These adjusted values, shown in column 4, indicate that the platinum point is probably lower than 1,773.5° C. From this it is concluded that:

Freezing point of platinum = 1,773° ± 1° C. (Int.).

Freezing point of iridium = 2,454° ± 3° C. (Int.).

The errors entering into the determination are somewhat difficult to evaluate. A summary of the estimated errors is given in table 6. The probable errors are all very much smaller and it is reasonably certain that the actual errors do not exceed those listed in the table.

TABLE 6.—*Summary of estimated errors*

Sources of error	Equivalent in °C.	
	Work based on gold point	Work based on platinum point
	°C.	°C.
Transmission of sectors	0.5	0.1
Effective wave length	1.0	.3
Photometric matching	.5	1.0
Departure from black body conditions	.7	.7
Impurity of metal	1.0	1.0
Reference temperature	0	1.0
Maximum error if all are of same sign	3.7	4.1

The value based on the direct measurement of the iridium to gold ratio is not dependent upon previous work and is the more reliable. In the absence of the other value, it would be considered good to ±3° C., since it is not likely that the errors listed are all of the maximum size and also all of the same sign. The satisfactory check obtained in the work based on the platinum point makes the estimate of ±3° C. for the final result a conservative one.

V. SUMMARY

The ratio of brightness of black bodies immersed in freezing iridium and freezing gold has been determined directly and in terms of the previously measured platinum to gold ratio. The platinum point is established as 1,773 ± 1° C. and the iridium point as 2,454 ± 3° C.

VI. ACKNOWLEDGMENTS

Acknowledgment is made to Wm. F. Roeser and F. R. Caldwell who gave able assistance throughout the work and served as observers.

VII. APPENDIX. PREPARATION AND PURITY OF THE IRIDIUM

By Edward Wichers

The purification of iridium is attended by unusual difficulties. The iterature on iridium does not include methods which can be depended upon for the complete elimination of impurities, even though they may be satisfactory for preparing metal of commercial purity. For this reason, and because the preparation of specimens of demonstrated purity has not been described, it seems rather unlikely that iridium of very high purity has been previously prepared.

All of the base metals ordinarily associated with iridium, as well as silver, gold, and probably palladium, can be removed by precipitating the iridium several times as ammonium chloroiridate, $(NH_4)_2IrCl_6$, provided proper precautions are taken. Platinum and ruthenium, on the other hand, cannot be separated from iridium in this way because they form chloro salts of the same order of solubility as the iridium salt. Even rhodium, which does not form an analogous, slightly soluble chloro salt, will contaminate the iridium compound with the utmost persistence, so that it is wholly impracticable, if not impossible, to get rid of rhodium in this way. No difficulty is experienced with osmium, although it forms a chloro salt similar to iridium, because it is volatilized as the tetroxide when the solution is digested with nitric acid or aqua regia, which is done repeatedly in the usual refining process.

When iridium is precipitated as ammonium iridium nitrite, platinum and ruthenium concentrate rapidly in the mother liquors and could probably be completely eliminated by several precipitations of that salt. This procedure can also be adapted to the separation of most of the base metals. However, in this instance it is rhodium which forms an analogous salt, somewhat less soluble than the iridium compound. Hence rhodium could be eliminated only by a long continued process of fractional precipitation, which is not very suitable when only a limited amount of material is available, and which in any case is not favorable to the purification of the more soluble of the two salts. Such a method would be better for freeing rhodium of iridium than vice versa.

Up to the present time no slightly soluble, easily handled, compound of iridium has been thought of which can be repeatedly precipitated and thereby effect the complete removal of rhodium. Small scale experiments, similar to an analytical procedure which has been de-

veloped in this laboratory [22] for the separation of rhodium from iridium, have shown that iridium can be freed of rhodium by precipitating the latter with trivalent titantium compounds. However, this reaction is not very practicable for even laboratory-scale refining operations. Earlier work [23] indicated that ruthenium could be eliminated by fractional precipitation with hydrogen sulphide, but that the yield of iridium was not very favorable. Later work has shown that this treatment also gets rid of rhodium and platinum. The poor yield (sometimes only 50 percent of fairly pure starting material) is offset by the simplicity of the operation and the fact that all three of the most persistent impurities are eliminated together. The procedure consists in saturating the acidified chloride solution (50 g of metal and 50 ml of concentrated hydrochloric acid per liter has been found to give satisfactory conditions of concentration) with hydrogen sulphide at room temperature and keeping it saturated for a week or longer, during which time platinum, rhodium, ruthenium, etc., slowly precipitate, together with a portion of the iridium. The precipitation is stopped when spectrographic examination of the iridium obtained from the filtered solutions shows no trace of other platinum metals. Foreign metals which are not completely precipitated by hydrogen sulphide at the prevailing acidity are then removed by repeated precipitation of ammonium chloroiridate, sometimes combined with one or more precipitations of ammonium iridium nitrite.

The iridium sponge, from which the ingot was prepared which was used in the experimental work described in this paper, was purified in two lots by the foregoing procedure, by H. A. Buchheit and R. K. Bell. The starting material was crude iridium residues from various sources, mostly obtained in the process of platinum refining by the United States Assay Office at New York, a portion of which was lent by the United States Mint and a portion obtained from the War Department. The crude residues contained large amounts of the remaining platinum metals, especially rhodium and platinum, as well as tin, iron, and other base metals. The iridium content of the residues probably averaged less than 25 percent.

After getting the residues into solution, mostly by fusion with alkaline oxidizing reagents, the iridium was concentrated somewhat by various procedures commonly employed to separate the platinum metals from each other and from base metals. The partially concentrated material was then subjected to fractional precipitation with hydrogen sulphide. One of the two lots, comprising about 60 percent of the metal used in the ingot, was finally purified from small amounts of base metals present, by twice converting the chloride solution to a nitrite solution (by heating with sodium nitrite), followed by the addition of ammonium chloride to precipitate ammonium iridium nitrite, and twice precipitating ammonium chloroiridate. The final purification of the other lot consisted in six precipitations as ammonium chloroiridate. Both lots of the ammonium chloroiridate were ignited and reduced under hydrogen to iridium sponge, samples of which were examined spectrographically to make sure that the material was of satisfactory purity.

---

[22] R. Gilchrist, B.S. Jour. Research, vol. 9, p. 547, 1932.
[23] E. Wichers, R. Gilchrist, and W. H. Swanger, Purification of the Six Platinum Metals, Trans. Am. Inst. Mining Met. Eng., vol. 76, p. 602, 1928.

After the completion of the work with the ingot, the arc spectrum of the metal [24] was photographed and compared with the arc spectrum of a sample of iridium sponge to which 0.02 percent each of platinum, rhodium, ruthenium, iron, and thorium (the last as oxide) had been added. The spectrum of the ingot showed no traces of any of the other platinum metals nor any other impurities except a faint trace of iron and silicon.

A further comparison of the ingot was then made with standards to which had been added 0.01 and 0.003 percent of iron. The intensity of the iron lines in the spectrum of the ingot was much less than in that of either standard and indicated the amount of iron to be 0.001 percent or less.

No standard containing silicon was prepared, but the ingot showed only a faint trace of the very sensitive line of wave length 2,881 A.

Spectrograms of standards which contained smaller admixtures of rhodium, ruthenium, platinum, and thorium than the one with which the ingot was directly compared, indicate that 0.002 percent of ruthenium and 0.005 percent of thorium would have been detected if present in the ingot. The sensitivity of rhodium was less well defined, but is probably of the same order as that of ruthenium. The sensitivity of platinum in these spectra may be limited to about 0.005 percent. However, experience in purifying iridium by fractional precipitation with hydrogen sulphide shows that platinum is eliminated much more rapidly than either rhodium or ruthenium. Hence it is highly probable that the amount of platinum, as well as of rhodium and ruthenium, was below 0.002 percent in each case. Osmium (and palladium) are usually removed in the preliminary purification and have never been detected during the final stages of purification. On the basis of both chemical and spectrographic evidence it seems reasonable to conclude that the iridium ingot, at the completion of the experimental work, contained less than a total of 0.01 percent of metallic impurities.

WASHINGTON, March 1, 1933.

[24] The spectrographic analyses were made by W. F. Meggers and B. F. Scribner.

THE PRECIPITATION AND TITRATION OF MAGNESIUM OXYQUINOLATE IN THE PRESENCE OF CALCIUM OXALATE, AND ITS APPLICATION IN THE ANALYSIS OF PORTLAND CEMENT AND SIMILAR SILICATES

By John C. Redmond

ABSTRACT

Data are presented showing that magnesium oxyquinolate can be precipitated and titrated in the presence of calcium oxalate. A rapid method for the determination of magnesium in portland cements is described.

CONTENTS

	Page
I. Introduction	823
II. Experimental	824
III. Recommended method for the rapid determination of magnesia in portland cement	825
1. Solutions required	825
2. Procedure	826
IV. Literature cited	826

I. INTRODUCTION

A rapid and accurate method for the determination of magnesia in portland cements and similar materials by the use of 8-hydroxyquinoline was described by Redmond and Bright (3)[1] in 1931. In this procedure, which has been in use for the routine analysis of portland cements at the Bureau of Standards for several years, the sample is dissolved in dilute hydrochloric acid, the R_2O_3 group and calcium are removed as usual, and magnesium then determined by precipitating with 8-hydroxyquinoline (1), dissolving the precipitate in acid, and titrating with a standard bromate solution. The work reported in this paper demonstrates that this method can be further shortened by omitting the removal of the calcium oxalate and precipitating and titrating the magnesium oxyquinolate in the presence of the calcium oxalate.

Shead and Valla (4) claim that magnesium oxyquinolate can be precipitated in the presence of calcium oxalate. In their method the combined precipitates of calcium oxalate and magnesium oxyquinolate are ignited, weighed, and lime subsequently determined by the

[1] The figures given in parentheses here and throughout the text relate to the reference numbers in the bibliography given at the end of this paper.

saccharate method. Bucherer and Meier (2) have described a method wherein the magnesium oxyquinolate is precipitated in the presence of calcium oxalate, and magnesium determined by their "filtration method." A brief description of the experimental work showing that the precipitated magnesium oxyquinolate can be titrated in the presence of calcium oxalate, together with complete directions for the application of the method in the analysis of portland cements, are given in the following sections. By using the method described, an experienced operator can determine magnesia in a portland cement or limestone in 1 to 1½ hours.

II. EXPERIMENTAL

Solutions of pure salts of magnesium, calcium, iron, and aluminum were used to obtain the various quantities of these elements present in the different test solutions. The procedures for separating magnesium from the several elements, and its precipitation and titration as the quinolate are given in section III.

Preliminary experiments showed that calcium once precipitated as the oxalate does not retain any 8-hydroxyquinoline, and that the presence of oxalic acid has no observable effect on the titration of 8-hydroxyquinoline with standard bromate and thiosulphate solutions. Further experiments showed that calcium must be precipitated as the oxalate, for otherwise more or less of it reacts with 8-hydroxyquinoline and precipitates as oxyquinolate with the magnesium. For instance, aliquot portions of solutions of magnesium chloride containing 0.0247 g of MgO indicated 0.0252, 0.0255, and 0.0270 g when adulterated with 0.0010, 0.0043, and 0.0300 g of CaO, respectively. Incidentally it was noted that the presence of iron or aluminum hydroxide causes errors in the precipitation and titration of magnesium oxyquinolate.

The results obtained by precipitating calcium as the oxalate and then precipitating magnesium in the presence of the calcium oxalate, dissolving the precipitate in hydrochloric acid, and titrating with a solution of bromate are shown in table 1. Each result is the average of two or more closely agreeing determinations. Two different methods were used to precipitate the calcium. In one case hot ammonium oxalate solution was added to a boiling faintly ammoniacal solution of the calcium and magnesium, and in the other case a boiling acid solution containing the magnesium and calcium, together with oxalic acid, was made ammoniacal by the dropwise addition of concentrated ammonia. The data show that for moderate amounts of lime and magnesia the results are sufficiently accurate for routine work. For high quantities of lime and magnesia the usual occlusion of magnesia that occurs when calcium oxalate is precipitated only once takes place no matter whether the calcium is precipitated in acid or ammoniacal solution. The addition of the 8-hydroxyquinoline prior to the calcium precipitation does not inhibit the occlusion of magnesia, for the results obtained are the same as when the reagent is added after the calcium precipitation.

TABLE 1.—*Results obtained by the precipitation of magnesium oxyquinolate in the presence of calcium oxalate*

Experiment no.	CaO taken	MgO taken	MgO found	Error	Remarks
	g	*g*	*g*	*g*	
1	0.034	0.0147	0.0146	−0.0001	Calcium oxalate precipitated in ammoniacal solution.
2	.060	.0147	.0148	+.0001	Calcium oxalate precipitated from acid solution by adding ammonia.
3	.170	.0195	.0194	−.0001	Same as in experiment 1.
4	.170	.0242	.0240	−.0002	Do.
5	.170	.0242	.0240	−.0002	Same as in experiment 2.
6	.300	.0049	.0049	.0000	Same as in experiment 1.
7	.300	.0147	.0144	−.0003	Same as in experiment 2.
8	.300	.0244	.0239	−.0005	Same as in experiment 1.
9	.300	.0244	.0236	−.0008	Same as in experiment 1, but calcium oxalate filtered before precipitating Mg.
10	.300	.0244	.0237	−.0007	Same as in experiment 1, 8-hydroxyquinoline added before oxalate precipitation.

The data given in table 2 were obtained by applying the recommended procedure to synthetic solutions which had been made to approximate solutions obtained from 0.5 g samples of portland cements. These solutions contained 0.020 g of Al_2O_3, 0.008 g of Fe_2O_3, 0.300 g of CaO, and the amounts of MgO shown in the table. The errors are no greater than are obtained in any procedure involving single precipitations with ammonium hydroxide and with ammonium oxalate, and are within commercial tolerances. By repeating the precipitation of the ammonium hydroxide group and of the calcium oxalate more accurate results can be obtained.

In addition to the data given in table 2, 0.8 g samples of Bureau of Standards standard sample of argillaceous limestone no. 1a (certificate value 2.19 percent MgO) were ignited for 30 minutes at 1,100° C. and magnesia was then determined by the recommended method. An average value of 2.14 percent magnesia was obtained.

TABLE 2.—*Results obtained for MgO in synthetic solutions of cement*

Experiment no.	MgO	
	Present	Found
	Percent	*Percent*
11	1.96	1.96
12	3.90	3.82
13	4.88	4.72
14	4.88	[1] 4.94

[1] R_2O_3 and CaO reprecipitated.

III. RECOMMENDED METHOD FOR THE RAPID DETERMINATION OF MAGNESIA IN PORTLAND CEMENT

1. SOLUTIONS REQUIRED

The solutions used in this procedure and their methods of preparation are those described by Redmond and Bright (3), with the exception of the method of standardization of the bromate-bromide solution. This is made as follows: To 200 ml of water in a 400-ml beaker add exactly 25 ml of the potassium bromate-potassium-bromide solution (0.2 *N*). Add 20 ml of hydrochloric acid (specific gravity

1.18), stir, and add immediately 10 ml of potassium iodide solution (25 percent). Mix well, and titrate at once with standard sodium thiosulphate solution (0.1 *N*) until nearly colorless. Add 2 ml of starch solution and titrate to the disappearance of the blue color.

2. PROCEDURE

To a 0.500 g sample in a 400-ml beaker add 10 ml of water and 10 ml of hydrochloric acid (specific gravity 1.18). Heat gently and grind any coarse particles with the flattened end of a glass rod until decomposition is complete. Dilute to 150 ml with hot water.

To the solution add three drops of methyl red (0.02 percent alcoholic solution), and then ammonium hydroxide (specific gravity 0.90) until the solution is distinctly yellow. Add macerated filter paper, and heat to boiling. Boil from 1 to 2 minutes, remove from the hot plate, and allow to stand until the precipitate has settled. Filter without delay, and wash the precipitate with a hot 2 percent solution of ammonium chloride. To the filtrate add 1 ml of ammonium hydroxide (specific gravity 0.90), and heat to boiling. When boiling, add 25 ml of a hot 4 percent solution of $(NH_4)_2CO_4.H_2O$ and continue boiling for 2 minutes. Digest on the steam-bath for 10 to 15 minutes.

Cool the solution to 70° C., add 20 ml[2] of a clear 1.25 percent solution of 8-hydroxyquinoline (25 g of the reagent dissolved in 60 ml of glacial acetic acid and diluted to 2 liters with water), and then 4 ml of ammonium hydroxide (specific gravity 0.90) per 100 ml of solution. Stir on a mechanical stirring machine for 15 minutes, and set aside until the precipitate has settled. Filter, and wash with hot dilute ammonium hydroxide (1+40). Dissolve the precipitate in 50 to 75 ml of hot dilute hydrochloric acid (1+9), dilute the resulting solution to 200 ml, and add 15 ml of hydrochloric acid (specific gravity 1.18). Cool to 25° C., and add from a pipette 25 ml of standard bromate-bromide solution (0.2 *N*). Stir and let stand for about 30 seconds to insure complete bromination. Add 10 ml of potassium iodide solution (25 percent), stir well, and then titrate with standard sodium thiosulphate solution (0.1 *N*) until the color of the iodine becomes faintly yellow. At this point add 2 ml of starch solution and titrate to the disappearance of the blue color.

The percentage of magnesia in a 0.5 g sample may be calculated as follows:

A = g of MgO per ml of standard sodium thiosulphate solution.
B = ml of standard sodium thiosulphate solution equivalent to 25 ml of standard bromate solution.
C = ml of sodium thiosulphate solution required in the titration.

Then

$(B-C)\times A$ = g of MgO.
g of MgO $\times 200$ = percent of MgO.

IV. LITERATURE CITED

1. Berg, R., Z. anal. Chem., vol. 71, p. 23, 1927.
2. Bucherer, H. Th., and Meier, F. W., Z. anal. Chem., vol. 82, pp. 1 to 44, 1930.
3. Redmond, J. C., and Bright, H. A., B.S. Jour. Research, vol. 6, pp. 113–120, 1931.
4. Shead, A. C., and Valla, R. K., Ind. Eng. Chem., Anal. ed., vol. 4, p. 246, 1932.

WASHINGTON, March 31, 1933.

[2] This amount suffices for 0.5 g samples containing 6 percent or less of magnesia. For cements of higher magnesia content proportionately more reagent should be added.

A NEW DESCRIPTION AND ANALYSIS OF THE ARC SPECTRUM OF CHLORINE

By C. C. Kiess

ABSTRACT

New types of photographic plates have made it possible not only to extend our knowledge of the chlorine arc spectrum beyond the infrared limit hitherto reached, but also to record many new lines in the regions of shorter wave length. There are now presented wave lengths for nearly twice as many lines as have hitherto been known. The new data have made it possible to revise and improve the analysis of Cl I with the results: (1) Many new terms have been detected; (2) previous erroneous classifications have been corrected.

CONTENTS

	Page
I. Introduction	827
II. Experimental procedure	827
III. Results	828
IV. Acknowledgment	839

I. INTRODUCTION

The description of the arc spectrum of chlorine presented in this paper constitutes an extension and revision of the work done four years ago at the Bureau of Standards by the writer in collaboration with T. L. deBruin.[1] At that time, we were able to photograph the spectrum out to wave length 9,876 A with plates sensitized with the dyes then available. The wave-length data thus obtained made it possible to establish the main features of the term structure of Cl I and to determine the ionization potential of the neutral chlorine atom. Owing, however, to the limitations of the sensitized photographic plates employed in that work, not all the features of the spectrum predictable from atomic theory could be recorded. The discovery of new photo-sensitizing materials by the Research Laboratory of the Eastman Kodak Co.[2] has made it desirable, therefore, to reinvestigate the arc spectrum of chlorine, both for the purpose of extending it into hitherto unexplored regions and to bring out with greater intensity those features which, in the previous work, had been recorded only fragmentarily. Since it will be necessary in this paper to refer frequently to the earlier paper, it will, hereafter, be briefly designated by RP73.

II. EXPERIMENTAL PROCEDURE

The light source used in the present work was a Geissler tube of the same type as that described in RP73. The chlorine generator of the new tube was charged, however, with palladium chloride, which is

[1] B.S. Jour. Research, vol. 2 (RP73), p. 1117, 1929.
[2] J. Opt. Soc. Am., vol. 21, p. 753, 1931; vol. 22, p. 204, 1932.

much less hygroscopic than the chloride of gold previously used. The chlorine vigorously attacked the hot platinum electrodes of the tube and had to be replenished from time to time until a state of equilibrium was attained, after which the tube was operated for over 200 hours without further admission of chlorine from the generator. The tube was excited by the uncondensed discharge from a 40,000-volt transformer.

The spectrograms were all obtained with the 21-foot concave grating ruled with 7,500 lines per inch. The mounting of this instrument has been described elsewhere.[3] Recently, however, the speed of this spectrograph has been considerably increased by substituting a collimating mirror of stainless steel for the tarnished speculum metal mirror. Nearly all the exposures to the first order infrared were made with only half the slit covered with a filter so that lines in the overlapping second order were also photographed. Both the first and second orders of the Fe arc spectrum were also photographed to supply the standards needed for the wave-length determinations. The exposures were of 24 hours duration for each setting of the spectrograph and covered the region from 3,000 A in the ultraviolet to 12,000 A in the infrared.

III. RESULTS

The new and revised wave lengths derived in this investigation are given in the first column of table 1. A total of 441 lines, believed to be characteristic of the arc spectrum of chlorine, is now listed as compared with the 225 lines reported in RP73. All the measurements made in the earlier and also the present series of observations have been combined into means which furnish a scale of wave lengths to which the new lines observed only on the recent spectrograms have been reduced. It is the results thus obtained that have been entered in the table. The intensities are estimates of the relative blackening produced by the lines, but owing to the variable spectral sensitivity of the plates, these estimates for groups of lines in different portions of the spectrum are not comparable with each other.

TABLE 1.—*Wave lengths in the arc spectrum of chlorine*

λ_{air}. I. A.	Intensity	ν_{vac} cm^{-1}	Term combination
10, 427. 52	0	9, 587. 38	
10, 420. 19	1	9, 594. 13	
10, 392. 45	5	9, 619. 73	$4s^2P_{0\frac{1}{2}}-4p^4D^{\circ}_{1\frac{1}{2}}$
10, 320. 00	4	9, 687. 27	
10, 315. 28	0	9, 691. 70	
10, 312. 11	1	9, 694. 69	
10, 305. 38	0	9, 701. 01	
10, 177. 40	1	9, 823. 00	$4s^2P_{0\frac{1}{2}}-4p^4D^{\circ}_{0\frac{1}{2}}$
10, 091. 64	40	9, 906. 48	$4s^2P_{1\frac{1}{2}}-4p^4D^{\circ}_{2\frac{1}{2}}$
10, 055. 93	1	9, 941. 66	
10, 002. 25	4	9, 995. 01	
9, 897. 79	3	10, 100. 50	
9, 875. 95	50	10, 122. 84	$4s^2P_{0\frac{1}{2}}-4p^2D^{\circ}_{1\frac{1}{2}}$
9, 815. 70	2	10, 184. 97	
9, 808. 46	5	10, 192. 49	$4s^2D_{1\frac{1}{2}}-4p^2P^{\circ}_{1\frac{1}{2}}$, ($^1D^1D$)

[3] B. S.Sci. Papers, vol. 18 (S441), p. 191, 1922.

TABLE 1.—*Wave lengths in the arc spectrum of chlorine*—Continued

λ_{air}. I. A.	Intensity	ν_{vac} cm^{-1}	Term combination
9, 806. 90	25	10, 194. 11	$4s^2D_{2½}-4p^2P^\circ_{1½}$, ($^1D^1D$)
9, 774. 64	1	10, 227. 75	
9, 744. 33	30	10, 259. 57	$4s^2P_{1½}-4p^4D^\circ_{1½}$
9, 702. 35	40	10, 303. 96	$4s^4P_{0½}-4p^4P^\circ_{1½}$
9, 669. 48	1	10, 338. 98	
9, 661. 90	20	10, 347. 20	$4s^2D_{1½}-4p^2P^\circ_{0½}$, ($^1D^1D$)
9, 632. 37	20	10, 378. 81	$4s^2P_{0½}-4p^2S^\circ_{0½}$
9, 608. 98	4	10, 404. 08	
9, 592. 20	75	10, 422. 28	$4s^2P_{1½}-4p^2D^\circ_{2½}$
9, 584. 77	50	10, 430. 36	$4s^4P_{1½}-4p^4P^\circ_{2½}$
9, 554. 96	4	10, 462. 90	$4s^2P_{1½}-4p^4D^\circ_{0½}$
9, 486. 89	25	10, 537. 97	$4s^4P_{0½}-4p^4P^\circ_{0½}$
9, 481. 93	3	10, 543. 49	$4s^2D_{2½}-5p^4P^\circ_{1½}$, ($^1D^3P$)
9, 452. 06	75	10, 576. 80	$4s^2P_{0½}-4p^2P^\circ_{1½}$
9, 419. 74	2	10, 613. 10	$4s^2D_{2½}-5p^4D^\circ_{3½}$, ($^1D^3P$)
9, 400. 76	1	10, 634. 65	
9, 393. 81	50	10, 642. 39	$4s^4P_{1½}-4p^4P^\circ_{1½}$
9, 371. 92	0	10, 667. 36	
9, 288. 82	60	10, 762. 68	$4s^2P_{1½}-4p^2D^\circ_{1½}$
9, 212. 39	3	10, 851. 98	$4s^2D_{1½}-5p^4P^\circ_{0½}$, ($^1D^3P$)
9, 197. 49	25	10, 869. 56	$4s^2P_{0½}-4p^4S^\circ_{1½}$
9, 191. 67	60	10, 876. 44	$4s^4P_{1½}-4p^4P^\circ_{0½}$
9, 121. 10	75	10, 960. 58	$4s^4P_{2½}-4p^4P^\circ_{2½}$
9, 073. 15	50	11, 018. 50	$4s^2P_{1½}-4p^2S^\circ_{0½}$
9, 069. 66	25	11, 022. 74	$4s^2D_{1½}-4p^2F^\circ_{2½}$, ($^1D^1D$)
9, 068. 39	3	11, 024. 30	$4s^2D_{2½}-4p^2F^\circ_{2½}$, ($^1D^1D$)
9, 045. 40	40	11, 052. 31	$4s^2P_{0½}-4p^2P^\circ_{0½}$
9, 038. 96	30	11, 060. 31	$4s^2D_{2½}-4p^2F^\circ_{3½}$, ($^1D^1D$)
8, 948. 01	50	11, 172. 60	$4s^4P_{2½}-4p^4P^\circ_{1½}$
8, 931. 20	2	11, 193. 63	$4s^2D_{2½}-5p^4D^\circ_{1½}$, ($^1D^3P$)
8, 918. 78	0	11, 209. 36	$4p^4D^\circ_{0½}-4d^4D_{1½}$
8, 912. 88	40	11, 216. 79	$4s^2P_{1½}-4p^2P^\circ_{1½}$
8, 846. 00	1	11, 301. 44	$4p^4D^\circ_{1½}-4d^4D_{2½}$
8, 815. 26	0	11, 340. 85	
8, 759. 93	0	11, 412. 49	$4p^4D^\circ_{1½}-4d^4D_{1½}$
8, 711. 58	1	11, 475. 83	$4s^2D_{1½}-5p^2S^\circ_{0½}$, ($^1D^3P$)
8, 686. 28	30	11, 509. 25	$4s^2P_{1½}-4p^4S^\circ_{1½}$
8, 641. 75	3	11, 568. 56	$4p^4D^\circ_{3½}-4d^4D_{3½}$
8, 628. 61	4	11, 586. 17	$4s^2D_{2½}-5p^2D^\circ_{1½}$, ($^1D^3P$)
8, 585. 96	100	11, 643. 72	$4s^4P_{1½}-4p^4D^\circ_{2½}$
8, 577. 98	7	11, 654. 56	$4p^4D^\circ_{3½}-4d^4D_{2½}$
8, 575. 25	75	11, 658. 27	$4s^4P_{0½}-4p^4D^\circ_{1½}$
8, 550. 46	20	11, 692. 07	$4s^2P_{1½}-4p^2P^\circ_{0½}$
8, 497. 32	5	11, 765. 19	$4p^4D^\circ_{2½}-4d^4D_{1½}$
8, 494. 52	0	11, 769. 07	
8, 472. 96	3	11, 799. 01	$4p^4S^\circ_{1½}-4d^2D_{2½}$
8, 467. 32	25	11, 806. 87	$4p^4D^\circ_{3½}-4d^4D_{3½}$
8, 428. 25	100	11, 861. 60	$4s^4P_{0½}-4p^4D^\circ_{0½}$
8, 422. 20	2	11, 870. 12	
8, 406. 20	10	11, 892. 72	$4p^4D^\circ_{3½}-4d^4D_{2½}$

TABLE 1.—*Wave lengths in the arc spectrum of chlorine*—Continued

λ_{air}. I. A.	Intensity	ν_{vac} cm^{-1}	Term combination
8, 403. 70	1	11, 896. 25	$4p^2P^0_{1½}-4d^4P_{2½}$
8, 397. 61	3	11, 904. 88	
8, 392. 48	2	11, 912. 16	
8, 383. 58	4	11, 924. 81	
8, 380. 54	2	11, 929. 13	
8, 375. 95	150	11, 935. 66	$4s^4P_{2½}-4p^4D^0_{3½}$
8, 355. 38	1	11, 965. 05	
8, 343. 97	4	11, 981. 41	
8, 333. 29	100	11, 996. 77	$4s^4P_{1½}-4p^4D^0_{1½}$
8, 330. 57	0	12, 000. 69	
8, 321. 43	1	12, 013. 87	
8, 311. 15	1	12, 028. 73	
8, 304. 69	5	12, 038. 08	$4p^2P^0_{1½}-6s^4P_{1½}$
8, 286. 67	5	12, 064. 26	
8, 280. 95	7	12, 072. 59	$4p^4S^0_{1½}-4d^2D_{1½}$
8, 273. 79	7	12, 083. 04	$4p^2D^0_{2½}-4d^4F_{3½}$
8, 271. 70	7	12, 086. 10	
8, 269. 15	10	12, 089. 82	
8, 267. 97	3	12, 091. 55	$4p^2P^0_{1½}-4d^2D_{2½}$
8, 258. 45	5	12, 105. 48	
8, 255. 70	1	12, 109. 52	
8, 244. 50	1	12, 125. 97	
8, 226. 60	2	12, 152. 35	
8, 221. 73	75	12, 159. 55	$4s^4P_{1½}-4p^2D^0_{2½}$
8, 220. 40	60	12, 161. 52	$4s^4P_{0½}-4p^2D^0_{1½}$
8, 212. 00	100	12, 173. 96	$4s^4P_{2½}-4p^4D^0_{3½}$
8, 206. 40	2	12, 182. 27	$4p^2P^0_{0½}-6s^4P_{0½}$
8, 203. 76	12	12, 186. 19	$4p^2D^0_{2½}-4d^2F_{3½}$
8, 200. 20	35	12, 191. 48	$4s^2D_{1½}-5p^2P^0_{1½}$, ($^1D^3P$)
8, 199. 02	35	12, 193. 23	$4s^2D_{2½}-5p^2P^0_{1½}$, ($^1D^3P$)
8, 194. 35	50	12, 200. 18	$4s^4P_{1½}-4p^4D^0_{0½}$
8, 175. 24	0	12, 228. 70	
8, 170. 09	10	12, 236. 40	$4p^2S^0_{0½}-6s^4P_{1½}$
8, 164. 76	1	12, 244. 40	
8, 161. 52	4	12, 249. 26	$4p^2D^0_{1½}-6s^4P_{2½}$
8, 129. 55	2	12, 297. 43	$4p^2D^0_{2½}-4d^4F_{2½}$
8, 121. 40	5	12, 309. 76	$4p^4S^0_{1½}-4d^4P_{1½}$
8, 117. 75	4	12, 315. 30	
8, 115. 40	2	12, 318. 87	
8, 094. 76	12	12, 350. 28	$4p^2D^0_{1½}-4d^4P_{2½}$
8, 087. 69	20	12, 361. 08	$4s^2D_{1½}-4p^2D^0_{2½}$, ($^1D^1D$)
8, 086. 67	75	12, 362. 63	$4s^2D_{2½}-4p^2D^0_{2½}$, ($^1D^1D$)
8, 085. 54	60	12, 364. 36	$4s^2D_{1½}-4p^2D^0_{1½}$, ($^1D^1D$)
8, 084. 48	35	12, 365. 98	$4s^2D_{2½}-4p^2D^0_{1½}$, ($^1D^1D$)
8, 051. 08	20	12, 417. 28	$4s^4P_{0½}-4p^2S^0_{0½}$
8, 044. 65	0	12, 427. 20	
8, 023. 30	18	12, 460. 28	$4p^4D^0_{1½}-4d^4F_{2½}$
8, 015. 57	45	12, 472. 31	$4s^2D_{1½}-5p^2P^0_{0½}$, ($^1D^3P$)
7, 997. 80	50	12, 500. 01	$4s^4P_{1½}-4p^2D^0_{1½}$
7, 989. 36	0	12, 513. 21	

TABLE 1.—*Wave lengths in the arc spectrum of chlorine*—Continued

λ_{air}. I. A.	Intensity	ν_{vac} cm^{-1}	Term combination
7, 985. 80	4	12, 518. 79	
7, 985. 10	1	12, 519. 88	
7, 980. 58	15	12, 526. 97	$4s^4P_{2\frac{1}{2}}-4p^4D^{\circ}_{1\frac{1}{2}}$
7, 976. 95	25	12, 532. 58	$4p^4P^{\circ}_{0\frac{1}{2}}-4d^4D_{1\frac{1}{2}}$
7, 974. 72	20	12, 536. 18	$4p^2D^{\circ}_{2\frac{1}{2}}-4d^2F_{2\frac{1}{2}}$
7, 968. 66	3	12, 545. 71	$4p^2D^{\circ}_{1\frac{1}{2}}-4d^2D_{2\frac{1}{2}}$
7, 962. 12	0	12, 556. 02	
7, 952. 49	15	12, 571. 22	$4p^4D^{\circ}_{0\frac{1}{2}}-4d^4F_{1\frac{1}{2}}$
7, 940. 65	2	12, 589. 97	$4p^2D^{\circ}_{2\frac{1}{2}}-6s^4P_{2\frac{1}{2}}$
7, 938. 90	8	12, 592. 74	
7, 935. 00	40	12, 598. 93	$4p^4D^{\circ}_{3\frac{1}{2}}-4d^4F_{3\frac{1}{2}}$
7, 933. 85	50	12, 600. 76	$4p^4D^{\circ}_{2\frac{1}{2}}-4d^4F_{4\frac{1}{2}}$
7, 924. 62	100	12, 615. 44	$4s^4P_{0\frac{1}{2}}-4p^2P^{\circ}_{1\frac{1}{2}}$
7, 915. 09	25	12, 630. 62	$4p^4P^{\circ}_{2\frac{1}{2}}-4d^4D_{0\frac{1}{2}}$
7, 899. 28	45	12, 655. 90	$4p^4P^{\circ}_{1\frac{1}{2}}-4d^4D_{2\frac{1}{2}}$
7, 898. 10	5	12, 657. 80	$4p^2P^{\circ}_{1\frac{1}{2}}-6s^4P_{0\frac{1}{2}}$
7, 893. 33	10	12, 665. 45	
7, 886. 00	6	12, 677. 22	
7, 878. 22	75	12, 689. 74	$4s^4P_{2\frac{1}{2}}-4p^2D^{\circ}_{2\frac{1}{2}}$
7, 872. 50	1	12, 698. 96	$4p^4D^{\circ}_{1\frac{1}{2}}-4d^2F_{2\frac{1}{2}}$
7, 870. 68	1	12, 701. 90	$4p^4D^{\circ}_{2\frac{1}{2}}-4d^2F_{3\frac{1}{2}}$
7, 839. 42	8	12, 752. 54	$4p^4D^{\circ}_{1\frac{1}{2}}-6s^4P_{2\frac{1}{2}}$
7, 837. 40	6	12, 755. 83	$4s^4P_{1\frac{1}{2}}-4p^2S^{\circ}_{0\frac{1}{2}}$
7, 830. 76	30	12, 766. 64	$4p^4P^{\circ}_{1\frac{1}{2}}-4d^4D_{1\frac{1}{2}}$
7, 825. 80	3	12, 774. 74	$4p^4D^{\circ}_{1\frac{1}{2}}-4d^4F_{1\frac{1}{2}}$
7, 821. 35	45	12, 782. 01	$4p^4P^{\circ}_{2\frac{1}{2}}-4d^4D_{2\frac{1}{2}}$
7, 815. 34	1	12, 791. 83	$4p^4D^{\circ}_{0\frac{1}{2}}-6s^4P_{1\frac{1}{2}}$
7, 810. 06	3	12, 799. 60	$4p^2S^{\circ}_{0\frac{1}{2}}-4d^4P_{1\frac{1}{2}}$
7, 805. 82	1	12, 807. 44	
7, 804. 25	2	12, 810. 01	
7, 802. 27	6	12, 813. 26	$4p^4D^{\circ}_{3\frac{1}{2}}-4d^4F_{3\frac{1}{2}}$
7, 798. 59	5	12, 819. 31	$4p^2D^{\circ}_{1\frac{1}{2}}-4d^2D_{1\frac{1}{2}}$
7, 790. 56	5	12, 832. 52	$4p^2D^{\circ}_{2\frac{1}{2}}-6s^4P_{1\frac{1}{2}}$
7, 787. 75	4	12, 837. 15	$4p^4D^{\circ}_{2\frac{1}{2}}-4d^4F_{2\frac{1}{2}}$
7, 777. 82	10	12, 853. 54	$4p^4D^{\circ}_{1\frac{1}{2}}-4d^4P_{2\frac{1}{2}}$
7, 771. 10	12	12, 864. 65	$4p^4P^{\circ}_{1\frac{1}{2}}-4d^4D_{0\frac{1}{2}}$
7, 769. 18	30	12, 867. 83	$4p^4P^{\circ}_{2\frac{1}{2}}-4d^4D_{2\frac{1}{2}}$
7, 758. 14	3	12, 886. 15	$4p^2D^{\circ}_{2\frac{1}{2}}-4d^2D_{2\frac{1}{2}}$
7, 754. 78	6	12, 891. 73	
7, 744. 94	125	12, 908. 11	$4s^4P_{0\frac{1}{2}}-4p^4S^{\circ}_{1\frac{1}{2}}$
7, 717. 57	100	12, 953. 89	$4s^4P_{1\frac{1}{2}}-4p^2P^{\circ}_{1\frac{1}{2}}$
7, 714. 56	0	12, 958. 94	
7, 702. 89	10	12, 978. 57	$4p^4P^{\circ}_{2\frac{1}{2}}-4d^4D_{1\frac{1}{2}}$
7, 697. 40	2	12, 987. 83	
7, 692. 97	7	12, 995. 31	$4p^4D^{\circ}_{1\frac{1}{2}}-6s^4P_{1\frac{1}{2}}$
7, 672. 44	25	13, 030. 08	$4s^4P_{2\frac{1}{2}}-4p^2D^{\circ}_{1\frac{1}{2}}$
7, 664. 35	1	13, 043. 83	
7, 659. 50	5	13, 052. 10	$4p^4D^{\circ}_{2\frac{1}{2}}-4d^2F_{2\frac{1}{2}}$ $4p^4D^{\circ}_{3\frac{1}{2}}-4d^4F_{2\frac{1}{2}}$
7, 656. 86	6	13, 056. 59	$4p^2D^{\circ}_{1\frac{1}{2}}-4d^4P_{1\frac{1}{2}}$

TABLE 1.—*Wave lengths in the arc spectrum of chlorine*—Continued

λ_{air}. I. A.	Intensity	ν_{vac} cm^{-1}	Term combination
7, 635. 08	1	13, 092. 30	
7, 633. 83	3	13, 096. 00	
7, 628. 35	1	13, 105. 29	$4p^4D^3_{3½}-6s^4P_{2½}$
7, 600. 05	0	13, 154. 19	
7, 561. 19	4	13, 221. 80	
7, 547. 06	100	13, 246. 55	$4s^4P_{1½}-4p^4S^1_{1½}$
7, 503. 80	0	13, 322. 92	$4p^4D^1_{1½}-4d^2D_{1½}$
7, 496. 48	1	13, 335. 93	
7, 492. 12	10	13, 343. 69	$4p^4D^3_{3½}-6s^4P_{2½}$
7, 489. 46	8	13, 348. 43	$4p^4D^3_{2½}-6s^4P_{1½}$
7, 462. 40	8	13, 396. 83	$4p^2D^3_{2½}-4d^4P_{1½}$
7, 459. 42	3	13, 402. 19	$4p^4D^3_{1½}-4d^2D_{2½}$
7, 454. 08	2	13, 410. 49	$4p^4D^5_{0½}-6s^4P_{0½}$
7, 444. 32	3	13, 429. 37	$4s^4P_{1½}-4p^2P^3_{0½}$
7, 437. 37	1	13, 441. 92	
7, 435. 71	7	13, 444. 91	$4p^4D^3_{3½}-4d^4P_{2½}$
7, 431. 33	0	13, 452. 84	
7, 414. 10	90	13, 484. 10	$4s^4P_{2½}-4p^2P^1_{1½}$
7, 382. 47	3	13, 541. 88	
7, 372. 65	1	13, 559. 91	$4p^4D^1_{1½}-4d^4P_{1½}$
7, 342. 74	3	13, 615. 15	$4p^4D^1_{1½}-6s^4P_{0½}$
7, 342. 00	1	13, 616. 52	$4p^2P^3_{0½}-4d^2P_{1½}$
7, 329. 33	3	13, 640. 06	$4p^4D^3_{3½}-4d^2D_{2½}$
7, 296. 38	1	13, 701. 66	
7, 256. 63	125	13, 776. 71	$4s^4P_{2½}-4p^4S^1_{1½}$
7, 252. 48	3	13, 784. 60	
7, 244. 76	3	13, 799. 29	$4p^4S^1_{1½}-4d^2P_{1½}$
7, 194. 94	5	13, 894. 83	$4p^4P^5_{0½}-4d^4F_{1½}$
7, 185. 68	2	13, 912. 74	$4p^4D^3_{3½}-4d^4P_{1½}$
7, 146. 38	5	13, 989. 25	
7, 127. 35	3	14, 026. 60	$4p^4P^3_{3½}-4d^4F_{2½}$
7, 125. 57	2	14, 030. 10	
7, 094. 20	8	14, 092. 14	$4p^2P^1_{1½}-4d^2P_{1½}$
7, 086. 80	25	14, 106. 86	$4p^4P^1_{1½}-6s^4P_{2½}$
7, 082. 35	3	14, 115. 72	$4p^4P^5_{0½}-6s^4P_{1½}$
7, 075. 64	3	14, 129. 10	$4p^4P^1_{1½}-4d^4F_{1½}$
7, 060. 18	2	14, 160. 05	$4p^4D^1_{1½}-4d^4P_{0½}$
7, 058. 25	1	14, 163. 90	$4p^2S^3_{1½}-5d^4D_{0½}$
7, 036. 30	5	14, 208. 10	$4p^4P^1_{1½}-4d^4P_{2½}$
7, 021. 99	1	14, 237. 06	
7, 019. 30	4	14, 242. 51	
7, 011. 24	3	14, 258. 89	
7, 008. 00	10	14, 265. 48	$4p^4P^3_{3½}-4d^2F_{2½}$
7, 006. 30	4	14, 268. 94	$4p^2P^1_{1½}-4d^2P^3_{0½}$
6, 995. 88	12	14, 290. 19	$4p^2S^3_{1½}-4d^2P_{1½}$
6, 981. 85	25	14, 318. 91	$4p^4P^3_{3½}-6s^4P_{2½}$
6, 979. 60	3	14, 323. 52	$4p^2P^1_{1½}-5d^4F_{2½}$
6, 977. 00	5	14, 328. 86	
6, 966. 80	8	14, 349. 84	$4p^4P^1_{1½}-6s^4P_{1½}$
6, 962. 50	6	14, 358. 70	

TABLE 1.—*Wave lengths in the arc spectrum of chlorine*—Continued

λ_{air}. I. A.	Intensity	ν_{vac} cm^{-1}	Term combination
6, 932. 90	25	14, 420. 00	$4p^4P^2_{3½}-4d^4P_{2½}$
6, 925. 35	6	14, 435. 73	
6, 924. 40	5	14, 437. 71	
6, 910. 32	6	14, 467. 02	$4p^2S^0_{½}-4d^2P_{0½}$
6, 872. 85	6	14, 546. 00	$4p^2D^1_{1½}-4d^2P_{1½}$
6, 865. 36	8	14, 561. 87	$4p^4P^2_{3½}-6s^4P_{1½}$
6, 854. 45	10	14, 585. 05	
6, 841. 74	6	14, 612. 14	$4p^4S^1_{1½}-5d^2D_{1½}$
6, 840. 23	15	14, 615. 37	$4p^4P^3_{3½}-4d^2D_{3½}$
6, 837. 60	5	14, 620. 99	$4p^2D^2_{3½}-5d^4D_{2½}$
6, 816. 50	2	14, 666. 24	$4p^4D^0_{0½}-5d^4D_{1½}$
6, 811. 50	3	14, 677. 01	$4p^4P^1_{1½}-4d^2D_{1½}$
6, 810. 04	15	14, 680. 23	$4p^4P^0_{0½}-4d^4P_{1½}$
6, 791. 92	3	14, 719. 32	$4p^4D^0_{0½}-5d^4D_{0½}$
6, 790. 20	2	14, 723. 05	$4p^2D^1_{1½}-4d^2P_{0½}$
6, 784. 45	1	14, 735. 53	$4p^4P^0_{0½}-6s^4P_{0½}$
6, 765. 20	3	14, 777. 46	$4p^2D^1_{1½}-5d^4F_{2½}$
6, 762. 30	2	14, 783. 80	$4p^4D^1_{1½}-5d^4D_{2½}$
6, 760. 05	2	14, 788. 82	
6, 757. 75	5	14, 793. 75	
6, 751. 54	4	14, 807. 27	$4p^2P^1_{1½}-5d^2D_{2½}$
6, 730. 24	5	14, 854. 22	$4p^4S^1_{1½}-5d^2F_{2½}$
6, 723. 40	4	14, 869. 33	$4p^4D^1_{1½}-5d^4D_{1½}$
6, 714. 65	4*d*?	14, 888. 71	$4p^4P^2_{3½}-4d^2D_{1½}$
6, 709. 90	15	14, 899. 25	
6, 703. 20	6	14, 914. 14	$4p^4P^1_{1½}-4d^4P_{1½}$
6, 699. 40	3	14, 922. 60	$4p^4D^1_{1½}-5d^4D_{0½}$
6, 697. 45	2	14, 926. 94	$4p^2S^0_{½}-5d^4P_{0½}$
6, 678. 39	10	14, 969. 54	$4p^4P^1_{1½}-6s^4P_{0½}$
6, 653. 80	1	15, 024. 86	
6, 643. 10	1	15, 049. 06	$4p^4D^1_{1½}-4d^2P_{1½}$
6, 637. 15	2	15, 062. 55	
6, 634. 60	0	15, 068. 34	$4p^4D^2_{3½}-5d^4D_{3½}$
6, 632. 75	0	15, 072. 55	
6, 611. 32	1	15, 121. 40	
6, 609. 26	7	15, 126. 12	$4p^4P^2_{3½}-4d^4P_{1½}$
6, 604. 57	7	15, 136. 86	$4p^4D^3_{3½}-5d^4D_{3½}$
6, 600. 10	3	15, 147. 11	$4p^2P^1_{1½}-5d^2F_{2½}$
6, 567. 35	3	15, 222. 64	$4p^4D^3_{3½}-5d^4D_{1½}$
6, 565. 90	1	15, 226. 01	$4p^4D^1_{1½}-4d^2P_{0½}$
6, 551. 28	3	15, 259. 98	
6, 550. 80	3	15, 261. 10	$4p^2D^1_{1½}-5d^2D_{2½}$ $4p^4D^0_{0½}-5d^4F_{1½}$
6, 542. 40	8	15, 280. 70	$4p^4P^0_{0½}-4d^4P_{0½}$ $4p^4D^1_{1½}-5d^4F_{2½}$
6, 536. 10	1	15, 295. 43	
6, 531. 39	20	15, 306. 45	$4p^4D^3_{3½}-5d^4D_{3½}$
6, 528. 12	0	15, 314. 12	
6, 526. 46	1	15, 318. 02	
6, 509. 00	2	15, 359. 11	$4p^2D^1_{1½}-5d^2D_{1½}$

TABLE 1.—*Wave lengths in the arc spectrum of chlorine*—Continued

λ_{air}, I. A.	Intensity	ν_{vac} cm^{-1}	Term combination
6, 502. 21	5	15, 375. 15	$4p^4D^2_{3½} - 5d^4D_{2½}$
6, 492. 76	0	15, 397. 52	
6, 490. 55	1	15, 402. 77	$4p^4D^2_{3½} - 4d^2P_{1½}$
6, 485. 38	1	15, 415. 05	
6, 475. 90	1	15, 437. 61	
6, 471. 45	3	15, 448. 23	
6, 464. 60	1	15, 464. 60	$4p^4D^1_{1½} - 5d^4F_{1½}$
6, 457. 14	1	15, 482. 46	$4p^4D^3_{0½} - 5d^4P_{0½}$
6, 455. 24	0	15, 487. 02	
6, 452. 75	1	15, 492. 99	
6, 450. 30	12	15, 498. 88	$4p^2D^3_{3½} - 5d^2F_{3½}$
6, 443. 76	2	15, 514. 61	$4p^4P^1_{1½} - 4d^4P_{0½}$
6, 440. 20	1	15, 523. 19	
6, 434. 79	15	15, 536. 24	$4p^4D^3_{3½} - 5d^4F_{3½}$
6, 425. 61	8	15, 558. 43	
6, 409. 64	0	15, 597. 20	
6, 408. 05	7	15, 601. 07	$4p^2D^1_{1½} - 5d^2F_{2½}$ $4p^2D^3_{2½} - 5d^2D_{2½}$
6, 398. 63	20	15, 624. 04	$4p^4D^3_{3½} - 5d^4F_{4½}$
6, 395. 66	0	15, 631. 29	
6, 394. 75	4	15, 633. 52	$4p^4D^2_{2½} - 5d^4F_{2½}$
6, 376. 28	3	15, 678. 80	
6, 373. 37	1	15, 685. 96	$4p^4D^1_{1½} - 5d^4P_{0½}$
6, 371. 40	2	15, 690. 81	
6, 367. 98	3	15, 699. 23	$4p^2D^3_{2½} - 5d^2D_{1½}$
6, 366. 83	2	15, 702. 07	
6, 366. 41	2	15, 703. 11	
6, 361. 19	2	15, 715. 99	
6, 347. 00	4	15, 751. 13	
6, 342. 72	2	15, 761. 76	
6, 341. 66	10	15, 764. 39	$4p^4D^1_{1½} - 5d^2D_{2½}$
6, 337. 59	0	15, 774. 51	$4p^4D^3_{1½} - 5d^4F_{3½}$
6, 334. 96	4	15, 781. 06	
6, 329. 65	0	15, 794. 30	
6, 326. 74	3	15, 801. 57	
6, 321. 59	6	15, 814. 44	
6, 304. 94	0	15, 856. 20	$4p^4D^2_{2½} - 5d^4P_{2½}$
6, 280. 20	5	15, 918. 67	
6, 276. 50	1	15, 928. 05	
6, 274. 51	0	15, 933. 10	
6, 252. 26	8	15, 989. 80	$4p^4P^3_{0½} - 5d^4D_{1½}$
6, 242. 54	4	16, 014. 70	$4p^4D^3_{3½} - 5d^2F_{3½}$
6, 231. 48	8	16, 043. 12	$4p^4P^3_{0½} - 5d^4D_{0½}$
6, 228. 68	1*d*?	16, 050. 34	
6, 226. 39	3	16, 056. 24	
6, 211. 55	6	16, 094. 60	$4p^4D^3_{3½} - 5d^4P_{2½}$
6, 194. 72	15	16, 138. 32	$4p^4P^1_{1½} - 5d^4D_{2½}$
6, 165. 38	1	16, 215. 12	$4p^4D^3_{2½} - 5d^2D_{1½}$
6, 162. 05	12	16, 223. 89	$4p^4P^1_{1½} - 5d^4D_{1½}$
6, 159. 80	0	16, 229. 81	

TABLE 1.—*Wave lengths in the arc spectrum of chlorine*—Continued

λ_{air}. I. A.	Intensity	ν_{vac} cm^{-1}	Term combination
6, 157. 85	2	16, 234. 95	
6, 151. 34	2	16, 252. 13	$4p^4D^3_{3½} - 5d^2F_{3½}$
6, 141. 79	4	16, 277. 40	$4p^4P^3_{1½} - 5d^4D_{0½}$
6, 140. 21	25	16, 281. 59	$4p^4P^3_{2½} - 5d^4D_{3½}$
6, 127. 00	0	16, 316. 70	
6, 114. 37	15	16, 350. 77	$4p^4P^3_{2½} - 5d^4D_{2½}$
6, 110. 38	1	16, 361. 07	
6, 082. 53	4	16, 435. 99	$4p^4P^3_{2½} - 5d^4D_{1½}$
6, 076. 45	1	16, 452. 43	
6, 073. 39	1	16, 460. 72	
6, 058. 33	0	16, 501. 64	
6, 042. 34	1	16, 545. 31	
6, 040. 43	2	16, 550. 51	
6, 037. 14	1	16, 559. 56	
6, 019. 71	6	16, 607. 51	
6, 003. 03	0	16, 653. 73	
5, 991. 42	4	16, 685. 92	
5, 972. 75	2	16, 738. 08	
5, 969. 86	0	16, 746. 18	
5, 965. 71	2	16, 757. 83	
5, 948. 40	4	16, 806. 60	$4p^4P^3_{0½} - 5d^4P_{0½}$
5, 936. 20	0	16, 841. 14	
5, 934. 00	1	16, 847. 38	$4p^4P^3_{2½} - 5d^4F_{2½}$
5, 930. 35	6	16, 857. 75	$4p^4D^3_{3½} - 6d^4D_{3½}$ $4p^4P^3_{1½} - 5d^4P_{2½}$
5, 916. 31	0	16, 897. 76	
5, 910. 75	0	16, 913. 65	
5, 908. 22	2	16, 920. 89	$4p^4D^3_{3½} - 6d^4D_{2½}$
5, 889. 14	1	16, 975. 71	
5, 880. 76	1	16, 999. 90	
5, 877. 53	2	17, 009. 25	
5, 866. 75	4	17, 040. 50	$4p^4P^1_{1½} - 5d^4P_{0½}$
5, 864. 44	0	17, 047. 21	
5, 861. 27	1	17, 056. 43	
5, 856. 70	8	17, 069. 74	$4p^4P^3_{2½} - 5d^4P_{2½}$
5, 847. 68	7	17, 096. 07	$4p^4D^3_{3½} - 6d^4D_{3½}$
5, 846. 70	8	17, 098. 94	
5, 844. 15	6	17, 106. 40	$4p^4P^1_{1½} - 5d^4P_{1½}$
5, 842. 39	1	17, 111. 55	
5, 839. 85	4	17, 118. 99	$4p^4P^1_{1½} - 5d^2D_{2½}$
5, 827. 44	2	17, 155. 45	
5, 826. 24	2	17, 158. 98	$4p^4D^3_{3½} - 6d^4D_{2½}$
5, 819. 44	0	17, 179. 03	
5, 817. 58	1	17, 184. 52	
5, 808. 59	1	17, 211. 12	
5, 806. 76	2	17, 216. 54	$4p^4P^1_{1½} - 5d^2D_{1½}$
5, 802. 84	5	17, 228. 17	$4p^4P^3_{1½} - 5d^2F_{3½}$
5, 799. 88	12	17, 236. 97	
5, 796. 26	15	17, 247. 73	
5, 774. 72	4	17, 312. 07	

TABLE 1.—*Wave lengths in the arc spectrum of chlorine*—Continued

λ_{air}. I. A.	Intensity	ν_{vac} cm^{-1}	Term combination
5, 772. 58	5	17, 318. 48	$4p^4P^2_{2½}-5d^4P_{1½}$
5, 769. 36	2	17, 328. 15	
5, 768. 30	2	17, 331. 34	$4p^4P^2_{2½}-5d^2D_{2½}$
5, 765. 55	3	17, 339. 60	
5, 726. 16	5	17, 458. 88	$4p^4P^1_{1½}-5d^2F_{2½}$
5, 711. 68	1	17, 503. 14	
5, 702. 02	1	17, 532. 79	
5, 686. 28	1	17, 581. 32	
5, 673. 01	1	17, 622. 45	
5, 660. 96	2	17, 659. 96	
5, 654. 20	1	17, 681. 07	
5, 620. 72	1	17, 786. 39	
5, 582. 28	1	17, 908. 87	
5, 580. 45	3	17, 914. 74	
5, 578. 13	3	17, 922. 16	$4p^4P^1_{1½}-6d^4D_{2½}$
5, 549. 21	1	18, 015. 59	
5, 541. 00	1	18, 042. 28	
5, 532. 13	8	18, 071. 21	$4p^4P^2_{2½}-6d^4D_{3½}$
5, 512. 95	4	18, 134. 08	$4p^4P^2_{2½}-6d^4D_{2½}$
5, 493. 14	3	18, 199. 48	
5, 484. 60	1	18, 227. 82	
5, 464. 31	1	18, 295. 50	
5, 401. 65	1	18, 507. 73	
5, 376. 32	1	18, 594. 93	
5, 338. 00	2	18, 728. 41	
5, 315. 10	1	18, 809. 10	
5, 307. 55	2	18, 835. 86	
5, 231. 41	2	19, 110. 00	
5, 140. 35	5	19, 448. 52	$4s^3P_{0½}-4p^3P^1_{1½}$, ($^3P^1D$)
5, 099. 80	8	19, 603. 16	$4s^3P_{0½}-4p^3P^2_{0½}$, ($^3P^1D$)
5, 074. 25	1	19, 701. 87	
4, 976. 62	10	20, 088. 37	$4s^3P_{1½}-4p^3P^1_{1½}$, ($^3P^1D$)
4, 952. 76	1	20, 185. 14	
4, 852. 70	8	20, 601. 35	$4s^3P_{1½}-5p^4D^2_{3½}$
4, 818. 64	2	20, 746. 96	$4s^3P_{0½}-5p^4S^1_{1½}$
4, 818. 42	3	20, 747. 91	$4s^3P_{1½}-5p^4P^2_{0½}$
4, 796. 76	2	20, 841. 60	$4s^3P_{0½}-5p^3D^1_{1½}$
4, 740. 71	10	21, 088. 01	$4s^3P_{1½}-5p^4D^1_{1½}$
4, 721. 24	8	21, 174. 97	$4s^3P_{1½}-5p^3D^2_{2½}$
4, 691. 53	12	21, 309. 07	$4s^3P_{1½}-5p^4D^2_{0½}$
4, 677. 76	7	21, 371. 79	$4s^3P_{1½}-5p^3S^2_{0½}$
4, 674. 40	2	21, 387. 15	$4s^3P_{1½}-5p^4S^1_{1½}$
4, 661. 22	18	21, 447. 63	$4s^3P_{0½}-5p^3P^1_{1½}$
4, 654. 05	10	21, 480. 67	$4s^3P_{1½}-5p^3D^1_{1½}$
4, 633. 91	0	21, 574. 03	
4, 631. 72	1	21, 584. 23	
4, 623. 96	10	21, 620. 45	$4s^3P_{0½}-4p^3D^1_{1½}$, ($^3P^1D$)
4, 601. 00	20	21, 728. 34	$4s^3P_{0½}-5p^3P^2_{0½}$
4, 580. 47	3	21, 825. 72	$4s^4P_{1½}-4p^3P^1_{1½}$, ($^3P^1D$)
4, 578. 17	4	21, 836. 69	$4s^4P_{0½}-5p^4P^1_{1½}$
4, 548. 06	1	21, 981. 25	
4, 545. 38	0	21, 994. 21	$4s^4P_{1½}-5p^4P^2_{2½}$
4, 526. 20	30	22, 087. 42	$4s^3P_{1½}-5p^3P^1_{1½}$
4, 491. 05	10	22, 260. 29	$4s^3P_{1½}-4p^3D^1_{1½}$, ($^3P^1D$)
4, 475. 31	15	22, 338. 57	$4s^4P_{1½}-5p^4D^2_{3½}$

TABLE 1.—*Wave lengths in the arc spectrum of chlorine*—Continued

λ_{air}. I. A.	Intensity	ν_{vac} cm^{-1}	Term combination
4, 469. 37	18	22, 368. 26	$4s^2P_{1½}-5p^2P°_{½}$
4, 446. 11	4	22, 485. 28	$4s^4P_{1½}-5p^4P°_{½}$
4, 445. 83	4	22, 486. 70	$4s^4P_{0½}-5p^4D°_{½}$
4, 438. 48	20	22, 523. 93	$4s^4P_{2½}-5p^4P°_{2½}$
4, 403. 03	15	22, 705. 27	$4s^4P_{2½}-5p^4P°_{1½}$
4, 402. 58	4	22, 707. 60	$4s^4P_{0½}-5p^4D°_{½}$
4, 390. 38	7	22, 770. 70	$4s^4P_{0½}-5p^2S°_{½}$
4, 389. 76	25	22, 773. 91	$4s^4P_{2½}-5p^4D°_{3½}$
4, 387. 55	6	22, 785. 38	$4s^4P_{0½}-5p^4S°_{1½}$
4, 379. 90	20	22, 825. 18	$4s^4P_{1½}-5p^4D°_{1½}$
4, 371. 55	5	22, 868. 78	$4s^4P_{2½}-5p^4D°_{3½}$
4, 369. 52	15	22, 879. 40	$4s^4P_{0½}-5p^2D°_{1½}$
4, 363. 30	20	22, 912. 02	$4s^4P_{1½}-5p^2D°_{2½}$
4, 337. 80	1	23, 046. 70	$4s^4P_{1½}-5p^4D°_{½}$
4, 323. 35	20	23, 123. 73	$4s^4P_{1½}-5p^4S°_{1½}$
4, 305. 55	1	23, 219. 33	$4s^4P_{0½}-5p^2D°_{1½}$
4, 280. 43	2	23, 355. 59	$4s^4P_{2½}-5p^4D°_{1½}$
4, 264. 59	5	23, 442. 34	$4s^4P_{2½}-5p^2D°_{2½}$
4, 226. 44	15	23, 653. 94	$4s^4P_{2½}-5p^4S°_{1½}$
4, 209. 68	12	23, 748. 11	$4s^4P_{2½}-5p^2D°_{1½}$
4, 147. 20	2	24, 105. 88	$4s^4P_{1½}-5p^2P°_{½}$
4, 139. 00	1	24, 153. 64	
4, 104. 78	3	24, 354. 99	$4s^4P_{2½}-5p^2P°_{1½}$
4, 032. 14	5	24, 793. 75	
3, 992. 81	2	25, 037. 96	
3, 944. 79	3	25, 342. 74	

d=double.

A detailed description of the theoretical term structure of neutral chlorine is given in RP73. All the prominent lines of the spectrum belong to three families of terms which have ^3P, ^1D, and ^1S of Cl II as limits. The terms of these families arise when one of the p electrons of the configuration $3s^2.3p^5$ becomes an ns, np, nd ... electron in the process of excitation. A much less conspicuous group of terms will arise when one of the s electrons is removed from the configuration $3s^2.3p^5$ and approaches $^3P°$ or $^1P°$ from the configuration $3s.3p^5$ of Cl II as limits. In table 2 are given the term groups resulting from the excitation processes just outlined.

TABLE 2.—*Theoretical terms of Cl I*

Electron configurations	Limiting terms of Cl II			
	^3P	^1D	^1S	$^3P°,^1P°$
$3s^2.3p^5$	$^2P°$			
$3s^2.3p^4.ns$	^3P ^4P	^2D	^2S	
$3s^2.3p^4.np$	$^2S°,^2P°,^2D°,^4S°,^4P°,^4D°$	$^2P°,^2D°,^2F°$	$^2P°$	
$3s^2.3p^4.nd$	$^2P,^2D,^2F,^4P,^4D,^4F$	$^2S,^2P,^2D,^2F,^2G$	^2D	
$3s.3p^6$				^2S

The revised list of Cl I terms is given in table 3. Comparison with the corresponding table of RP73 will show the following corrections and extensions. New values have been assigned to the $^2S°$ terms of the $4p$ and $5p$ groups, which otherwise remain unchanged; the nd groups, in which only the ^4D term had previously been established with certainty, are now practically completed, with the finding of the ^4F and ^4P terms, and also the corresponding doublet terms; the terms with $\Delta\nu = 1.70$, previously provided with the symbol ^2X, are now definitely designated as $4s^2D$ belonging to the ^1D family. With the terms now established for Cl I a total of 269 lines, or 61 percent of those given in table 1, has been classified. This is approximately twice the number classified in RP73.

It should be noticed that the total quantum numbers of the nd electrons have been increased by 1. Although the terms coming from the $3d$ electron have not been established, yet there is good reason to believe that they are not of the same order of stability as those of the $4s$ electron. deBruin's [4] analysis of singly ionized argon, which is isoelectronic with neutral chlorine, shows that the $3d$ terms have nearly the same values as those of the $4s$ electron; but in the arc spectrum of argon the $3d$ terms lie about 20,000 cm^{-1} higher than the $4s$ terms. Similarly, in Cl II the analysis of Kiess and deBruin [5] shows that the $3d$ terms are next in stability after the $4s$ terms; but if the Cl I terms of the nd sequences are approximately represented by Rydberg's formula then those of the $3d$ electron should fall close to the level of the $4p$ terms, near 18,000 cm^{-1}, in which case the lines through which they must be established will lie in the infrared beyond the limit reached in table 1.

TABLE 3.—*Observed terms of Cl I*

Term type	ν	$\Delta\nu$	Series electron	Term type	ν	$\Delta\nu$	Series electron
$^3P_{1½}$	104, 991	881	$3p$	$^4D_{3½}$	21, 101. 36	238. 26	$4p+{}^3P$
$^3P_{0½}$	104, 110			$^4D_{2½}$	20, 863. 10	353. 01	
$^4P_{2½}$	33, 037. 00	530. 20	$4s+{}^3P$	$^4D_{1½}$	20, 510. 09	203. 36	
$^4P_{1½}$	32, 506. 80	338. 44		$^4D_{0½}$	20, 306. 73		
$^4P_{0½}$	32, 168. 36			$^2D_{2½}$	20, 347. 31	340. 35	
$^3P_{1½}$	30, 769. 56	639. 80		$^2D_{1½}$	20, 006. 96		
$^3P_{0½}$	30, 129. 76			$^2S_{0½}$	19, 751. 02		
$^3D_{2½}$	20, 875. 32	1. 70	$4s+{}^1D$	$^2P_{1½}$	19, 552. 96	475. 40	
$^3D_{1½}$	20, 873. 62			$^2P_{0½}$	19, 077. 56		
$^4P_{3½}$	22, 076. 46	212. 05	$4p+{}^3P$	$^4S_{1½}$	19, 260. 32		
$^4P_{1½}$	21, 864. 41	233. 96		$^2P_{1½}$	10, 681. 33	154. 83	$4p+{}^1D$
$^4P_{0½}$	21, 630. 45			$^2P_{0½}$	10, 526. 50		

[4] Proc. Acad. Sci. Amsterdam, vol. 31, p. 771, 1928; vol. 33, p. 198, 1930.
[5] Soon to be published in Bureau of Standards Journal of Research.

TABLE 3.—*Observed terms of Cl I*—Continued

Term type	ν	$\Delta\nu$	Series electron	Term type	ν	$\Delta\nu$	Series electron
$^2F_{3½}$	9, 815. 00			$^4P_{0½}$	6, 349. 78		
		35. 95					
$^2F_{2½}$	9, 850. 95		$4p+{}^1D$	$^2F_{3½}$	8, 161. 15	350. 09	
$^2D_{3½}$	8, 512. 62			$^2F_{2½}$	7, 811. 06		
		3. 32					$4d+{}^3P$
$^2D_{1½}$	8, 509. 30			$^2D_{2½}$	7, 461. 15	273. 61	
$^4P_{2½}$	10, 513. 07			$^2D_{1½}$	7, 187. 54		
		181. 35					
$^4P_{1½}$	10, 331. 72			$^2P_{1½}$	5, 460. 90	176. 90	
		310. 15					
$^4P_{0½}$	10, 021. 57			$^2P_{0½}$	5, 284. 00		
$^4D_{3½}$	10, 263. 09			$^4P_{2½}$	7, 757. 63	242. 83	
		94. 84					
$^4D_{2½}$	10, 168. 25			$^4P_{1½}$	7, 514. 80		$6s+{}^3P$
		486. 68				619. 76	
$^4D_{1½}$	9, 681. 57			$^4P_{0½}$	6, 895. 04		
		221. 08					
$^4D_{0½}$	9, 460. 49		$5p+{}^3P$	$^4D_{3½}$	5, 794. 98	68. 69	
$^2D_{3½}$	9, 594. 69			$^4D_{2½}$	5, 726. 29		
		305. 70				85. 51	
$^2D_{1½}$	9, 288. 99			$^4D_{1½}$	5, 640. 78		
						53. 39	
$^2S_{0½}$	9, 397. 72			$^4D_{0½}$	5, 587. 39		
$^4S_{1½}$	9, 382. 70			$^4F_{4½}$	5, 477. 32		
						150. 47	
$^2P_{1½}$	8, 682. 16			$^4F_{3½}$	5, 326. 85		
		280. 80				97. 37	
$^2P_{0½}$	8, 401. 36			$^4F_{2½}$	5, 229. 48		
						183. 90	
$^4D_{3½}$	9, 294. 51			$^4F_{1½}$	5, 045. 58		$5d+{}^3P$
		85. 92					
$^4D_{2½}$	9, 208. 59			$^4P_{3½}$	5, 006. 70		
		110. 75				248. 70	
$^4D_{1½}$	9, 097. 84			$^4P_{1½}$	4, 758. 00		
		98. 02				65. 88	
$^4D_{0½}$	8, 999. 82			$^4P_{0½}$	4, 823. 88		
$^4F_{4½}$	8, 500. 60			$^2F_{3½}$	4, 848. 59		
		236. 41				442. 87	
$^4F_{3½}$	8, 264. 19		$4d+{}^3P$	$^2F_{2½}$	4, 405. 72		
		214. 49					
$^4F_{2½}$	8, 049. 70			$^2D_{2½}$	4, 745. 68		
		314. 25				97. 66	
$^4F_{1½}$	7, 735. 45			$^2D_{1½}$	4, 648. 02		
$^4P_{2½}$	7, 656. 40			$^4D_{3½}$	4, 005. 40		
		706. 20				62. 87	$6d+{}^3P$
$^4P_{1½}$	6, 950. 20			$^4D_{2½}$	3, 942. 53		
		600. 42					

IV. ACKNOWLEDGMENT

In conclusion, it is a pleasure to acknowledge my indebtedness to Dr. E. Wichers, of the Bureau staff, who prepared the palladium chloride used in the experimental work.

WASHINGTON, April 20, 1933.

RP571

THE EFFECT OF GASOLINE VOLATILITY ON THE MISCIBILITY WITH ETHYL ALCOHOL

By Oscar C. Bridgeman and Dale W. Querfeld

ABSTRACT

Data are presented on the effect of the volatility of gasoline on its miscibility with ethyl alcohol containing various amounts of water. Samples of gasoline having different volatilities were obtained by two methods—first, fractional distillation of an original gasoline and second, blending of refinery and natural gasolines. The more volatile gasolines were found to be more miscible with alcohol, in that they produced mixtures having lower critical solution temperatures than similar mixtures containing less volatile gasoline. Comparatively small differences were found in the miscibility with ethyl alcohol of gasolines having the same volatility but different composition.

CONTENTS

		Page
I.	Introduction	841
II.	Description of gasoline samples	841
III.	Experimental data	843
IV.	Conclusions	850

I. INTRODUCTION

In a previous paper[1] data were presented on the critical solution temperatures of mixtures, in various proportions, of eight different gasolines with ethyl alcohol containing various percentages of water. The experimental results were suggestive in indicating that differences in the volatility of various gasolines might account for most of the differences found in the critical solution temperatures of mixtures of ethyl alcohol and these gasolines. Differences in the crude from which the gasoline was refined, or differences in composition of cracked and straight-run gasolines of about the same volatility, appeared to have comparatively little effect on the critical solution temperatures. In order to obtain more direct experimental evidence regarding the effect of the volatility of gasoline on its miscibility with ethyl alcohol, the investigation described in the present paper was undertaken.

II. DESCRIPTION OF GASOLINE SAMPLES

Three of the gasolines used in the previous investigation were "topped", so as to reduce the temperature at 90 percent evaporated to approximately the same value in the three cases. This "topping" process was accomplished by distilling the gasoline in a laboratory

[1] Bridgeman and Querfeld, Critical Solution Temperatures of Mixtures of Gasoline, Ethyl Alcohol and Water, B.S. Jour. Research, vol. 10 (RP560), p. 693, May 1933.

still, stopping the distillation at an appropriate stage, and discarding the residue left in the distillation flask. Distillation of the product thus obtained, employing A.S.T.M. standard method D86–30, was used to determine when a sufficient percentage of the distillate had been collected. By the above procedure, the 90 percent temperatures of gasolines nos. 1, 7, and 8 were reduced by 46°, 38°, and 41° C., respectively, to a value which was close to 152° C. in all three cases. This particular value of 152° C. was chosen since the volatility of the Pennsylvania straight-run gasoline no. 1, after removal of the heavier fractions, was thereby made almost identical with that of the Rumanian straight-run gasoline no. 2, and permitted a direct comparison of the critical solution temperatures for two gasolines of the same volatility but of widely different chemical characteristics.

In order to evaluate the effect on critical solution temperatures produced by lowering the 10 percent distillation temperature of the gasoline, blends of natural gasoline with gasoline no. 1 were prepared. Two different natural gasolines were employed and the blends contained 10, 20, and 30 volume percent of the respective natural gasoline. These blends were prepared at 0° C. in order to minimize evaporation of the lighter constituents. In addition to the measurements made on the above gasolines and blends, some supplementary data were obtained on six commercial gasolines, presumably mixtures of straight-run and cracked products.

Distillation and specific gravity data are given in table 1 for the various gasolines and blends, and for the two natural gasolines used in blending with gasoline no. 1.

TABLE 1.—*Identification data on gasolines*

No.	Description	Distillation temperatures at stated percentages evaporated			60°/60° specific gravity
		10 percent	50 percent	90 percent	
		°C.	°C.	°C.	
1	Straight-run Pennsylvania	76	135	199	0.738
9	Gasoline no. 1 distillate	69	107	153	.720
2	Straight-run Rumania	70	109	152	.734
7	Cracked gasoline	54	126	188	.754
10	Gasoline no. 7 distillate	53	96	150	.722
8	Cracked gasoline	69	142	194	.773
11	Gasoline no. 8 distillate	60	102	153	.734
18	10 percent natural gasoline A+90 percent no. 1	64	128	197	.731
19	20 percent natural gasoline A+80 percent no. 1	55	119	196	.721
20	30 percent natural gasoline A+70 percent no. 1	42	104	192	.707
21	10 percent natural gasoline B+90 percent no. 1	69	128	197	.736
22	20 percent natural gasoline B+80 percent no. 1	61	120	195	.727
23	30 percent natural gasoline B+70 percent no. 1	57	111	193	.719
12	Commercial gasoline	61	130	180	.742
13	do	58	123	181	.742
14	do	68	127	175	.743
15	do	69	136	186	.752
16	do	65	124	174	.741
17	do	66	131	187	.752
	Natural gasoline A	24	31	52	.632
	Natural gasoline B	43	58	101	.678

III. EXPERIMENTAL DATA

The apparatus and procedure used in the present work were identical with those previously described. A description of the aqueous ethyl alcohol solutions employed is given in table 2.

TABLE 2.—*Concentrations of ethyl alcohol solutions*

No.	60°/60° specific gravity	Volume percent alcohol at 60° F.	Volume percent water at 60° F.	No.	60°/60° specific gravity	Volume percent alcohol at 60° F.	Volume percent water at 60° F.
A	0.79820	99.144	1.110	E	0.81269	95.845	5.178
A1	.79826	99.131	1.127	E1	.81274	95.833	5.193
A2	.79835	99.112	1.151	E2	.81257	95.875	5.143
				E3	.81293	95.787	5.248
B	.80202	98.337	2.133				
B1	.80207	98.325	2.149	F	.81608	94.987	6.196
B2	.80199	98.344	2.124	F1	.81609	94.984	6.201
B3	.80210	98.318	2.157	F2	.81615	94.970	6.218
				F3	.81623	94.948	6.244
C	.80565	97.528	3.139				
C1	.80580	97.492	3.182	G	.81948	94.097	7.243
C2	.80586	97.479	3.199	G1	.81940	94.119	7.217
C3	.80586	97.479	3.199	G2	.81961	94.061	7.285
				G3	.81949	94.094	7.246
D	.80917	96.703	4.145				
D1	.80927	96.679	4.175	H	.82264	93.243	8.237
D2	.80930	96.672	4.184	H1	.82281	93.196	8.291
D3	.80941	96.645	4.216	H2	.82275	93.210	8.275
				H3	.82275	93.210	8.275

With each of the three fractionated gasolines, mixtures containing from 10 to 90 volume percent of gasoline, by even steps of 10 percent, were prepared with the alcohol solution of each concentration, and measurements of the critical solution temperature were made. No measurements were made on those mixtures having critical solution temperatures outside of the approximate range from +65° C. to −65° C. The data on the three gasolines are given in tables 3, 4, and 5 where for comparison the values previously obtained on the gasolines before fractionation are also included. It is seen that the decrease in the 90 percent distillation temperatures of the gasolines has produced a marked lowering in the critical solution temperatures. This lowering is shown graphically in figure 1 for fuels nos. 9 and 1, the latter being the original gasoline. The lowering in critical solution temperature as the result of removing the heavier fractions of the gasoline becomes less (*a*) as the percentage of gasoline in the mixture increases and (*b*) as the percentage of water in the alcohol solution increases. For mixtures with the alcohol solution of the C series (97.5 percent alcohol), the lowering in critical solution temperature resulting from the average decrease of 42° C. in 90 percent distillation temperature was on the average 18° C. for mixtures containing 50 percent gasoline and 7° C. for mixtures containing 90 percent gasoline.

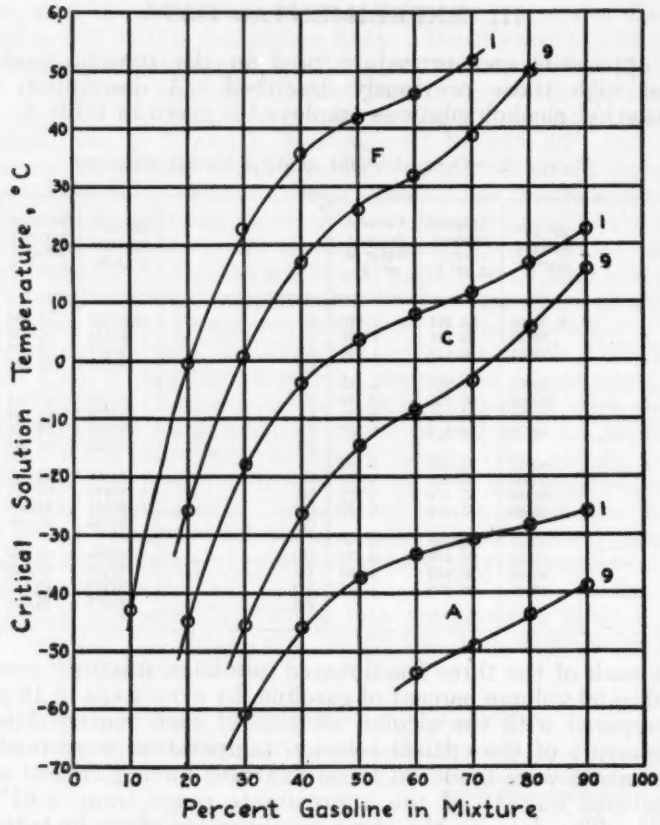

FIGURE 1.—*Comparison of data on the critical solution temperatures of mixtures in various proportions of ethyl alcohol and gasolines nos. 1 and 9*

Gasoline no. 9 is the more volatile fraction of gasoline no. 1 and the differences between the curves represent the effect of change in volatility. The letters between each pair of curves indicate the alcohol solutions used, the concentrations of which are recorded in table 2.

TABLE 3.—*Critical solution temperatures in ° C. of alcohol mixtures with gasolines nos. 9 and 1*

No.	Alcohol solution	Volume percent gasoline in mixture								
		10	20	30	40	50	60	70	80	90
9	A						−54.0	−49.1	−43.9	−39.0
1	A			−61.0	−46.2	−37.4	−33.4	−31.0	−28.3	−26.4
9	B1				−47.1	−35.2	−28.1	−23.9	−17.0	−9.3
1	B		−60.0	−36.8	−24.0	−15.1	−10.3	−7.4	−2.5	.8
9	C			−45.4	−26.8	−15.0	−8.9	−3.9	5.2	15.3
1	C		−45.0	−18.0	−4.1	3.7	7.7	11.3	16.6	22.3
9	D			−28.5	−9.9	1.0	7.5	12.1	20.9	31.0
1	D	−60.6	−26.2	−3.2	11.5	18.7	22.4	26.6	33.1	39.4
9	E		−39.6	−12.3	5.5	14.5	20.3	26.1	35.6	47.9
1	E	−54.7	−12.7	11.3	24.3	30.8	34.4	39.5	47.7	52.9
9	F		−25.0	1.5	17.4	26.2	31.6	38.8	49.6	
1	F	−43.2	.3	22.5	35.3	41.6	45.7	51.6		
9	G		−12.6	13.6	28.2	36.7	42.3	50.3		
1	G	−30.2	12.6	33.7	45.0					
9	H	−49.2	−1.4	24.1	38.3	46.1				
1	H	−19.3	23.2	43.2						

TABLE 4.—*Critical solution temperatures in ° C. for alcohol mixtures with gasolines nos. 10 and 7*

No.	Alcohol solution	Volume percent gasoline in mixture								
		10	20	30	40	50	60	70	80	90
10	A1									
7	A1									−53.1
10	B2						−56.4	−49.0	−41.2	−28.9
7	B1					−49.8	−44.8	−40.1	−30.9	−19.9
10	C2				−55.6	−41.3	−31.3	−24.9	−16.5	−.1
7	C1			−59.9	−40.0	−26.8	−19.3	−15.9	−9.3	2.8
10	D2			−56.4	−35.4	−22.6	−14.2	−8.1	1.9	18.3
7	D1			−38.8	−21.6	−10.9	−4.6	.7	9.6	24.5
10	E2			−41.0	−19.7	−6.8	−.3	6.4	18.0	37.5
7	E1		−50.2	−23.7	−6.5	3.5	8.6	14.8	24.4	42.6
10	F2		−55.9	−25.2	−5.7	5.6	12.1	19.6	32.6	
7	F1		−37.0	−9.1	6.2	14.7	20.2	27.0	39.0	
10	G2		−41.6	−11.3	6.7	17.0	23.3	31.8	46.8	
7	G1		−23.6	4.0	18.0	25.8	32.0	39.4	51.4	
10	H2		−28.7	.3	17.3	26.9	34.0	43.0	54.4	
7	H1	−58.1	−11.6	14.5	27.4	35.5	41.1	50.5		

TABLE 5.—*Critical solution temperatures in ° C. for alcohol mixtures with gasolines nos. 11 and 8*

No.	Alcohol solution	Volume percent gasoline in mixture								
		10	20	30	40	50	60	70	80	90
11	A2									−57.6
8	A1								−51.7	−45.6
11	B3						−52.7	−47.3	−40.0	−27.7
8	B1				−50.9	−40.9	−34.9	−28.2	−22.7	−13.9
11	C3				−52.8	−39.6	−30.4	−24.7	−15.9	−2.0
8	C1			−48.8	−30.0	−18.5	−13.3	−9.2	−.8	9.8
11	D3			−56.1	−34.7	−21.0	−13.1	−6.9	3.9	20.1
8	D1		−56.8	−28.2	−12.0	−1.5	2.1	8.2	15.9	27.4
11	E3			−38.0	−17.4	−4.7	1.2	8.4	19.2	39.0
8	E1	[1]−42.3	[1]−14.1	1.9	11.2	15.5	21.9	31.5	45.9	
11	F3		−53.8	−23.1	−3.8	7.1	13.3	20.0	33.9	
8	F1		−27.2	−.7	14.1	21.8	26.6	33.3	44.3	
11	G3		−39.4	−9.5	7.9	18.2	24.2	31.0	47.7	
8	G1		−13.6	13.3	25.4	33.1	37.6	45.8		
11	H3		−26.4	2.0	18.4	27.9	36.0	43.8	57.8	
8	H1	−49.8	−2.0	22.0	34.6	41.8				

[1] Solution E2.

For the blends of gasoline no. 1 with the two natural gasolines, measurements of the critical solution temperature were made only on alcohol mixtures containing 50 and 75 percent of the blend, since the primary object of the research was to investigate this range. The results obtained are given in tables 6 and 7. The slight differences in alcohol content of the different solutions used are not sufficient to vitiate the comparison, being equivalent to less than 1° C. difference in critical solution temperature. The data for the mixtures containing 75 percent of gasoline are shown graphically in figures 2 and 3, where the volume percent of water in the mixture is plotted against the critical solution temperature. Decrease in the 10 percent distillation temperature of the gasoline by addition of natural gasoline results in a lowering of the critical solution temperature, which on

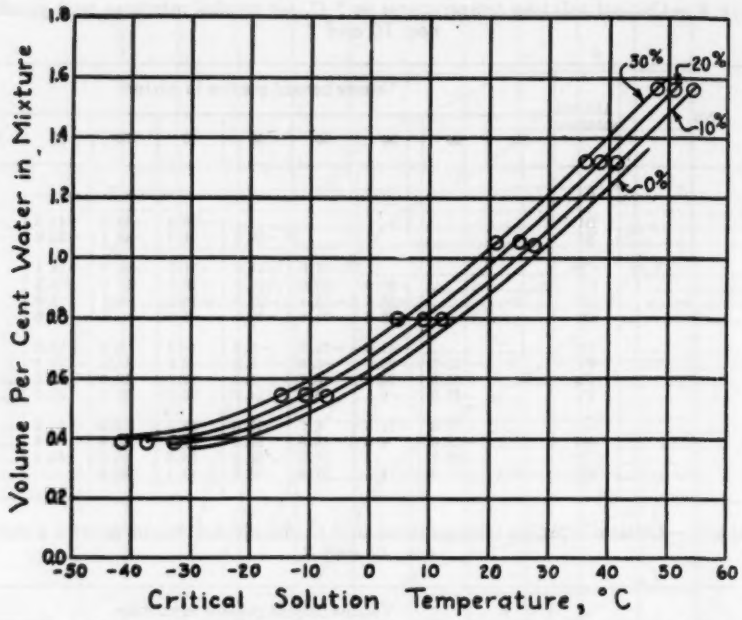

FIGURE 2.—*Data on the critical solution temperatures of mixtures containing 25 percent of ethyl alcohol of various water contents and 75 percent of blends of gasoline no. 1 with natural gasoline A in the proportions indicated on the curves.*

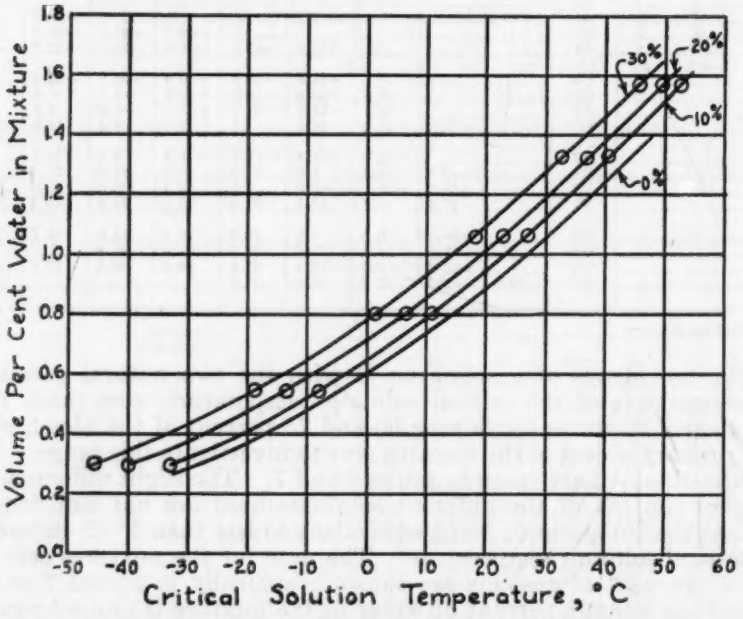

FIGURE 3.—*Data on the critical solution temperatures of mixtures containing 25 percent of ethyl alcohol of various water contents and 75 percent of blends of gasoline no. 1 with natural gasoline B in the proportions indicated on the curves.*

the average is 4° C. for each 10 percent addition of natural gasoline A and 3° C. for each 10 percent addition of natural gasoline B. For mixtures with the alcohol solution of the C series (97.5 percent alcohol), the lowering in critical solution temperature resulting from a decrease in the 10 percent distillation temperature of 20° C. was about 8° C. on the average, being only slightly different in the case of the two natural gasolines.

TABLE 6.—*Critical solution temperatures in ° C. for alcohol mixtures with gasolines containing various added percentages of natural gasoline A*

Gasoline no.	Amount of natural gasoline A	50 percent gasoline in mixture		75 percent gasoline in mixture	
		Alcohol solution	Critical solution temperature	Alcohol solution	Critical solution temperature
	Percent		° *C.*		° *C.*
1	0	A	−37.4	A	−30.1
18	10	A1	−41.2	A2	−33.6
19	20	A1	−46.2	A2	−40.1
20	30	A1	−53.3	A2	−46.2
1	0	B	−15.1	B	−5.0
18	10	B1	−16.8	B3	−8.4
19	20	B1	−20.4	B3	−13.9
20	30	B1	−29.5	B3	−19.0
1	0	C	3.7	C	13.7
18	10	C1	.7	C3	10.7
19	20	C1	−3.5	C3	6.3
20	30	C1	−10.5	C3	1.5
1	0	D	18.7	D	29.9
18	10	D1	15.9	D3	26.5
19	20	D1	11.2	D3	22.5
20	30	D1	5.3	D3	18.0
1	0	E	30.8	E	43.0
18	10	E1	27.9	E3	40.3
19	20	E1	23.9	E3	36.4
20	30	E1	18.5	E3	32.3
1	0	F	41.6	F	----
18	10	F1	38.6	F3	52.8
19	20	F1	35.0	F3	49.2
20	30	F1	29.7	F3	45.7
1	0	G	----	----	----
18	10	G1	49.0	----	----
19	20	G1	45.2	----	----
20	30	G1	39.5	----	----

TABLE 7.—*Critical solution temperatures in ° C. for alcohol mixtures with gasolines containing various added percentages of natural gasoline B*

Gasoline no.	Amount of natural gasoline B	50 percent gasoline in mixture		75 percent gasoline in mixture	
		Alcohol solution	Critical solution temperature	Alcohol solution	Critical solution temperature
	Percent		° *C.*		° *C.*
1	0	A	−37.4	A	−30.1
21	10	A1	−39.9	A2	−32.7
22	20	A1	−44.3	A2	−37.2
23	30	A1	−49.2	A2	−41.4
1	0	B	−15.1	B	−5.0
21	10	B2	−16.9	B3	−7.1
22	20	B2	−21.3	B3	−10.7
23	30	B2	−26.1	B3	−15.0
1	0	C	3.7	C	13.7
21	10	C2	2.1	C3	12.5
22	20	C2	−1.7	C3	9.4
23	30	C2	−6.2	C3	4.8
1	0	D	18.7	D	29.9
21	10	D2	16.9	D3	28.2
22	20	D2	13.1	D3	24.8
23	30	D2	9.1	D3	21.5
1	0	E	30.8	E	43.0
21	10	E2	28.6	E3	41.5
22	20	E2	25.3	E3	38.4
23	30	E2	21.7	E3	36.1
1	0	F	41.6	F	----
21	10	F2	39.4	F3	53.9
22	20	F2	36.4	F3	51.0
23	30	F2	33.0	F3	48.2
1	0	G	----	----	----
21	10	G2	49.3	----	----
22	20	G2	46.4	----	----
23	30	G2	43.2	----	----

Since the Pennsylvania gasoline no. 9, produced by topping gasoline no. 1, has the same volatility as the Rumania gasoline no. 2, within experimental error, a direct comparison is possible between the critical solution temperatures of two gasolines of equal volatility but of widely different chemical characteristics. Data on these two gasolines are given in table 8, and it is seen that gasoline no. 2 has somewhat lower critical solution temperatures. The difference is almost constant, being on the average 6.7° C. This difference represents about the maximum which is likely to be found between any two straight-run gasolines of the same volatility refined from different crude oils. Greater differences might be found, however, between a straight-run and a 100 percent cracked gasoline of equal volatility.

TABLE 8.—*Comparison of critical solution temperatures in ° C. for mixtures with alcohol of the Pennsylvania gasoline no. 9 and of the Rumania gasoline no. 2 of equal volatility*

No.	Alcohol solution	Volume percent gasoline in mixture								
		10	20	30	40	50	60	70	80	90
9	A						−54.0	−49.1	−43.9	−39.0
2	A					−67.0	−60.7	−55.6	−52.3	−47.9
9	B				−47.1	−35.2	−28.1	−23.9	−17.0	−9.3
2	B				−56.5	−43.6	−35.3	−30.4	−24.2	−16.2
9	C			−45.4	−26.8	−15.0	−8.9	−3.9	5.2	15.3
2	C			−53.5	−34.5	−21.5	−15.0	−10.8	−3.0	7.6
9	D			−28.5	−9.9	1.0	7.5	12.1	20.9	31.0
2	D		−59.9	−35.4	−16.5	−5.4	−.2	5.8	14.5	27.0
9	E		−39.6	−12.3	5.5	14.5	20.3	26.1	35.6	47.9
2	E		−47.9	−18.5	−1.3	8.5	14.0	19.7	29.4	41.9
9	F		−25.9	1.5	17.4	26.2	31.6	38.8	49.6	
2	F		−33.2	−1.5	11.1	20.1	25.6	32.4	44.4	
9	G		−12.6	13.6	28.2	36.7	42.3	50.3		
2	G		−20.4	7.3	22.2	30.7	36.5	44.4		
9	H	−49.2	−1.4	24.1	38.3	46.1				
2	H	−57.0	−7.8	17.7	32.2	40.7	46.4			

As a supplement to the information presented in this paper and the previous one, some data were obtained on six branded gasolines purchased on the open market, and are given in table 9. The differences in the critical solution temperatures of comparable mixtures containing any of the six commercial gasolines are very small.

TABLE 9.—*Critical solution temperatures in °C. for alcohol mixtures with various commercial gasolines*

(*a*) 50 PERCENT GASOLINE IN MIXTURE

Alcohol solution	Gasoline no.					
	12	13	14	15	16	17
A1	−58.8	−59.5	−60.6	−56.2	−58.8	−58.3
B1	−33.5	−34.1	−36.9	−29.5	−36.7	−34.1
C1	−13.3	−15.1	−16.5	−10.9	−17.1	−15.1
D1	1.5	−.1	−.5	4.1	−.6	1.5
E1	14.9	12.7	13.1	17.3	12.8	14.7
F1	26.5	24.4	24.6	28.6	24.2	25.9
G1	37.0	34.5	34.9	39.8	34.7	36.3
H1	47.3	44.1	44.4	47.9	44.3	45.6

(*b*) 75 PERCENT GASOLINE IN MIXTURE

A2	−49.4	−52.3	−51.0	−47.1	−52.6	−51.1
B3	−22.0	−24.0	−22.6	−18.9	−23.8	−22.7
C3	−.8	−3.2	−1.5	1.8	−2.9	−1.7
D3	15.3	13.7	14.9	18.1	14.0	15.3
E3	29.5	27.9	29.5	32.3	28.4	29.0
F3	42.8	41.0	42.2	44.9	41.6	42.0
G3	54.3	52.7	54.3	55.8	53.3	53.8

IV. CONCLUSIONS

The present work indicates that an increase in the volatility of a gasoline produces a marked lowering in the critical solution temperatures of its mixtures with ethyl alcohol. Differences in the critical solution temperatures of mixtures containing gasolines of the same volatility but of different composition were found to be comparatively small.

WASHINGTON, April 15, 1933.

RP572

CREEP AND STRUCTURAL STABILITY OF NICKEL-CHROMIUM-IRON-ALLOYS AT 1,600° F.

By W. A. Tucker and S. E. Sinclair

ABSTRACT

A study was made of the creep characteristics at 1,600° F. (870° C.) of 15 alloys covering a range from 1 to 75 percent nickel and from 3 to 55 percent chromium. The results were compared with those of a previous investigation at 1,000° F. (538° C.) on similar alloys.

In the investigation at 1,000° F. (538° C.) of the nickel-chromium-iron system, it was found that the alloys containing little or no iron, 50 to 80 percent nickel and 20 to 50 percent chromium exhibited the greatest resistance to creep. At 1,600° F. (870° C.), the strongest alloys are those containing approximately equal parts of nickel and chromium, and not more than 30 to 40 percent iron.

As part of a metallographic study the attempt was made to distinguish between the effect on structure of elevated temperature alone and of elevated temperature and stress combined. A comparison was made between the structure in specimens used in the creep test and that in the unstressed specimens of the same alloys annealed at 1,600° F. (870° C.) for periods ranging from 100 to 1,000 hours or quenched in iced brine from that temperature. In nearly all cases the quenched specimens were similar in structure to the annealed materials which indicates that these alloys were not readily heat treated.

Carbide precipitation and agglomeration of the carbide at the grain boundaries were most pronounced in both the binary iron-chromium alloys and the ternary iron-chromium-nickel alloys of higher chromium content. Prolonged heating, of both stressed and unstressed specimens, did not produce any pronounced changes in the structure of the binary iron-chromium alloys or the ternary alloys except those containing 50 percent or more of nickel.

CONTENTS

	Page
I. Introduction	851
II. Materials	852
III. Methods of study	853
1. Creep tests	853
2. Microstructural examination	854
IV. Results	855
1. Rates of creep	855
2. Microstructural changes	857
V. Discussion	858
1. Creep	858
2. Structure	861
VI. Summary	862

I. INTRODUCTION

The stresses producing creep of 1 percent in 1,000 hours in a number of cast nickel-chromium-iron alloys at 1,000° F. (538° C.) have been reported by French, Kahlbaum, and Peterson.[1] The present study

[1] H. J. French, Wm. Kahlbaum, and A. A. Peterson, Flow Characteristics of Special Fe-Ni-Cr Alloys and Some Steels at Elevated Temperatures, B.S. Jour. Research, vol. 5 (RP192), pp. 125-183, July 1930.

gives information on creep at 1,600° F. (870° C.) of similar materials, together with observations on the accompanying structural changes. To facilitate the comparison of the results of the earlier work with those of the present tests, the data of the earlier tests have been summarized graphically and included in this report to show the rates of creep at 1,000° F.

II. MATERIALS

The alloys used are listed in table 1. They cover a range from 1 to 75 percent nickel and from 3 to 55 percent chromium. Eight alloys (72 to 79, inclusive, table 1) were kindly prepared for this investigation by the Michiana Products Corporation, Michigan City, Ind. The preparation was similar to that employed at this Bureau for the corresponding alloys used in the tests at 1,000° F. (538° C.). Ingots 1½ inches in diameter and 6 inches long were cast in chill molds and were quartered longitudinally after heat-treatment (table 1). Specimens of 0.250 inch diameter were machined from the quarters. Four of the other materials (DH, OS, CA, and MS, table 1) were secured originally for use in "short-time" tensile tests at elevated temperatures. They represent the "as cast" materals. In addition to the cast alloys, one wrought material, representing a widely used commercial nickel-chromium heat-resistant alloy (76–20, table 1) was tested.

TABLE 1.—*Composition and heat treatment of nickel-chromium-iron alloys tested for creep at 1,600° F.*

Alloy designation	C	Mn	P	S	Si	Cr	Ni	Form of material	Heat treatment of alloys before the creep tests
	Per cent	*Per cent*	*Per cent*	*Per cent*	*Per cent*	*Per cent*	*Per cent*		
72	0.41	0.17			[1]0.50	[1]12.91	[1]1.36	1½-inch round ingots.	1,650° F., 1 hour, furnace cooled.
73	.19	.32			[1].51	[1]27.54	[1]2.36	do	1,800° F., 2 hours, air cooled.
74	.37	.34	0.023	0.009	1.13	55.80	.82	do	1,900° F., 3 hours, air cooled.
75	.03	.28	.042	.005	.54	17.20	24.00	do	2,000° F., 3 hours, air cooled.
76	.26	.27			[1]1.10	[1]30.94	[1]33.00	do	1,900° F., 3 hours, air cooled.
77	.33	1.00			[1].51	[1]18.02	[1]50.62	do	Do.
78	.22	1.30	.019	.036	1.01	[1]18.00	72.80	do	Do.
79	.25	.31	.023	.022	.13	3.00	31.20	do	1,450° F., 1 hour, furnace cooled.
76–20	.15					20.60	76.00	1¼-inch round rod.	Mill annealed.
DH [2]	.87	.85			1.10	13.72	58.45	1¼-inch round castings.	As cast.
OS [2]	.95	.79			1.77	19.18	40.42	do	Do.
CA [2]	.18	.96			1.16	16.70	74.62	do	Do.
MS [2]	.52	.44			1.57	15.62	25.18	do	Do.

[1] Manufacturer's analysis; all others were made at the Bureau of Standards by H. A. Bright and H. M. Fowler.

[2] Secured originally from various sources for use in "short-time" tensile tests at elevated temperatures.

The compositions and heat-treatments of the alloys used in the tests at 1,000° F. are given in table 2.

TABLE 2.—*Composition and heat treatment of nickel-chromium-iron alloys tested for creep at 1,000° F.*[1]

Alloy designation	C	Mn	Si	Cr	Ni	Form of material	Heat treatment of alloys before the creep tests
	Percent	*Percent*	*Percent*	*Percent*	*Percent*		
1,000	0.19	0.75	0.69	----------	----------	1½-inch octagonal castings.	1,650° F., ½ hour, air cooled.
1,001	.25	.80	.89	----------	Balance.	----do----------	1,500° F., ½ hour, air cooled.
1,002	.24	.88	.52	----------	68.5	----do----------	1,650° F., ½ hour, air cooled.
1,003	.18	.75	.57	----------	30.6	----do----------	1,450° F., 1 hour, furnace cooled.
1,004	.24	.59	.39	14.6	----------	----do----------	1,650° F., 2 hours, furnace cooled.
1,005	.38	.73	.82	30.2	----------	----do----------	1,800° F., 2 hours, air cooled.
1,006	.49	.68	1.01	55.3	----------	----do----------	1,900° F., 3 hours, air cooled.
1,007	.51	.74	.75	18.3	78.2	----do----------	Do.
1,008	.24	.88	1.14	46.3	49.7	----do----------	Do.
1,009	.41	.53	.78	14.8	58.7	----do----------	Do.
1,010	.11	.54	.77	16.4	25.5	----do----------	2,000° F., 1 hour, air cooled.
1,011	.11	.59	.87	27.2	35.4	----do----------	1,900° F., 3 hours, air cooled.
1,024	Commercial nickel shot remelted and cast in ingots.					----do----------	1,500° F., ½ hour, air cooled.

[1] See footnote 1 (text), p. 851.

III. METHODS OF STUDY

1. CREEP TESTS

The method for determining creep was the same as previously described.[2] The specimen had a diameter of 0.250 inch and a gage length of 2 inches and was loaded as indicated in figure 1. The gage length was defined by means of fine platinum wires in grooves on the edge of the shoulder at each end of the reduced section. Elongation was measured by means of a traveling micrometer microscope.

At the middle of the gage length, the temperature at the surface of the specimen exceeded the temperature at the center of the specimen by 2° F. at 1,600° F. This was determined by two thermocouples. A platinum platinum-rhodium thermocouple of 0.008 inch diameter wire covered with porcelain insulation was inserted in a very small hole extending radially to the center of a calibration specimen. Another thermocouple of 0.025 inch diameter chromel-alumel wire fastened to the surface of this specimen at the middle of the gage length indicated a temperature 2° F. higher than the one embedded in the metal. Further temperature measurements on the surface of the calibration specimen at the shoulder just outside of the reduced section indicated that the maximum temperature decrease along the surface of the specimen was 9° F. (5° C.). Thus, with surface temperature of 1,600° F. (870° C.) at the center of the gage length the temperature of the surface at each shoulder was 9° F. (5° C.) lower.

The creep tests made were of 500 to 700 hours' duration. The total creep during these periods was sufficient to permit the detection of rates of creep of the order of 10^{-6} inch per inch per hour.

[2] Wm. Kahlbaum and Louis Jordan, Creep at Elevated Temperatures in Chromium-Vanadium Steels Containing Tungsten or Molybdenum, B.S. Jour. Research, vol. 9 (RP481), p. 441, September 1932.

2. MICROSTRUCTURAL EXAMINATION

A metallographic study was made of specimens representative of the materials before and after the creep tests. In addition to the determination of the structural changes occurring as result of creep, an attempt was made for the purpose of ascertaining whether or not the rate of structural changes in these alloys might be accelerated by stress, and to distinguish between the effect on structure of elevated temperature alone and of elevated temperature and stress combined.

Townsend has observed that, in the case of lead sheath, the precipitation and coalescence of antimony from solid solution are accelerated

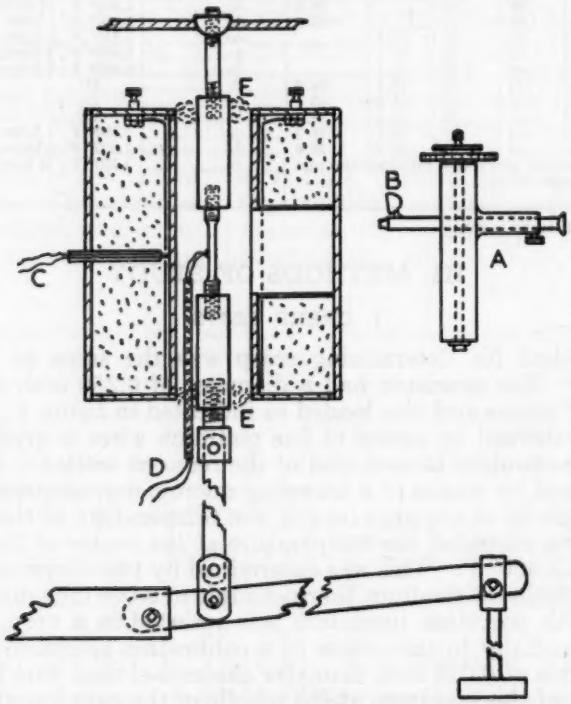

FIGURE 1.—*Diagram of vertical test unit for creep tests at elevated temperatures.*

A, traveling micrometer microscope; *B*, illuminator; *C*, thermocouple which actuates automatic controller; *D*, specimen temperature recording thermocouple; *E*, asbestos packing to minimize convection currents within the furnace.

by strain. Some authorities believe a similar condition exists in duralumin. A precipitation of $CuAl_2$ along the slip planes has been observed in portions of duralumin propellers which have been subjected to high stresses.

The metallographic specimens representative of the structural condition after creep were cut from the reduced sections of the test bars which had undergone creep at several loads and for different periods of time. Comparison specimens of the same alloys, protected from oxidation by being packed in sand and charcoal, were heated in an automatically controlled electric muffle furnace at 1,600° F. (870° C.) for periods varying from 100 to 1,000 hours. Two specimens of

each alloy were removed after each successive 100-hour heating period up to 1,000 hours. One specimen was quenched in iced brine; the other was transferred to another furnace at the same temperature (1,600° F.) and allowed to cool slowly in the furnace. The treatment selected was intended to retain the structure existing at the high temperature

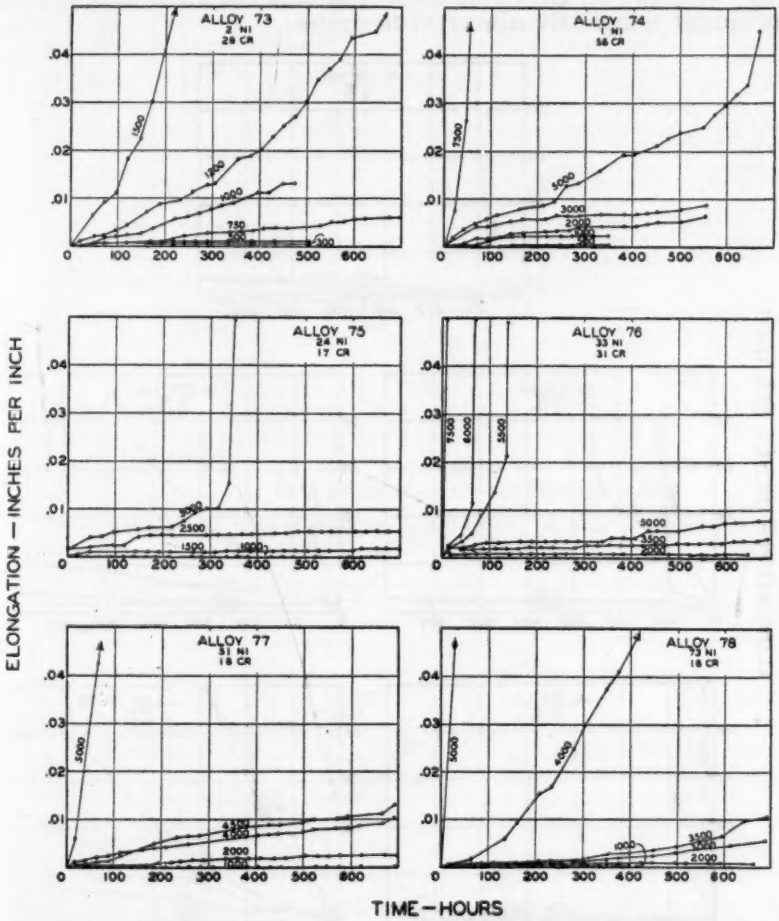

FIGURE 2.—*Time-elongation curves of nickel-chromium-iron alloys tested at 1,600° F. (870° C.).*

The number over each curve indicates the stress in lb./in.² at which the creep test was made. The arrows terminating some of the curves indicate the direction of the next point which was not included in the chart.

in the first case and in the other to produce a structure more nearly representative of that resulting in service from slow cooling.

IV. RESULTS

1. RATES OF CREEP

The time-elongation curves for the alloys tested at 1,600° F. and at the various loads are shown in figures 2 and 3 and the average rates of creep in figure 4.

Data are not given for the creep of the alloy containing 13 percent chromium and 1.4 percent nickel (no. 72) nor for the one containing 31 percent nickel and 3 percent chromium (no. 79). Neither alloy had sufficient resistance to oxidation at 1,600° F. (870° C.) to permit the carrying out of the creep tests. After several hundred hours at 1,600° F. (870° C.) the entire cross section of the 0.250-inch test bars was almost completely converted to oxides.

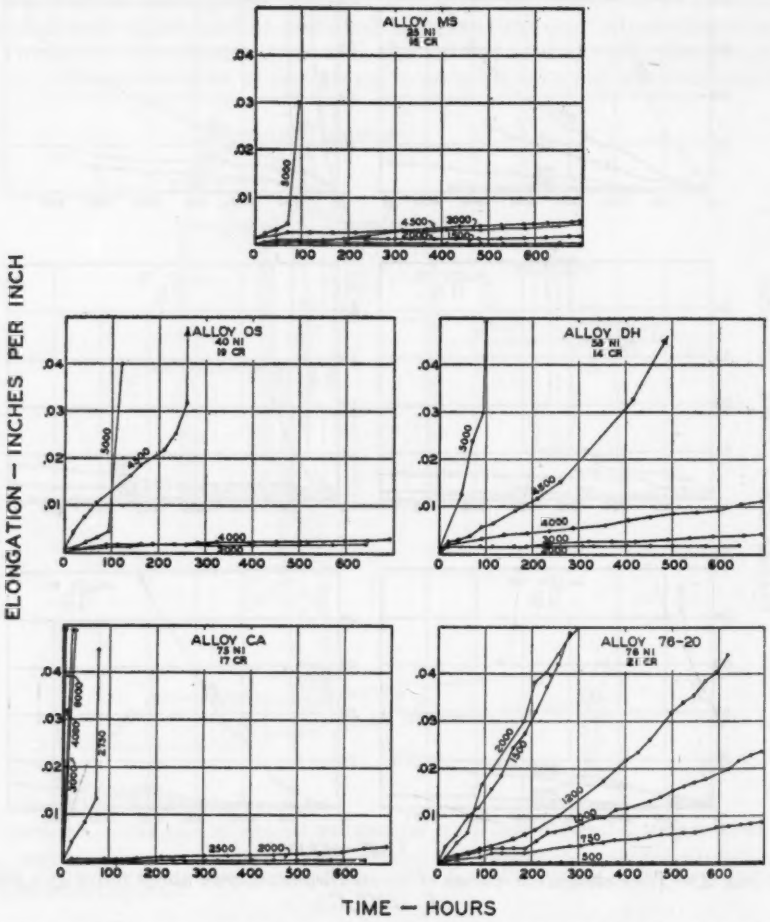

FIGURE 3.—*Time-elongation curves of nickel-chromium-iron alloys tested at 1,600° F. (870° C.).*

The number over each curve indicates the stress in lb./in.² at which the creep test was made. The arrows terminating some of the curves indicate the direction of the next point which was not included in the chart.

The remaining alloys showed excellent resistance to oxidation at 1,600° F. (870° C.). The oxide was confined to a slight discoloration of the surface in most cases. Alloys of the 25 percent nickel-15 percent chromium type (75 and MS, table 1) were practically without any oxide discoloration on the surface at the end of 700 hours.

Figure 5 shows the rates of creep of the nickel-chromium alloys tested at 1,000° F. in the earlier work.

2. MICROSTRUCTURAL CHANGES

The conclusions concerning the factors which influence the structural changes during creep at elevated temperatures were based upon

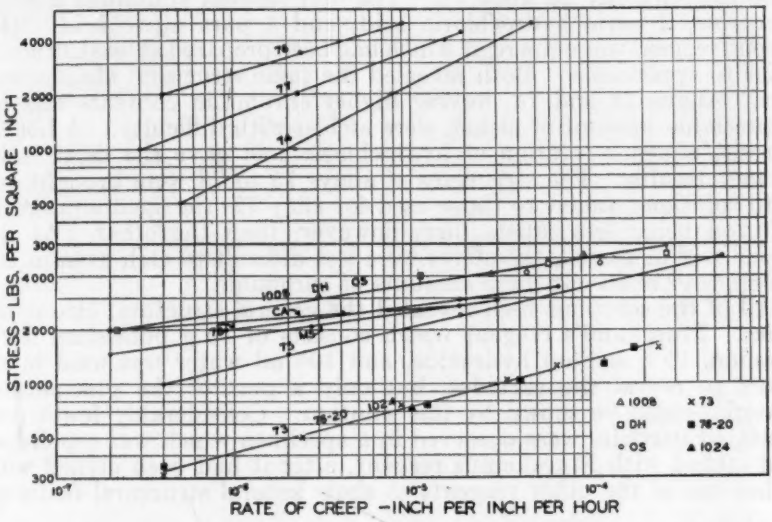

FIGURE 4.—*Average rates of creep in "second stage" of nickel-chromium-iron alloys tested at 1,600° F. (870° C.).*

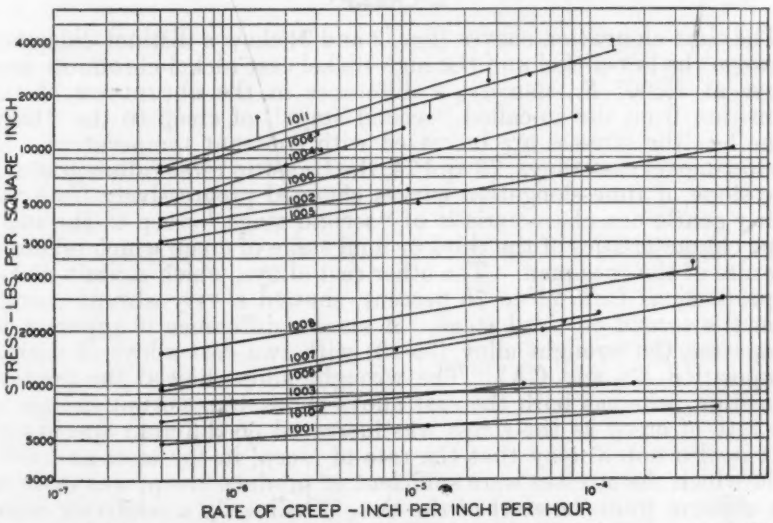

FIGURE 5.—*Average rates of creep in "second stage" of nickel-chromium-iron alloys tested at 1,000° F. (538° C.).*

the observations made on alloys 72 to 78 (table 1). Representative micrographs are shown (figs. 6, 7, and 8).

The specimens heated at 1,600° F. without stress showed very similar structural features in nearly all cases regardless of whether

they had been cooled slowly from the annealing temperature or had been quenched in iced brine.

The etching reagents used for alloys 72 to 78 differed somewhat with the different compositions of the alloys. Two reagents were used satisfactorily on alloy 72. The first reagent contained 2 parts glycerine, 2 parts hydrochloric acid, and 1 part nitric acid. The second reagent was aqua regia which had been prepared at least 20 hours prior to application. Both revealed the same structural characteristics. Alloys 73 and 74, having higher chromium contents and no appreciable amount of nickel, were etched with difficulty. A hot 50 percent aqueous solution of hydrochloric acid gave the most satisfactory results. The structures of alloys 75 to 78 were brought out with solutions similar to those used for alloy 72, the aged aqua regia solution being less satisfactory, however, than the other. As the nickel was increased, the alloys were less difficult to etch even in the presence of relatively large amounts of chromium.

All of the solutions used revealed the general structural characteristics. Murakami's reagent which consists of 10 g potassium ferricyanide, 10 g sodium hydroxide, and 100 ml water was used in an effort to reveal the carbides, but only a part of the precipitated material could be shown by this solution. Considerably fewer precipitated particles were observed in a specimen which was repolished and etched with Murakami's reagent, after it had been etched with either one of the other reagents to show general structural features.

V. DISCUSSION

1. CREEP

The time-elongation curves (figs. 2 and 3) show a distinct difference between the low-nickel and the high-nickel cast nickel-chromium-iron alloys at 1,600° F., namely, a difference in the abruptness of the transition from the so-called "second stage" of creep to the "third stage" as the stresses are increased with constant temperature. In the low-nickel cast alloys, 73 and 74, the transition was rather gradual. The slope of time-elongation curves changed progressively from the rather gentle one characteristic of "second stage" creep to the steep slope characteristics of the third or final stage of creep which precedes fracture of the specimen. The other cast alloys, which contain nickel in proportions from 25 to 75 percent, showed a very abrupt change from the second to third stage. A similar difference is apparent in comparing the wrought alloy (76-20) with two cast alloys of similar composition (78 and CA). The wrought alloy showed the gradual transition, whereas both the cast alloys showed an abrupt change in the rate of creep as the stress was increased on different specimens.

It is also noteworthy that the rate of creep, in the tests at 1,600° F. in which the stresses were sufficient to produce creep, was more or less uniform from the start of the test. Ordinarily a relatively rapid rate of creep takes place in the first few hours of test which is generally designated as the "first stage" or "initial creep." The rate gradually decreases as the test proceeds. This stage, "secondary creep", is intermediate between the initial rapid elongation immediately following the application of the load and the rapid rate of creep immediately preceding fracture.

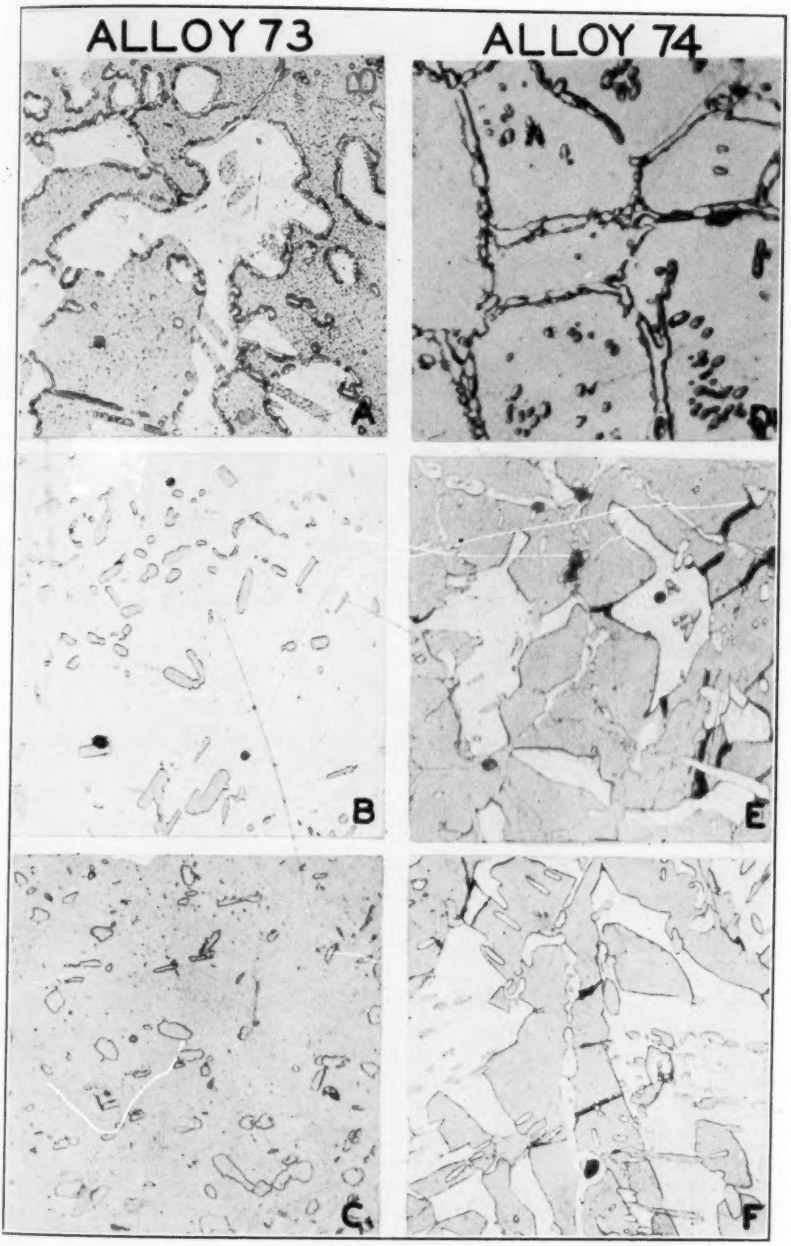

FIGURE 6.—*Structure of nickel-chromium-iron alloys relatively low in nickel and high in chromium.*

Alloy 73: *A*, original condition; *B*, annealed at 1,600° F. for 1,000 hours; and *C*, broken in creep test after 314 hours at 1,600° F. and 1,500 lbs./in.²

Alloy 74: *D*, original condition; *E*, annealed at 1,600° F. for 1,000 hours; and *F*, tested in creep for 348 hours at 1,600° F. and 1,000 lbs./in.²

Etchant, hot 50 percent aqueous solution of hydrochloric acid. Magnification, 500 ×.

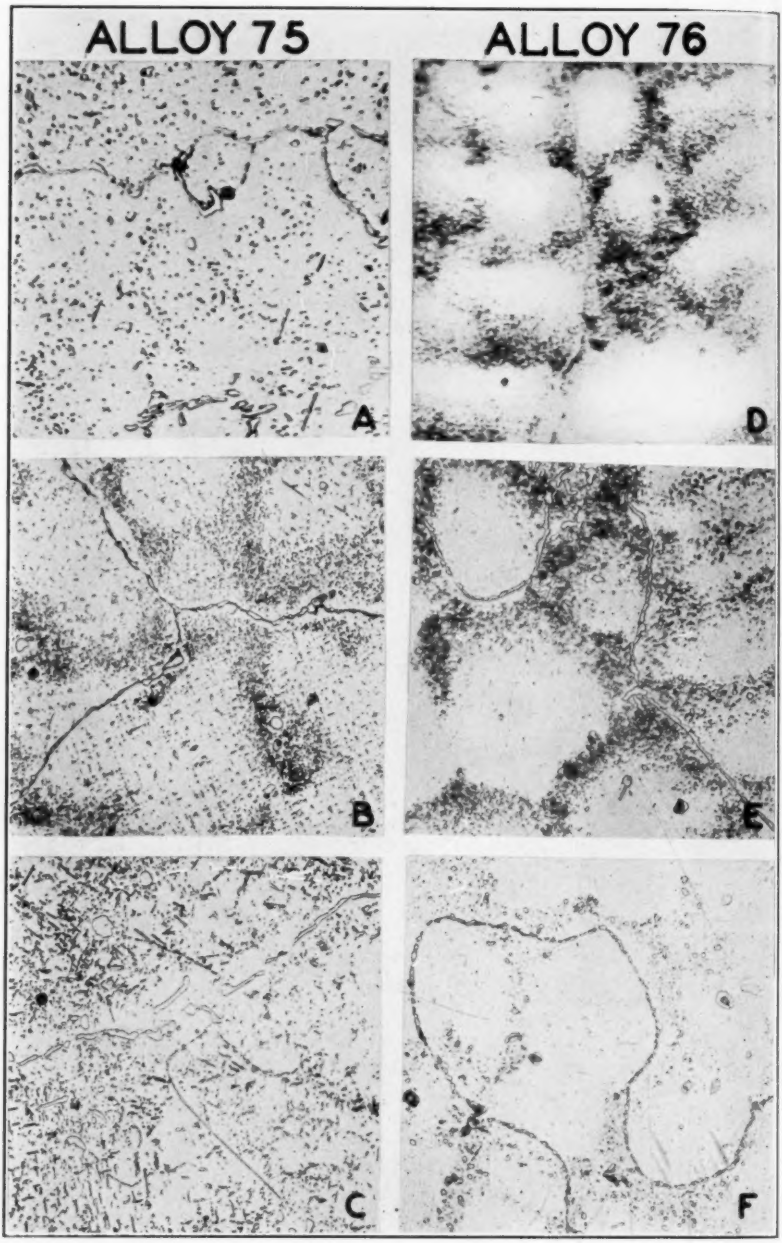

FIGURE 7.—*Structure of nickel-chromium-iron alloys containing approximately equal amounts of nickel and chromium.*

Alloy 75: *A*, original condition; *B*, annealed at 1,600° F. for 1,000 hours; and *C*, tested in creep for 700 hours at 1,600° F. and 2,500 lbs./in.²

Alloy 76: *D*, original condition; *E*, annealed at 1,600° F. for 1,000 hours; and *F*, tested in creep for 696 hours at 1,600° F. and 5,000 lbs./in.²

Etchant, aqua regia (see text). Magnification, 500 ×.

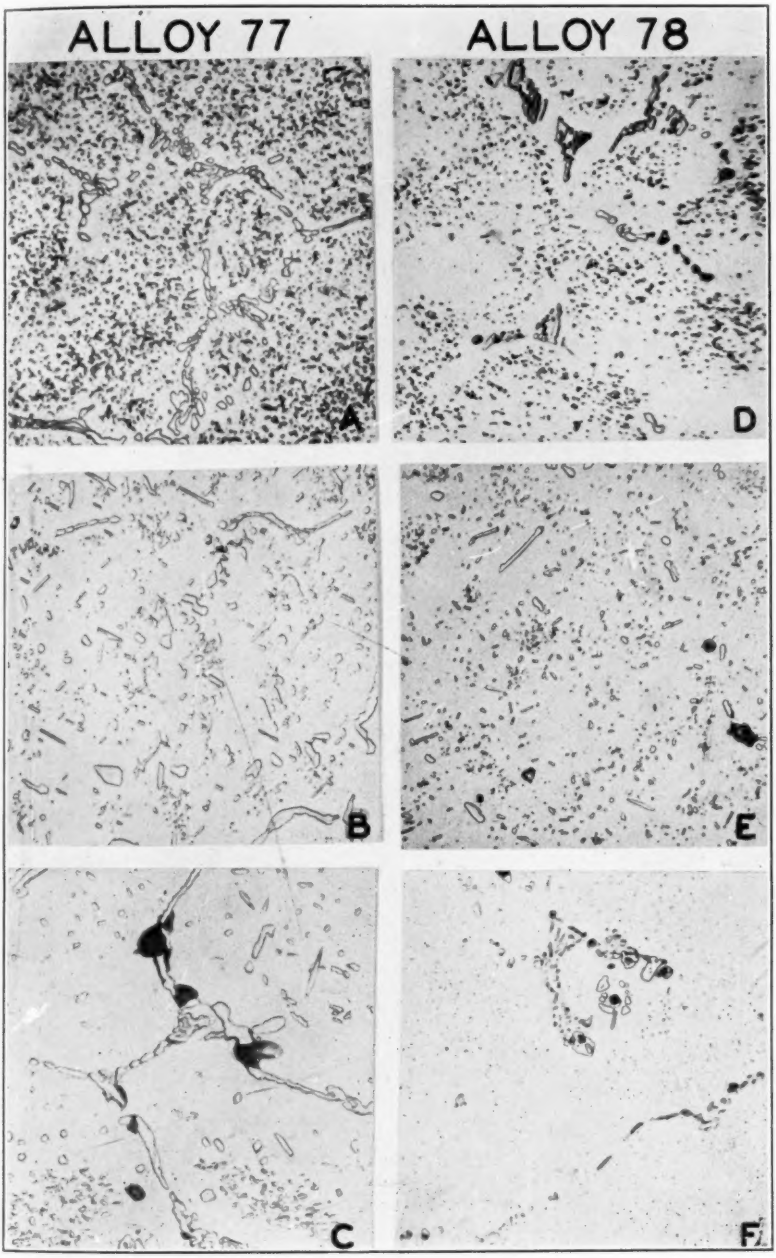

FIGURE 8.—*Structure of nickel-chromium-iron alloys containing relatively high amounts of nickel and intermediate amounts of chromium.*

Alloy 77: *A*, original condition; *B*, annealed at 1,600° F. for 1,000 hours; and *C*, tested in creep for 689 hours at 1,600° F. and 4,000 lbs./in.^{2}

Alloy 78: *D*, original condition; *E*, annealed at 1,600° F. for 1,000 hours: and *F*, tested in creep for 689 hours at 1,600° F. and 4,000 lbs./in.^{2}

Etchant, aqua regia (see text). Magnification, 500 ×.

These three stages of creep were not so pronounced at 1,600° F (870° C.) as at the lower temperatures. If the applied load was sufficient to produce appreciable elongation at the beginning of the test, the rate in most cases continued fairly constant throughout the duration of the test. The very low loads which produced no measurable elongation in 700 hours showed practically no initial deformation upon application of the load.

The difference in the resistance to creep (which was of the order of 0.1 percent in 1,000 hours at 1,600° F.) of alloys of different chemical composition is shown in figure 9.[3] The ternary alloys containing approximately equal proportions by weight of nickel and chromium and not more than 30 to 40 percent iron showed the highest resistance to creep. In the binary iron-chromium alloys the resistance to creep was found to increase as the chromium content is increased from about 20 to 60 percent. An addition of nickel up to 30 percent increased the resistance to creep of iron-chromium alloys containing between 15 and 40 percent chromium. An increase above 30 percent might, however, have little effect on the resistance to creep of iron-nickel-chromium alloys containing between 10 and 25 percent chromium.

Alloys having a composition which places them in the vicinity of the "pure iron corner" of the ternary diagram and for some distance from pure iron on the iron-nickel side of the diagram (alloys 72 and 79) do not resist oxidation and scaling in air at 1,600° F. as well as do the other alloys studied.

These experimental results are in accord with the prediction by Dean [4] that " * * * alloys in the vicinity of equal percentages of iron, nickel, and chromium and those in the iron-chromium series between 20 and 40 percent chromium with varying amounts of nickel * * * will furnish the alloys of the future, where conditions of economy, excellent mechanical and physical properties, and extreme resistance to high temperature oxidation must be fulfilled." This prediction was not based on the results of creep tests, but was made as a result of determinations of hardness, thermal expansion, electrical resistivity, and resistance to oxidation. Dean also stated that alloys to the right of a line (dotted line, fig. 9) drawn from 100 percent nickel to 20 percent chromium in the iron-chromium series are resistant to oxidation at 1,830° F. (1,000° C.). In the present work both cast and wrought alloys of the 75 nickel-20 chromium type were tested. The resistance to creep of the cast alloys (CA and 78, fig. 4) was very considerably greater than that of the wrought alloy (76–20, fig. 4).

In the previous investigation [5] of alloys it was found that alloys containing little or no iron, 50 to 80 percent nickel, and 20 to 50 percent chromium exhibited the greatest resistance to creep at 1,000° F. (538° C.). The greatest resistance to creep was obtained in castings containing about 50 percent each of nickel and chromium. Such an alloy might be expected to offer difficulties in the foundry and has the serious disadvantage of being extremely brittle. A summary of the results of the earlier work is given in figure 10, which shows the

[3] In order to make figure 9 more complete and accurate in the "pure nickel corner" and on the nickel-chromium side a very limited number of creep tests were made at 1,600° F. on nickel (alloy 1024, table 2) and on an alloy containing approximately equal parts of nickel and chromium (alloy 1008, table 2). Test specimens of these two materials were taken from material used in the investigation at 1,000° F.

[4] An investigation of some of the physical properties of the iron-nickel-chromium system, Walter A. Dean. Rensselaer Polytechnic Institute, Engineering and Science Series No. 26, June 1930, pp. 31–55.

[5] See footnote 1, p. 851.

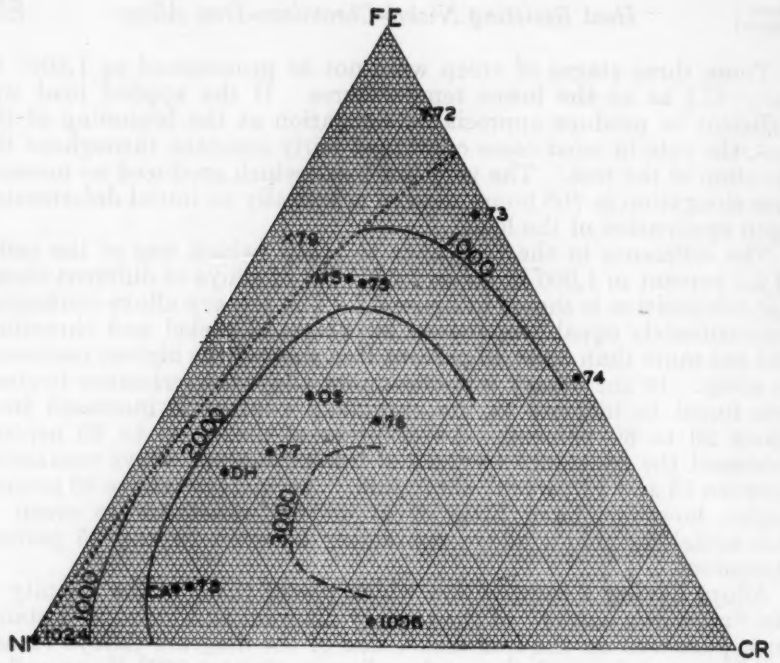

FIGURE 9.—*Stresses in lb./in.² required to produce 0.1 percent creep in 1,000 hours at 1,600° F. (870° C.) in the nickel-chromium-iron ternary system*

Compositions of the alloys tested are indicated.

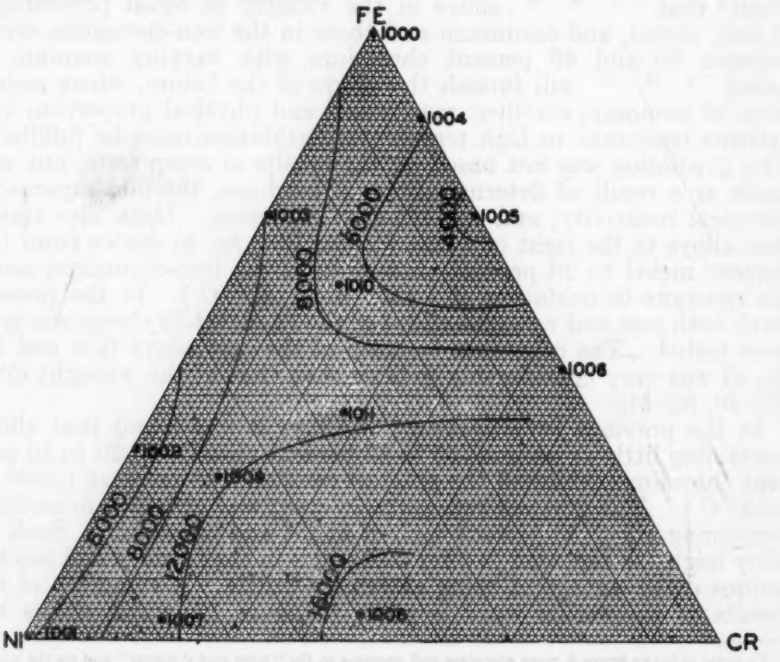

FIGURE 10.—*Stresses in lb./in.² required to produce 0.1 percent creep in 1,000 hours at 1,000° F. (538° C.) in the nickel-chromium-iron ternary system*

Compositions of the alloys tested are indicated.

approximate stresses producing creep of the order of 0.1 percent in 1,000 hours at 1,000° F. (538° C.).

The compositions of the alloys possessing the greatest load-carrying ability at 1,000° F. are not identical with the corresponding alloys at 1,600° F. (870° C.). The changes are most clearly demonstrated by comparing figures 9 and 10. At 1,600° F. (870° C.) the strongest alloys were those containing approximately equal parts of nickel and chromium, and not more than 30 to 40 percent iron. Neither chromium nor nickel alone appeared to contribute to its alloys with iron superior resistance to creep.

The stresses which at 1,600° F. fail to produce creep exceeding 10^{-6} inch per inch per hour in 700 hours range from about 2,500 lb./in.^{2} for the alloy containing equal parts of nickel, chromium, and iron to about 400 lb./in.^{2} for the 28 percent chromium alloy. This gives some indication of the extremely low loads at which creep takes place at 1,600° F. (870° C.) for the group of materials investigated.

All of the alloys of the present study that broke during creep tests failed with very little elongation, 7 percent or less, and practically no reduction of area.

2. STRUCTURE

The structural changes resulting from heating were not pronounced in either the unstressed or stressed specimens of the cast nickel-chromium-iron alloys.

An increase in the chromium content of the binary iron-chromium alloys causes an increase in the stability of the structural constituents. This stability is at a maximum in alloy 74 (fig. 6, (*d*), (*e*), and (*f*)). No marked difference in the amount or location of the carbide constituent could be seen in the structures of the original, annealed, or stressed specimens.

Prolonged heating in the absence of stress did not produce any marked changes in the structure of the ternary alloys of intermediate and high chromium-content (fig. 7, (*a*), (*b*), (*d*), and (*e*)).

The ternary alloys having an intermediate chromium content and 50 to 75 percent nickel showed slight structural changes after being subjected to a prolonged annealing (fig. 8, (*a*), (*b*), (*d*), and (*e*)). As the nickel content is increased the structural stability is decreased and the carbide particles are agglomerated to a greater extent.

The effect of stress at 1,600° F. has, generally speaking, a tendency to accelerate the rate of structural changes in the entire group of alloys studied. This effect is perhaps most readily illustrated in figure 6, (*b*), and (*c*). The stressed specimen, C, was loaded so that fracture occurred after 314 hours. The structure shows very coarse agglomerated carbide particles. The structure of the specimen, B, annealed at the same temperature for 1,000 hours resembles very closely that of the stressed specimen. The structure of specimens annealed at 1,600° F. for different periods up to 700 hours did not possess the degree of agglomeration which is observed in the stressed specimen or the specimen annealed for 1,000 hours. The application of stress apparently had accelerated the structural change in this alloy to a very marked extent. Approximately one third of the time at the same temperature was needed to produce a similar structure in the stressed specimen as in the unstressed specimen. The accelerating effect of stress was noticeable in all the alloys except alloy 74.

The rate of diffusion and agglomeration was increased in all the alloys studied, excepting alloy 74, to such a degree that the stressed specimens more closely approached an equilibrium condition than the unstressed specimens which had been annealed for several hundred hours longer than the duration of the creep test.

VI. SUMMARY

The creep characteristics at 1,600° F. (870° C.) of 15 different alloys, covering a range of chemical composition from 1 to 75 percent nickel and from 3 to 55 percent chromium, were determined. The results of these determinations are compared with those of a previous investigation at 1,000° F. (538° C.) on similar alloys.

In the previous investigation it was found that those alloys containing little or no iron, 50 to 80 percent nickel, and 20 to 50 percent chromium exhibited the greatest resistance to creep. At 1,600° F. (870° C.) the strongest alloys are those containing approximately equal parts of nickel and chromium and not more than 30 to 40 percent iron.

A metallographic study was made to determine what structural changes took place during creep. The attempt was made to distinguish between the effect on structure of elevated temperature alone and of elevated temperature and stress combined. A comparison was made between the structure in specimens used in the creep test and that in unstressed specimens of the same alloys annealed at 1,600° F. (870° C.) for periods ranging from 100 to 1,000 hours or quenched in iced brine from that temperature. In nearly all cases materials quenched in iced brine after heating were similar in structure to the annealed materials which indicates the extreme lack of susceptibility of alloys of this type to heat treatment.

An increase in the chromium content of both the binary alloys of iron and chromium and the ternary alloys results in an increase in the carbide precipitation and a greater agglomeration at the grain boundaries. The changes in structure which occurred after prolonged annealing were noticeable in the binary alloys containing up to 30 percent chromium and in the ternary alloys with large amounts of nickel.

The combination of prolonged heating and stressing caused structural changes in all the alloys with the exception of alloy 74. There is a distinct indication that the effect of stress had accelerated the rate of diffusion and agglomeration of the carbides. The structures in the stressed specimens indicate that these specimens approached an equilibrium condition at a rate sometimes three times as great as that in the corresponding specimens annealed at the same temperature.

WASHINGTON, April 18, 1933.

INDEX TO VOLUME 10

A

	Page
Acid, sulphuric, viscosity of, RP566	781
Acidity of leather, pH as measure of, RP547	559
Acidity of soils, RP539	413
Aircraft propellers, vibrations of, RP556	659
Alcohol fuels, solubility of aqueous solutions of ethyl alcohol in gasoline {RP560	693
{RP571	841
Alkaline earths, long-wave arc spectra of alkalis and, RP558	669
Alkalis and alkaline earths, long-wave arc spectra of, RP558	669
Alloys, thermoelectric properties of platinum-rhodium, RP537	373
Alloys, white-metal, RP512	1
white-metal bearing, RP512	1
Altitude, effect of, on limit of safe operation of gas appliances, RP553	619
Aluminum, determination in nitriding steels, RP533	327
Ampholyte, isoelectric region of, RP543	475
Amplifier, a resistance-coupled, for measuring ionization currents, RP550	583
Amplifiers, sensitive pulse, elimination of back ground "noise" in, RP522	151
Analysis of cement, determination of magnesia by, RP569	823
Analysis of Cl 1, RP570	827
Annealing, effect on temperature coefficient of elastic moduli, RP531	289
Antenna system for elimination of night effects in radio range-beacon reception, RP513	7
Antimony, effect of, in batteries, RP567	795
Apparatus for purification of hydrocarbons by crystallization from solvents at low temperatures, RP552	609
Apparatus for separating solids from liquids by centrifuging at liquid air temperatures, RP552	609
Appliances, gas, the effect of altitude on limits of safe operation of, RP553	619
Arc spectra, long-wave, of alkalis and alkaline earths, RP558	669
Arc spectra of manganese and rhenium, RP564	757
Arc spectrum of chlorine, RP570	827
Argon, infrared spectrum of, RP540	427
Austenitic steel, magnetic balance for inspection of, RP532	321

B

Balance, magnetic, for the inspection of austenitic steel, RP532	321
Barium, arc spectrum of, RP558	669
Basil, J. L., H. K. Herschman and, "Tin-free" bearing bronze, RP551	591
——, ——, White-metal bearing alloys: Mechanical properties at different temperatures and service tests, RP512	1
Batten plates, measurements of strain in, RP559	685
I-beams, measurements of strain in, RP559	685
Bearing metals, bronzes, RP551	591
Bennett, Ekert G., An apparatus for magnetic testing at high magnetizing forces, RP547	567
Beryllium bronze, temperature coefficient of elastic moduli of, RP531	289
Blends, gasoline, ethyl alcohol, water {RP560	693
{RP571	841
Boeckner, C., and F. L. Mohler, Scattering of electrons by ions and the mobility of electrons in a cesium discharge, RP535	357
Bomb calorimetry, benzoic acid as standard-izing substance for, RP546	525
correction of results of, to a common temperature, RP546	525
reduction of data of, to a common basis, RP546	525
sources of error in, RP546	526
standard states for, RP546	525
standardization of condition for, RP546	525
thermodynamics of, RP546	525
Bowker, R. C., and E. L. Wallace, The influence of pH on the deterioration of vegetable-tanned leather by sulphuric acid, RP547	559
Brass, temperature coefficient of elastic moduli of, RP531	289
Brewster, J. F., and F. P. Phelps, The preparation of optically stable sugar solutions for colorimetric analysis, RP536	365
Brick walls, compression strength of steel columns incased in, RP520	123
Bridgeman, Oscar C., and Dale Querfeld, Critical solution temperatures of mixtures of gasoline, ethyl alcohol, and water, RP560	693
——, ——, The effect of gasoline volatility on the miscibility with ethyl alcohol, RP571	841
Bright, H. A., and Robert M. Fowler, Determination of aluminum in nitriding steels by the use of 8-hydroxyquinoline, RP533	327
Bromine, oxidation of sugars with, RP534	337
Bronzes, leaded bearing, RP551	591
Brooks, H. B., H. L. Dryden, L. B. Tuckerman and, A method of exciting resonant vibrations in mechanical systems, RP556	659
Brunn, Johannes H., and Mildred M. Hicks-Brunn, 1, 1-dimethylcyclopentane and 2-methylhexane in a midcontinent petroleum, RP542	465
Bruun, Mildred M. Hicks, and Johannes H. Bruun, 1, 1-dimethylcyclopentane and 2-methylhexane in a midcontinent petroleum, RP542	465
Buildings, wind pressure on, RP545	493

C

Cadmium, use of, in batteries, RP567	795
Calcium, arc spectrum of, RP558	669
Calderwood Dam, measurements of strain on, RP559	685
measurement of strain on model of, RP559	685
Caldwell, Frank R., Thermoelectric properties of platinum-rhodium alloys, RP537	373
Calibration of platinum-rhodium thermocouples, RP530	275
Calorimeter, Thomas recording gas, RP519	99
Carbon dioxide, vapor pressure of, RP538	381
Carroll, Burt H., and C. M. Kretchman, Photographic reversal by desensitizing dyes, RP541	449
——, *and Donald Hubbard,* The photographic emulsion: The mechanism of hypersensitization, RP525	211
Cells, standard, effect of service temperature condition on, RP518	89
Cement, determination of magnesia in, RP569	823
Cesium, arc spectrum of, RP558	669
Cesium positive column, recombination radiation in the, RP565	771
Chlorine terms, RP570	827
Chlorine wave lengths, RP570	827
Chromium vanadium steel, temperature coefficient of elastic moduli of, RP531	289

Page

Circle, dyadic, RP559 685
Circle of strain, RP559 685
Clay in concrete, RP529 257
Classification of Cl 1, RP570 827
Cloth, creaseability of, RP555 647
drape of, RP555 647
feel or handle of, RP555 647
flexural hysteresis of, RP555 647
flexural resilience of, RP555 647
stiffness of, RP555 647
Coblentz, W. W., R. Stair, and J. M. Hogue, Measurement of ultraviolet solar radiation in various localities, RP517 79
Color sensitivity, RP525 211
Colorimetric analysis, preparation of optically stable sugar solutions for, RP536 365
Columns, gypsum fire protection for, RP563 737
steel, compressive strength of, incased in brick walls, RP520 123
Combination of wool and silk with positive and negative ions, RP543 475
Combustion, heat of, RP546 525
See also Bomb calorimetry.
temperature coefficient of, RP546 525
Compressibility of textiles and similar materials, RP561 705
Compressional properties of textiles and similar materials, RP561 705
Compressive strength of brick walls, RP520 123
Compressive strength of steel columns incased in brick walls, RP520 123
Compressometer for textiles and similar materials, RP561 705
Concrete, absorption of, containing clay, RP529 257
compressive strength of, containing clay, RP529 257
Concrete containing clay admixtures, RP529 257
freezing and thawing tests of, RP529 257
Concrete, permeability of, containing clay, RP529 257
Cone deformation temperature (enamels), RP524 189
Counting chambers, Geiger-Müller tube counters, RP526 229
Craig, D. N., C. L. Snyder, G. W. Vinal and, Composition of grids for positive plates of storage batteries as a factor in influencing the sulphation of negative plates, RP567 795
——, *G. W. Vinal and,* The viscosity of sulphuric-acid solutions used for battery electrolytes, RP566 781
Creaseability of cloth and similar materials, RP555 647
Critical solution temperatures; mixtures of gasoline, ethyl alcohol, and water: RP560 693, RP571 841
Crystallization of ether-soluble rubber hydrocarbon, RP544 479
Crystallization of petroleum hydrocarbons from liquid methane, RP552 609
Curtiss, L. F., A resistance-coupled amplifier for measuring ionization currents, RP550 583
——, Temperature effect and its elimination in Geiger-Müller tube counters, RP526 229
——, The elimination of back ground "noise" in sensition pulse amplifiers, RP522 151

D

Dahl, A. I., Wm. F. Roeser and, Conditions affecting the freezing temperature of silver, RP557 661
Deformation temperature (enamels), RP524 189
Denison, L. A., Methods for determining the total acidity of soils, RP539 413
Desensitizers, photographic, RP541 449
Deterioration of leather, RP547 559
Determination of magnesia in portland cement, RP569 823
Diamond, H., The cause and elimination of night effects in radio range-beacon reception RP513 7
Digges, T. G., Effect of lathe cutting conditions on the hardness of carbon and alloy steels, RP516 77

Page

1, 1-dimethylcy clopentane, RP542 465
Dioxide, carbon, vapor pressure of, RP538 381
Directive radio beacon, elimination of night effects in use of, RP513 7
Dosage, X-ray, RP527 233
Drape of cloth and similar materials, RP555 647
Dryden, H. L., H. B. Brooks, L. B. Tuckerman and, A method of exciting resonant vibrations in mechanical systems, RP556 659
——, *and George C. Hill,* Wind pressure on a model of the Empire State Building, RP545 493
Duralumin, temperature coefficient of elastic moduli of, RP531 289
Dyadic circle, RP559 685

E

Effect of temperature on bearing alloys, RP512
Eiseman, John H., Francis A. Smith, and Cecil J. Merritt, The effect of altitude on the limits of safe operation fo gas applicances, RP553 619
Elastic moduli, temperature coefficient of, RP531 289
Electromotive force of Standard cells, effect of temperature conditions on, RP518 89
Electron scattering by ions, RP535 357
Elimination of night effects in radio range-beacon reception, RP513 7
Elinvar, temperature coefficient of elastic moduli, of RP531 289
Empire State Building, wind pressure on a model of, RP545 493
Enamel, porcelain (fusibility), RP524 189
Enamels, first-coat, fusibility, RP524 189
fusibility, RP524 189
viscosity of, RP524 189
viterous (fusibility), RP524 189
Ethylbenzene, content of, in petroleum, RP554 639
infrared absorption by, RP554 639
isolation of, from petroleum, RP554 639
physical properties of, RP554 639
presence of, in petroleum, RP554 639
Eutectics, composition of, ethylbenzene-*m*-xylene, RP554 639
—— ——, ethylbenzene-*p*-xylene, RP554 639
Excitation of resonant vibrations in mechanical systems, RP556 659
Expansion of refractories to 1,800° C., RP562 715
Expansion, thermal measurements by interference method, RP515 59

F

Feel or handle of cloth and similar materials, RP555 647
Fiock, E. F., D. C. Ginnings, H. F. Stimson, N. S. Osborne and, The pressure of saturated water vapor in the range 100° to 374° C., RP523 155
Fire clay and special refractories, expansion of, RP562 715
Fire tests of gypsum column protections, RP563 737
Flexometer for cloth and similar materials, RP555 647
Flexural properties of cloth and similar materials, RP555 647
Fluidity of battery electrolytes, RP566 781
Fowler, Robert M., H. A. Bright and, Determination of aluminum in nitriding steels by the use of 8-hydroxyquinoline, RP533 327
Frandsen, Mikkel, The heat capacity, heat of sublimation, and heat of solution of phosphorus pentoxide, RP514 35
Freezing point of ethylbenzene-*m*-xylene, RP554 639
Freezing point of ethylbenzene-*p*-xylene, RP554 639
Freezing point of iridium, RP568 809
Freezing temperature of silver, RP557 661
Fusibility tests (enamels), RP524 189
Fusion properties (enamels), RP524 189

G

Page

Gages, comparison of fused quarts gages with steel gages, RP528 249
screw micrometer, for rubber specimens, RP549 575
Gas appliances, the effect of altitude on limits of safe operation, of RP553 619
Gas calorimeter, Thomas recording, RP519 99
Gasoline, critical solution temperatures of mixtures with ethyl alcohol and water: RP560 693
RP571 841
effect of volatility on critical solution temperatures of mixtures with ethyl alcohol and water, RP571 841
Geiger-Müller tube counters, RP526 229
Ginnings, D. C., H. F. Stimson, E. F. Fiock, N. S. Osborne and, The pressure of saturated water vapor in the range 100° to 374° C., RP523 155
Gluconic δ lactone, RP534 337
Glucose, isomeric forms in aqueous solution, RP534 337
oxidation of β and, RP534 337
Ground coat enamels (fusibility), RP524 189
Gusset plates, measurements of strain in, RP559 685
Gypsum fire protections for columns, RP563 737

H

Hardness, effect of lathe cutting conditions on the hardness of carbon and alloy steels, RP516 77
Hardness or softness of textiles and similar materials, RP561 705
Harris, Albert L., A. H. Stang, and J. W. Mc Burney, compression strength of steel columns incased in brick walls, RP520 123
Harris, Milton, The combination of silk and wool with positive and negative ions, RP543 475
Harrison, W. N., and B. J. Sweo, Some fusion properties of ground coat enamels as influenced by composition, RP524 189
Heat, absorption of (enamels), RP124 189
Heat absorption temperatures (enamels), RP524 189
Heat of combustion. *See* Combustion, heat of.
Heat-resisting nickel-chromium-iron alloys, RP572 851
Heindl, R. A., The thermal expansion of refractories to 1,800° C., RP562 715
Henning, F., and H. T. Wensel, The freezing point of iridium, RP568 809
Heptane, isomer of, in petroleum, RP542 465
Herschman, H. K., and J. L. Basil, "Tin-free" leaded bearing bronze, RP551 591
——, ——, White-metal bearing alloys: Mechanical properties at different temperatures and service tests, RP512 1
High temperature, mechanical properties of leaded bronzes, at RP551 591
High voltage apparatus, RP527 233
High voltage measurements, RP527 233
High voltage X-ray generators, RP527 233
High voltage X-ray tubes, RP527 233
Hill, George C., Hugh L. Dryden and, Wind pressure on a model of the Empire State Building, RP545 493
Hogue, J. M., R. Stair, W. W. Coblentz and, Measurements of ultraviolet solar radiation in various localities, RP517 79
Holders for supporting gages in comparator, RP528 249
Holt, W. L., Screw micrometer gages for rubber specimens, RP549 575
Houseman, M. R., G. H. Keulegan and, Temperature coefficient of the moduli of metals and alloys used as elastic elements, RP531 289
Hubbard, Donald, Burt H. Carroll and, The photographic emulsion: The mechanism of hypersensitization, RP525 211
Humphreys, C. J., and W. F. Meggers, Further description and analysis of the first spectrum of xenon, RP521 139
——*William F. Meggers* and, Infrared spectra of neon, argon, and krypton, RP540 427

Page

Hydrocarbons, isolation of difficulty crystallizable, from petroleum, RP552 609
petroleum, ethylbenzene one of, RP554 639
isolation of ethylbenzene from, RP554 639
purification of, by crystallization from liquid methane, RP552 609
8-hydroxyquinoline, use of, in determining aluminum in nitriding steels, RP533 327
in determination of magnesia, RP569
Hypersensitization, mechanism of, RP525 211
Hysteresis effects on unsaturated standard cells, R P518 89
flexur], of cloth and similar materials, RP5a55 647

I

Impurities, effect of, on silver point, RP557 661
Indicator, electric contact used as an, in measuring machine, RP528 249
Infrared arc spectra of manganese and rhenium, RP564 757
Infrared spectra of neon, argon, and krypton, RP540 427
Infrared standards, RP521 139
Interference method of thermal expansion, RP515 59
Ionization currents, a resistance-coupled amplifier for measuring, RP550 583
Ions, scattering by, RP535 357
Iridium, freezing point of, RP568 809
Isbell, Horace S., and Ward Pigman, The oxidation of alpha and beta glucose and a study of the isomeric forms of the sugar in solution, RP534 337
Isoelectric point of silk, RP543 475
Isoelectric point of wool, RP543 475
Isoelectric region of ampholyte, RP543 475

J

Jessup, R. S., The Thomas recording gas calorimeter, RP519 99

K

Keulegan, G. H., and M. R. Houseman, Temperature coefficient of the moduli of metals and alloys used as elastic elements, RP531 289
Kiess, C. C., A new description and analysis of the arc spectrum of chlorine, RP570 827
Kretchman, C. M., Burt H. Carroll and, Photographic reversal by desensitizing dyes, RP541 449
Krypton, infrared spectrum of, RP540 427

L

Lathe tests, effect of cutting conditions on the hardness of carbon and alloy steels, RP516 77
Lead alloys for storage batteries, RP567 795
Leaded bronzes, effect of various additions on dispersion of lead in, RP551 591
Leather, deterioration of, by sulphuric acid, RP547 559
Leather, influence of pH on deterioration of, RP547 559
Leslie, R. T., Purification of hydrocarbons by crystallization from liquid methane. Isolation of 2-methylheptane from petroleum, RP552 609
Light, infrared, absorption by ethylbenzene of, RP554 639
Loads due to wind, RP545 493
Locomotive side rod, measurement of strain in, RP559 685

M

McBurney, J. W., A. H. Stang, Albert L. Harris and, Compressive strength of steel columns incased in brick walls, RP520 123
Machinability, effect of lathe cutting conditions on the hardness of carbon and alloy steels, RP516 77
Magnesia, determination of, in portland cement, RP569 823
Magnetic testing at high magnetizing forces, apparatus for, RP548 567

Page

Manganese, infrared arc spectrum of, RP564
Mechanical properties of bearing alloys, RP512 7
Mechanical properties of bearing alloys at different temperatures, RP512 7
Mechanical properties of white metal bearing alloys, RP512 7
Mechanical systems, excitation of vibrations in, RP556 659
Meggers, W. F., C. J. Humphreys and, Further description and analysis of the first spectrum of xenon, RP521 139
——, Long-wave arc spectra of alkalis and alkaline earths, RP558 669
——, *and C. J. Humphreys,* Infrared spectra of neon, argon, and krypton, RP540 427
——, The infrared arc spectra of manganese and rhenium, RP564 757
Melting point of iridium, RP568 809
Melting point of rubber hydrocarbon, RP544 479
Merritt, Cecil J., Francis A. Smith, John H. Eiseman and, The effect of altitude on the limits of safe operation of gas appliances, RP553 619
Merritt, George E., The interference method of measuring thermal expansion, RP515 59
Methods for determining isoelectric points and the possibilities and limitations of such methods, RP543 475
2-methylheptane, isolation of, from petroleum, RP552 609
Methylhexane, 2-, RP542 465
Meyer, C. H., and M. S. Van Dusen, The vapor pressure of liquid and solid carbon dioxide, RP538 381
Micrometer, electrically controlled, RP528 249
Micrometer gages for rubber, RP549 575
Mitchell, Nolan D., Fire tests of columns protected with gypsum, RP563 737
Model of Calderwood Dam, measurements of strain on, RP559 685
Model tests, wind pressure, RP545 493
Moduli, temperature coefficient of elastic, RP531 289
Modulvar, temperature coefficient of elastic moduli of, RP531 289
Mohler, F. L., Recombination radiation in the cesium positive column, RP565 771
——, *C. Boeckner and,* Scattering of electrons by ions and the mobility of electrons in a cesium discharge, RP535 357
Monel metal, temperature coefficient of elastic moduli of, RP531 289
Moon, Charles, Apparatus for comparison of length of gages, RP528 249

N

Neon, infrared spectrum of, RP540 427
Nickel-chromium-iron alloys, heat resisting, RP572 851
Nickel silver, temperature coefficient of elastic moduli of, RP531 289
Nickel steel, temperature coefficient of elastic moduli of, RP531 289
Night effects, elimination of, in radio range-beacon reception, RP513 7
Nitriding steels, determination of aluminum in, RP533 327

O

Optical pyrometry, RP568 809
Optically stable sugar solutions for colorimetric analysis, preparation of, RP536 365
Osborne, N. S., H. F. Stimson, E. F. Frock, and D. C. Ginnings, The pressure of saturated water vapor in the range 100° to 374° C., RP523 155
Osgood, Wm. R., and Rolland G. Strum, The determination of stresses from strains on three intersecting gage lines and its application to actual tests, RP559 685
Oxidation of sugars with bromine water, RP534 337
Oxygen dissolved in silver, RP557 661

P

Page

Park, J. H., Effect of service temperature conditions on the electromotive force of unsaturated portable standard cells, RP518 89
Parsons, D. A., Clay in concrete, RP529 257
Petroleum, 1, 1-dimethylcyclopentane and 2-methylhexane in, RP542 465
ethylbenzine in, RP554 639
isolation of ethylbenzine from, RP554 639
pH of leather, influence on deterioration, RP547 559
Phelps, F. P., J. F. Brewster and, The preparation of optically stable sugar solutions for chlorimetric analysis, RP536 365
Phosphor bronze, temperature coefficient of elastic moduli of, RP531 289
Phosphorus pentoxide, heat capacity, and heat sublimation, RP514 35
Photographic emulsions, the mechanism of hypersensitization, RP525 211
Photographic reversal by desensitizing dyes, RP541 449
Pigman, Ward, Horace S. Isbell and, The oxidation of alpha and beta glucose and a study of the isomeric forms of the sugar in solution, RP534 337
Piano wire, temperature coefficient of elastic moduli of, RP531 289
Plane stress, determination of state of, from measurements of strain, RP550 685
Platinum-rhodium alloys, thermoelectric properties of, RP537 373
Platinum to platinum-rhodium thermocouples, RP530 275
Porcelain enamel (fusibility), RP524 189
Portland cement, determination of magnesia in, RP569 823
Positive column, recombination radiation in the cesium, RP565 771
Potassium, arc spectrum of, RP558 669
Pressure, vapor, of carbon dioxide, RP538 381
Pressure, wind, on structures, RP545 493
Propellers, vibration of aircraft, RP556 659
Protection of standard cells against temperature disturbances, RP518 89
Pulse amplifier, elimination of "noise" in, RP522 151
Pyrometry, optical, RP568 809

Q

Querfeld, Dale, Oscar C. Bridgeman and, Critical solution temperatures of mixtures of gasoline, ethyl alcohol, and water, RP560 693
——, ——, The effect of gasoline volatility on the miscibility with ethyl alcohol, RP571 841

R

Radio range-beacon, elimination of night effects in use of, RP513 7
Reaction rates for the oxidation of sugars, RP534 337
Recombination radiation in the cesium positive column, RP565 771
Recording gas calorimeter, Thomas, RP519 99
Rectifiers, X-ray, RP527 233
Redmond, John C., The precipitation and titration of magnesium oxyquinolate in the presence of calcium oxalate, and its application in the analysis of portland cement and similar silicates, RP569 823
Reference tables for platinum-rhodium thermocouples, RP530 275
Refractories, expansion of, to 1,800° C., RP562 715
Resilience, compressional, of textiles and similar materials, RP561 705
flexural, of cloth and similar materials, RP555 647
Resonant vibrations, method of exciting, RP556 659
Reversal, photographic, by desensitizing dyes, RP541 449
Rhenium, infrared arc spectrum of, RP564 757
Rigidity modulus, temperature coefficient of, RP531 289

Page

Roeser, Wm. F., and A. I. Dahl, Conditions affecting the freezing temperature of silver, RP557 561
—, *and H. T. Wensel,* Reference tables for platinum to platinum-rhodium thermocouples, RP530 275
Rose, jr., F. W., Joseph D. White and, Isolation of ethylbenzine from an Oklahoma petroleum, RP554 639
Rubber, analysis of crystalline, RP544 479
crystallization of ether-soluble hydrocarbon, RP544 479
Rubber gases, RP549 575
Rubber hydrocarbon, melting point of, RP544 479
optical properties of crystalline, RP544 479
purification, crystallization, composition, and properties of ether-soluble, RP544 479
Rubidium, arc spectrum of, RP558 669

S

Safety of gas appliances at different altitudes, RP553 619
Sanford, Raymond L., A magnetic balance for the inspection of austenitic steel, RP532 321
—, *and Evert G. Bennett,* An apparatus for magnetic testing at high magnetizing forces, RP548 567
Saturation pressure of steam, RP523 155
Saturation pressure of water, RP523 155
Saylor, Charles Proffer, Henry J. Wing, W. H. Smith and, The preparation and crystallization of pure ether-soluble rubber hydrocarbon: Composition, melting point, and optical properties, RP544 479
Schiefer, Herbert F., The compressometer, an instrument for evaluating the thickness, compressibility, and compressional resilience of textiles and similar materials, RP561 705
—, The flexometer, an instrument for evaluating the flexural properties of cloth and similar materials, RP555 647
Sensitization, spectral, RP541 449
Service tests of bearing alloys, RP512 1
Service tests of white-metal bearing alloys, RP512 1
Silicates, determination of magnesia in, RP569 823
Silico-manganese steel, temperature coefficient of elastic module of, RP531 289
Silk, combination of, with positive and negative ions, RP543 475
isoelectric point of, RP543 475
Silver, freezing temperature of, RP557 661
Sinclair, S. E., W. A. Tucker and, Creep and structural stability of nickel-chromium-iron alloys, RP572 851
Smith, Francis A., Cecil J. Merritt, John H. Eiseman and, The effect of altitude on the limits of safe operation of gas appliances, RP553 619
Smith, W. H., Charles Proffer Saylor, and Henry J. Wing, The preparation and crystallization of pure ether-soluble rubber hydrocarbon: Composition, melting point, and optical properties, RP544 479
Snyder, C. L., D. N. Craig, G. W. Vinal and, Composition of grids for positive plates of storage batteries as a factor in influencing the sulphation of negative plates, RP567 693
Sodium, arc spectrum of, RP558 669
Soil acidity, method for determining total, RP539 413
Soils, determination of acidity of, RP539 413
Solar radiation, ultraviolet, in various localities, RP517 79
Solubility, aqueous solutions of ethyl alcohol in gasoline: RP560 693, RP571 841
Solution, heat of, phosphorus pentoxide, RP514 35
Solutions, isomeric forms of glucose in, RP534 337
Specific heat of phosphorus pentoxide, crystals, and vapor, RP514 35
Spectra, infrared, of neon, argon, and krypton, RP540 427

Page

Spectra of xenon, RP521 139
Spectral sensitivity, RP525 211
Spectrum, infrared absorption, of ethylbenzene, RP554 639
Spring materials, temperature coefficient of elastic moduli of, RP531 289
Spectrum of neutral Cl atom, RP570 827
Stainless steel, temperature coefficient of elastic moduli of, RP531 289
Stair, R., J. M. Hogue, W. W. Coblentz and, Measurements of ultraviolet solar radiation in various localities, RP517 79
Stang, A. H., J. W. McBurney, Albert L. Harris and, Compressive strength of steel columns in brick walls, RP520 123
Standard cells, effect of service temperature conditions on, RP518 89
Standard wave lengths, RP521 139
Steam, saturated vapor pressure of, RP523 155
Steel, magnetic balance for inspection of austenitic, RP532 321
nitriding, determination of aluminum in, RP533 327
Steels, effect of lathe cutting conditions on the hardness of carbon and alloy steels, RP516 77
temperature coefficient of elastic moduli of, RP531 289
Stiffness of cloth and similar materials, RP555 647
Stimson, H. F., E. F. Flock, O. C. Ginnings, N. S. Osborne and, The pressure of saturated vapor in the range 100° to 374° C., RP523 155
Stoneburner, C. F., Lauriston S. Taylor and, Operation of thick-walled X-ray tubes on rectified potentials, RP527 233
Storage batteries, electrolyte, RP566 781
grid materials for, RP567 795
Strain, circle of, RP559 685
measurements of, to determine stress, RP559 685
on Calderwood Dam, RP559 685
on model of Calderwood Dam, RP559 685
Stress, determination of, from strains on three interesting gage lines, RP559 685
Stress distribution in vibrating propellers, method of measurement, RP556 659
Strontium, arc spectrum of, RP558 669
Structures, wind pressure on, RP545 493
Strum, Rolland G., Wm. R. Osgood and, The determination of stresses from strains on three intersecting gage lines and its application to actual tests, RP559 685
Sublimation, heat of, phosphorus pentoxide, RP514 35
Sugar solutions, composition of, RP534 337
Sugar solutions for colorimetric analysis, preparation of optically stable, RP536 365
Sulphation of battery plates, RP567 795
Sulphuric acid, deterioration of leather by, RP547 559
Sulphuric acid, viscosity of, RP566 781
Sweo, B. J., W. N. Harrison and, Some fusion properties of ground coat enamels as influenced by composition, RP524 189

T

Tables, reference, for platinum-rhodium thermocouples, RP530 275
steam, saturation pressure of, RP523 155
Taylor, Lauriston S., and C. F. Stoneburner, Operation of thick-walled X-ray tubes on rectified potentials, RP527 233
Temperature coefficient of moduli of materials used as elastic elements, RP531 289
Temperature effects on unsaturated standard cells, RP518 89
Temperature of freezing iridium, RP568 809
Temperature of freezing silver, RP557 661
Test, methods of (enamels-fusibility), RP524 189
Testing, magnetic, at high magnetizing forces, apparatus for, RP548 567
Tests for fusibility (enamels), RP524 189
Tests, model, wind pressure, RP545 493
Terms of Cl I, RP570 827

Page

Textiles, compressibility of, RP561 705
compressional resilience of, RP561 705
hardness or softness of, RP561 705
thickness of, RP561 705
Thermal expansion measurements, interference method, RP515 59
Thermocouples, calibration at silver point, RP557 661
platinum-rhodium, RP530 275
Thermoelectric properties of platinum-rhodium alloys, RP537 373
Thickness gages for rubber, RP549 575
Thickness of textiles and similar materials, RP561 705
Thomas recording gas calorimeter, RP519 99
Total acidity of soils, RP539 413
Transformers, X-ray, RP527 233
Transmission line antenna system for determination of night effects in radio range-beacon reception, RP513 7
Transmitting antenna system for use at radio range-beacon stations to eliminate night effects, RP513 7
Tube counters, Geiger-Müller, RP526 229
Tucker, W. A., and S. E. Sinclair, Creep and structural stability of nickel-chromium-iron alloys, RP572 851
Tuckerman, L. B., H. L. Dryden, and H. B. Brooks, A method of exciting resonant vibrations in mechanical systems, RP556 659

U

Ultraviolet calibration of dosage intensity meters, RP517 79
Ultraviolet radiometry, RP517 79
Ultraviolet solar radiation in various localities, RP517 79
Unequal heating of standard cells, RP518 89
Unsaturated standard cells, effect of service temperature conditions on, RP518 89

V

Van Dusen, M. S., C. H. Meyer and, The vapor pressure of liquid and solid carbon dioxide, RP538 381
Vapor pressure of carbon dioxide, RP538 381
Vapor pressure of steam, RP523 155
Vapor pressure of water, RP523 155
Vinal, G. W., and D. N. Craig, The viscosity of sulphuric-acid solutions used for battery electrolytes, RP506 781

Page

Vinal, D. N. Craig, and C. L. Snyder, Composition of grids for positive plates of storage batteries as a factor in influencing the sulphation of negative plates, RP567 795
Viscosity of enamels, RP524 189
Viscosity of sulphuric acid, RP506 781
Vitreous enamels (fusibility), RP524 189

W

Wallace, E. L., R. C. Bowker and, The influence of pH on the deterioration of vegetable-tanned leather by sulphuric acid, RP545 559
Washburn, Edward W., Standard states for bomb calorimetry, RP546 525
Water, concentration of saturated vapor of, effect of gas pressures upon, RP546 525
Water, Saturation pressure of, RP523 155
Water, vapor pressure of, RP523 155
Wear resistance of leaded bronzes, RP551 591
Wensel, H. T., F. Henning and, The freezing point of iridium, RP568
White, Joseph D., and F. W. Rose, Jr., Isolation of ethylbenzine from an Oklahoma petroleum, RP554 639
White-metal alloy, RP512 1
White-metal bearing alloys, RP512 1
Wind pressure on a model of the Empire State Building, RP545 493
Wing, Henry J., Charles Proffer Saylor, W. H. Smith and, The preparation and crystallization of pure ether-soluble rubber hydrocarbon: Composition, melting point, and optical properties, RP544 479
Wool, combination of, with positive and negative ions, RP543 475
Wool, isoelectric point of, RP543 475

X

Xenon, first spectrum of, RP521 139
X-ray dosage, RP527 233
X-ray emission, RP527 233
X-ray generators, RP527 233
X-ray measurements, RP527 233
X-ray tubes, RP527 233

Y

Young's modulus, temperature coefficient of, RP531 289

(Cut here)

SUPERINTENDENT OF DOCUMENTS,
Government Printing Office,
Washington, D.C.

DEAR SIR: Send me the Bureau of Standards publications marked X below. I enclose remittance [1] to cover the cost.

Mark X	Title of publication	Price		Amount enclosed
		United States, Canada, Cuba, Newfoundland, Republic of Panama	Foreign countries	
-------	Commercial Standards Monthly (one year)	$1.00	$1.60	----------
-------	Bureau of Standards Journal of Research [2] (one year)	2.50	3.25	----------
-------	Blue buckram bound volumes 1 to 6 of above journal are now available--each volume	[3] 2.75	[3] 3.50	----------
-------	Technical News Bulletin (one year)	.50	.70	----------
-------	Standards Yearbook 1933	1.00	1.20	----------
	Total remittance	----------	----------	----------

Send to----------
Number and Street----------
City and State (or County)----------

[1] Remittances should be either in the form of a post-office money order, coupons (issued for the specific purpose of purchasing Government publications), express money order, New York draft, or cash, at the sender's risk.
[2] This issue completes volume 10. Volume 11 will commence with the July (1933) issue. Your subscription should be submitted at once to insure starting with no. 1 of volume 11.
[3] These prices are for volumes 1 to 6. Commencing with volume 7 the price will be $3 and $3.50 (foreign).

BUREAU OF STANDARDS JOURNAL OF RESEARCH

CONTENTS OF RECENT NUMBERS—Continued

March 1933 (Vol. 10, No. 3)

RP531. Temperature coefficient of the moduli of metals and alloys used as elastic elements. G. H. Keulegan and M. R. Houseman. Price 5 cents.

RP532. A magnetic balance for the inspection of austenitic steel. Raymond L. Sanford. Price 5 cents.

RP533. Determination of aluminum in nitriding steels by the use of 8-hydroxyquinoline. H. A. Bright and Robert M. Fowler.

RP534. The oxidation of alpha and beta glucose and a study of the isomeric forms of the sugar in solution. Horace S. Isbell and Ward Pigman.

RP535. Scattering of electrons by ions and the mobility of electrons in a cæsium discharge. C. Boeckner and F. L. Mohler. Price 5 cents.

RP536. The preparation of optically stable sugar solutions for colorimetric analysis. J. F. Brewster and F. P. Phelps. Price 5 cents.

RP537. Thermoelectric properties of platinum-rhodium alloys. Frank R. Caldwell. Price 5 cents.

RP538. The vapor pressure of liquid and solid carbon dioxide. C. H. Meyer and M. S. Van Dusen.

RP539. Methods for determining the total acidity of soils. I. A. Denison.

April 1933 (Vol. 10, No. 4)

RP540. Infra-red spectra of neon, argon, and krypton. William F. Meggers and C. J. Humphreys.

RP541. Photographic reversal by desensitizing dyes. Burt H. Carroll and C. M. Kretchman.

RP542. 1, 1-dimethylcyclopentane and 2-methylhexane in a midcontinent petroleum. Johannes H. Brunn and Mildred M. Hicks-Brunn.

RP543. The combination of silk and wool with positive and negative ions. Milton Harris

RP544. The preparation and crystallization of pure ether-soluble rubber hydrocarbon: Composition, melting point, and optical properties. W. H. Smith, Charles Proffer Saylor, and Henry J. Wing.

RP545. Wind pressure on a model of the Empire State Building. Hugh L. Dryden and George C. Hill.

RP546. Standard states for bomb colorimetry. Edward W. Washburn.

RP547. The influence of pH on the deterioration of vegetable-tanned leather by sulphuric acid. R. C. Bowker and E. L. Wallace.

RP548. An apparatus for magnetic testing at high magnetic forces. Raymond L. Sanford and Evert G. Bennett.

May 1933 (Vol. 10, No. 5)

RP549. Screw micrometer gages for rubber specimens. W. L. Holt.

RP550. A resistance-coupled amplifier for measuring ionization currents. L. F. Curtiss.

RP551. "Tin-free" leaded bearing bronze. H. K. Herschman and J. L. Basil.

RP552. Purification of hydrocarbons by crystallization from liquid methane. Isolation of 2-methylheptane from petroleum. R. T. Leslie.

RP553. The effect of altitude on the limits of safe operation of gas appliances. John H. Eiseman, Francis A. Smith, and Cecil J. Merritt.

RP554. Isolation of ethylbenzene from an Oklahoma petroleum. Joseph D. White and F. W. Rose, Jr.

RP555. The flexometer, an instrument for evaluating the flexural properties of cloth and similar materials. Herbert F. Schiefer.

RP556. A method of exciting resonant vibrations in mechanical systems. L. B. Tuckerman, H. L. Dryden, and H. B. Brooks.

RP557. Conditions affecting the freezing temperature of silver. Wm. F. Roeser and A. I. Dahl.

RP558. Long-wave arc spectra of alkalis and alkaline earths. William F. Meggers.

RP559. The determination of stresses from strains on three intersecting gage lines and its application to actual tests. Wm. R. Osgood and Rolland G. Sturm.

RP560. Critical solution temperatures of mixtures of gasoline, ethyl alcohol, and water. Oscar C Bridgeman and Dale W. Querfeld.

Research papers, where price is given, are already available, and others will be available in the near future as separates for purchase from the Superintendent of Documents, United States Government Printing Office, Washington, D.C

BUREAU OF STANDARDS JOURNAL OF RESEARCH

CONTENTS OF RECENT NUMBERS

December 1932 (Vol. 9, No. 6)

RP501. Isolation of the three xylenes from an Oklahoma petroleum. Joseph D. White and F. W. Rose, Jr. Price 5 cents.

RP502. Characteristic equations of vacuum and gas-filled tungsten-filament lamps. L. E. Barbrow and J. Franklin Meyer. Price 5 cents.

RP503. The calorimetric determination of the intrinsic energy of gases as a function of the pressure. Data on oxygen and its mixtures with carbon dioxide to 40 atmospheres, at 28° C. Frederick D. Rossini and Mikkel Frandsen. Price 5 cents.

RP504. Shear tests of reinforced brick masonry beams. D. E. Parsons, A. H. Stang, and J. W. McBurney. Price 5 cents.

RP505. The measurement of low-voltage X-ray intensities. Lauriston S. Taylor and C. F. Stoneburner. Price 5 cents.

RP506. A multi-range potentiometer and its application to the measurement of small temperature differences. H. B. Brooks and A. W. Spinks. Price 5 cents.

RP507. The density of some soda-lime-silica glasses as a function of the composition. F. W. Glaze, J. C. Young, and A. N. Finn. Price 5 cents.

RP508. Coiled-filament resistance thermometers. C. H. Meyers. Price 5 cents.

RP509. Deflection of cosmic rays by a magnetic field. L. F. Curtiss. Price 5 cents.

RP510. The system: CaO-B_2O_3. Elmer T. Carlson. Price 5 cents.

RP511. A metal-connected glass electrode. M. R. Thompson. Price 5 cents.

January 1933 (Vol. 10, No. 1)

RP512. White-metal bearing alloys: Mechanical properties at different temperatures and service tests. Harry K. Hershman and John L. Basil. Price 5 cents.

RP513. The cause and elimination of night effects in radio range-beacon reception. H. Diamond. Price 10 cents.

RP514. The heat capacity, heat of sublimation, and heat of solution of phosphorus pentoxide. Mikkel Frandsen. Price 5 cents.

RP515. The interference method of measuring thermal expansion. George E. Merritt. Price 5 cents.

RP516. Effect of lathe cutting conditions on the hardness of carbon and alloy steels. T. G. Digges. Price 5 cents.

RP517. Measurements of ultra-violet solar radiation in various localities. W. W. Coblentz, R. Stair, and J. M. Hogue. Price 5 cents.

RP518. Effect of service temperature conditions on the electromotive force of unsaturated portable standard cells. J. H. Park. Price 5 cents.

RP519. The Thomas recording gas calorimeter. R. S. Jessup. Price 5 cents.

RP520. Compressive strength of steel columns incased in brick walls. Albert I. Harris, A. H. Stang, and J. W. McBurney. Price 5 cents.

RP521. Further description and analysis of the first spectrum of xenon. C. J. Humphreys and W. F. Meggers. Price 5 cents.

February 1933 (Vol. 10, No. 2)

RP522. The elimination of background "noise" in sensitive pulse amplifiers. L. F. Curtiss. Price 5 cents.

RP523. The pressure of saturated water vapor in the range 100° to 374° C. N. S. Osborne, H. F. Stimson, E. F. Fiock, and D. C. Ginnings. Price 10 cents.

RP524. Some fusion properties of ground coat enamels as influenced by composition. W. N. Harrison and B. J. Sweo. Price 5 cents.

RP525. The photographic emulsion: The mechanism of hypersensitization. Burt H. Carroll and Donald Hubbard. Price 5 cents.

RP526. Temperature effect and its elimination in Geiger-Müller tube counters. L. F. Curtiss. Price 5 cents.

RP527. Operation of thick walled X-ray tubes on rectified potentials. Lauriston S. Taylor and C. F. Stoneburner. Price 5 cents.

RP528. Apparatus for comparison of length of gages. Charles Moon. Price 5 cents.

RP529. Clay in concrete. D. A. Parsons. Price 5 cents.

RP530. Reference tables for platinum to platinum-rhodium thermocouples. Wm. F. Roeser and H. T. Wensel. Price 5 cents.

Research papers, where price is given, are already available, and others will be available in the near future as separates for purchase from the Superintendent of Documents, United States Government Printing Office, Washington, D.C.